Proceedings of the 3rd International Brain-Computer Interface Workshop and Training Course 2006

September 21-24 2006
Graz University of Technology, Austria

G.R. Müller-Putz, C. Brunner, R. Leeb, R. Scherer,
A. Schlögl, S. Wriessnegger, G. Pfurtscheller

Verlag der Technischen Universität Graz 2006

Laboratory of Brain-Computer Interfaces
Institut für Semantische Datenanalyse/Knowledge Discovery
Graz University of Technology, Austria

Verlag der Technischen Universität Graz
http://www.ub.tugraz.at/Verlag

ISBN-10: 3-902465-46-8
ISBN-13: 978-3-902465-46-7

Bibliografische Information der Deutschen Bibliothek:
Die Deutsche Bibliothek verzeichnet diese Publikation in der
Deutschen Nationalbibliografie; detaillierte bibliografische Daten sind im Internet über
http://dnb.ddb.de/ abrufbar.

Printed by TU Graz/Büroservice, Graz, Austria

PREFACE

This book contains the scientific contributions to the 3rd International Brain-Computer Interface Workshop and Training Course 2006, held in Graz, Austria.

From the very beginning about 15 years ago, a growing number of research groups around the world started to develop and investigate Brain-Computer Interfaces (BCIs). To date, alternative approaches or prototypes, using different types of electrophysiological brain signals or metabolical changes in the brain, training/control paradigms or operating modes, are available and to be evaluated in practical use.

Exemplarily, the use of an asynchronous BCI, which analyses the brain signals sample by sample and therefore, produces a decision sample by sample is mandatory for a real world application. The challenge here is to define a system which deals not only with the intentional control (e. g., motor imagery-related brain patterns), but also to handle the non-control state. During non-control the same pattern may occur as during the control-state leading to an unwanted control signal. Therefore the minimization of false positives is the main challenge in asynchronous BCIs. With such a system users gain full control over timing and speed of communication.

The rapid progress in this field became possible due to advances both in methods of signal analysis and in information technology, allied to a better understanding of the psychophysiological correlates of the crucial parameters. It is important to note that improvements in the emerging field of BCI research and development depend largely on cooperation between scientists and research groups of different fields. The interdisciplinary co-operation among neuroscientists, engineers, psychologists, and rehabilitation specialists is a necessary requisite. But also constructive collaboration and exchange of experiences and information between the involved research groups as well as creating the right community of young people are essential for a field like this.

After the positive responses to the 1st and 2nd BCI meetings in 2002 and 2004, we were encouraged to organize a third meeting in Graz. In this 3rd International Brain-Computer Interface Workshop and Training Course 2006 we tried to distinguish more between the Training Course, which is especially for new researchers in the field, and the Workshop, the scientific part of the meeting. The Training Course is completely separated from the meeting and participants should learn to set up a BCI system beginning with electrode montage, paradigm design, feature extraction and classification up to realize online and real-time feedback. The current Workshop was defined as a scientific conference where researchers can present their own work either in form of a talk or a poster presentation. For this purpose we encouraged the participants to submit short papers, which were peer-reviewed and are published in this issue. The BCI meetings held in Graz, Austria, may be considered as an European initiative in the field of EEG-based Brain-Computer Interfaces that contributes to a stronger orientation towards scientific cooperation.

We are lucky that outstanding experts in the field, Theresa Vaughan (Wadsworth Center, USA), José del R. Millán (IDIAP, Switzerland), Riita Salmelin (HUT, Finland) were able to accept our invitation to present keynote addresses at the Workshop.

This issue is devoted to the scientific contributions of the participants. As can be seen, these contributions cover a wide range of topics, including methods of signal processing and feature extraction, new methods of classification, different types of presenting feedback, and software/hardware development. Aside from reports on healthy volunteers, also studies in disabled people are reported. With respect to the brain signals used, a variety of different approaches on how to detect user-initiated or evoked changes in EEG signals have been taken.

We gratefully acknowledge the support of the Graz University of Technology for providing the facilities and thank the staff of the Institute of Knowledge Discovery, BCI-Lab, for their dedicated assistance.

We hope that the content and scope of our program may contribute to a successful and constructive 3rd International Brain-Computer Interface Workshop and Training Course 2006!

The editorial board

Group of the 2nd International Brain-Computer Interface Workshop and Training Course 2004.

Contents

THEORETICAL AND EXPERIMENTAL BASIS FOR THE DEVELOPMENT OF DIRECT NONINVASIVE BCI

R. Grave de Peralta Menendez[1], J. del R. Millán[2], P. Morier[2], S. L. Gonzalez Andino[1]

[1]Electrical Neuroimaging Group, Geneva University Hospital, Geneva
[2]IDIAP Research Institute. Rue du Simplon 4, 1920 Martigny, Switzerland
E-mail: Rolando.Grave@hcuge.ch

SUMMARY: This paper proposes the use of non-invasively estimated local field potentials (eLFP) produced by ELECTRA as a safe and efficient alternative to the highly invasive procedures currently in use for neuroprosthesis control. Here we present theoretical and experimental evidences justifying eLFP estimation and its advantages. To illustrate the capabilities of this approach we compare eLFP with intracranial recordings (IR) for the same task. The results show that eLFP non-invasively estimated from the EEG are as informative as invasive IR opening new possibilities for the design of direct noninvasive BCIs.

INTRODUCTION

Recent experiments have shown the possibility to use the brain electrical activity to directly control the movement of robots or prosthetic devices in real time. Such neuroprostheses can be invasive or non-invasive, depending on how the brain signals are recorded. In principle, invasive approaches will provide a more natural and flexible control of neuroprostheses, but their use in humans is debatable given the inherent medical risks. Non-invasive approaches mainly use scalp electroencephalogram (EEG) signals and their main disadvantage is that these signals represent the noisy spatiotemporal overlapping of activity arising from very diverse brain regions; i. e., a single scalp electrode picks up and mixes the temporal activity of myriads of neurons at very different brain areas. In order to combine the benefits of both approaches, we propose to rely on the non-invasive estimation of local field potentials (eLFP) in the whole human brain from the scalp measured EEG data using a ELECTRA inverse solution [1, 2]. The goal of ELECTRA is to de-convolve or unmix the scalp signals attributing to each brain area its own temporal activity. This paper presents the theoretical and experimental evidences that support the irrotational source model of ELECTRA. To illustrate the capabilities of this approach we compare the classification results of eLFP non invasively estimated from the EEG with intracranial recordings (IR) during a visuo-motor task.

MATERIALS AND METHODS

Basic equations: Poisson equation describes the relationship between scalp surface EEG and the (primary) current density vector (J^p) under the quasi-static approximation of Maxwell equations [2]. Assuming a simple head model with unitary conductivity and denoting by G the Green function, it can be written in any of the two following forms:

$$V(r) = \int_V \nabla \cdot J^p(r_v) G(r, r_v) \tag{1}$$

$$\nabla \cdot \nabla V = \nabla \cdot J^p \tag{2}$$

Where V denotes the electrical potential at scalp site r and r_v stand for points that belong to the brain volume.

Experiment description: We recorded scalp EEG data and intracranial data in 4 subject and two patients performing a visuo-motor reaction time task requiring left or right finger responses as described in [3]. Unless otherwise specified, the term data will denote both EEG and IR data.

EEG recording: The electroencephalogram (EEG) was continuously monitored at 500 Hz during the whole experiment from 125 scalp electrodes (Electric Geodesic Inc. system, USA). Recordings were done using a cephalic reference placed at the vertex. Off-line processing of the data consisted of 1) transformation of the EEG data to the common average reference, 2) rigorous rejection of trials contaminated by ocular or movement artifacts through careful visual inspection, and 3) bad channel selection and interpolation. Fourteen electrodes from the lowest circle on the electrode array, i. e., closest to neck and eyes, were excluded a posteriori because of their likeliness to pick up muscular artifacts.

eLFP: EEG recordings obtained from previous step were transformed into local field potential estimates (eLFP) using the inverse matrix associated to the irrotational source model (ELECTRA) described in [1] and [2]. This yielded LFP estimates for 4024 brain voxels distributed all over the gray matter of a realistic head model.

Intracranial recording: Two patients that underwent intracranial recordings (IR) for presurgical epilepsy evaluation performed the same visuo-motor reaction time task as used in the healthy subjects. IR were recorded at 200 Hz from subdural electrodes covering motor cortex and parietal and temporal areas of one hemisphere. The covering of motor areas was assessed by direct electrical cortical stimulation. The local ethical committee approved the experiments, and written informed consent was obtained in all cases.

Analysis Window and features computation: Data from the 111 EEG channels and the 4024 eLFP (virtual) channels were transformed to the frequency domain. To avoid muscular artifacts (that might be present in the EEG) the shortest reaction time of each

subject was used to define the eLFP analysis window. For the IC recording the mean reaction time (what could favor this modality) was used as the analysis window.

Classification details: For both modalities the whole data set was divided in two halves. The first half was used as a learning set and the second one as the testing set. The best 150 features (from all possible channels and frequencies) were selected using the discriminative power [3] on the learning set. Classification was based on the linear OSU-SVM and the leave-one-out method on the testing set.

RESULTS

As for any vector field, the primary current density vector can be written as the sum of a solenoidal vector field plus an irrotational vector field plus the gradient of a harmonic function, i. e., $J^p = \nabla\phi + \nabla \times A + \nabla H$. Substituting this expression into (1) demonstrates that only the irrotational part $\nabla\phi$ can produce the potential V (i. e., the EEG).

Feeding the irrotational part $\nabla\phi$ into (2) proves that the scalar function ϕ (potential) has the same Laplacian, and thus, the same sources and sinks as V.

Concurrent experimental evidence was provided by Plonsey [4] who stated that "the fields measured do not even arise from J but rather from secondary sources only. These secondary sources, in turn, depend on both the electrical field and the interfaces, and hence are related to $\nabla \cdot J$ and the geometry".

In summary, we can say that the scalar potential field ϕ contains valuable information about the potentials generated inside the brain and that by estimating it we can: 1) Reduce the number of unknowns by a factor of three. 2) Facilitate the inclusion of a priori information from others scalar modalities. 3) Reduce the problem to a physical measurable magnitude, i. e., potentials instead of current density vector, which can be experimentally assessed.

Table 1 shows that the results obtained for invasive IR in two patients are not better than the results obtained with non invasive eLFP computed from the EEG in 4 subjects.

	Correct classification rate (%)
IR 1	91
IR 2	94
eLFP 1	98
eLFP 2	93
eLFP 3	91
eLFP 4	99

Table 1: Classification results for the two patients (IR) and estimated local field potentials (eLFP) of the 4 normal subjects.

CONCLUSION

This paper shows the connection between the external potential field (EEG) and the potential distribution inside the brain volume. The estimation of this potential field is equivalent to use the irrotational source model of ELECTRA [1]. As shown by the experimental results, this non-invasively estimated field (eLFP) performs as well, or better, than the IR obtained with invasive methods during the classification task discussed here. This suggests that eLFP, might be considered as a safe and efficient alternative for the development of direct non invasive BCIs.

ACKNOWLEDGEMENT

Work supported by the SNSF grant 3152A0-100745, the SNSF NCCR "IM2", and the European IST Programme FET Project FP6-003758.

REFERENCES

[1] Grave de Peralta R, Gonzalez SL, Morand S, Michel CM and Landis T. Imaging the electrical activity of the brain: ELECTRA. Hum Brain Mapp, 2000; 9: 1-12.

[2] Grave de Peralta Menendez R, Murray MM, Michel CM, Martuzzi R, Gonzalez Andino SL. Electrical Neuroimaging Based on Biophysical Constraints. Neuroimage, 2004; 21: 527-539.

[3] Gonzalez Andino SL, Grave de Peralta Menendez R, Thut G, Millán JdR, Morier P, Landis T. Very high frequency oscillations (VHFO) as a predictor of movement intentions. Neuroimage, 2006; in press.

[4] Plonsey R. The nature of sources of bioelectric and biomagnetic fields. Biophys J, 1982; 39: 309-12.

PARAMETERIZATION OF WAVELETS FOR OPTIMIZED SIGNAL REPRESENTATION IN THE CLASSIFICATION OF MOVEMENT-RELATED CORTICAL POTENTIALS

D. Farina[1], O. F. do Nascimento[1], M. F. Lucas[2], C. Doncarli[2]

[1]Center for Sensory-Motor Interaction (SMI), Department of Health Science and Technology, Aalborg University, Aalborg, Denmark
[2]IRCCyN, École Centrale de Nantes, Nantes, France
E-mail: df@hst.aau.dk

SUMMARY: We present a method for the classification of movement-related cortical potentials (MRCPs). The feature space was built from the coefficients obtained from a discrete dyadic wavelet transformation (DWT). The parameterization of the mother wavelet, within the multi-resolution framework, allowed the selection of an infinite number of sets of basis functions to project the signals. Using this parameterization, the mother wavelet was optimized in order to minimize classification error. Classification was performed with the support vector machine approach. A representative example of application to the classification of MRCPs generated by ballistic plantar-flexions at two force levels is presented. In this example, classification error ranged from 5 %, with optimization of the wavelet, to 34 %, with fixed wavelet in the worst case, showing the importance of a signal-based selection of the feature space.

INTRODUCTION

A successful classification depends on an adequate representation of the signals in a relevant space (feature extraction). Many features have been proposed for classification of electroencephalographic (EEG) signals for the use in brain-computer interfaces (BCI), such as parameters of autoregressive models, Fourier transformation coefficients, and wavelet transform coefficients. However, to our knowledge, the extraction features adapted to the characteristics of the signal in order to minimize classification error, has not been attempted. Discrete wavelet transform (DWT) coefficients may be adapted to the set of signals to be classified since they depend on the choice of the mother wavelet. However, classification using DWT as projection in the feature space was previously based on the a-priori selection of the mother wavelet.

Therefore, our aims are 1) to propose a signal-dependent wavelet transformation through parameterization of the analysis filters in the multi-resolution analysis (MRA) framework, and 2) to show the advantage of wavelet parameterization over the selection of fixed wavelets in a representative example of classification of movement-related cortical potentials (MRCP).

MATERIALS AND METHODS

The classification method is based on the representation of the signal in a feature space built through the DWT and parameterization of the analysis filter. The analysis filter, which defines the mother wavelet, is then optimized with the criterion of minimum classification error.

Feature extraction: The DWT decomposes a signal $f(x)$ on a basis where all functions are dilated and translated versions of a prototype function ψ, called mother wavelet. The projections of the signal into these basis functions return detail coefficients

$$d_f(j,k) = \langle f(x), \psi_{j,k}(x) \rangle ,$$

where

$$\psi_{j,k}(x) = 2^{-j/2}\psi(2^{-j}x - k).$$

Approximation coefficients $a_x(j,k)$ are obtained by projecting the signal on dilated and translated versions of the scaling function φ,

$$a_f(j,k) = \langle f(x), \varphi_{j,k}(x) \rangle ,$$

where

$$\varphi_{j,k}(x) = 2^{-j/2}\varphi(2^{-j}x - k).$$

The set of approximation and detail coefficients can be alternatively computed by Mallat's algorithm with the application of a filter bank [1] (MRA).

In the MRA framework, the scaling function φ and its associated mother wavelet ψ are related to the filters h and g (used for computation of the DWT through a filter bank) by the two-scale recursive relations

$$\varphi(x/2) = \sqrt{2}\sum_n h[n]\varphi(x-n),$$

$$\psi(x/2) = \sqrt{2}\sum_n g[n]\varphi(x-n).$$

For orthogonal wavelets, g can be deduced from h from the relation $g[k] = (-1)^{1-k}h[1-k]$, thus h defines ψ. To generate an orthogonal MRA wavelet, h must satisfy some constraints. For a FIR filter of length L, there are $L/2+1$ sufficient conditions to ensure the existence and orthogonality of the scaling function and wavelets [2]. Thus, $L/2-1$ degrees of freedom remain to design the filter h. The lattice parameterization described by Vaidyanathan [3] allows the design of h via unconstrained optimization. The L coefficients of h can be expressed in term of $L/2-1$ new free parameters. If $L=4$, we need one single parameter α and h is given as:

$$h[0] = (1-\cos(\alpha)+\sin(\alpha))/(2\sqrt{2})$$

$$h[1] = (1+\cos(\alpha)+\sin(\alpha))/(2\sqrt{2})$$

$$h[2] = (1+\cos(\alpha)-\sin(\alpha))/(2\sqrt{2})$$

$$h[3] = (1 - \cos(\alpha) - \sin(\alpha))/(2\sqrt{2})$$

If $L = 6$, we need a 2-component design vector and h is given by:

$$\begin{aligned} i = 0, 1 : h[i] &= [(1 + (-1)^i \cos\alpha + \sin\alpha) \cdot \\ &\quad \cdot (1 - (-1)^i \cos\beta - \sin\beta) + \\ &\quad + (-1)^i 2 \sin\beta \cos\alpha]/(4\sqrt{2}) \\ i = 2, 3 : h[i] &= \frac{1 + \cos(\alpha - \beta) + (-1)^i \sin(\alpha - \beta)}{2\sqrt{2}} \\ i = 4, 5 : h[i] &= 1/\sqrt{2} - h(i-4) - h(i-2) \end{aligned}$$

For other values of L, expressions of h are given in [4]. This parameterization allows the definition of an infinite number of wavelet representations through the selection of a finite set of parameters. While the a-priori selection of a wavelet for best classification is not possible, a training set of signals may be used to estimate the probability of classification error for each wavelet and thus to select the wavelet leading to the lowest error.

Feature space: The wavelet coefficients are partly localized in time and scale. However, localization in time may be a problem for comparison due to the lack of alignment of the signals. In order to make the representation space insensitive to time alignment, different features can be selected. One possibility is to use the normalized marginals of the DWT, defined as:

$$m_f(j) = \sum_{k=0}^{N/2^j - 1} c_f(j,k), \qquad j = 1 \ldots J$$

$$c_f(j,k) = \frac{|d_f(j,k)|}{\sum_{j=1}^{J} \sum_{k=0}^{N/2^j - 1} |d_f(j,k)|}$$

where J is the deepest level of the decomposition ($J = \lfloor \log_2 N \rfloor$). In this case, the features representing the signal f are the components of the vector $M_f = [m_f(1), \ldots, m_f(J)]$. The vector M_f contains information on the distribution of the wavelet coefficients over J bands.

Other choices are entropy, root mean square or any other processing of wavelet coefficients in the different subbands. In the following, the marginals were used.

Classification: Support vector machine (SVM) algorithm was used for binary classification in the representative results shown below. The idea is to construct, in the feature space H, a linear decision function from the hyperplane with maximum margin, i. e., which is at maximum distance from all the data points and classifies them correctly. This corresponds to looking for a normal vector w and a parameter b corresponding to the hyperplane whose equation is $w\Phi(x) + b = 0$, where $K(x, x') = \langle \Phi(x), \Phi(x') \rangle$ is the kernel.

For each parameterized wavelet, the classifier was applied to the training set and optimized for the parameters of the kernel. The estimated minimum classification error was used to select the optimal wavelet.

Representative example of application: Representative results are shown for the classification of MRCPs generated by different force levels in one subject (23 years), who was instructed to perform plantar-flexions of the right foot reaching torque levels at 40 % or 60 % of maximal force as fast as possible. Each task was repeated 60 times with inter-trial intervals of 12 s [5]. Epochs of 1.5 s prior the movement from Cz channel sampled at 500 Hz were used for classification.

RESULTS

The two classes could be separated with a minimum classification error of 5 % when the optimization of the wavelet was implemented. With fixed wavelets the classification error could be as large as 34 % (Figure 1).

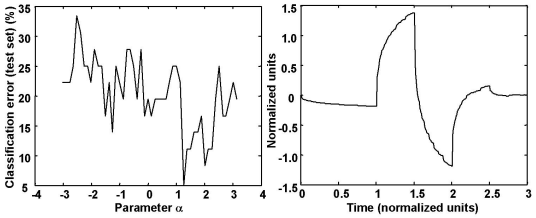

Figure 1: Classification error (test set) for the 50 wavelets used in the optimization procedure (left). Optimal wavelet corresponds to a classification error of 5 %, worst wavelet to a classification error of 34 %. Best wavelet in this case is shown on the left.

DISCUSSION

We presented and evaluated a feature extraction method optimized for the aim of classification. The DWT allows the selection of an infinite set of basis functions through a set of parameters. The optimal parameters can be chosen on the basis of the specific training set and thus adapted to the subject. The importance of wavelet optimization was shown by comparison of the results obtained with different wavelets (Figure 1). The method can be extended to the multichannel case to further improve performance.

REFERENCES

[1] Mallat SG. A theory of multiresolution signal decomposition: the wavelet representation. IEEE Trans Pattern Anal Machine Intell, 1989; 11(7): 674–693.

[2] Maitrot A, Lucas MF, Doncarli C, Farina D. Signal-dependent wavelets for electromyogram classification. Med Biol Eng Comput, 2005; 43(4): 487–492.

[3] Vaidyanathan PP. Multirate Systems and Filter Banks. Wellesley-Cambridge Press, 1996.

[4] Burrus CS, Gopinath RA, Guo H. Introduction to wavelets and wavelet transforms. Prentice Hall, 1997; 53–66

[5] Do Nascimento OF, Nielsen KD, Voigt M. Relationship between plantar-flexor torque generation and the magnitude of the movement-related potential. Exp Brain Res, 2005; 160: 154–165.

THE USE OF FUZZY INFERENCE SYSTEMS FOR CLASSIFICATION IN EEG-BASED BRAIN-COMPUTER INTERFACES

F. Lotte

IRISA-INSA (National Institute of Applied Sciences) Rennes, France
E-mail: fabien.lotte@irisa.fr

SUMMARY: This paper introduces the use of a Fuzzy Inference System (FIS) for classification in EEG-based Brain-Computer Interfaces (BCI) systems. We present our FIS algorithm and compare it, on motor imagery signals, with three other popular classifiers, widely used in the BCI community. Our results show that FIS outperformed a Linear Classifier and reached the same level of accuracy as Support Vector Machine and neural networks. Thus, FIS-based classification is suitable for BCI design. Furthermore, FIS algorithms have two additional advantages: they are readable and easily extensible.

INTRODUCTION

Most BCI systems use classification algorithms to identify specific mental activities. Several classification algorithms have been used to design BCIs, such as linear classifiers, Support Vector Machines (SVM) or neural networks [9]. Surprisingly, fuzzy classifiers have been scarcely used by the BCI community. However, fuzzy classifiers were proved efficient for several classification problems [1], including non-stationary biomedical signals classification [2] and brain research [3].

A specific kind of fuzzy classifiers, namely Fuzzy Inference System (FIS), has three main advantages: it is readable, extensible [4], and a universal approximator [5]. Therefore, in this paper, we propose to use a FIS for BCI design.

In the following paper we will first describe the FIS algorithm that we have set-up to classify EEG data corresponding to motor imagery. Then, we will report on an evaluation of the FIS classifier as compared with three other classifiers: Linear Classifier, Neural Network, and SVM.

FIS ALGORITHM USED

The FIS that we used is based on Chiu's algorithm [4]. This algorithm is robust to noise and according to its author, it is generally more efficient than Neural Networks.

Training of the FIS: As any FIS, our algorithm uses fuzzy "if-then" rules. Three steps are required to learn the fuzzy rules from N dimensionnal data:

1. *Clustering of training data.* First, a clustering algorithm, known as "substractive clustering" [4], is applied to the training data of each class. This algorithm is used because it is noise resistant and can automatically determine the number of clusters. It requires the user to specify the clusters radius R_a.

2. *Generation of the initial fuzzy rules.* A fuzzy "if-then" rule is generated for each cluster found previously. For a given cluster j, belonging to class Cl_i, the generated fuzzy rule is:

   if X_1 is A_{j1} and X_2 is A_{j2} and ...
   then class is Cl_i

   X_k is the k^{th} element of a feature vector X and A_{jk} is a gaussian membership function:

   $$A_{jk}(X_k) = \exp\left\{-\frac{1}{2}\left(\frac{X_k - x_{jk}}{\sigma_{jk}}\right)^2\right\} \quad (1)$$

   where x_{jk} is the k^{th} element of the vector representing the center of the cluster, and σ_{jk} is a positive constant, which is initialy the same for all A_{jk}.

3. *Optimization of the fuzzy rules.* Last, each membership function A_{jk} is tuned according to gradient descent formulas [4]:

   $$x_{jk} \Leftarrow x_{jk} - \lambda\frac{\partial E}{\partial x_{jk}} \text{ and } \sigma_{jk} \Leftarrow \sigma_{jk} - \lambda\frac{\partial E}{\partial \sigma_{jk}} \quad (2)$$

   where λ is a positive learning rate and E a classification error measure. To increase accuracy, membership functions can be "two-sided" Gaussian functions [4], with a plateau and different standard deviations on the left and right sides, as displayed in Figure 1.

FIS Classification: Once trained, the FIS can classify a new feature vector X using its set of fuzzy rules. The output class of X corresponds to the class associated with the rule j for which $\prod_{k=1}^{N} A_{jk}(X_k)$ is the highest. Thus, the standard multiplication is used as the *and* operator.

CLASSIFYING MOTOR IMAGERY WITH FIS

EEG data: The data used corresponds to the EEG data set IIIb of the BCI competition III. Three subjects had to imagine left or right hand movements. Hence, the two classes to be identified are "Left" and "Right". EEG were recorded using electrodes C3 and C4, and were filtered between 0.5 and 30 Hz (see [6] and [7] for further details).

Feature extraction: Band Power (BP) features were extracted, in a statistically optimal time window, for both electrodes C3 and C4. The optimal time window was found to start 0.4 s after the beginning of the feedback presentation for subject 1 and 1.4 s for subjects 2 and 3. It was 2.5 s long for subject 1 and 1.5 s long for

subjects 2 and 3. The most reactive frequency bands were selected using a statistical paired t-test which compared the two classes means for all overlapping 2 Hz frequency bands between 1 Hz and 30 Hz. As expected, the optimal frequencies for discrimination were found in the α and β bands. This led to a four dimensional feature vector: [$C3_\alpha$, $C3_\beta$, $C4_\alpha$, $C4_\beta$] in which Cp_y is the BP value for eletrode Cp in the y band. Naturally, the exact frequency bands depended on the subject.

FIS Classifier: The FIS algorithm was trained using the data set and the features described above. For each subject, two fuzzy rules were extracted. The rules obtained for the first subject are displayed on Figure 1.

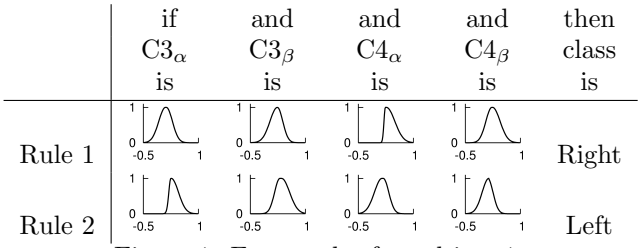

Figure 1: Fuzzy rules for subject 1

The interpretation of the rules shows that the power for electrode C3, in the α and β bands, is lower during imagined right hand movements than during imagined left hand movements. A symmetric behaviour can be observed for electrode C4. In EEG research, this phenomenon is known as contralateral Event-Related Desynchronisation (ERD) [10]. This proved that FIS classifiers are readable systems which can be useful to extract knowledge about the brain dynamics. Another advantage of FIS is that fuzzy rules, such as rules made by brain experts, could be easily added as "a priori information".

PERFORMANCES EVALUATION

Our FIS was compared to three other popular classifiers widely used in the BCI community [9]: an SVM with gaussian kernel, a MultiLayer Perceptron (MLP) which is a neural network and a perceptron as a Linear Classifier (LC). Implementation of LC, SVM and MLP was achieved using the Torch C++ library [8]. The optimal values for the hyperparameters of all classifiers (radius R_a for the FIS, regularization parameter C for the SVM, etc.) were chosen using 10-fold cross validation. The four classifiers were compared using the same test set and the same features as described above. Table 1 sums up the accuracy obtained by each classifier.

Table 1: Accuracy of the different classifiers

Subject	FIS	SVM	MLP	LC
Subject 1	86.7 %	86.8 %	86.6 %	84.1 %
Subject 2	74.7 %	75.9 %	75.5 %	71.8 %
Subject 3	75.7 %	75.4 %	74.6 %	72.7 %
Mean	79 %	79.4 %	78.9 %	76.2 %

Our results show that our FIS outperformed LC and reached the same level of accuracy as SVM and MLP. Finally, the average computation time to classify a feature vector using an FIS is 0.008 ms. Thus, the algorithm is suitable for a real-time and online use within a BCI system.

CONCLUSION

In this paper we have described the use of a Fuzzy Inference System (FIS) for classification in Brain-Computer Interfaces. An FIS classifier outperformed a linear classifier and was found as accurate as Support Vector Machine or neural networks for the classification of motor imagery. Furthermore, FIS classifier is fast, readable and easily extensible which make it suitable and useful for real-time BCI design.

ACKNOWLEDGEMENT

This work was supported by the French National Research Agency and the National Network for Software Technologies within the Open-ViBE project.

REFERENCES

[1] Bezdek JC. Computing with uncertainty. IEEE Communications Magazine, 1992.

[2] Chan FHY, Yang YS, Lam FK, Zhang YT, Parker PA. Fuzzy EMG classication for prosthesis control. IEEE Trans Rehab Eng, 2000.

[3] Bay OF, Usakli AB. Survey of fuzzy logic applications in brain-related researches. J Med Syst, 2003.

[4] Chiu SL. An efficient method for extracting fuzzy classication rules from high dimensional data. J Adv Comp Int, 1997.

[5] Wang LX. Fuzzy systems are universal approximators. IEEE Int Conf Fuzzy Syst, 1992.

[6] Leeb R, Scherer R, Lee F, Bischof H, Pfurtscheller G. Navigation in virtual environments through motor imagery. CVWW'04, 2004.

[7] Vidaurre C, Schlögl A, Cabeza R, Scherer R, Pfurtscheller G. A fully on-line adaptive brain computer interface. Biomed Tech Band Special issue, 2004; 49.

[8] Collobert R, Bengio S, Mariethoz J. Torch: a modular machine learning software library. IDIAP-RR, 2002; 02–46.

[9] Blankertz B, Müller KR, Curio G, Vaughan TM, Schalk G, Wolpaw JR et al. The BCI competition 2003: Progress and perspectives in detection and discrimination of eeg single trials. IEEE Trans Biomed Eng, 2004.

[10] Pfurtscheller G, Klimesch W. Event-related synchronization and desynchronization of alpha and beta waves in a cognitive task. Induced rhythms in the brain, 1992.

REGULARISED CSP FOR SENSOR SELECTION IN BCI

J. Farquhar, N. J. Hill, T. N. Lal, B. Schölkopf

Max Planck Institute for Biological Cybernetics, Tübingen, Germany
E-mail: jdrf@tuebingen.mpg.de

SUMMARY: The Common Spatial Pattern (CSP) algorithm is a highly successful method for efficiently calculating spatial filters for brain signal classification. Spatial filtering can improve classification performance considerably, but demands that a large number of electrodes be mounted, which is inconvenient in day-to-day BCI usage. The CSP algorithm is also known for its tendency to overfit, i. e. to learn the noise in the training set rather than the signal. Both problems motivate an approach in which spatial filters are sparsified. We briefly sketch a reformulation of the problem which allows us to do this, using 1-norm regularisation. Focusing on the electrode selection issue, we present preliminary results on EEG data sets that suggest that effective spatial filters may be computed with as few as 10–20 electrodes, hence offering the potential to simplify the practical realisation of BCI systems significantly.

INTRODUCTION

BCI data sets typically consist of multiple time-series that are highly correlated, particularly so when measured by EEG, since EEG signals suffer from a high degree of spatial blurring. When transduction is based on a nonlinear transformation of the time-series, such as one that extracts band-power for the detection of Event-Related Desynchronisation (ERD), a *spatial filtering* preprocessing stage that performs *source separation* before nonlinear feature extraction will often improve results (see for example [1]). This can be done by Independent Component Analysis, or in some cases by the computationally much cheaper Common Spatial Pattern (CSP) method [2] and related algorithms [3, 4, 5].

One practical problem with spatial filtering is that it typically requires a large number of electrodes to be applied, whereas in everyday clinical application it is desirable to have to apply only a few. An additional problem associated with the supervised CSP algorithm in particular is its tendency to *overfit*, leading to poor generalisation (for illustration and discussion of this effect see [1, 4, 5]). This is a particular problem when the number of electrodes is large, and when the number of available trials is small.

Both problems argue for an approach which can *sparsify* the spatial filters that one computes, i. e. to force them to be based on a small number of electrodes, and to trade this characteristic off against performance on the training data. The goal is twofold: firstly to identify (based on an initial setting with a full EEG cap) which electrodes should be attached in future sessions and which can be omitted; secondly to *regularise* the computation of spatial filters, leading to improved generalisation in cases where overfitting is a problem. Regularisation by sparsification is a common approach in machine learning, and was described in the context of a CSP-like algorithm by Dornhege et al. [5]. The latter authors apply regularisation in the domain of the temporal FIR filters used in their algorithm. Here we apply the same principle to the spatial filters themselves, focusing on the question: what is the tradeoff between number of electrodes and performance, within the CSP framework?

THE RCSP ALGORITHM

CSP operates on the covariance matrix Σ_T between the d channels, computed using all trials, and the class-covariance matrix Σ_c which is computed using only trials from a given class c. Each filter is a vector $\boldsymbol{w}$ of length d, found by maximising the variance in one class whilst simultaneously minimising the variance in the other class(es). Equivalently, CSP can be seen as maximising the *Rayleigh quotient* which is the ratio of the variance of the filtered signal in class c to its variance overall. In addition to this criterion, we add a regularisation term incorporating a cost hyperparameter C. As is common in regularisation-by-sparsification approaches, our C is a penalty term on the L1-norm (i. e. the sum of the absolute values of the elements) of $\boldsymbol{w}$. Our $\boldsymbol{w}$ is therefore found by solving the following unconstrained optimisation problem:

$$\arg\max_{\boldsymbol{w}} \frac{\boldsymbol{w}^\top \Sigma_c \boldsymbol{w}}{\boldsymbol{w}^\top \Sigma_T \boldsymbol{w}} - \frac{C|\boldsymbol{w}|_1}{\sqrt{d}|\boldsymbol{w}|_2}. \qquad (1)$$

The first term is the Rayleigh quotient: optimising this alone (i. e. setting $C = 0$) can be shown to be equivalent to solving the generalised eigenvalue problem $\Sigma_c \boldsymbol{w} = \lambda \Sigma_T \boldsymbol{w}$, which gives the ordinary CSP solution. We obtain a solution to (1) using the conjugate gradient method (see [6]). Once each filter is found, subsequent filters are found by *deflating* Σ_c as follows:

$$\Sigma_c \leftarrow \Sigma_c \left(I - \frac{\boldsymbol{w}^\top \boldsymbol{w} \Sigma_T}{\boldsymbol{w}^\top \Sigma_T \boldsymbol{w}} \right) \qquad (2)$$

and then iterating the procedure. If C is set to 0, (1) and (2) together recover the ordinary CSP decomposition in full. With $C > 0$, we call the algorithm regularised CSP or rCSP, and its solutions are sparser, i. e. the resulting $\boldsymbol{w}$ vectors have fewer non-zero entries, meaning that fewer electrodes are used.

EXPERIMENTS

We tested the effect of varying C on the data from a number of two-class motor imagery experiments without feedback. 39-channel EEG was recorded from each subject as they performed 400 trials of imagined left-

or right-hand movement. Regularised CSP was applied using the 7–30 Hz band, and a linear Support Vector Machine was used to classify the resulting variances of the spatially filtered signals. Offline performance was estimated using 2 repeats (with different random seeds) of 10-fold cross-validation, and the SVM's own regularisation parameter was optimised using 10-fold cross-validation nested within that (i. e. within the training subset of each outer fold).

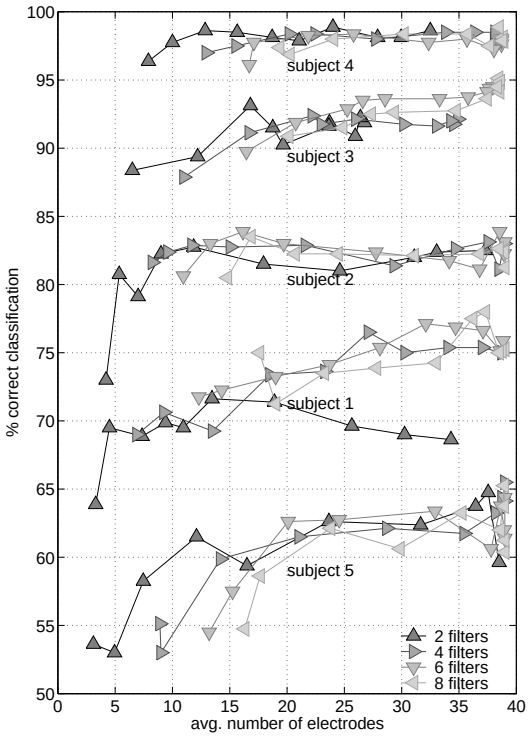

Figure 1: Classification accuracy for 5 subjects, as a function of number of electrodes required.

We varied the number of filters we wished to extract, $n \in \{2, 4, 6, 8\}$, and the cost parameter $C \in \{0, 0.01, 0.02, 0.05, 0.1, 0.2, 0.5, 1, 2, 5\}$. For each setting, we plot classification accuracy (averaged across the 20 outer folds) against the number of electrodes required in total to implement the n computed filters (also averaged across outer folds). We show results for 5 of the 6 subjects—the sixth subject showed similar trends, but we omit his results for readability since the curves overlap those of subjects 1 and 5.

Figure 1 gives a quantitative impression of the effect of the number of electrodes needed. For some subjects (for example, subjects 2 and 4) the curves are surprisingly flat: using only two spatial filters, one can reduce the number of electrodes to around 10 without any appreciable drop in classification accuracy. For the others, best performance was achieved with the maximum available number of electrodes, although close-to-optimal performance may still be achieved with around 20. In practice, the optimal choice of C and n should, as in most CSP implementations, be found for each subject by cross-validation.

Note that these are only preliminary results—our subjects started with a relatively small number of electrodes, 39, which meant they were widely spaced relative to those, say, a 128-electrode cap. It is possible that sparser electrode montages are effective if the candidate electrodes are more closely spaced.

CONCLUSION

Formulating the CSP problem as a Rayleigh quotient optimisation allows us to modify the formulation easily, with potential applications in both spatial and spatio-spectral filtering. The current modification, rCSP, allows automatic selection of a subset of electrodes during the optimisation of the spatial filter, showing that in some cases the number of electrodes can be reduced to 20 or fewer with little loss in performance.

REFERENCES

[1] Hill NJ, Lal TN, Schröder M, Hinterberger T, Widman G, Elger C. E, Schölkopf B, Birbaumer N. Classifying event-related desynchronization in EEG, ECoG and MEG signals. In: Dornhege G, Millán JdR, Hinterberger T, McFarland DJ, and Müller K-R (Eds.), Towards Brain-Computer Interfacing. MIT Press, Cambridge, MA, 2006. In press.

[2] Koles ZJ, Lazar MS, and Zhou SZ. Spatial patterns underlying population differences in the background EEG. Brain Topography, 1990; 2(4): 275–284.

[3] Wang Y, Berg P, Scherg M. Common spatial subspace decomposition applied to analysis of brain responses under multiple task conditions: a simulation study. Clin Neurophysiol, 1999; 110(4): 604–614.

[4] Lemm S, Blankertz B, Curio G, and Müller K-R. Spatio-spectral filters for robust classification of single trial EEG. IEEE Transactions on Biomedical Engineering, 2004; 52(9): 993–1002.

[5] Dornhege G, Blankertz B, Krauledat M, Losch F, Curio G, and Müller K-R. Optimizing spatiotemporal filters for improving brain-computer interfacing. In: Weiss Y, Schölkopf B, and Platt J (Eds.), Advances in Neural Information Processing Systems 18. MIT Press, Cambridge, MA, 2006.

[6] Bishop CM. Neural Networks for Pattern Recognition. Oxford University Press, 1995.

HIGH FREQUENCY BANDS AND ESTIMATED LOCAL FIELD POTENTIALS TO IMPROVE SINGLE-TRIAL CLASSIFICATION OF ELECTROENCEPHALOGRAPHIC SIGNALS

P. W. Ferrez[1], F. Galán Moles[1], A. Buttfield[1],
S. L. Gonzalez Andino[2], R. Grave de Peralta Menendez[2], J. del R. Millán[1]

[1]IDIAP Research Institute, Martigny, Switzerland
[2]Neurology Department, Geneva University Hospital, Switzerland
E-mail: pierre.ferrez@idiap.ch

SUMMARY: Non-invasive brain-computer interfaces are traditionally based on slow, mu or beta rhythms. However, there is mounting evidence that neural oscillations up to 200 Hz play important roles in processes such as attention, perception, motor action and conscious experience. In this preliminary study we propose to extend the investigations to the complete frequency spectrum and to compare the high frequency bands with the usual low frequencies. It appears that the 70–130 Hz band and the 170–230 Hz band performs better than the traditional 2–40 Hz band. In a second step we applied the same analysis to the estimated local field potentials from the scalp EEG. The same frequency bands show the best performances, and the use of eLFP leads to an increase of performances of ∼5 %.

INTRODUCTION

Recent experiments have shown the possibility of using the brain's electric activity to directly control the movement of robots or prosthetic devices in real time [1, 2, 3]. For humans, non-invasive methods based on electroencephalogram (EEG) are preferable because of ethical concerns and medical risks and it's widely hypothesized that EEG signals could form the basis of a brain-computer interface (BCI) in order to provide an alternative communication channel to paralyzed people.

Non-invasive BCIs can be classified according to the electrophysiological signal they use. With some systems the subject learns to modulate the amplitude of mu (8–12 Hz) or beta (16–26 Hz) rhythms [4], while some other systems use slow cortical potentials [5] or the P300 event-related potentials [6]. However, there is mounting evidence that neural oscillations play important roles in processes such as attention and motor action. Recent studies in rats and cats report a correlation between neural oscillations above 100 Hz and extending up to 200 Hz with attentive exploration and visual processing [7]. While human electrophysiology has consistently investigated the functional role of gamma band oscillations, the range of frequencies above 80 Hz remains largely unexplored.

The basic question addressed in this paper is to investigate the potential use of high frequency bands to improve performance and accuracy of a BCI. Therefore we enlarged our investigations to the complete frequency spectrum and we compared the performances of different frequency bands. Furthermore, we also used the previously introduced non-invasive estimation of local field potentials (eLFP) in the whole human brain from the scalp EEG using recently developed distributed linear inverse solution termed ELECTRA [8].

MATERIALS AND METHODS

We recorded scalp EEG from four healthy volunteers (25–31 years, 2 women) performing three different mental tasks. The mental tasks were: imagination of left arm movement, imagination of right arm movement and word association. Subjects had no prior BCI training and did not receive online feedback in order not to bias performance towards any kind of preselected features (i. e. frequency bands or scalp EEG vs. eLFP). Subjects were asked to fixate a central white point and to perform the mental task associated to the visual stimulus that appeared 1.5 s later. In a trial, subjects performed a single task for 5.5 s but, for the analysis of the signals, we rejected the first 1.5 s to avoid the presence of evoked potentials associated to the appearance of the visual stimulus. Each subject performed 15 sessions on 2 different days, one session consisting of 18 trials with a random delay of about 2.5 s in between each single trial.

EEG potentials were recorded at 512 Hz with 64 electrodes covering the whole scalp. For both scalp EEG and eLFP analysis, samples were computed 16 times per second. A sample consisted of the power spectrum density, computed over the last second, at a given frequency for a number of channels. We chose 15 bands of variable resolution (higher at low frequencies and bands of 20 Hz above 50 Hz): 2–6 Hz, 8–14 Hz, 16–24 Hz, 26–36 Hz, 38–48 Hz, 52–70 Hz, 72–90 Hz . . . 232–250 Hz. Feature selection was then performed for both scalp EEG and eLFP analysis using a variant of the Relief method, which has been successfully applied to the selection of relevant features for a BCI [8]. We applied this method to select the 10 most relevant EEG electrodes out of 64 and the 100 most relevant voxels out of 4024 in the 3D reconstruction of the brain activity.

Each single sample (48 in each trial) was finally fed to a Gaussian classifier [4] for the recognition of the mental task executed by the subject. The output of this statistical classifier is an estimation of the posterior class probability distribution for a sample, i. e. the probabilities that the input vector belongs to one of the three classes.

For each subject, the 30 sessions were split into 6 groups of 5 consecutive sessions each. For each frequency band we performed the feature selection and trained a classifier using the 5 sessions of a group and we evaluated the performance of this classifier on the 5 sessions of the following group.

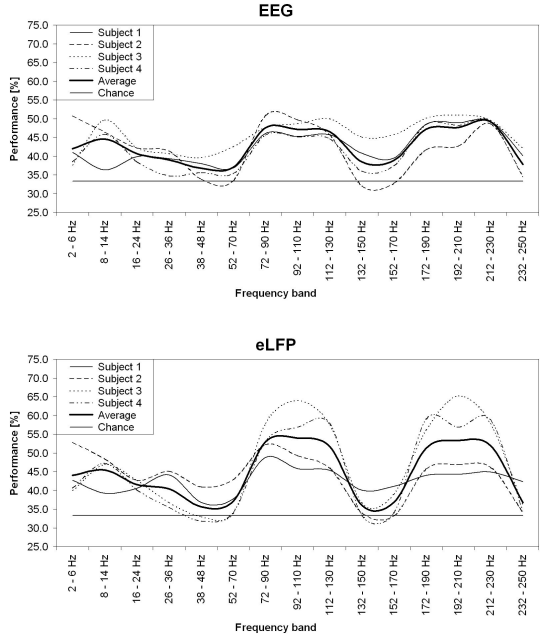

Figure 1: Average of the classification performances for the four subjects plus the average of them using EEG signals and estimated local field potentials for a 3-class BCI. In both cases we can see an increase in performances between 70 and 130 Hz as well as between 170 and 230 Hz compared to the traditionally used 2–40 Hz band. Furthermore, the use of eLFP leads to an increase of performances of $\sim$5 %

RESULTS

Figure 1 shows the average performance for the four subjects plus the average of them for each frequency band using scalp EEG (top) and eLFP (bottom). For both scalp EEG and eLFP, the best performances are reached for frequencies between 70 and 130 Hz and between 170 and 230 Hz. The peak average performance is 49.2 % for the scalp EEG and 54.0 % for the eLFP. The high frequency bands perform better than the traditional low frequencies (49.2 % vs. 44.6 % for scalp EEG and 54.0 % vs. 45.5 % for eLFP). Furthermore eLFP outperform scalp EEG for all discriminant frequency bands.

In the case of scalp EEG, the selected electrodes are outside the midline and cover also the anterio-frontal areas as expected. Regarding the selected voxels, there are 3 clear clusters in the sensorimotor cortex and the right anterior area.

DISCUSSION

The reported results suggest that high frequency bands carry information that is useful for the classification of mental tasks in a BCI context. Frequencies between 70 and 130 Hz and between 170 and 230 Hz outperformed the traditional 2–40 Hz band. Furthermore, the use of eLFP lead to an increase of performances of $\sim$ 5 %. Performances are not very high for a 3-class BCI, but it should be noticed that we have tried to classify every single sample computed every 62.5 ms and that subjects had no prior BCI training and did not receive any feedback. The combination of several frequency bands could also lead to significantly higher performances. The next important step consists in the online verification of the reported improvements by integration of both high frequencies and eLFP into the BCI.

ACKNOWLEDGMENTS

This work is supported by the Swiss National Science Foundation NCCR “IM2” and by the European IST Programme FET Project FP6-003758.

REFERENCES

[1] Carmena JM et al. Learning to control a brain-machine interface for reaching and grasping by primates. PLoS Biol, 2003; 1(2): 193–208.

[2] Pfurtscheller G, Neuper C. Motor imagery and direct brain-computer communication. Proc of the IEEE, 2001; 89: 1123–1134.

[3] Millán JdR et al. Non-invasive brain-actuated control of a mobile robot by human EEG. IEEE Trans Biomed Eng, 2004; 51: 1026–1033.

[4] Wolpaw JR et al. Brain-computer interfaces for communication and control. Clin Neuro, 2002; 113: 767–791.

[5] Birbaumer N et al. The thought translation device (TTD) for completely paralyzed patients. IEEE Trans Rehab Eng, 2000; 8: 190–193.

[6] Farwell LA and Donchin E. Talking off the top off your head: Toward a mental prosthesis utilizing event-related brain potentials. Electroenchephalogr Clin Neurophysiol, 1988; 70: 510–523.

[7] Siegel M and Konig P. A functional gamma-band defined by stimulus-dependent synchronization in area 18 of awake behaving cats. J Neuroscience, 2003; 23: 4251–4260.

[8] Grave de Peralta R et al. Non-invasive estimation of local field potentials for neuroprosthesis control. Cogn Process, 2005; 6: 59–64.

PHASE SYNCHRONISATION IN MEG FOR BRAIN-COMPUTER INTERFACES

M. Bensch[1], W. Rosenstiel[1], M. Bogdan[1,2]

[1]Department of Computer Engineering, Eberhard-Karls-Universität Tübingen, Tübingen, Germany
[2]Department of Computer Engineering, Universität Leipzig, Leipzig, Germany
E-mail: bensch@informatik.uni-tuebingen.de

SUMMARY: We present offline results for classification accuracy based on synchronisation features from MEG and compare these to the more well-known autoregressive (AR) coefficients.

INTRODUCTION

This paper aims to show that phase synchronisation features can be used successfully in Brain-Computer Interfaces (BCI) based on magnetoencephalography (MEG). While the MEG is not portable, short preparation time, high spatial resolution and signal quality make it simple to test new algorithms. This can increase motivation for patients who are still mobile.
Phase synchronisation has been associated with mental tasks previously [1]. Results in the field of BCIs based on EEG have been published by Gysels et al. [2] and others. Gysels found that synchronisation measures combined with the classical power spectral density (PSD) estimates can lead to improved results compared to using one measure only. Due to synchrony being a measure for channel *pairs*, n channels result in $O(n^2)$ features, making feature selection a vital ingredient for the high number of MEG channels.
In an offline analysis, we compare synchronisation features to the AR (model order 2) results to be found in Lal et al. [3]. We use the same data and feature selection methods as in their experiment to foster a fair comparison. A combination of different feature types is also examined.

MATERIALS AND METHODS

Experimental setup: MEG signals of 10 healthy subjects ($\mathcal{A}$ – $\mathcal{J}$) were recorded at 625 Hz from 150 channels. The task was imagined left little finger or tongue movement. The cue duration was 500 ms. The classification interval began after a further 500 ms and lasted for 3 s. Please see [3] for further details.
Preprocessing: To enable a comparison with the findings in [2], we employ similar preprocessing. However, we investigate 3 frequency bands: 8–16 Hz and 16–24 Hz (known to be linked to motor tasks) and 8–40 Hz which encompasses the most relevant frequencies. These bands are extracted by applying a linear phase FIR bandpass filter to the signal.
The phase locking value (PLV) characterising the stability of phase differences between two channels is calculated as follows:

$$PLV = \left| < e^{j\Delta\varphi(t)} > \right| \qquad (1)$$

where $\Delta\varphi(t)$ is the phase difference of two signals at time t. We calculate the instantaneous phase by Hilbert transform [4]. The operator $< . >$ returns the average PLV for a given time window. We use 3 non-overlapping time windows, 1 s each.
Spectral coherence characterising the linear dependence of two channels in a given frequency band f is calculated as follows:

$$\gamma^2_{XY}(f) = \frac{|< C_{XY}(f) >|^2}{< C_{XX}(f) >< C_{YY}(f) >} \qquad (2)$$

where $C_{XY}(f)$ is the cross-power spectrum between two signals $x(t)$ and $y(t)$ at a given frequency band f and $C_{XX}(f)$ is the autospectrum.
We concentrate on the central 75 MEG channels (2775 features) to speed up calculations and to avoid artifacts, which are usually prevalent on the outer sensors. Per trial we obtain 3 frequency bands and 3 time windows. By ROC inspection, we found that the 8–40 Hz frequency band is best for most subjects. The following results are shown for this frequency band. The most discriminative time window varied across subjects.

RESULTS

The error estimation method we use (nested cross-validation), employing a linear SVM and Recursive Feature Elimination (RFE), is explained in [3]. The high amount of features forced us to reduce the number of outer cross-validation folds from 50 to 20. We also use a fast RFE initially discarding 50 % of the features per iteration, which might have a slight negative influence on the α error estimate (Table 1). This estimate is for the number of selected features with a deviation of no more than two standard errors from the lowest error estimate during the cross-validation.

Table 1: Results for 8–40 Hz PLV features

Sub.	α-Estimate	All Features	Nr Feat.
$\mathcal{A}$	0.301 ± 0.077	0.322 ± 0.049	7 ± 16.4
$\mathcal{B}$	0.351 ± 0.101	0.374 ± 0.055	2 ± 2.3
$\mathcal{C}$	0.477 ± 0.062	0.416 ± 0.075	11 ± 13
$\mathcal{D}$	0.140 ± 0.052	0.121 ± 0.047	4 ± 2.7
$\mathcal{E}$	0.443 ± 0.087	0.378 ± 0.072	4 ± 4.9
$\mathcal{F}$	0.374 ± 0.061	0.275 ± 0.071	8 ± 6.6
$\mathcal{G}$	0.397 ± 0.061	0.349 ± 0.070	6 ± 6.6
$\mathcal{H}$	0.210 ± 0.061	0.220 ± 0.037	1 ± 0.8
$\mathcal{I}$	0.338 ± 0.079	0.349 ± 0.052	5 ± 3.3
$\mathcal{J}$	0.481 ± 0.068	0.401 ± 0.063	7 ± 9.8
Ø	0.351 ± 0.111	0.321 ± 0.091	6 ± 6.6

The number of selected features used for the α-estimate is displayed in the third column of Table 1. For each subject, accuracy for the best time window is shown.

Table 2: Results for 8–40 Hz PLV+AR features

Sub.	α-Estimate	All Features	Nr Feat.
$\mathcal{A}$	0.230 ± 0.057	0.245 ± 0.061	8 ± 11
$\mathcal{B}$	0.314 ± 0.080	0.345 ± 0.069	5 ± 9.6
$\mathcal{C}$	0.531 ± 0.072	0.461 ± 0.061	5 ± 6.3
$\mathcal{D}$	0.046 ± 0.034	0.041 ± 0.026	14 ± 7.4
$\mathcal{E}$	0.370 ± 0.071	0.326 ± 0.048	9 ± 8.0
$\mathcal{F}$	0.244 ± 0.076	0.208 ± 0.054	2 ± 1.8
$\mathcal{G}$	0.305 ± 0.092	0.229 ± 0.086	13 ± 13
$\mathcal{H}$	0.168 ± 0.072	0.213 ± 0.058	2 ± 0.7
$\mathcal{I}$	0.365 ± 0.066	0.292 ± 0.064	10 ± 9.8
$\mathcal{J}$	0.480 ± 0.065	0.453 ± 0.063	14 ± 21
$\emptyset$	0.305 ± 0.143	0.281 ± 0.125	8 ± 9.0

Results for the combination PLV+AR features show an improvement over the accuracies for a single feature type (Table 2). This result includes PLV features from all time windows ($2775 \cdot 3$ PLV + $150 \cdot 2$ AR features). Note that we do not group the AR features channel-wise as in [3].
A comparison of PLV, coherence (Coh), AR and PLV+AR is shown in Figure 1.

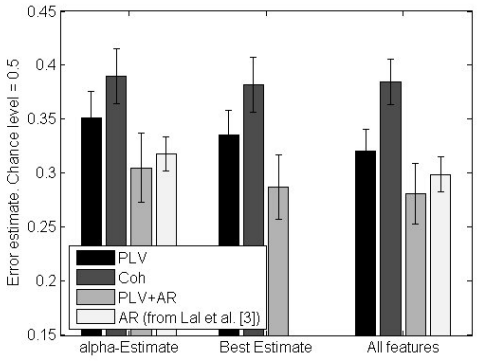

Figure 1: Comparison of 3 error estimation methods for 4 feature types

DISCUSSION
PLV features are better than Coh features, which is consistent with the findings in [2]. Although PLV+AR has the lowest error, the difference between PLV+AR and AR is not significant. The average number of features was reduced to 8 by RFE, increasing the mean error by less than 3 %.

CONCLUSION
Our offline results propose that synchronisation features could become a valuable addition to MEG BCIs. Cross-validation results suggest that some subjects would significantly benefit from using the PLV+AR combination instead of AR alone. Future work will concentrate on the combination of synchronisation features with other well-known features such as PSD.

ACKNOWLEDGEMENTS
Thanks to Jeremy Hill for software and Thomas Navin Lal and Michael Schröder for their error estimation code and helpful discussions.

REFERENCES

[1] Rodriguez E, George N, Lachaux JP, Martinerie J, Renault B, Varela FJ. Perception's shadow: long-distance synchronization of human brain activity. Nature, 1999; 397: 430–433.

[2] Gysels E, Celka P. Phase synchronisation for the recognition of mental tasks in a brain computer interface. IEEE Trans Neural Syst Rehab Eng, 2004; 12(4): 406–415.

[3] Lal TN, Schröder M, Hill J, Preissl H, Hinterberger T, Mellinger J, et al. A Brain Computer Interface with Online Feedback based on Magnetoencephalography. De Raedt, L, Wrobel S (Ed.). Proc of the 22nd Int Conf on Machine Learning, 2005; 465–472.

[4] Le Van Quyen M, Foucher J, Lachaux J, Rodriguez E, Lutz A, Martinerie J, et al. Comparison of Hilbert transform and wavelet methods for the analysis of neural synchrony. J Neurosci Methods, 2001; 111: 83–98.

TIME-DEPENDENT DEMIXING OF TASK-RELEVANT EEG SOURCES

N. J. Hill, J. Farquhar, T. N. Lal, B. Schölkopf

Max Planck Institute for Biological Cybernetics, Tübingen, Germany
E-mail: jez@tuebingen.mpg.de

SUMMARY: Given a spatial filtering algorithm that has allowed us to identify task-relevant EEG sources, we present a simple approach for monitoring the activity of these sources while remaining relatively robust to changes in other (task-irrelevant) brain activity. The idea is to keep spatial *patterns* fixed rather than spatial filters, when transferring from training to test sessions or from one time window to another. We show that a fixed spatial pattern (FSP) approach, using a moving-window estimate of signal covariances, can be more robust to non-stationarity than a fixed spatial filter (FSF) approach.

INTRODUCTION

Since EEG data are highly spatially blurred, it is often beneficial to apply a *spatial filtering* algorithm such as Independent Component Analysis (ICA) or the Common Spatial Pattern (CSP) method. Either method may return a (let's assume, square) matrix W such that sources S are estimated from data matrix X (s sensors by t time samples) by premultiplication $\mathrm{S} = \mathrm{WX}$. Each row of W gives us a *spatial filter*, i. e. a vector of sensor weightings for estimating one source signal. We refer to the columns of the mixing matrix $\mathrm{A} = \mathrm{W}^{-1}$ as *spatial patterns*: each one shows, for a given source, that source's relative amplitude as received at the s different sensors.

It is common practice to obtain spatial filters on one set of data X_1 (computing W from the training trials only, using ICA or CSP), infer which sources are relevant to the task, and then apply the corresponding rows of W to some new test data X_2 (perhaps from a subsequent feedback session). A potential drawback is that an optimized spatial filter can only be guaranteed to remain optimal for estimating a given source as long as the spatial patterns of the *other* sources remain constant: changing any column of A may easily affect *all* rows of A^{-1}. So a spatial filter optimized for listening to a particular part of the motor cortex in the presence of, say, prominent frontal-cortex activity may look different from a spatial filter optimized for listening to the same source in the presence of prominent occipital activity. It seems reasonable to hypothesize that, over the course of a motor-imagery BCI experiment, the spatial patterns for relevant sources will change relatively little (we will assume that the positions of the sources in the motor cortex, and the spectral content of the signals they generate, are relatively constant). By contrast we might expect the spatial patterns in the rest of the decomposition to change more significantly, particularly in transfer between training and feedback sessions (when conditions of visual stimulation and general arousal change), but also perhaps with regard to other factors like tiredness, hunger, thirst or cognitive activity. For this reason, we outline a simple approach based on fixed spatial patterns (FSP) rather than fixed spatial filters (FSF).

FIXED SPATIAL PATTERN (FSP) DEMIXING

Both ICA and CSP can be seen as performing a *whitening* or decorrelation, followed by a rotation, in the s-dimensional space of sensors:

$$\begin{array}{rcccl} \mathrm{S} & = & \mathrm{WX} & = & \mathrm{RPX} \\ \mathrm{X} & = & \mathrm{AS} & = & \mathrm{P}^{-1}\mathrm{R}^{-1}\mathrm{S}. \end{array}$$

The whitening matrix P can be any matrix such that $\mathrm{P}^\top\mathrm{P} = \Sigma^{-1}$, where Σ is the sensor covariance matrix. The rotation matrix R is optimized according to some criterion (class difference in projected variance for CSP, independence of outputs for ICA). Let us assume that we have used one of these methods to estimate P_1 and R_1 from training data X_1, and have partitioned the mixing matrix A_1 into two sets of columns, $\mathrm{A}_1 = \left[\mathrm{A}_1^{[r]} : \mathrm{A}_1^{[i]}\right]$ corresponding to the task-relevant and irrelevant sources respectively. We then observe test data X_2 and estimate a new P_2 from it. We now want a new R_2 that will best separate our sources, but under the constraint that the relevant columns of the resulting A_2 be the same as they were in A_1.

As in the spatially constrained ICA (SCICA) approach described in [1], we partition R_2^{-1} into constrained and unconstrained columns, $[\mathrm{C} : \mathrm{U}]$. The FSP constraint gives us $\mathrm{C} = \mathrm{P}_2\mathrm{A}_1^{[r]}$. Since it is unlikely that $\mathrm{P}_1 = \mathrm{P}_2$, we cannot assume that columns C are orthonormal. However, like [1] we will assume that C and U occupy orthogonal subspaces. This allows us to write R_2 as a vertical concatenation of pseudoinverses, to obtain:

$$\mathrm{W}_2 = \mathrm{R}_2\mathrm{P}_2 = [\mathrm{C} : \mathrm{U}]^{-1}\mathrm{P}_2 = \left[\begin{array}{c} (\mathrm{C}^\top\mathrm{C})^{-1}\mathrm{C}^\top \\ (\mathrm{U}^\top\mathrm{U})^{-1}\mathrm{U}^\top \end{array}\right]\mathrm{P}_2.$$

If, like [1, 2], we were using this technique to correct the EEG for *artifacts* with known spatial patterns $\mathrm{A}_1^{[r]}$, we would then have to proceed to optimize the U (making the further assumption that columns U are orthonormal) in order to estimate the remaining sources. However, since we have already decided that the remaining sources are irrelevant, we can ignore the lower rows of W_2 and hence U. Substituting for C, we obtain:

$$\mathrm{W}_2^{[r]} = (\mathrm{A}_1^{[r]\top}\Sigma_2^{-1}\mathrm{A}_1^{[r]})^{-1}\mathrm{A}_1^{[r]\top}\Sigma_2^{-1} \qquad (1)$$

This simple formula requires only the fixed spatial patterns $\mathrm{A}_1^{[r]}$ and a new estimate Σ_2 of the covariance of

the sensor signals from which we want to extract the corresponding sources.

DEMONSTRATION

We present a preliminary illustration that this approach can make motor-imagery BCI classification more robust to changes in task-irrelevant brain activity. We use 7 two-class data sets. The first is the 118-channel EEG dataset IVc from BCI Competition III: we took the 500–1500 msec interval of each trial in both training and test set, with the 0 class removed, resulting in 210 training trials and 280 test trials of left-hand/foot motor imagery. The other 6 are imagined left/right hand movement data sets from our lab, each consisting of 400 trials of 39-channel EEG. We use the first 200 as training and the second 200 as test points.

First, we perform ordinary CSP on the training trials with a wide-band (7–30 Hz) temporal filter. We invert the full s-by-s filter matrix and keep the first 4 and last 4 spatial patterns as our $\mathrm{A}_1^{[r]}$. Next, we track the activity of the sources associated with these 8 patterns throughout the whole data set (training and test trials). For each trial i, we obtain spatial filters W_i using equation (1) with a moving estimate of the covariance: each Σ_i is obtained from the last n trials including the current one, i. e. trials $(i-n+1)\ldots i$. After applying the spatial filter, we compute the log amplitude spectrum using the Welch's short-time Fourier transform method. We then normalize the vector of amplitude features for each trial and source. Using this feature set, we then classify using a linear Support Vector Machine, finding the regularization parameter by 10-fold cross-validation within the training set.

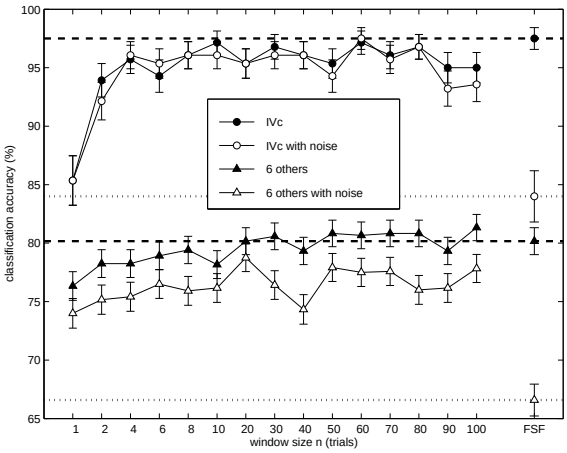

Figure 1: Performance of FSP and FSF methods

The one hyperparameter that needs to be set is the size of the moving window, n. In practice this could be found by cross-validation, or perhaps by adding a known artificial signal to the data, in a known artificial spatial pattern, and empirically determining the value of n that allows it to be recovered most accurately. Here, we simply present the results for each of a range of values, to see its effect on test set performance.

In Figure 1, filled symbols show the results for data set IVc (circles) and for the average of the 6 subjects in the other study (triangles)—the individual subject results were broadly consistent with the average, but we do not have space to show them individually here. The dashed lines show, for comparison, the performance of a fixed spatial *filter* approach analogous to ordinary CSP-based methods: the W_i were simply the original filters found using the training trials, held constant for all trials. We can see that, for a sufficient window size, say $n \geq 20$, the moving-window FSP approach does not perform significantly better or worse than the FSF approach.

At this preliminary stage we cannot say whether the algorithm is not sensitive enough to non-stationarities in the data to improve performance, or whether these particular data sets do not suffer from a significant non-stationarity problem in the first place (our six data sets were all single-session without feedback). However, we can demonstrate the moving-window FSP approach's robustness to non-stationarity by *introducing* non-stationarity into the data. In a second set of tests, we added two Gaussian noise sources to the test trials only. This introduces a difference in the training and test distributions, resulting in clear problems for the FSF method (dotted lines). Both artificial noise sources had fixed spatial patterns (chosen randomly), but their amplitudes drifted over time: one increased linearly from $a/2$ to $2a$ over the course of the entire test set, and the other decreased from $2a$ down to $a/2$, with a chosen such that the FSF method suffered about a 10–15 % degradation in performance. Open symbols show performance on the noisy data. Comparison of the filled and open symbols shows that the introduction of non-stationary noise into the test set did not greatly affect the moving-window FSP method's performance (hardly at all for some subjects, like IVc), and hence it performed better than the FSF approach for nearly all values of n. This suggests that it is a promising candidate for dealing with non-stationarities in EEG data, although a wider range of data sets will be required in order to see whether it is effective at coping with the kind of non-stationarities that occur in reality.

REFERENCES

[1] Hesse CW, James CJ. The FastICA algorithm with spatial constraints. IEEE Sig Proc, Letters, 2005; 12: 792-795.

[2] Ille N, Berg P, Scherg M. Artifact correction of the ongoing EEG using spatial filters based on artifact and brain signal topographies. J Clin Neurophysiol, 2002; 19(2): 113-124.

AN ITERATIVE ALGORITHM FOR SPATIO-TEMPORAL FILTER OPTIMIZATION

R. Tomioka[1,2], G. Dornhege[2], K. Aihara[1], K.-R. Müller[2]

[1]Dept. Mathematical Informatics, IST, The University of Tokyo, Japan
[2]Fraunhofer FIRST.IDA, Berlin, Germany
E-mail: ryotat@first.fhg.de

SUMMARY: We propose a simultaneous spatio-temporal filter optimization algorithm for the single trial electroencephalography (EEG) classification problem. The algorithm is a generalization of the Common Spatial Pattern (CSP) algorithm, which incorporates non-homogeneous weighting of the cross-spectrum matrices. The spectral weighting coefficients and the spatial filter are alternately updated. The validation results on 162 motor-imagery BCI datasets show that the proposed method outperforms wide-band filtered CSP in most datasets and gives comparable accuracy to Common Sparse Spectral Spatial Pattern (CSSSP) with far less computational cost. The proposed method is highly interpretable and modular at the same time because the temporal filter is parameterized in the spectral domain.

INTRODUCTION

A Common Spatial Pattern (CSP) [1] based classifiers for the motor-imagery BCI system has been successful in extracting subject specific discriminative spatial patterns. However, the problem of choosing the temporal filter or the spectral band on which CSP works has not been fully investigated in spite of recent efforts [2, 3].

We propose a novel simultaneous spatio-spectral filter optimization technique and compare the classification accuracy on 162 motor-imagery BCI datasets with three conventional techniques, namely, Common Spatial Pattern (CSP) [1], Common Spatio Spectral Pattern (CSSP) [2], Common Sparse Spectral Spatial Pattern (CSSSP) [3].

MATERIALS

We use 162 datasets of motor-imagery BCI experiment from 29 healthy subjects. Each dataset contains EEG signal recorded during 200-400 trials of one of the pairwise combinations of three motor imagination tasks, namely right hand (R), left hand (L) or foot (F) (see [3] for the detail).

METHODS

Preprocessing: We band-pass filter the signal from 7–30 Hz and cut out the interval of 500–3500 ms after the appearance of the visual cue on the screen from the continuous EEG signal for each trial of imaginary movement.

Spatio-spectral filter: Let us denote by $X \in \mathbb{R}^{d\times T}$ the EEG signal of a single trial of imaginary motor movement, where d is the number of electrodes and T is the number of sampled time-points in a trial. We consider a binary classification problem where each class, e. g. right or left hand imaginary movement, is called positive (+) or negative (−) class. The task is to predict the class label for a single trial X.

In this paper, we use a feature vector, namely *log-variance feature*, defined as follows:

$$\phi_j(X;\boldsymbol{w}_j,\boldsymbol{\alpha}^{(j)}) = \log\sum_{k=1}^{T}\alpha_k^{(j)}\boldsymbol{w}_j^T V_k \boldsymbol{w}_j \qquad (1)$$
$$(j=1,\ldots,J),$$

where $\boldsymbol{w}_j \in \mathbb{R}^d$ is a spatial projection that projects the signal into a single dimension, $\boldsymbol{\alpha}^{(j)} = \left\{\alpha_k^{(j)}\right\}_{k=1}^{T}$ is the spectrum of the temporal filter, which is homogeneous ($\alpha_k = 1\ \forall k$) in the case of conventional CSP algorithm, and $V_k := \hat{\boldsymbol{x}}_k\hat{\boldsymbol{x}}_k^\dagger \in \mathbb{C}^{d\times d}\,(k=1,\ldots,T)$ are the cross-spectrum matrices. The training of a classifier is composed of two steps. In the first step, the coefficients $\boldsymbol{w}_j$ and $\boldsymbol{\alpha}^{(j)}$ are optimized. In the second step, the Linear Discriminant Analysis (LDA) classifier is trained on the feature vector.

Since the covariance matrix of the temporally filtered signal can be written as $V(\boldsymbol{\alpha}) := \sum_{k=1}^{T}\alpha_k V_k$, we solve the following problem for the optimization of the spatial projection (angled brackets $\langle\cdot\rangle^c$ denote expectation within a class $c \in \{+,-\}$):

$$\max_{\boldsymbol{w}\in\mathbb{R}^d} \quad \frac{\boldsymbol{w}^T\langle V(\boldsymbol{\alpha})\rangle^+\boldsymbol{w}}{\boldsymbol{w}^T\langle V(\boldsymbol{\alpha})\rangle^-\boldsymbol{w}}$$

Writing the spectrum of the spatially projected signal as $\{s_k(\boldsymbol{w})\}_{k=1}^{T}$, we set the spectral coefficients $\boldsymbol{\alpha} = \{\alpha_k\}_{k=1}^{T}$ as follows:

$$\alpha_k \propto \begin{cases} \frac{\left(s_k^{(+)}-s_k^{(-)}\right)\left(s_k^{(+)}+s_k^{(-)}\right)}{v_k^{(+)}+v_k^{(-)}} & \text{if } s_k^{(+)}-s_k^{(-)}>0 \\ & \text{and } k\in I_{[7,30]}, \\ 0 & \text{otherwise,} \end{cases}$$

where $I_{[7,30]}$ is the set of DFT indices corresponding to 7–30 Hz, and the following short hands are used: $s_k^{(c)} := \langle s_k(\boldsymbol{w})\rangle^c$ and $v_k^{(c)} := \mathrm{Var}\left[s_k(\boldsymbol{w})\right]^c$.

Since both the spatial projection and the spectral coefficients depend on the other, we alternately update them starting from a CSP with homogeneous spectral filter. The process is illustrated in Figure 1.

RESULTS

Figure 2 shows the improvements in the 10×10 cross-validation error by iteratively updating spatio spectral filter for six subjects. We use the log-variance feature (1) with $n_{\mathrm{of}} = 3$ features for each class and LDA as a

classifier. The odd steps correspond to the spatial projection updates; the even steps are spectral updates. Although major improvements were often observed at the second step (spectral update), further improvements were also observed after the third step (CSP recalculation). For some subjects (e. g. in subject F) systematic increases in the cross-validation errors were observed.

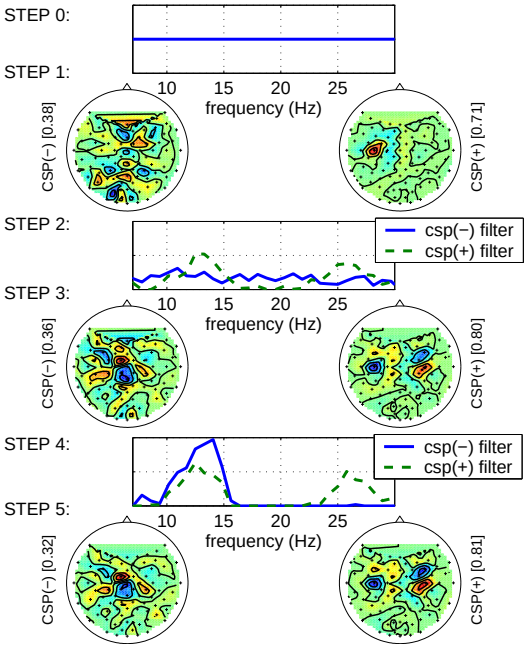

Figure 1: The topographical pattern of the CSP projection and the spectrum of the filter are shown for each step of iteration for a Left (−) vs. Foot (+) dataset. The iteration starts from a homogeneous spectral filter (step 0) and the spatial projection and spectral filter are updated alternately (step 1–5). Note that although we use $n_{\mathrm{of}} = 3$ features for each class, only the top patterns are shown here for the visualization purpose.

Table 1: The 25 %-tile point, the median, and the 75 %-tile point of chronological test errors over 162 datasets are shown for CSP, CSSP, CSSSP, and the proposed method.

	CSP (7–30 Hz)	CSSP	CSSSP	proposed (20 steps)
25 %-tile	10.6	6.67	7.00	8.00
median	23.8	21.1	21.0	19.7
75 %-tile	35.8	33.6	36.4	35.3

Table 1 shows the comparison of test errors of four algorithms, namely CSP [1], CSSP [2], CSSSP [3], and the proposed method. Here, the validation was done in the chronological manner, i. e. all methods were trained on the first half of the samples and applied on the remaining half. The time-lag parameter τ for CSSP and the regularization constant C for CSSSP were chosen by cross validation on the training set (see [2, 3]).

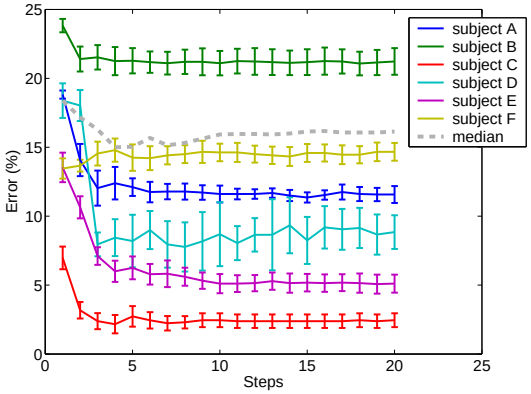

Figure 2: The cross-validation error at each step of iteration is shown for six subjects. The median over 162 datasets is also shown (dashed line). The odd steps and the even steps correspond to spatial projection updates and the spectral filter updates, respectively. Note that the first step is the CSP with white spectral filter over 7–30 Hz.

CONCLUSION

We have proposed a spatio-spectral filter optimization algorithm for the single trial EEG classification problem; the method is based on iterative updates of spectrally weighted CSP and the spectral coefficients. The validation results on 162 BCI datasets show that the proposed method outperforms wide-band filtered CSP [1] and gives comparable results with CSSP [2] and CSSSP [3] with far less computational cost.

REFERENCES

[1] Ramoser H, Müller-Gerking J, Pfurtscheller G. Optimal spatial filtering of single trial EEG during imagined hand movement. IEEE Trans Rehab Eng, 2000; 8(4): 441–446.

[2] Lemm S, Blankertz B, Curio G, Müller K-R. Spatio-spectral filters for improved classification of single trial EEG. IEEE Trans Biomed Eng, 2005; 52(9): 1541–1548.

[3] Dornhege G, Blankertz B, Krauledat M, Losch F, Curio G, Müller K-R. Combined optimization of spatial and temporal filters for improving brain-computer interfacing. IEEE Trans Biomed Eng, 2006; accepted.

ACCURATE HAND TRAJECTORY PREDICTION BY REAL AND SYNTHETIC EEG

R. Grave de Peralta Menendez[1], P. Morier[1], J. del R. Millán[2], S. L. Gonzalez Andino[1]

[1]Neurology Department, Geneva University Hospital, 24 Rue Micheli du Crest, 1211 Geneva 14
[2]IDIAP Research Institute. Rue du Simplon 4, 1920 Martigny, Switzerland
E-mail: Rolando.Grave@hcuge.ch

SUMMARY: Non-invasive real-time prediction of hand trajectories by neural signals might allow considerable progress in neuroprosthetic. Here we evaluate the accuracy that can be obtained when fitting and predicting hand trajectories from scalp recorded and synthetic EEG for two different hand movements: 1) elliptic 2D movements and 2) reaching/approaching 3D movements. We show that both, recorded EEG data and synthetic data serve to accurately fit the explored hand trajectories. Indeed, the smooth synthetic data fits the model better than the measured data. A cross-validation procedure was used to predict the hand position coordinates in the second part of the trials after training the model with the initial half. Also here the synthetic EEG data yielded significantly high ($p < 0.0001$) correlations between the predicted and recorded hand trajectories for the 70 % of trials. We conclude that irrespective of the existence of a casual relationship, it is always possible to fit hand trajectories by a multivariate time series of similar frequency content.

INTRODUCTION

Neural signals directly recorded from the cortex of monkeys have been used to accurately drive the 3D movement of robotic arms. Extension of these devices to paralyzed individuals are challenging because of the inherent risks linked to neurosurgery. Besides, the quality of recordings with long-term implanted devices degrades with time. Thus, one might wonder if non-invasive scalp recorded signals are informative enough to allow for predictions of hand trajectories whith the accuracy required to drive neuroprosthetic devices. Some recent results using magnetoencephalography indicate that this might be possible since rather accurate prediction of hand trajectories were obtained in ten subjects from 248 MEG channels.

In mathematical terms, the problem of predicting hand trajectories from neural recordings consists in finding a model in which the hand position coordinates (the dependent variable) are written as a function of the neural activity (independent variable). One widely employed model postulates a linear relationship between the hand position at time t and the past of neural activity (ARX models). A potential risk in this type of models is the so-called overfitting that occurs when the number of independent variables surpasses the number of dependent variables. The danger of overfitting is that good forecasting and model fitting might arise for time series bearing no causal relationship. The purpose of this paper is to illustrate the dangers of overfitting in the problem of predicting 2D and 3D hand trajectories from EEG and synthetic EEG (computer generated EEG).

MATERIALS AND METHODS

Hand Movements: We explored two different types of movements represented in Figure 1: M1 – periodic three dimensional elliptic movements (Figure 1a) and M2 – non-periodic reaching/approaching movements (Figure 1b) in which the subject's hand started from the keyboard, grasped and object from a tray and approached the object to the mouth.

Hand Position (HP) recordings: The 3D hand position coordinates were recorded with a hand position tracking system using a sampling frequency of 130 Hz.

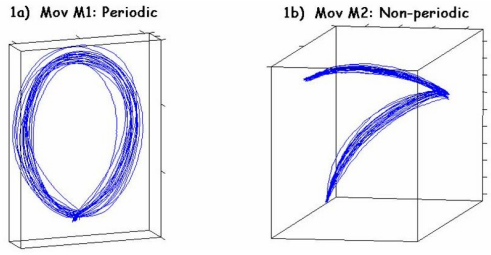

Figure 1: Trajectories recorded with the hand tracking device for periodic and non-periodic movements.

EEG Recordings: The EEG was recorded from 111 scalp electrodes (Electric Geodesic System) using a sampling frequency of 1000 Hz. The EEG was simultaneously recorded with the HP data for the case of movement M1 for 61 trials. A random subset of 20 electrodes was selected for the analysis reported here.

Synthetic EEG data (fEEG) generation: Generated as combinations of sinusoidal waves of random phases.

Data Preprocessing: The differences in sampling frequency between the HP and EEG recordings yield time series of different lengths. We therefore resampled the EEG and HP data using FFT interpolation to obtain time series of 1000 samples length each one. We also discarded the coordinate with the smallest spatial variation for movement M1 after realizing that the movement was essentially planar.

Model: Lets consider the two following multivariate time series: $Y(t)$, the two-dimensional time series describing the hand position coordinates at time t.

$V(t)$ the N-dimensional time series describing the scalp recorded (synthetic) EED data recorded at N scalp electrodes.

A linear relationship between the HP coordinates and the neural activity can be assumed linear and written as:

$$Y(t) = B_1 \cdot V(t) + B_2 \cdot V(t-T) + \ldots + B_m \cdot u(t-mT) + e(t)$$

Where $B_1 \ldots B_m$ are the model coefficients, m is the model order ($m = 10$ here), and $e(t)$ is a noise term.

RESULTS

Movement M1, EEG data, model fitting: The fitting of the model to the 20 randomly selected EEG channels yield to very high correlation coefficients (cc) between the fitted and the measured hand position coordinates (cc x-coordinate = 0.9905, cc y-coordinate = 0.9913).

Movement M1, synthetic data, model fitting: The synthetic data (20 synthetic EEG channels) yield perfect fitting to the hand position data (cc x-coordinate = 1, cc y-coordinate = 1). Figure 2 shows the original and fitted hand trajectories (x-coordinates top panels, y-coordinates lower panels).

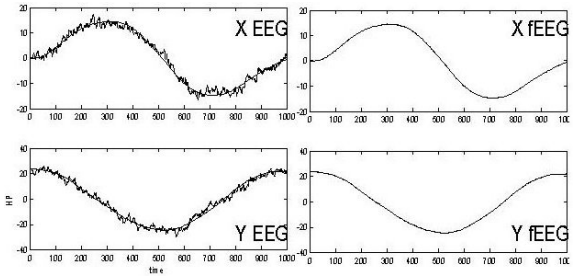

Figure 2: Example of original and fitted hand trajectories using EEG (left) and synthetic EEG (right).

Movement M2, synthetic data, model fitting: The synthetic EEG data also lead to excellent fitting of the non-periodic movement 3D trajectories. Figure 3 shows an example of the fitting for each independent coordinate and the cc values.

Movement M1, synthetic EEG data, hand trajectory forecasting: For prediction we divided the trials (pairs of fEEG and HP data for each performed movement) into two groups: 1) The training group formed by 25 trials and 2) the test group formed by 31 trials. The model was fitted with the training set and then used to predict hand trajectories over the test set. The fictitious EEG data predicted the hand trajectories with correlation values significant at the 0.0001 level in more than the 70 % of the test trial. In the 16 % of the remaining trials one coordinate was correctly predicted. In only the 14 % percent of the test trials were the hand trajectories incorrectly predicted.

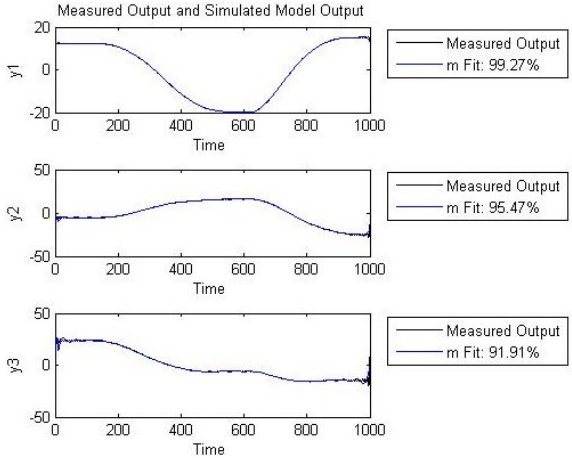

Figure 3: Fitting of non-periodic data using synthetic EEG.

DISCUSSION

The results presented here indicate that hand position trajectories can be better fitted with computer generated data than with recorded EEG data. This effect is due to the existence of oscillations in the EEG data not present in the hand trajectories and is independent of the possible movement artifacts. A perfect fit to the hand trajectories can be obtained for smoothed EEG data. The perfect fitting obtained with computer simulated data is not due to the use of smooth two dimensional periodic movements since, for 3D non-periodic movements, the fitting is also excellent. In this latter case, the lack of periodicity influences the fitting at the beginning and end of the time series. Finally, the forecasting capabilities of the synthetic data are also excellent.

CONCLUSION

Both, neural signals and synthetic signals show excellent capabilities to model 2D and 3D hand trajectories. Synthetic data are able to predict such trajectories with adequate accuracies while bearing absolutely no relationship with the hand position data. These results therefore introduce a note of caution when analyzing experiments in which the number of time series containing the neural data surpasses the dimensions of the hand coordinates. In such cases, it is impossible to decide if the obtained accuracy is due to model overfitting or to actual neurophysiological information contained in the neural data.

ACKNOWLEDGEMENT

Work supported by the SNSF grant 3152A0-100745, the SNSF NCCR "IM2", and the European IST Programme FET Project FP6-003758.

REFERENCES

[1] Chapin JK. Using multi-neuron population recordings for neural prosthetics. Nature Neurosci, 2004; 7: 452–455.

[2] Georgopoulos AP, Langheim JP, Leuthold AC, Merkle AN. Magnetoencephalographic signals predict movement trajectory in space. Experimental Brain Research, 2005; 16: 132–135.

EEG SINGLE-TRIAL CLASSIFICATION OF FOUR CLASSES OF IMAGINARY WRIST MOVEMENTS BASED ON GABOR COEFFICIENTS

A. Vučković, F. Sepulveda

BCI Group, Department for Computer Science, University of Essex, Colchester, UK
E-mail: vuckovic@essex.ac.uk

SUMMARY: The aim of the study was to classify up to four direction distinctive imaginary wrist movements based on single-trial EEG recordings. The algorithm was based on the Gabor transformation for features extraction and recurrent neural networks for classification. Classification rate of four different movements (flexion, extension, pronation and supination) was up to 71.7 % with an average of 62.3 % in all seven subjects. The average classification rate of any three selected movements was 67 % and the average classification rate of any two movements was 79.2 %. Surprisingly, 66 % of the features included in classification belong to the gamma region. This is the first study showing results of classification of such large number of movement classes on a single joint .

INTRODUCTION

Detection of single-trial imaginary movements generally utilizes EEG analysis in space, time and frequency domains. However, current approaches are limited as different classes are mainly related to different limbs [1]. To detect different types of movement for a single limb/joint, the number of classes should increase. However, this is difficult to achieve because the usual spatial information cannot be exploited as the movements to be classified activate the same region of the brain. In this study, we tried to achieve detection of up to four different types of imaginary kinesthetic movements of the right hand.

MATERIALS AND METHODS

Experimental Procedure: Seven healthy right handed volunteers (24.9 ± 2.5) participated in the study. All subjects signed a consent form. Subjects were asked to perform four kinesthetic imaginary right wrist movements: flexion (F), extension (E), pronation (P) and supination (S). All subjects except subject 6 had no experience in similar experiments but were asked to perform a session of real movements prior to the imaginary one. At time $t = 0$ s, a warning sign (a rectangle) appeared on the screen for 0.25 s. At $t = 1$ s, an arrow pointing in one of the following directions was shown: right (F), left (E), up (P), and down (S). The arrow indicated the movement to be executed (letters in parenthesis above). The arrow stayed on for 3 s and for that time the subject was asked to keep the hand in the required position. The time between the arrow's disappearance and the new warning was random, between 5 and 8 s. The order of movements was also random. Each subject performed 60 movements of each type, totaling 240 movements divided in four sessions.

Recording procedure: EEG was recorded using a 64 channel ActiveTwo system (Biosemi-TM) at 256 samples/s. The reference was the right mastoid. EMG was bipolarly recorded from the *flexor carpi radialis* and the *extensor carpi radialis* to check if there was any real movement. Horizontal and vertical EOG were recorded from the right eye as well.

Data Pre-Processing: EOG was removed using independent component analysis (EEGLAB, SCCN). The component containing EOG artifact was removed and EEG was reconstructed from the rest of components, then referenced and filtered (high pass at 0.5 Hz, low pass at 80 Hz, stopband at 50 Hz). Epochs of 5 s were extracted, starting 1 s before the warning and up to 4 s after it. A baseline (50 ms of EEG starting 1 s before the warning) was subtracted from the rest of the epoch. Independent components (IC) were calculated based on epoched EEG. Only 3 s long epochs showing IC while the arrow was on the screen were included in the analysis.

Joint Time-Frequency Analysis: Gabor coefficients (GC) (time window 120 ms, frequency band 2 Hz) were calculated on the independent components. Only GCs corresponding to 8–70 Hz were included in the final analysis. For 64 components and one 3 s epoch, this yielded 49600 coefficients. To find the coefficients that gave the best separation between the four classes, the Davis-Bouldin Index (DBI) [2] was calculated for four groups and two-dimensional variables (real and imaginary part of GC). Five hundred (about 1 %) of the coefficients with the lowest DBI were used for classification with a neural network.

Neural Network Training: A recurrent Elman network was used. Thirty trials of each movement were used for training and the rest were used for classification testing. The input layer consisted of 1000 neurons (500 absolute values and 500 phases values of the chosen GC) plus previous values of the hidden layer, hidden layer had 250 neurons and the output had 4, 3 or 2 neurons, depending on the classification task.

RESULTS

Table 1 shows recognition rates for four different imaginary wrist movements (flexion F, extension E, pronation P and supination S) for all subjects. Table 2 shows the average recognition rate for all subjects for four possible combinations of three different imaginary movements. Table 3 shows an average recognition rate for all subjects for six possible combinations of two imaginary wrist movements.

From the 500 selected best features, 7.3 ± 2.2 % were in the alpha (8–12 Hz) band, 29.0 ± 7.5 % were in the

beta (13–30 Hz) band, 46.4 ± 5.6 % were in the lower gamma (31–50 Hz) band and 20.1 ± 2.0 % were in the higher gamma (51–70 Hz) band.

Table 1: Recognition rate for four imaginary wrist movements for each subject and the average value for all subjects

Subject	F	E	P	S	Average
1	67	83	70	67	71.7
2	68	58	82	65	68.2
3	57	67	70	73	66.7
4	60	63	67	67	64.3
5	63	50	67	57	59.2
6	63	63	43	50	54.7
7	40	43	57	67	51.8
Total Average: 62.3 ± 10.4					

Table 2: Average recognition rate for all subjects for all combinations of three imaginary wrist movements

FEP	66.7 ± 10.9
FES	67.0 ± 13.3
FPS	68.8 ± 8.0
EPS	65.4 ± 13.1
Average	67.0 ± 11.3

Table 3: Average recognition rate for all subjects for all combinations of two imaginary wrist movements

FE	79.0 ± 9.7
FP	80.2 ± 9.2
FS	79.5 ± 7.6
EP	77.4 ± 14
ES	79.9 ± 9.3
PS	79.4 ± 8.7
Average	79.2 ± 9.9

The stopping criteria for network training was a minimum gradient of 10^{-6}, that typically resulted in a mean square error MSE $= 9 \cdot 10^{-8}$. To check for possible overfitting, the MSE was chosen as a stopping criteria. For MSE $= 10^{-3}$, the average recognition rate was 61.8 ± 7.2 and for MSE $= 10^{-5}$ it was 61.7 ± 6.8. Both mean values are worse than the one shown in Table 1. The number of neurons in the hidden layer was also varied. The results, shown in Table 4, don't show any clear trend that would indicate overfitting.

Table 4: Average recognition rate for all subjects as a function of the number of neurons in the hidden layer

50	63.1 ± 2.5
100	59.7 ± 9.0
150	60.1 ± 10.7
200	58.9 ± 9.1
250	62.3 ± 10.4

DISCUSSION

Single trial EEG classification of different types of imaginary movements on the same joint is a difficult task because the spatial distribution of the EEG signals cannot be expected to yield relevant information. Therefore, the analysis has to be focused on time domain and/or frequency analysis. The Gabor Transform is a useful tool because it provides the most precise information about both amplitude and phase and has a fixed time-frequency windows in the whole time-frequency domain.

Similar single-trial studies have been restricted to two class separation problems, such as the classification of intention to generate a shoulder versus elbow torque, with a classification accuracy of 89 % [3]. However, the latter study was performed on only 4 subjects and using 163 electrode EEG. A four class single trial study has been performed to classify imaginary movement in four different limbs [1]. The results of our study: 62.3 % average recognition rate of four movements, 67 % of three movements and 79 % of two movements are encouraging results for the following reasons: a) imaginary movements about the same joint were classified, b) single trial classification c) not previously trained subjects d) no subjectively discarded data and d) only EOG was removed using ICA. Further, the results are from seven subjects, which is a larger number than in most of comparable studies. An interesting result of this study was that 66 % of all GC used for classification belong to gamma band (30–70 Hz). Combinations of left and right wrist imaginary movements could potentially enable separation of eight different classes. In the future, a number of training sessions has to be increased and different types of classifiers have to be applied in order to increase the classification accuracy.

CONCLUSION

Using a time-frequency approach and neural-network based classifier of single trial movements, it was possible to classify four different types of imaginary wrist movements. The most important features for classification of movement were in the gamma band.

ACKNOWLEDGEMENT

This work was supported by the EPSRC (Grant GR/T09903/01).

REFERENCES

[1] Pfurtscheller G, Brunner C, Schlögl A, Lopes da Silva FH. Mu rhythm (de)synchronization and EEG single-trial classification of different motor imagery tasks. NeuroImage, 2006; 11(1): 54–59.

[2] Sepulveda F, Meckes M, Conway BA. Cluster Separation Index Suggests Usefulness of Non-Motor EEG Channels in Detecting Wrist Movement Direction Intention. Proc IEEE ICS 2004, Singapore, 2004; 2: 943–947.

[3] Deng J, Yao J, Dewald JPA. Classification of the intention to generate a shoulder versus elbow torque by means of a time-frequency synthesized spatial patterns BCI algorithm. J Neural Eng, 2005; 2: 131–138.

FEATURE DIMENSIONALITY REDUCTION BY MANIFOLD LEARNING IN BRAIN-COMPUTER INTERFACE DESIGN

J. Q. Gan

BCI Group, Department of Computer Science, University of Essex, Colchester CO4 3SQ, UK
E-mail: jqgan@essex.ac.uk

SUMMARY: Unsupervised manifold learning for dimensionality reduction has drawn much attention in recent years. This paper applies two manifold learning methods for the first time to feature dimensionality reduction in brain-computer interface (BCI) design, and compares them with principal component analysis (PCA) and supervised PCA that is mathematically equivalent to the common spatial patterns (CSP) method. Their abilities to reveal embedded low-dimensional submanifolds or subspaces of high-dimensional BCI data and to preserve or improve the data separability are analysed. Experimental results on asynchronous BCI data from 3 subjects are presented. As the methods are unsupervised, they are particularly suitable for adaptive and asynchronous BCI.

INTRODUCTION

In BCI system design, a well-known problem is how to handle a very large amount of features extracted from multi-channel EEG signals. When the number of extracted features is over hundreds or even thousand, the training of a BCI classifier would be problematic due to the overfitting problem caused by highly noisy BCI data and the lack of representative data in the high-dimensional feature space.

Feature selection is a commonly used approach for solving this problem [7]. Although it offers good interpretation, the dimensionality of the constructed new feature space usually can or has to be further reduced, resulting in better classification performance. Projecting high-dimensional features onto a low-dimensional new feature space is another well-known approach, which can be regarded as high-level feature extraction or feature fusion [2].

This paper investigates on two manifold learning methods [3, 8] for BCI feature dimensionality reduction, and compares their performance with other unsupervised and supervised methods [2, 4]. The focus of investigation will be on whether nonlinear projections can produce better new feature space than linear ones and whether unsupervised approach to BCI feature dimensionality reduction is likely to perform as well as supervised approach or even better.

MANIFOLD LEARNING METHODS

In recent years, unsupervised manifold learning methods have been developed for nonlinear dimensionality reduction, such as Laplacian Eigenmap [1], ISOMAP [9], and locally linear embedding (LLE) [8]. There are four common steps in these methods: 1) computing nearest neighbours of input data, 2) constructing a weighted graph using neighbourhood relations, 3) deriving a matrix based on the graph as an optimal criterion, and 4) producing projected data from the top or bottom eigenvectors of this matrix. The differences among these methods lie in the definitions of the weights and optimal criteria.

Unlike linear projection methods, the results of nonlinear manifold learning methods are projected data themselves rather than projection matrixes or functions. Therefore, for classification after a training phase, a nonlinear projection function has to be learnt from the obtained projected data, e. g., by neural networks. To overvome this problem, a locality preserving projection (LPP) method has been developed, which is linear but provides good approximation to the nonlinear Laplacian Eigenmap [1, 3].

Although the manifold learning methods are unsupervised, they make use of structural knowledge within the data, such as locality and proximity relations, and thus suitable for classification applications. Without the need of class labels, they are especially suitable for adaptive and asynchronous BCI. This paper applies LLE and LPP to dimensionality reduction of asynchronous BCI data, and presents results in terms of separability on training data, optimal embedding dimension chosen by cross-validation, and prediction performance on testing data, in comparison with PCA and supervised PCA (SPCA) [2, 4] that shares the same idea as CSP filters [6].

EXPERIMENTAL RESULTS

The data used here is for asynchronous BCI and from 3 subjects, each performing 3 mental tasks in a random order during 4 recording sessions respectively. During a session of 4 minutes, a subject performed self-paced mental tasks, each lasting about 15 seconds. EEG signals were recorded from 32 channels. Power spectral density (PSD) features were extracted and 96 features were selected. Detailed description of data recording and preprocessing can be found in [5].

The first 3 sessions from each subject were used for 3-fold cross-validation of the LDA classifiers (using one against the rest mechanism), with features resulted from 4 dimensionality reduction methods as inputs. The average classification accuracies on training data were used to examine the separability of the features resulted from various projections. Figure 1 illustrates the classification accuracies on Subject 1 after the features are projected by PCA, LLE, LPP, and SPCA, respectively, onto low-dimensional subspaces or submanifolds. It shows that LPP achieves the best result among the unsupervised methods and almost matches

SPCA. The results on Subjects 2 and 3 have also been obtained, which show the similar trends of the 4 methods although the accuracies are lower. In order to analyse the best embedding dimensions identified by the 4 methods and their corresponding classification accuracies on validation data, Figure 2 gives a performance comparison among the 4 methods on validation data from Subject 1. It can be seen that LPP is able to find the lowest subspace producing the best cross-validation performace. The result of LLE is not so stable, but it is worth further investigation in the future. Results on Subjects 2 and 3 also lead to observations similar to the above.

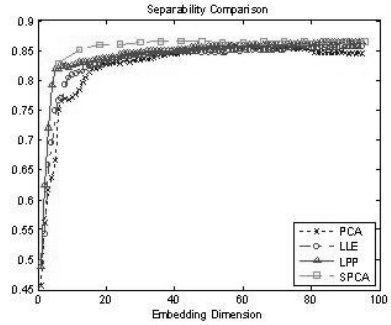

Figure 1: Separability comparison, using any two of the first three sessions from Subject 1 as training data and averaging over three folds.

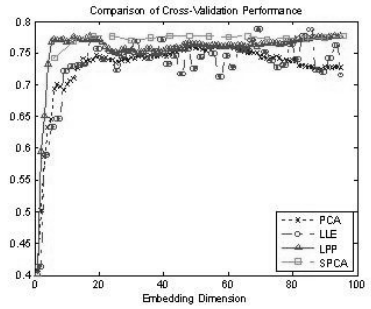

Figure 2: Comparison of performance on validation data from Subject 1, averaging over three folds.

By using the optimally reduced dimensions obtained from the cross-validation, in comparison with the situation of no dimensionality reduction, the 4 methods were further evaluated in terms of their classification accuracies on testing data which is the 4^{th} session from each subject.

Table 1: Performance comparison on testing data

Projection methods	Feature dimensions	Subj 1 (%)	Subj 2 (%)	Subj 3 (%)	Ave (%)
None	96, 96, 96	81.14	69.99	55.25	68.79
PCA	57, 32, 37	80.37	68.52	54.21	67.70
LLE	18, 12, 31	78.34	73.47	45.79	65.87
LPP	12, 4, 56	82.56	73.33	59.97	71.95
SPCA	18, 12, 60	81.48	72.12	59.06	70.89

The results are given in Table 1, which show that LPP and SPCA improve the classification performance on all subjects and more significantly on Subjects 2 and 3 whose EEG signals are of poorer quality than Subject 1. It is interesting that unsupervised method LPP slightly outperforms supervised method SPCA. Not surprisingly, PCA degrades the classification performance in comparison with no dimensionality reduction. LLE does not produce good results in this experiment, especially on Subject 3. Further investigation would be required to find out why.

DISCUSSION AND CONCLUSION

Although the original feature vectors were obtained through feature selection, their dimensionality can still be reduced dramatically by manifold learning, leading to average classification accuracy improvement of over 3 %. Unsupervised method LPP is able to match or even outperform supervised method SPCA, and would be advantageous in adaptive and asynchronous BCI. In theory, LLE is capable of revealing nonlinear low-dimensional submanifolds embedded in high-dimensional features. The experimental results in this paper have not shown its advantage. However, it is worth further investigation.

ACKNOWLEDGEMENT

The work was partly supported by the UK EPSRC under grant EP-D030552-1. The author would like to acknowledge with thanks the use of the asynchronous BCI data provided by JdR Millán, and thank Dell Zhang for useful discussions on manifold learning.

REFERENCES

[1] Belkin M, Niyogi P. Laplacian eigenmaps and spectral techniques for embedding and clustering. Proc NIPS, 2001; 585–591.

[2] Gan JQ. On optimal criteria of linear projections for classification. Proc UKCI, London, UK, 2005; 61–66.

[3] He X, Niyogi P. Locality preserving projections. Proc NIPS, Vancouver, Canada, 2003.

[4] Koren Y, Carmel L. Robust linear dimensionality reduction. IEEE Trans Vis Comp Graph, 2004; 10(4): 459–470.

[5] Millán JdR. On the need for on-line learning in brain-computer interfaces. Proc IJCNN, Budapest, Hungary, 2004; 2877–2882.

[6] Müllr-Gerking J, Pfurtscheller G, Flyvbjerg H. Designing optimal spatial filters for single-trial EEG classification in a movement task. Clin Neurophysiol, 1999; 110: 787–798.

[7] Pg H, Long F, Ding C. Feature selection based on mutual information: Criteria of max-dependency, max-relevance, and min-redundancy. IEEE Trans Patt Anal Mach Intell, 2005; 27(8): 1226–1238.

[8] Roweis ST, Saul KS. Nonlinear dimensionality reduction by locally linear embedding. Science, 2000; 290: 2323–2326.

[9] Tenenbaum JB, de Silva V, Langford JC. A global geometric framework for nonlinear dimensionality reduction. Science, 2000; 290: 2319–2323.

NARROW BAND SPECTRAL ANALYSIS FOR MOVEMENT ONSET DETECTION IN ASYNCHRONOUS BCI

C. S. L Tsui, A. Vučković, R. Palaniappan, F. Sepulveda, J. Q. Gan

BCI Group, Computer Science Department, University of Essex, Colchester, United Kingdom
E-mail: csltsu@essex.ac.uk

SUMMARY: Asynchronous Brain-Computer Interfaces (BCI) offer more natural mode of human-machine interaction, allowing users to make voluntary and self-paced mental activities. However, it is difficult to discriminate intentional user control from idle with this approach. In this paper, we propose a method that requires minimal user training for accurate onset detection of real movements using optimal spectral features from selected electrodes. We obtained true positive rates of 100 %, 87.5 %, and 72.5 % for 3 subjects respectively. The results also indicate a potential of the method for detecting onset of imagery movements.

INTRODUCTION

In recent years, there has been active research on techniques for detecting mental activities in asynchronous BCI designs [1, 2, 3]. In our approach here, narrow band spectral analysis of the electroencephalogram (EEG) from 8–45 Hz is conducted, because it covers mu, beta, and lower gamma frequency components, each having its own distinctive characteristics during real and imagery movements [4]. The onset detector presented in this paper has combined EEG spectral feature extraction, feature selection to reduce feature space dimension, and a decision mechanism to detect onset from classification results. We present the methodology in the following section, followed by results and discussions, and a conclusion.

MATERIALS AND METHODS

Subjects and motor task: 3 right-handed subjects (2 males and 1 female) were sitting comfortably with right arm resting on the arm rest. They were asked to perform the same real movements 40 times on their own pace in one session (session lasted 534, 338 and 400 seconds for Subject 1, 2, and 3, respectively). There was no cue from the system to instruct the subjects when to make a movement (i. e., random inter-trial interval), but subjects were asked to leave at least 4 seconds between two movements. The designed movements were: extending right wrist, holding for about 1–2 seconds, and relaxing.

EEG and EMG Acquisition: EEG signals were recorded with 64 electrodes according to the International 10-10 Standard (ActiveTwo, Biosemi, The Netherlands). We used electromyogram (EMG) to record muscle activities for establishing correct onset and offset time points for self-paced movements. This allows training data to be labelled according to the real movement activities. EMG was recorded bipolar, from extensor carpi radialis muscle. Both EEG and EMG were sampled at 1024 Hz, but downsampled to 256 Hz for offline analysis. No artefact rejection or EOG correction was employed.

EEG data labelling: The continuous EEG data were labelled into 4 classes. Samples of 1.5 seconds prior to EMG onset were labelled as "preparation". Samples between an EMG onset and offset of one movement were labelled as "execution". Samples of 1.5 seconds after an EMG offset were labelled as "after execution". Samples that did not fall into one of the above classes were labelled as "baseline", as they are supposed to be irrelevant to the movement.

Feature extraction and selection: EEG data were filtered with common average reference. To extract features for narrow band spectral analysis, the Thomson Multitaper Method was used to estimate the power spectral density (PSD) of each EEG channels over a 1 second moving window with an overlap of 7/8 seconds. The PSD over 8–27 Hz was sampled and averaged every 2 Hz, and over 28–45 Hz it was sampled and averaged every 3 Hz, resulting in a vector of 16 features. For 64 channels, there are 1024 features in total.

Davis Bouldin Index (DBI) [5] was used to select a subset of the best features. N features that maximise the validity of "preparation" against other classes were selected, and another N features that maximise the validity of "execution" against other classes were also selected. Therefore, $2N$ features were selected in total.

Classification and onset recognition: A naive Bayes classifier was used to deal with the 4 class problem, To find an EEG onset, a moving decision window that checks the past 11 classification results[1] was applied at each time point in feature space. In the moving window, if there were 2 (for Subjects 1 & 2) or 3 (for Subject 3) predicted "preparation", followed by 3 "execution", then the current position of this window was recognised to be an EEG onset. This sort of detection would be less sensitive to noise, because "preparation" correlates to "execution" and an individual false classification of "preparation" or "execution" would not lead to a false-positive detection. In performance evaluation, a predicted EEG onset is regarded as correct, if there is a real movement onset that occurs either 2 seconds before or after this predicted point.

Performance evaluation was conducted by 10-fold cross-validation. Each fold had 4 trials for testing and 36 trials for training. The number of true-positive (TP) detections and the number of false-positive (FP)

[1] It is a reasonable length. Shorter windows resulted in lower FP rate but also lower TP rate. Longer windows resulted in higher FP rate and were sensitive to noise.

detections from all the folds were combined to produce true-false difference (TF %) that is an event-by-event measurement. Given that E is the total number of movements or events (i. e., $E = 40$), TF % is defined by $\mathrm{TF}\,\% = (\mathrm{TP}/E - \mathrm{FP}/(E+\mathrm{FP})) \cdot 100$ (Townsend et al. [1] counted multiple detections during an event as a single TP. However, in this paper we counted M detections during an event as a single TP, and add $M-1$ to total number of FP).

Table 1: Performance with optimal number of features selected from 64 (top) and 37 (bottom) channels respectively. Dev is the averaged time between correctly detected and real movement onset.

Subject	$2N$	TF %	TP/E (%)	FP	Dev (ms)
1	16	95.24	40/40 (100)	2	325
2	10	69.13	35/40 (87.5)	9	788
3	28	59.46	29/40 (72.5)	6	688
1	14	86.39	39/40 (97.5)	5	556
2	30	70.91	32/40 (80.0)	4	922
3	40	57.61	29/40 (72.5)	7	575

Table 2: Selected features that give the results as shown in Table 1. In each sub-table, left column shows features that optimise the detection of "preparation" and right column shows features that optimise the detection of "execution".

Subject 1 ($2N = 16$)			
CP1	34–36 Hz	CP4	10–11 Hz
FC1	31–33 Hz	P4	10–11 Hz
CPz	34–36 Hz	CP2	10–11 Hz
FC1	28–30 Hz	P4	8–9 Hz
P3	8–9 Hz	CP4	12–13 Hz
P3	16–17 Hz	P2	10–11 Hz
FCz	31–33 Hz	P4	12–13 Hz
P1	10–11 Hz	Pz	10–11 Hz
Subject 2 ($2N = 10$)			
Cz	28–30 Hz	CP3	10–11 Hz
Cz	26–27 Hz	CP1	10–11 Hz
FCz	28–30 Hz	CP3	8–9 Hz
C1	28–30 Hz	CP3	12–13 Hz
C1	18–19 Hz	P1	10–11 Hz
Subject 3 ($2N = 28$)			
CPz	20–21 Hz	P5	18–19 Hz
CP3	18–19 Hz	CP5	16–17 Hz
P2	20–21 Hz	P5	16–17 Hz
CP3	22–23 Hz	Pz	20–21 Hz
CP3	16–17 Hz	CP3	20–21 Hz
CP5	14–15 Hz	CP1	20–21 Hz
CP5	18–19 Hz	CPz	22–23 Hz
C3	22–23 Hz	CP3	14–15 Hz
P5	14–15 Hz	CP2	22–23 Hz
CP5	12–13 Hz	P2	22–23 Hz
P5	20–21 Hz	CPz	18–19 Hz
P5	12–13 Hz	CP2	20–21 Hz
CP5	10–11 Hz	CP1	22–23 Hz
P7	18–19 Hz	P5	22–23 Hz

RESULTS AND DISCUSSION

Classification performance depends on the number of selected features. The method was evaluated by cross-validation, with $2N$ ranging from 2 to 100. The optimal values of $2N$ are shown in Table 1 (top), where the features were selected from 64 channels (1024 features). Subject 1 produced the best overall result, with 100 % TP rate and TF % = 95.24. Subjects 2 and 3 produced similar results: though Subject 2 had a higher TP rate (87.5 %) and TF % = 69.13, whilst Subject 3 had less FP detection. Table 1 also shows the averaged time deviation.

The selected channels and frequency components (i. e., features) are also explicitly given in Table 2. It is interesting to note that some features selected for Subjects 1 and 2 are from lower gamma band, which dominate the "preparation". Although rarely found in the human EEG, study in [4] has shown the existence of gamma band activities shortly before movement onset, which is then followed by mu rhythm activities.

Previous ERD/ERS research [6] showed that during real movements, EEG activity can be found in both contralateral and ipsilateral hemispheres, but in the case of imaginary movements only contralateral hemisphere gets activated. In order to make the conditions similar to imaginary movements, Table 1 (bottom) shows the results with features selected only from the contralateral hemisphere. Even with fewer available features, only a slight drop in TF % was found for Subject 3, but almost a 10 % drop for Subject 1. This is because for Subject 1, the best selected features that optimise the detection of "execution" are from ipsilateral hemisphere which gets activated after the contralateral one during real movements. The results in Table 1 (bottom) indicate a potential of our method for detecting onset of imagery movements.

CONCLUSION

An onset detection method for asynchronous BCI is presented in this paper, which shows some promise for detection of self-paced real movements, and potentially of imagery movements. New experimental protocol and extension to deal with imagery movements will be investigated in our future research. There is also much room for improving the feature selection method.

ACKNOWLEDGEMENT

This work was partly supported by the UK EPSRC under grant EP-D030552-1 and grant GR/T09903/01.

REFERENCES

[1] Townsend G, Graimann B, Pfurtscheller G. Continuous EEG classification during motor imagery Simulation of an asynchronous BCI. IEEE Trans Neural Syst Rehab Eng, 2004; 12(2): 258–265.

[2] Borisoff JF, Mason SG, Bashashati A, Birch GE. Brain-computer interface design for asynchronous control applications: Improvements to the LF-ASD asynchronous brain switch. IEEE Trans Biomed Eng, 2004; 51(6): 985–992.

[3] Millan JdR. Adaptive brain interfaces. Communications of the ACM, 2003; 46(3): 74–80.

[4] Pfurtscheller G, Neuper C. Motor imagery and direct brain-computer communication. Proc IEEE, 2001; 89(7): 1123–1134.

[5] Bezdek JC, Pal NR. Some new indexes of cluster validity. IEEE Trans Systems, Man and Cybernetics, 1998; 28(3): 301–315.

[6] Neuper C, Pfurtsheller G. Motor imagery and ERD. Pfurtscheller G, Lopes da Silva FH Handbook of Electroencephalography and Clinical Neurophysiology - Event-related Desynchronization, Elsevier, Netherlands, 1999; 303–325.

INVERSE PROBLEM APPLIED TO BCIS: KEEPING TRACK OF THE EEG'S BRAIN DYNAMICS USING KALMAN FILTERING

R. Lehembre, Q. Noirhomme, B. Macq

Communications and remote sensing laboratory,
Université catholique de Louvain, Louvain-la-Neuve, Belgium
E-mail: lehembre@tele.ucl.ac.be

SUMMARY: In this paper, we use Kalman filtering to improve inverse solutions for BCI applications. The algorithm is tested on EEG data from the BCI 2003 competition. The aim of this work is to improve the spatial resolution of the EEG using the inverse model and take profit of their excellent time resolution with the Kalman filter. Preliminary results show a 4 % improvement by our additionnal Kalman filtering.

INTRODUCTION

Current research in BCI are mainly conducted directly on the EEG signals. These signals have a very good time resolution but suffer from a low spatial resolution. This shortcoming can not only be explained by the limited number of electrodes placed on the scalp but also because electrodes and sources are separated by the skull which is responsible of the diffusion of electric signals transmitted out of the brain. The Inverse Problem (IP) offers an improvement of this spatial resolution with the projection of the EEG measurements on dipoles distributed on a head model. The IP adds an information prior to the EEG (i. e. brain's geometry, electromagnetic transmission inside the brain) and therefore could be helpful in BCI applications based on the localisation of motor tasks. Already a few steps have been taken in that direction [1, 2, 3] and show promising results. To go further in that path we suggest improving inverse solutions by taking into account the temporal evolution of the EEG. It has recently been shown [4] that Kalman filtering is a suitable approach for this purpose although it has mainly been tested on simulated data. The main challenge in using this method with real EEG data is that we still know very little of the brain dynamics, and thus it seems difficult to find an accurate model. We will show in the following how, in the case of BCI applications, it is possible to elude this problem. We will first describe the data we used as well as the head model for the inverse problem. Then the application of Kalman filtering to the IP will be described. Finally, preliminary results will be presented and discussed.

MATERIALS AND METHODS

Data [5]: Provided by Fraunhofer-FIRST, Intelligent Data Analysis Group, and Freie Universität Berlin, Department of Neurology, Neurophysics Group.

This dataset was recorded from a normal subject during a non-feedback session. The task was to press with the index and little fingers the corresponding keys in a self-chosen order and timing 'self-paced key typing'. 28 EEG channels were measured at positions of the international 10/20-system. Signals were recorded at 1000 Hz with a band-pass filter between 0.05 and 200 Hz. There are 416 epochs (316 for the training set and 100 for the test set) of 500 ms length.

Head Model: For simplicity reasons, a simple four concentric spheres head approximation was used. As few as 400 dipoles were fitted on a half-sphere just below the cortex. They are orientated perpendicular to the cortex. We chose a small number of dipoles to cope with computational expenses and also because the activity we are looking at is located in the cortex.

Kalman filtering: The inverse problem can be viewed as a Kalman filtering problem where the measurements are the EEG, $\phi(t)$, and the states, $J(t)$, are the values of the current of each dipole. The measurement equation is:

$$\phi(t) = GJ(t) + \epsilon \tag{1}$$

where G (commonly called the lead field matrix) represents the electromagnetic model of the head and is a projection from the electrode space to the dipole space. For simplicity reasons we used a first order linear approximation for the state equation where A is the dynamical model matrix:

$$J(t) = A(t)J(t-1) \tag{2}$$

Since we do not know how the currents in each dipole are linked, we adopt a very simple model linking current at time t and position d, namely $j(d,t)$, to current $j(d,t-1)$ and currents at time $t-1$ on neighbouring positions as in expression (3). This makes sense in our case since we work specifically on regions located in the left and right motor cortex. Thus the dipoles located in these regions are probably correlated.

$$j(d,t) = a(t)j(d,t-1) + \frac{1}{4}b(t)\sum_{d'\epsilon D(d)} j(d',t-1) \tag{3}$$

The second expression on the right hand side expresses the contribution of d's neighbors. Since the dipoles are located on a surface, each dipole has four neighbors. We suppose that all neighbors have the same contribution. As was pointed out in the introduction, brain dynamics are yet to be known and of course, this model is not precise enough to track the temporal evolution. Nonetheless in the particular case of the data we analyse here, it is possible to have improved inverse solutions by introducing the supposed dynamics that appear when we take out the mean for one movement. For example, taking a dipole located in the middle

of the right (resp. left) cortex, and taking the mean of the signal provided by this dipole over a few trials when the user moved his left (resp. right) hand, it is possible to observe a slowly decreasing curve.
Therefore, we can improve the inverse solution corresponding to a given task by giving a temporal dependency for A, and giving a gradually ascending value for the $a(t)$ that corresponds to dipoles located in the right or left cortex. We then face a model selection problem since we use two models, one for the left and one for the right hand movement.

PRELIMINARY RESULTS

Algorithms were only tested on the test set, and the inverse problem was not optimized. The classifier consisted simply in comparing the mean of the signal for the dipoles in the right and left motor cortex. The inverse problem alone gave a 72 % good classifications while the inverse problem with the Kalman approach gave 76 % good classifications.

DISCUSSION

Although these results are certainly inferior to the best results obtained on this dataset, they show that Kalman filtering can be used and can improve results obtained with the inverse problem. On the other hand, recent work based on [1] using the same head model, but with an optimized classifier, reports a 82 % good classification. Hopefully, this result can be improved with the method described here. Possible improvements will be obtained by using a better classifier, improving the temporal model and using better features than just the mean of the signal.

CONCLUSION

Kalman filtering has been applied to the inverse problem and used in the case of BCI applications. The main challenge of this method is to find an accurate model for the brain dynamics. One way to achieve this is by using different models that enlight only one task. A model selection can then decide which model is the most suitable one.

ACKNOWLEDGMENTS

Rémy Lehembre is supported by a grant from the Belgian NSF (FRIA). Quentin Noirhomme is supported by a grant from the Région Wallonne. Special thanks to Jacek Czyz for his constant support.

REFERENCES

[1] Noirhomme Q, Macq B. EEG imaging methods applied to brain-computer interface. SPIE Medical Imaging 2006, San Diego, USA, Feb 11–16, 2006; Proc SPIE 6143.

[2] Qin L, Ding L, He B. Motor imagery classification by means of source analysis for brain computer interface applications. J of Neural Eng, 2004; 1: 131–134.

[3] Grave de Peralta Menendez R, González Andino S, Perez L, Ferrez PW, Millán JdR. Non-invasive estimation of local field potentials for neuroprosthesis control. Cogn Process, 2005; 6: 59–64.

[4] Galka A, Yamashita O, Ozaki T, Biscay R, Valdés-Sosa P. A solution to the dynamical inverse problem of EEG generation using spatiotemporal Kalman filtering. NeuroImage, 2004; 23: 435–453.

[5] Blankertz B, Curio G, Mäller K-R. Classifying singletrial EEG: Towards brain computer interfacing, Advances in Neural Inf. Proc Systems NIPS 01, Diettrich TG, Becker S, Gharamani Z, Eds, 2002; 14.

BRAIN COMPUTER INTERFACING IN SPACE-TIME-FREQUENCY DOMAIN

K. Nazarpour, L. Shoker, S. Sanei

Centre of Digital Signal Processing, Cardiff School of Engineering, Cardiff University, Cardiff CF24 3AA, United Kingdom
E-mail: NazarpourK@cf.ac.uk

SUMMARY: Two novel Space-Time-Frequency (STF) approaches for Brain Computer Interfacing (BCI) are presented. The first algorithm is based on extending of a precise time-frequency masking method to accommodate spatial information in BCI. In this method EEG trials are classified based on the motion vectors of the extracted EEG sources and their locations over the scalp. In the second algorithm, using parallel factor analysis (PARAFAC), the STF decomposition of EEG is proposed. Results of using PARAFAC shows that for each EEG trial there are two factors in μ band. The spatial distribution of the factor with ERD time characteristics is classified to indicate the subject's intention of left/right index movement imagination. We can reliably distinguish between left and right index movements by using these developed STF methods.

INTRODUCTION

Studies of medical imaging have established cortical sensorimotor systems are activated during imagery as well as real motions. It has been established that planning and execution of movement leads to a short-lasting amplitude attenuation following by amplification in the μ rhythm known as event-related (de-) synchronization (ERD/ERS) [1]. These brain activities are spatially smeared when volume conducted through the scalp, thus their exact localization is sophisticated. Also the clearest ERD/ERS may occur at different frequency bands and in different time points. This fact motivated us to develop hybrid space-time-frequency approaches for BCI. In this paper, we briefly introduce the two methods where in both, in addition to the time and frequency information of the EEG signals, the spatial information provide crucial indicators of intended motion.

Based on the assumption that the electrical sources in brain might move during index imagination, we developed a moving source tracker after clustering of the highly active regions of the time-frequency maps of 64 channels EEG signals. In the second method in order to remove the background activity subspace of recorded EEG, we developed the PARAFAC algorithm on the complex wavelet transformed filtered EEG signal with a static spatial mask over the sensorimotor area. The spatial distribution of the factor with ERD time characteristics is classified to indicate the subject's imagination. The support vector machines classifier has been used for the two approaches. The data of the first approach was provided by King's College Hospital, London where an able bodied subject was seated with arms resting on a table. The second method has been implemented on the EEG signals of 2 subjects participating in *NIPS2001 BCI Workshop* datasets.

FIRST METHOD

Preliminary, the EEGs are transformed into the time-frequency domain and then the TF representation of each electrode is arranged into a matrix where each element represents the x-y coordinates of the electrode. Then, space-time-frequency masks are created and the components within the masks are clustered. Using k-mean clustering followed by the Gap statistics method enables us to estimate the number of disjoint factors, representing the brain's active sources, accurately. The cluster centers are one of the features used by the classifier. The other significant feature is the directionality of the moving reconstructed source signal which is deduced from its cross correlation with the raw EEGs. A block diagram of the proposed system is shown in Figure 1. Using this approach classification rates up to 75.5 % have been gained when Gaussian RBF kernel is used for the SVM classifier. The results are detailed in Table 1. Interested reader is referred to [2] for details of this approach.

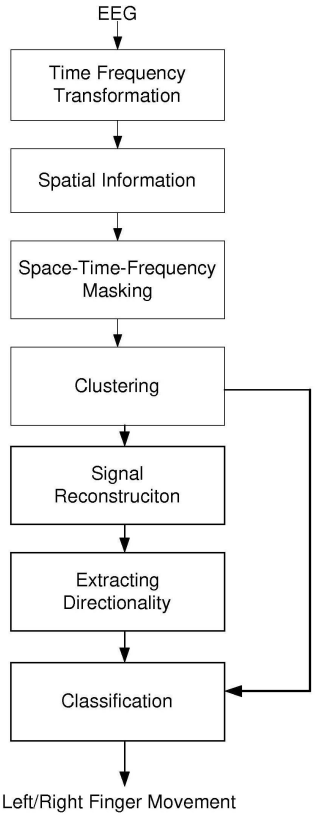

Figure 1: The diagram of STF based atom extraction and classification algorithm [2]

Table 1: The performance of the classifier based on the average (standard deviation) number of correctly classified points. Three kernels are compared in the classification.

Kernel	Average classification rate (%) (s. d.)		
	Overall	Right	Left
Gaus. RBF	75.50 (1.0)	75.16 (1.2)	69.43 (1.5)
Cubic Poly.	65.30 (1.4)	66.15 (1.0)	64.36 (1.0)
Linear	61.01 (1.3)	60.34 (1.4)	56.51 (1.0)

SECOND METHOD

In this approach, we decomposed the time-varying EEG spectrum of different channels using PARAFAC. It has long been known that unique multi-linear decomposition of multi-way arrays of data is possible using PARAFAC. We showed that PARAFAC is capable of successfully space-time-frequency decomposition of the EEG for BCI. This makes use of the fact that multichannel evolutionary spectra are multi-way arrays, indexed by electrode, time, and frequency. The inherent uniqueness of the PARAFAC solution leads to single trial EEG decomposition with a minimum a priori assumptions such as independencies of channels.

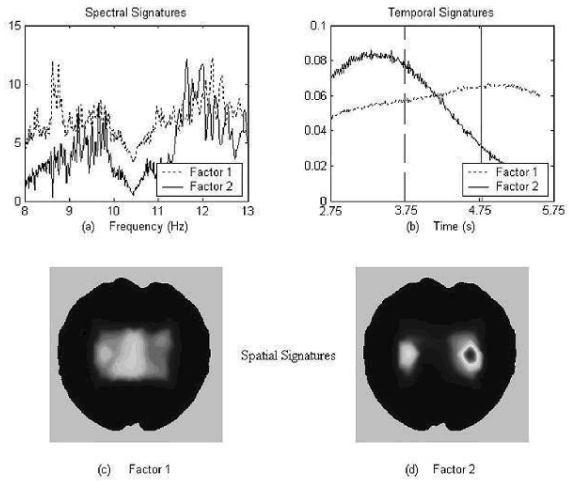

Figure 2: Sample Space Time Frequency decomposition of the 15 channel EEG signal recorded during LEFT index imagination. The factor demonstrated with solid line indicates a clear ERD in the contralateral hemisphere. (a) Spectral contents of the two identified factors, (b) Temporal profile of the two identified factors and the onset of preparation and execution cues are shown in vertical dashed and solid lines, respectively, (c) and (d) Topographic mapping of EEG for the two factors.

One sample result for left index imagination is shown in Figure 2. Figure 2 (a) shows the spectral contents of the two factors identified by PARAFAC in the μ band. Figure 2 (b) is of great interest where two temporal profiles are illustrated. Note that the blue and red vertical lines indicate onset of "L/R" and "X" cues for preparation and execution, respectively. Figure 2 (b) shows that even before "X" which occurs at time point 3.75 s, the subject has started imagination. The dotted curves of Figure 2 (a, b) correspond to Figure 2 (c), where obviously occurs under. Note that red and blue areas indicate the level of activity of the channels normalized between zero and one (left ear is left and the nose is up). The results come along with previous researches where it is elaborated that an ERD may be mostly recorded on the contralateral hemisphere in μ band [1]. The second factor occurs simultaneously within the brain but manifests the background activity of brain-due its temporal signature. The spatial distribution of the ERD factor is introduced to the SVM classifier as feature. The best achieved classification rate implementing this method was 76.22 % with Gaussian RBF kernels [3].

CONCLUSION

In this paper, two STF hybrid approaches for BCI are presented. The first approach effectively utilizes the spatial information of the localized a rhythms and directionality of the moving sources. In the second approach, the potential of PARAFAC to jointly STF decompose the time-varying spectrum of multichannel EEG, enables spatially localization of the ERD factor in contralateral hemisphere clearly in parallel with time and frequency. The classifications have been done by using the SVM and promising results achieved.

REFERENCES

[1] Pfurtscheller G, Lopes da Silva FH. Handbook of Electroencephalography and Clinical Neurophysiology Event-related desynchronization, Elsevier, Amsterdam, Netherlands, 1999.

[2] Shoker L, Sanei S, Nazarpour K, Sumich A. A novel space-time-frequency masking approach for quantification of EEG source propagation with application to brain computer interfacing, in Proc EUSIPCO 2006, Florence, Italy, 2006.

[3] Nazarpour K, Sanei S, Shoker L, Chambers JA. Parallel space-time-frequency decomposition of EEG signals for brain computer interfacing, in Proc EUSIPCO 2006, Florence, Italy, 2006.

ENGINEERING THE BRAIN SIGNALS – PREPROCESSING

H. Singh, E. Hines, N. Stocks, C. Syan

School of Engineering, University of Warwick, UK
E-mail: harsimrat.singh@warwick.ac.uk

SUMMARY: The central element in each brain computer interface (BCI) is a translational algorithm that converts electrophysiological input from the user into output that controls external devices [1]. The focus of our BCI group is to improve the accuracy and efficacy of the techniques used to develop this translational algorithm, thereby making an impact on increasing the transfer rates for online BCI systems. In this paper, we report on the preliminary analysis of the multi task, multi-channel brain data and study the methods to segregate it into useful sequences providing distinct features for the development of an efficient learning algorithm.

INTRODUCTION

The concept of BCI development evolved from motor imagery which is then transformed into control signals [2]. The key characteristics of precision, responsiveness and interpretability by which the development of BCI is ranked, are not only dependent on the good performance of the classifier, but also on the choice of proper parameters characterizing signal features [3]. This feature extraction process is boosted, if the data channel selection is based on its ability to provide information about the mental tasks, being performed by the subject. Thus, Principal Component Analysis (PCA) studies on the multi-channel data acquire importance for the selection of the appropriate channels with maximum information. Furthermore, the paper covers object oriented filter design which gives better trade off analysis between the stop band attenuation and the filter order which is perceived to have positive effect on the transfer rates of BCIs.

DATA

The dataset used here is provided by the University of Tbingen, Germany and other participating universities as a part of the BCI competition 2005 [4]. The subject had to perform a series of tasks as imagined movements of either the left small finger or the tongue. The 3 second trials were performed using 8×8 ECoG platinum electrode grid, placed on the contralateral (right) motor cortex. To avoid visually evoked potentials, the recording started 0.5 s after the visual cue.

METHODOLOGY

The intent is to extract more exhaustive knowledge for the feature extraction process so that the classification of this multi-channel training data is accurate and effective. By and large, the concept of motor imagery is related to spatial location of the recording sites of the head. This idea helps significantly, to shrink the multi channel data and reject the channels which are likely to be of less use in terms of the information they contain about the left or right motor imagery. Since it is known that the left small finger movement should correspond to right part of the head, the recording paradigm clearly implies that all the channels contain the information about the right motor cortex. So there is a need to extract those channels with maximum information about the tasks. This is done through PCA, a technique for reducing the number of correlated variables in a data set without significant loss of information. Since the training data trials are labelled as 1 and -1, we know that the two consecutive trials are two different tasks. After the rejecting the channels having less information, we propose to calculate band powers for the selected channels to be used as features for the learning algorithm. In the second phase, an object oriented approach using MATLAB is employed to design filters to segregate data into frequency bands namely 0.5–7 Hz, 8–12 Hz, 13–29 Hz and 30–50 Hz. These frequency bands are so selected that the tasks performed by the subject fall into one of them. The band power in each of the selected channels is used as a means of classifying the task. This also indicates the prominent frequency band corresponding to each of the two tasks. This concept is novel [5, 6] because firstly, the methodology is implemented on the data collected with the help of ECoG grid and the identified key principal components determine the channel selection. Secondly, filter design is object oriented. The filter design becomes quite systematic with object based approach i. e. the trade-off analysis between the stopband attenuation and the filter order becomes less cumbersome. As we know that the filter order is directly proportional to the delay between the input and output in time (the computation time to implement the filter), so the stopband attenuation can be iterated to select filter order with the least distortion. The iterations are based on the dynamics of the data in terms of its statistical measures and amplitude ranges. Lower filter order would mean less multiplications and subtractions, therefore less computational time. Figure 1 (a) is a schematic representation of the methodology and 1 (b) shows the parameters for the band pass filter design.

RESULTS AND CONCLUSION

Bar charts in Figure 2 (a) and 2 (b) show large range of variation in channels. This implies that there is more rigorous brain activity going on in specific areas of the brain. The challenge lies in selection of channels with limited independent information about the tasks. Firstly, the data is normalised by their second moments. PCA transforms the data set of correlated variables into a new set of uncorrelated variables, called

the principal components (PCs). The PCs are orthogonal and are sequenced in terms of the variability they represent. They correspond to the directions in which the input data has the largest variances. Before doing the PCA we make sure that the channels are correlated by using scatter plots between two channels. Scatter plot between channel 1 and 2 in Figure 2 (c) shows a cluster of points in the straight line i. e. for every value in the first channel, there is a corresponding value in the second channel, hence, correlated. Figure 2 (d) shows somewhat less correlation between another set of channels. Hence, it is observed that some channels are more correlated than others.

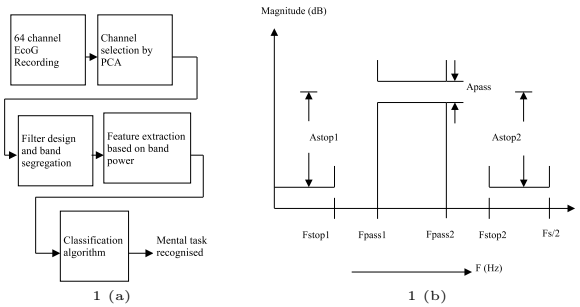

Figure 1 (a): Methodology Flow; 1(b): filter design

There is a need to find a hypothetical spatial location of electrodes in the grid which would give clearer conceptual fundamentals about the correlation between channels because we perceive that the channels adjacently placed in the grid might be closely correlated. It is observed that the range of data is up to 20 dB for all channels, so for the filter design, we regulate stopband attenuation around this value. The ripple in the pass band is kept at 0.5. This gives a direct form, FIR equiripple stable filter, with linear phase and very clean attenuation of 20 dB as shown in Figure 2 (e). Stable elliptic filter with filter order of 12, Figure 2 (f) has been designed with identical parameters for comparison. It exhibits non linear phase, but since our application concerns band power, the non linearity in phase doesn't have large impact on the results. It is concluded that PCA analysis is a useful tool to extract information and reduce the size of data. But the recording paradigm of using 8×8 grid makes it complicated to answer queries like, the electrode placement in a grid might result in a distinguishable correlation between the adjacently placed electrodes, which could mislead our conclusions. There is a need to perform more comprehensive statistical analysis on the data to understand the distribution of the data before applying PCA to be able to choose specific channels. Even the scree plots and eigen value ratios in percent are not able to explain the selection of channels. In order to use PCA for this type of multi channel data it must be somewhat modified to take into account the data structure and the recording paradigm. The spectral power in each band can be computed and power difference in two different channels for the same band can also be computed which can act as features for the learning algorithm. The authors are working on this idea and results will be published soon.

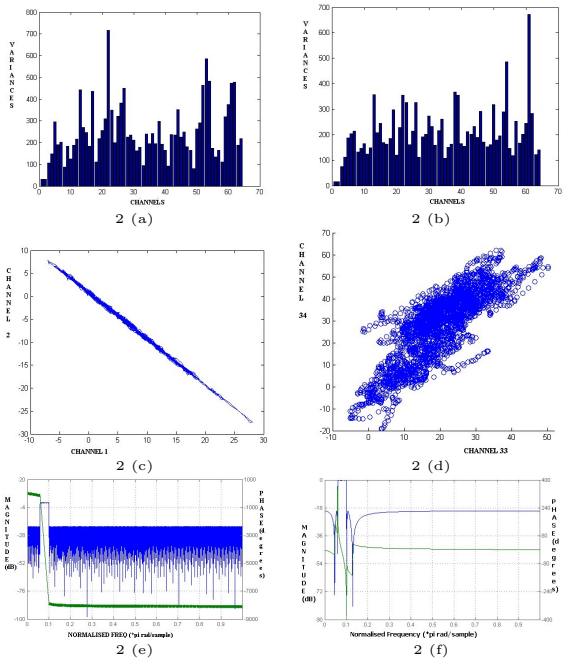

Figure 2(a) and 2(b): Bar charts show variances of 64 channels for first task and second task respectively before PCA. 2(c) and 2(d): Scatter plots show correlation between channels for the first task. 2(e) and 2(f): Magnitude and phase responses for the equiripple filter and elliptic filters respectively

ACKNOWLEDGEMENT

The authors thank the organizers of the BCI Competition III for the dataset. Singh acknowledges support for WPRF Research Fellowship and ORS.

REFERENCES

[1] Wolpaw JR, Birbaumer N, Heetderks WJ, McFarland D, Peckham P, Schalk G, et al. Brain-computer interface technology: A review of the first international meeting, IEEE Trans Rehab Eng, 2000; 8: 164–173.

[2] Wolpaw JR, Birbaumer N, McFarland DJ, Pfurtscheller G, Vaughan TM. Brain computer interfaces for communication and control. Clin Neurophysiol, 2002; 113: 767–791.

[3] Singh H, Hines E, Stocks N, Syan C. Computational methodologies in the Brain Computer Interface Research, Proc CARS & FOF 2006, VIT, India 2006 (Conference Proceeding).

[4] ida.first.fhg.de/projects/bci/competition_iii/

[5] Palaniappan R. Brain computer interface design using band powers extracted during mental tasks, Proc IEEE EMBS Neural Engineering, Arlington, Virginia, 2005; 321–324 (Conference proceeding).

[6] Singh H, Upendra K, Singh S, Jain VK. EEG Signal Analysis: An opening to the Brain Computer Interface Proc Intern Conf on Soft Computing, Chennai, India, May 2004 (Conference proceeding).

CROSSECTIONAL INVESTIGATION OF WRIST MOVEMENT INTENTION CLASSIFICATION IN EEG SIGNALS

B. Hubais, F. Sepulveda, I. Navarro

BCI Group, Department of Computer Science, University of Essex, UK
E-mail: bahuba@essex.ac.uk

SUMMARY: This study looked into classification of wrist movements for left and right hands across user with an unbiased selection of feature/channel sets. The 10 best feature/channel sets as determined by the Davies-Bouldin Index (linear separability) were used. The features were then classified using a multi-layered perceptron (MLP). Classification of *executed* movements across users (classifier trained on data from one set of subjects but tested on data from another) was promising: near 80 % correct classification in some cases. Data scaling improved the performance more than MLP retraining on parts of the test user's data. On the other hand, *imaginary* movements proved more difficult (near 60 % mean correct recognition), with the exception of 1 user whose results greatly improved with MLP retraining (near 100 % correct classification of left vs. right wrist imaginary movements).

INTRODUCTION

The study looked into wrist movements for left and right hands. For each of 21 EEG channels, 776 features from time, frequency and joint time-frequency domains were investigated. Classification was investigated across users, i. e. the MLPs were trained on data from one subject but tested on data from another. To determine the features and channel combinations with the highest class separability, the Davies-Bouldin Index (DBI) [1] was used.

MATERIALS AND METHODS

Experimental Protocol: Four able-bodied male subjects participated in the study. Data were acquired using a MindSet system with a 10/20 ear-referenced 21 electrode setup. The subjects looked at a monitor where commands were given as to which hand to move. More details about the protocol can be found in [1].

Data Processing: Data were run through an analogue antialiasing second order Butterworth filter and sampled at 256 Hz. The data were then filtered using band-specific Butterworth zero-phase filters: 6^{th} order filter to extract the Delta band, and 12^{th} order filter to extract the Theta band, Alpha band, Beta band, Gamma band, and for the combined bands. The data were then downsampled to 128 Hz. No effort was made to remove EOG artefacts so as to examine the robustness of the features.

The 12^{th} order filter was used as it was the lowest order that returned a 40 dB SNR between the signal and mains power. The delta band filter used a smaller order than the other filters because of numerical errors in Matlab that did not allow the use of a higher order filter.

Feature Selection: The following features were extracted for selection of the best set for classification:

- Amplitude variance of the signal
- Windowed amplitude variance of the signal
- Maximum/minimum power and dominant frequency of autocorrelation
- 6^{th} order autoregressive model, 6 coefficients and noise variance [2]
- 4^{th} order autoregressive moving average model, 4 coefficients and noise variance
- Total signal power

The features were calculated for each of the specific EEG bands. All windowed features used non overlapping 125 ms windows. Based on the DBI values for each feature, the 10 best (lowest DBI) were used in the classification of left versus right hand movements.

Classification: The data from three subjects were used for training, while the data from a fourth subject were used for testing (for all combinations of subjects). The data from the test subjects were later also scaled using 50 and 95 percentile width in the data's distribution before re-calculating the features and the results re-evaluated.

Retraining was also used to assess its effect on classification results. To this end, one third of a test subject's data were set aside for testing. The remaining 2/3 of the test subject's data were used for retraining to assess the effect of the amount of retraining data used, as follows: First, the first 1/3 of the retraining data were used to continue training an MLP that had previously been trained on the data from the other subjects. In another case, the first 2/3 of the retraining data were used, and, finally, the full retraining set was used. This was combined with random initialization of the data sets.

The classification task was also repeated five times for each data set and the average performance was computed. The classifiers used were multilayer-perceptrons with five to fifty hidden neurons (in increments of five) with the training goal set to 0.2 mean squared error (MSE).

RESULTS AND DISCUSSION

Cross-user results without classifier retraining or data scaling: As expected, the initial cross-user results were very disappointing (first bar in the plots in Figure 1).

These results were found to reflect the large differences between the users' feature distributions.

Cross-user results with 95 percentile scaling: The results (second bars in the plots Figure 1) showed that scaling improved the executed movement classification, but the imagined movement classification remained relatively unchanged. The results for the imaginary movements were more in line with the non scaled data results.

Cross-user results with 50 percentile scaling: This scaling had similar effects (third bars in Figure 1) as the 95 percentile scaling but to a lesser degree. It is also important to notice that the scaling did not have a substantial effect on the imaginary movement results, as in the 95 percentile results.

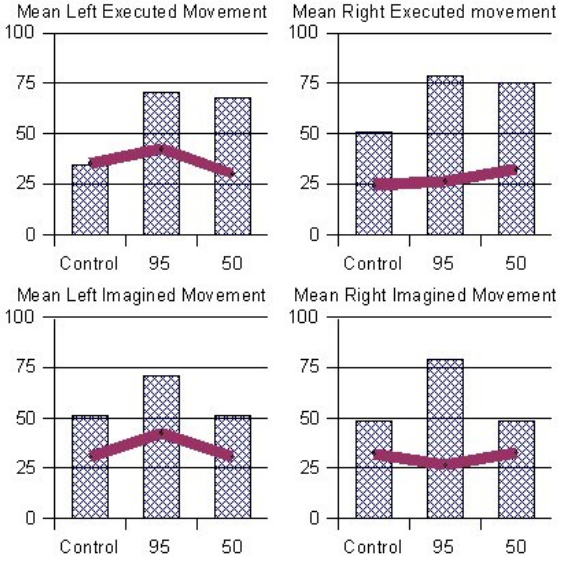

Figure 1: Effect of data scaling on cross-user results. Bars: mean correct classification. Thick lines: standard deviations. Controls: no data scaling.

Cross user results with classifier retraining: The results of retraining the MLPs with one third, two third, and all of the retraining data from a subject were disappointing, as can be seen in Figure 2. There was little improvement with respect to the classification without retraining or scaling (i. e. controls in Figure 1).

Best results: Results for User 3 were special in that, when retraining was used, his results where close to 100 % correct classification for both left and right imagined hand movements. This could be due to the distribution of his data being a subset of the distributions for the other subjects.

CONCLUSION

In this crossectional study, scaling of the test subjects' data to the range of the training data showed potential in improving the classifier's performance for *executed* movements. On the other hand, neither scaling nor retraining showed significant improvement in *imaginary* movements, with the exception of the case for Subject 3. It is possible that the retraining data were not sufficient to improve the results, or, that the subjects employed different strategies for the motor imagery task.

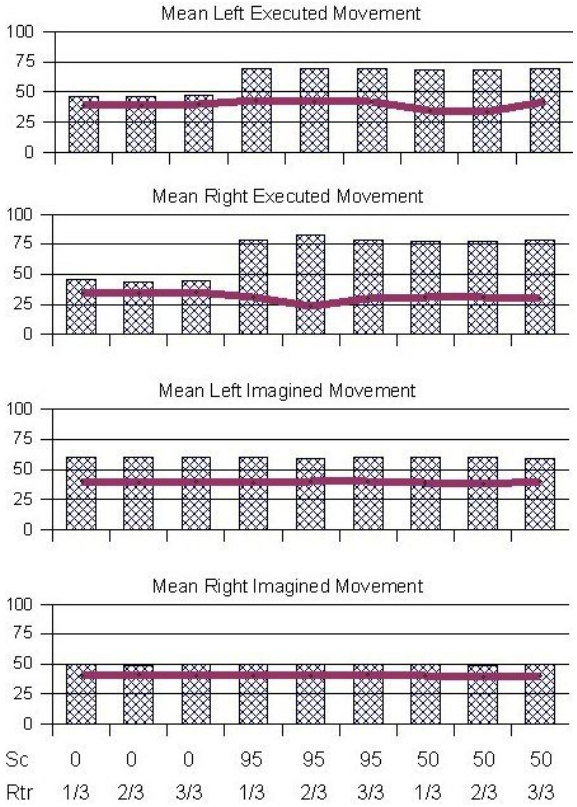

Figure 2: Cross-user results with retraining and scaling. Sc: scaling percentile factor (0 = no scaling). Rtr: retraining data size (as a fraction of the full retraining set)

ACKNOWLEDGEMENT

B. Hubais is sponsored by Etisalat University College, a subdivision of the Emirates Telecommunication Corporation (ETISALAT), United Arab Emirates.
This project has also been funded the UK's EPSRC (Project GR/T09903/01).

REFERENCES

[1] Sepulveda F, Meckes M, Conway BA. Cluster Separation Index Suggests Usefulness of Non-Motor EEG Channels in Detecting Wrist Movement Direction Intention. Proc of the 2004 IEEE Conf on Cybernetics and Intelligent Systems, Singapore, 2004; paper FM6.1.

[2] Pfurtscheller G, Neuper C, Schlögl A, Lugger K. Separability of EEG signals recorded during right and left motor imagery using adaptive autoregressive parameters. IEEE Trans Rehabil Eng, 1998; 6(3): 316–25.

REAL-TIME FEEDBACK SOLUTION APPLIED TO THE MOTOR IMAGERY BASED BCI PROTOCOL

S. Parini, L. Maggi, L. Piccini, G. Andreoni

Bio-engineering Department, Polytechnic of Milan, Italy
E-mail: sergio.parini@polimi.it

SUMMARY: In this paper we propose a new method for the synthesis of a biofeedback for Motor Imagery BCI protocol with no need of a preliminary frequency screening session. We discuss a solution based on the index of the percentage of desynchronization estimated after an envelope demodulation. Starting from an algorithm without a priori knowledge about the relevant frequencies of the subject, an auto calibrating incremental adaptive algorithm produces a feedback as significant as a feedback obtained on the basis of the knowledge of the relevant frequencies.

INTRODUCTION

A Brain Computer Interface is a man-machine interface based on the mutual interaction between the computer and the brain: the former should be capable to translate the signal generated by the user through a classification algorithm, while the latter should learn the correct mental strategy on the basis of the computer behaviour. This approach leads to the generation of a more repeatable and more effective signal. When the user is aware of a physiological activity which usually does not perceive, he or she can learn how to partially control it. This phenomenon is called biofeedback. When biofeedback is applied to the BCI it is possible to establish a virtuous loop, which could improve the performances of the whole system. In order to achieve such a result a real-time feedback is needed: in this way the user can obtain an higher level of control over the system by understanding the action-reaction mechanism behind it. An efficient training system should help the user to provide a better signal. In this work we face the issue of subjects training on the ERD/ERS based Motor Imagery Protocol. Usually the biofeedback is generated by a classifier trained on a previous training set. In this way the generated feedback magnitude reflects the probability that the extracted feature belongs to a particular population of the training set; as a consequence, in case of a low quality training set, the user should learn to repeat a low quality signal.

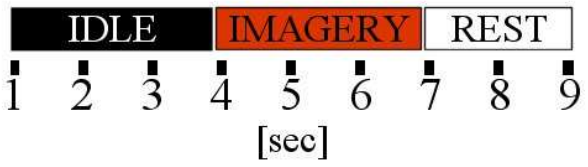

Figure 1: The adopted epoch structure

MATERIALS AND METHODS

Setup: The signal was acquired from the scalp above the sensorymotor cortex using two bipolar channels centered on locations C3 and C4. The training protocol was based on a modified version of the epoch structure proposed by the Graz University of Technology. A scheme of the adopted structure is reported in Figure 1. In this preliminary study, three subjects were asked to perform a training session of 80 epochs based on the imagination of hands movements. A feedback value for each channel was presented to the user by means of two level bars as instantaneous indexes of the lateralized motor imagery.

The algorithm: The proposed solution aimed at modelling the in-band desynchronization using the integral of the amplitude modulation envelope (AM) computed on data windows of fixed length and overlap. In Figure 2 is reported an example of the fitting properties of the AM envelope method [1] on a 1 second data window filtered in the generic mu-band (8–12 Hz).

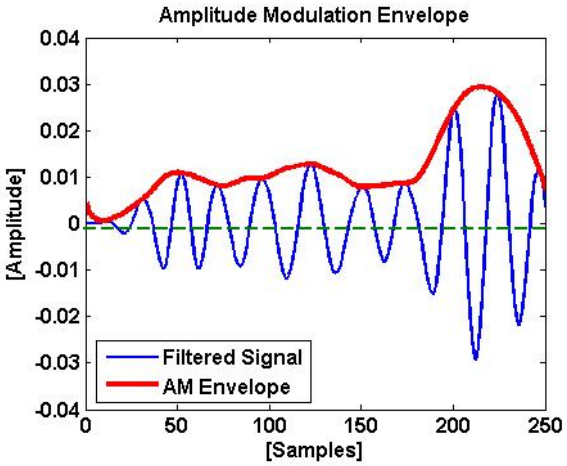

Figure 2: The amplitude modulation envelope

The developed algorithm used an incremental approach in order to progressively adapt to the subject relevant frequencies. This was achieved by identifying those portions of the 4–30 Hz band in which the event-related information was concentrated. By using a bank of 4 Hz amplitude passband filters centered on the 6–28 Hz frequency range, the windowed signal acquired from each channel was separated into its components. For each i^{th} component the AM_i value was computed and consequently, according to the current event-label, the mean values ($\bar{x}_{OFF,i}$ for the idling phase, $\bar{x}_{ON,i}$ for the controlateral imagery phase) and the standard deviation values ($S_{OFF,i}$, $S_{ON,i}$) were updated. During the controlateral activity phase a set of weights, each

related to a specific component, was computed by evaluating two parameters: the current desynchronization in respect to the $\bar{x}_{OFF,i}$ value and a gradient descent analysis based on the mean value. According to the information gathered at time t, three main states could be identified:

$$\bar{x}_{OFF,i}(t-1) - \mathrm{AM}_{\mu,i}(t) \begin{cases} < \varphi \cdot S_{OFF,i}(t-1) \Rightarrow \text{LOSS} \\ \geq \varphi \cdot S_{OFF,i}(t-1) \Rightarrow \text{other} \end{cases}$$

$$\text{other} \Rightarrow [\bar{x}_{ON,i}(t) - \bar{x}_{ON,i}(t-1)] \begin{cases} \leq 0 \Rightarrow \text{GAIN} \\ > 0 \Rightarrow \text{STABLE} \end{cases}$$

where $\varphi \in (0, 1]$ identifies the fraction of $S_{OFF,i}$ to be used as desynchronization threshold. The LOSS state identified a decrease ($\delta_{LOSS,i}$) of the weight related to i^{th} component, while the GAIN state corresponded to an increase ($\delta_{GAIN,i}$) of the weight value. During the STABLE state the weight value were not modified.

$$\begin{aligned} \delta_{LOSS,i} &= -\alpha \cdot \left(2\varphi - \frac{\bar{x}_{OFF,i}(t-1) - \mathrm{AM}_{\mu,i}(t)}{S_{OFF,i}(t-1)} \right) \\ \delta_{GAIN,i} &= \alpha \cdot \left(\frac{\bar{x}_{OFF,i}(t-1) - \mathrm{AM}_{\mu,i}(t)}{S_{OFF,i}(t-1)} \right) \end{aligned}$$

where α is a parameter by which the effect of a single update step is adjusted. The gain and loss quantities identified by $\delta_{LOSS,i}$ e $\delta_{GAIN,i}$ were chosen in order to be proportional to the current distance of the AM_i feature from the desynchronization threshold identified by the quantity $\varphi \cdot \sigma_{OFF,i}$. At each analysis step the feedback value was computed as follows:

$$\begin{aligned} \mathrm{AM}_{tot}(t) &= -(\bar{\mathbf{x}}_{OFF}(t-1) - \mathbf{AM}(t)) \times \\ &\quad \times \left(\frac{\mathbf{w}(t-1)}{\sum_i w_i(t-1)} \right)^T \end{aligned}$$

where $\bar{\mathbf{x}}_{OFF} = \{x_{OFF,i}\}$, $\mathbf{AM}_{OFF} = \{\mathrm{AM}_i\}$ and $\mathbf{w} = \{w_i\}$. The current feedback value was finally scaled according to the variability of a reference population. This latter was incrementally evaluated during the idling phase, corresponding to the first three seconds of each epoch.

RESULTS AND CONCLUSION

We evaluated the performances of the proposed method by comparing relevant frequencies, identified by means of an offline method, with the weights assigned to each signal component and using the presented incremental solution. The offline method consisted in the maximization of the mutual information [2] values obtained by analyzing the output of a supervised classifier. This was based on a linear discriminant analysis which used as features the RMS amplitudes, evaluated on 4 Hz bands centered on the 6–28 Hz frequency range. It is worth noting that the values of mutual information, identified using the offline method, reflected the values of the final weights computed incrementally on the same dataset (Figure 3).

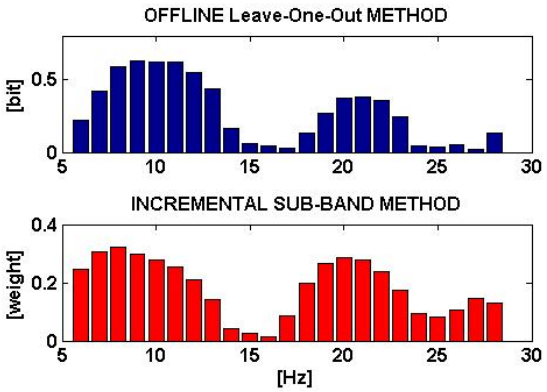

Figure 3: The results of the two methods applied on the training dataset correspondent to subject S1

We evaluated the time courses of the mutual information (MI) computed from the difference of the feedback outputs from channel C3 and C4 from the whole dataset (Figure 4). In spite of the incremental method settling time, the MI obtained with no a-priori knowledge regarding the subject relevant frequencies, reflects the time course obtained with the reference method on predetermined optimal frequencies.

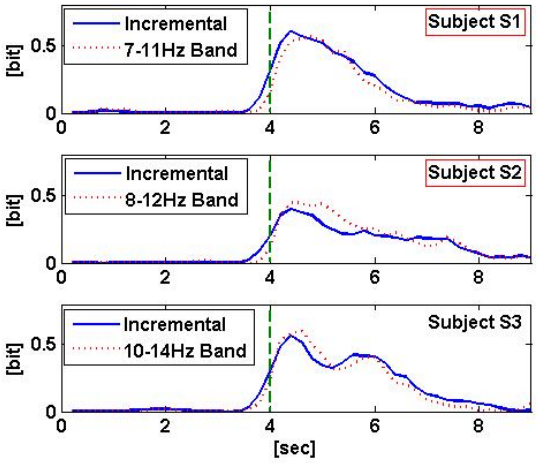

Figure 4: Time courses of mutual information obtained both with the proposed incremental method (continuous line) and the relevant band method (dotted line)

ACKNOWLEDGEMENT

This work was partially supported by a grant from IIT and a grant from ST Microelectronics.

REFERENCES

[1] Clochon P, et al. A new method for quantifying EEG event-related desynchronization: amplitude envelope analysis. Electroenceph Clin Neurophysiol, 1996; 98: 126–129.

[2] Schlögl A, Neuper C, Pfurtscheller G. Estimating the mutual information of an EEG-based Brain-Computer-Interface. Biomed Tech, 2002; 47(1-2): 3–8.

A FUZZY LOGIC CLASSIFIER DESIGN FOR ENHANCING BCI PERFORMANCE

P. Herman, G. Prasad, T. M. McGinnity

School of Computing and Intelligent Systems, Intelligent Systems Engineering Laboratory, Ulster University, Magee Campus, Derry, BT48 7JL, N. Ireland
E-mail: p.herman@ulster.ac.uk

SUMMARY: This work is aimed at enhancing inter-session performance of Brain-Computer Interface (BCI) classification. The effective handling of uncertainties associated with changing brain dynamics is considered to be a key issue. Since fuzzy logic (FL) has been recognized as a functional and well-suited approach to capturing the effects of uncertainty, the research has been concentrated on the development of an FL classifier for a BCI system. The emphasis is placed on type-2 (T2) FL methodology that has recently shown a higher potential in dealing with uncertain data than its classical type-1 (T1) FL counterpart. In this work a case study was conducted using ECoG recordings made available as part of BCI competition III. Due to the high dimensionality of the signal, two-stage feature selection was devised. The overall performance of the developed BCI was assessed in off-line simulations based on the classification accuracy (CA). Comparative analysis of the designed T2FL and T1FL systems suggests that T2FL has superior capability in effective dealing with inter-session variability of the ECoG dynamics in the given subject.

INTRODUCTION

Despite intensive research in the BCI area, there are still problems impeding the advancement of practical applications. One of the challenges is the effective handling of uncertainties associated with variability in brain dynamics. This research deals with some aspects of this problem at the level of a classifier. The case study reported here is based on two-session electrocorticogram (ECoG) recordings provided as part of the BCI Competition III. The principal objective set by the organisers, which was to devise a classifier maintaining high level of classification accuracy (CA) over more than one session recorded with a few days' interval without re-training, constitutes the essence of the BCI enhancement attempted in this work. The problem of inter-session BCI generalisation has been tackled with varying degree of success. Schlögl et al. [4] made an attempt to assess the effect of non-stationarities and long-term variability of the brain dynamics on the performance of a BCI system. The multi-session data analysis confirmed the existence of long-term changes that could not be effectively handled by the multi-session linear discriminant analysis (LDA) classifier. Similarly, the results of two-session experiments reported in [1] showed a significant drop in the CA obtained on session II with session I used as training data. There has been some research performed on adaptive BCI classification [5, 6] aimed at reducing the effect of spontaneous EEG variations. In most cases, these classifiers are designed under the assumption of a specific feature distribution to handle within-session changes, which leads to their frequent adjustments.

In this work off-line analysis was undertaken to illustrate the concept of a multi-session BCI classifier that can function effectively without a mechanism of adaptation. To this end, fuzzy logic (FL) methodology was employed due to its distinctive capabilities in capturing the effects of non-deterministic variations described in uncertainty terms [3]. Recently, the type-2 (T2) FL, has emerged as a powerful approach to handling more than static imprecision in data [3].

MATERIALS AND METHODS

Data: The ECoG trials were recorded from one subject performing imagination of left small finger and tongue movement using 8×8 ECoG electrode grid in two sessions, 276 and 100 trials, with a week-long interval. Each trial was recorded with a sampling rate of 1000 Hz for 3 s.

Feature Analysis: To begin with, three types of features were extracted from the 64-channel signal. They were calculated independently in 3 overlapping time windows (window length of 1040 samples and overlap of 80 samples) and concatenated within channels to represent a 64-dimensional trial. First, power in the frequency bands adjusted to individualised ERD/ERS features [1] was estimated using the short time Fourier transform (STFT). Second, the corresponding wavelet packets coefficients were evaluated with Symlet-8 mother wavelet. Thirdly, reflection coefficients of an autoregressive (AR) model of order 4 were extracted.

The following feature selection procedure was then applied: First, channel selection was tackled using Fisher discriminant analysis, which led to the reduction to 12 channels with the most discriminative properties. Next, a genetic algorithm was applied to select a type of feature sub-vector (**STFTf**, **WPf**, **ARf**) assigned to each of the 12 channels. The cost function was the mean CA of 4-fold cross-validation (CV) on session I. As a result, only 4 channels were assigned a feature sub-vector:

$$\mathbf{V} = \left(\mathbf{STFTf}^{ch_{i_1}}, \mathbf{STFTf}^{ch_{i_2}}, \mathbf{ARf}^{ch_{i_3}}, \mathbf{WPf}^{ch_{i_4}}\right)$$

Fuzzy Classification: The results of off-line analysis with classification in a given feature space being made at the end of every trial are reported. The emphasis

is laid on T2FL approach and the results of its application are compared with that of T1FLS and LDA in terms of CA.

The concept of T2 FL is based on fuzzy sets (FSs) that are themselves fuzzy. Instead of being two-dimensional, a T2 FS is three-dimensional with the two-dimensional domain of support for membership functions called a foot of uncertainty (FOU) [3]. In this work, the simplified approach of the Interval T2 (IT2) FSs [3] with constant membership function over the FOU was adopted.

The fuzzy classifier was designed in two steps: an initial structure was found and then its parameters were tuned. The signal features representing ECoG trials and the corresponding class labels were clustered using the multi-pass version of a mapping-constrained agglomerative (MCA) algorithm developed in this work [2]. This allowed for maintaining the consistency in the input-output space mapping and led to enhancement of the performance of the T2FLS-based classifier.

The clusters in the input-output space, defined by the means ($\mathbf{m_{INP}}$, m_{OUT}) and standard deviations ($\mathbf{s_{INP}}$, s_{OUT}), were translated into T1 fuzzy rules. The consequent FSs were singleton corresponding to class labels equal to m_{OUT} ($s_{OUT} = 0$). Next, T2 fuzzy rule-base was formed by replacing T1 FSs with T2 FSs in each rule:

$$\text{IF } R_1 \text{ is } \tilde{A}_1 \text{ AND } \ldots \text{ AND } R_n \text{ is } \tilde{A}_n$$
$$\text{THEN class is } C = [c_{left}, c_{right}]$$

where $R_1, \ldots, R_n$ are the fuzzified components of an input feature vector $\mathbf{V}$, n is their number and $\tilde{A}_1, \ldots, \tilde{A}_n$ denote IT2FSs with uncertain means [3] that model rule antecedents and C is the centroid of the consequent T2FS representing the class that the input feature vector is assigned to. The antecedent Gaussian IT2 FSs are described by pairs of means, $m_1^{(i)}$ and $m_2^{(i)}$, plus the standard deviations $s^{(i)}$ $(i = 1, \ldots, n)$, and the consequents are characterized by two points, c_{left} and c_{right}. Thus, additional parameters, $\mathbf{\Delta m}$ and Δc, were introduced to define a T2 fuzzy rule:

$$\mathbf{m_1} = \mathbf{m_{INP}} - \mathbf{\Delta m}, \quad \mathbf{m_2} = \mathbf{m_{INP}} + \mathbf{\Delta m}, \quad \mathbf{s} = \mathbf{s_{INP}},$$
$$c_{left} = m_{OUT} - \Delta c, \quad c_{right} = m_{OUT} + \Delta c$$

The parameters $\mathbf{\Delta m}$ and Δc determined the initial bounds of the uncertainty modelled. They were selected in combination with the learning process by an extensive search in 4-fold CV setup over session I.

The parameters of the initial FSs were tuned in the next step. The training algorithm implements the concept of gradient-descent with the mean-square error to be minimised. The enhanced version of a classical learning algorithm for FLSs [3] was developed in this work, which increased the computational efficiency [2].

RESULTS AND DISCUSSION

Selection of the classifiers' initial parameters and estimation of their overall efficacy was performed using a 4-fold CV on session I data. The mean CA rates with 95 % confidence intervals (CI) are reported in Table 1.

Table 1: Comparative analysis of BCI classifiers

	Session I – CV CA ± 95 % CI [%]	Session II – test CA [%]
T2FLS	**82.14 ± 1.78**	**87.00**
T1FLS	81.36 ± 1.77	85.00
LDA	81.43 ± 2.29	80.00

There are no significant differences in performance between the classifiers on the training session I. They accommodated within-session variability of ECoG features to a comparable extent. Next, LDA along with the T2FLS and T1FLS in their optimal initial configurations were trained on session I and tested on session II in one pass. The purpose of this analysis was to assess session-to-session performance transfer of the classifiers. The results presented in Table 1 demonstrate superior capabilities of the T2FLS in accounting for changes in the dynamics of ECoGs recorded at distant times from the given subject. This is in accord with the outcome of similar analysis for EEG-based BCI [2]. However, the enhancement achieved here by exploiting T2FL methodology is less substantial when compared to the T1FLS's performance. It is hypothesised that this effect can be due to lower degree of noise and artefacts contributing to both short and long-term changes in stochastic properties of the ECoG dynamics.

CONCLUSION

The ECoG case study analysed in this work demonstrated the potential of FL approach to handling inter-session variability of the signal characteristics. More subjects and more sessions have to be examined in order to validate these findings.

REFERENCES

[1] Guger C, Edlinger G, Harkam W, Niedermayer I, Pfurtscheller G. How many people are able to operate an EEG-based brain-computer interface (BCI)? IEEE Trans Neural Sys Rehab Eng, 2003(6); 11(2): 145–147.

[2] Herman P, Prasad G, McGinnity TM. Critical Observations on Type-2 Fuzzy Logic Approach to Uncertainty Handling in a Brain-Computer Interface Design. to appear in Proc IPMU 2006, Paris, France, July 2006.

[3] Mendel JM. Uncertain Rule-Based Fuzzy Logic Systems: Introduction and New Directions. Prentice-Hall, USA, 2001.

[4] Schlögl A, Vidaurre C, Pfurtscheller G. Assessing nonstationarities in BCI data. BCI 2005 Workshop, Rensellarville, NY, USA, Jun 2005.

[5] Sykacek P, Roberts SJ, Stokes M. Adaptive BCI based on variational bayesian kalman filetring: an empirical evaluation. IEEE Trans Biomed Eng, May 2004; 51(5): 719–727.

[6] Vidaurre C, Schlögl A, Cabeza R, Scherer R, Pfurtscheller G. About adaptive classifiers for brain computer interfaces. Biomedizinische Technik, 2004; 49(1): 85–86.

USER SPECIFIC TEMPLATE MATCHING FOR EVENT DETECTION USING SINGLE CHANNEL EEG

C. J. Haw, D. Lowne, S. Roberts

Information Engineering Department, University of Oxford, Oxford, UK
E-mail: chaw@robots.ox.ac.uk

SUMMARY: A major problem with Brain Computer Interface (BCI) technology is the variability of performance when applied to multiple users. We introduce a user-specific training scheme that builds a signal template specific to each user based on EEG recordings. As a feature we use the slow cortical change associated with a movement known as the *Bereitschaftspotential* (BP) measured using one bi-polar channel placed between C3 and A1 in the 10-20 standard electrode scheme. Signal processing techniques such as embedding, median and exponential weighting filters as well as normalisation of data and simulated annealing are implemented to make the template as robust as possible. Results still indicate a large variability in performance with accuracies from 59 % up to 86 %. It is expected that the results of this classification will be most useful in a multi-feature classification scheme. The simplicity of the training protocol and the number of electrodes used for detection are useful when considering clinical application of BCIs.

INTRODUCTION

Two of the major challenges facing current BCI systems are the high subject variability in performance [1] and the complexity in practical clinical applications due to the placement and recordings of many electrodes. Here we investigate the effectiveness of a user specific detection system based on the the *Bereitschaftspotential* (BP). Previous work [2] has shown that the BP can be of value in predicting the onset of movements and hence in constructing a real-time BCI. Our system attempts detection of the movements using only one electrode channel (as opposed to 21 channels used in [2]). We present some background on the BP, our template building methods and the detection of the single trial. Results are followed by a brief discussion and conclusion.

THE BEREITSCHAFTSPOTENTIAL

The BP, also known as the readiness potential, is a slow cortical change associated with movements and movement planning. It has been suggested that the BP only materializes with exact movement synchronization over ensemble averaging, indicating the sensitivity of its presence to external noise factors. In previous experiments we have found the shape of the BP to vary considerably between subjects hence providing the motivation for a user-specific template matching system. To accurately locate the BP, synchronization of signal segments is carried out by aligning EMG signals from electrodes on the appropriate muscles.

BUILDING THE TEMPLATE

One template for each subject is obtained from four (in some cases three) trials each containing 6 movements, 3 left and 3 right. Only movements corresponding to the contra-lateral channel are used to build that channel's ensemble (a total of 12 movements per template). The raw EEG data is filtered (using an embedding filter [3]) and segmented.

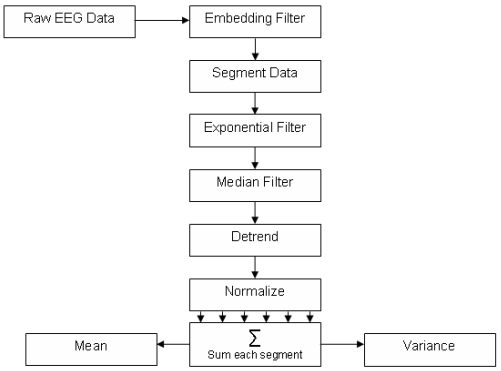

Figure 1: Information flow

The individual segments are then aligned (using concurrently-recorded EMG) and processed further using the signal processing techniques shown in Figure 1. Figure 2 shows a typical template with error bars.

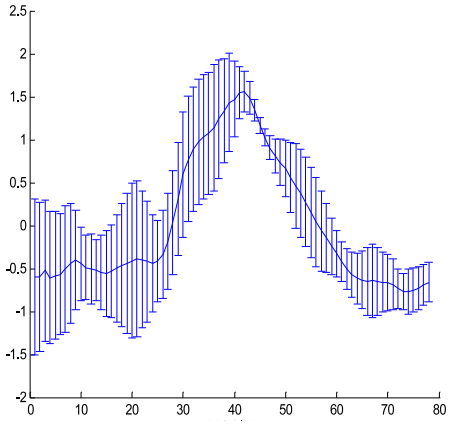

Figure 2: A typical user specific template with error bars ($f_s = 40\,\mathrm{Hz}$)

CLASSIFICATION OF A SINGLE TRIAL

We compare a window of the template and the real data based on:

Correlation & P-Values: Found by calculating the Pearson's correlation coefficients. P-values from these coefficients (using a Student's t test) give us the probability that the correlation between the two signals happened by chance based on the number of samples considered. We apply a simulated annealing to the P-value [4] to deflate parts of the signal that likely to be correlated by chance.

The error: The variance of the template, shown by the error bars in Figure 2, allows us to place more emphasis on sections of the template that match while the error bars are small. Conversely where the error bars are large we have less confidence in a match. By treating each sample in the template as an independent Gaussian distribution we can calculate the probability of each unseen point x_n being generated from a corresponding point in the template y_n using:

$$P\left(x_n|y_n\right) = \frac{1}{2\pi\sigma_n^2} e^{-\frac{(x_n-y_n)^2}{2\sigma_n^2}}$$

This probability (totaled over the window at a particular time step) is expressed as a multiplier to penalize the correlation where the error is large and to instill confidence where the error is small.

EXPERIMENTAL PROCEDURE

We test 5 different subjects (AF, AO, HH, CB, SA) asked to make actual finger movements when faced with a cue. For each subject we record 5 sets of roughly 27 s each. We record correlation, annealed P-value, confidence, and a combination value representing the product of the confidence multiplier and the P-value. Successful movement detection is regarded when the combination value is greater than 0.2 within one second before and half a second after the movement cues.

RESULTS

Figure 3 shows a typical response from the best subject AF.

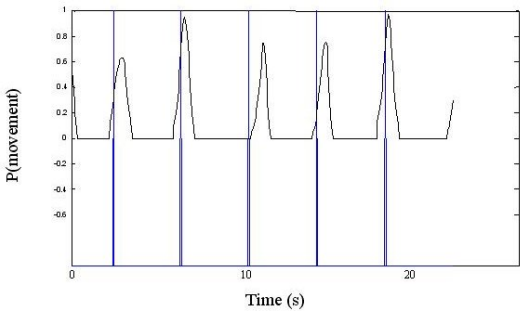

Figure 3: Probability of movement in a good subject, vertical lines are the movements.

Table 1

Subject	No. Mov	Detected +	False +	% (acc)
AF	28	24	5	86 %
HH	25	12	15	48 %
SA	23	19	9	83 %
CB	21	16	3	76 %
AO	27	16	7	59 %
TOTAL	**124**	**87**	**39**	**70 %**

DISCUSSION

Although the results show variability in performance between users it is promising to see that a single channel electrode analysis can result in good detection ($> 85\,\%$) accuracies. Further investigation using the same subjects with a different methodology is recommended in order to evaluate the effect on the method in user performance variability. The poor performances match with templates that were deemed "featureless", or simplistic resulting in a large number of false positives being detected. Having the result expressed as a probability between 0 and 1 (see Figure 3) we can easily fold our information here into a multi-feature classification scheme.

CONCLUSION

User performance variability remains evident after the application of the user-specific template matching scheme. However, in some subjects the BP has been successfully used from a single electrode analysis to predict movements with accuracy greater than 85 %, with a low false positive rate (5/24). This suggests viable use of the algorithm as part of an information fusion approach [5] to detecting movement planning.

REFERENCES

[1] Blankertz B, et al. Enhancing brain-computer interfaces by machine learning techniques. in Proc MLUI, 2003, Whistler, Canada.

[2] Krauledat M, et al. The Berlin Brain Computer Interface for rapid response. Biomed Tech, 2004; 49(1): 61–62.

[3] Haykin S. Adaptive Filter Theory (3rd Edition). Prentice-Hall, Upper Saddle River, New Jersey, 1996.

[4] Aaarts E, Korst J. Simulated Annealing and Boltzmann Machines. John Wiley & Sons, New York, 1989.

[5] Burke D, et al. A parametric feature extraction and classification strategy for BCI. IEEE Trans Neural Syst Rehabil Eng, 2005; 13(1): 12–7.

NEUROELECTRICAL SOURCE IMAGING OF MU RHYTHM CONTROL FOR BCI APPLICATIONS

M. Mattiocco[1], D. Mattia[1], F. Babiloni[1,2], S. Bufalari[1], M. G. Marciani[1,3], F. Cincotti[1]

[1]Clinical Neurophysiopathology Unit, Fondazione Santa Lucia IRCCS, Roma, Italy
[2]Dept. of Human Physiology and Pharmacology, Univ. of Rome "La Sapienza", Rome, Italy
[3]Dept. of Neuroscience, Univ. of Rome "Tor Vergata", Rome, Italy
E-mail: m.mattiocco@hsantalucia.it

SUMMARY: In the last decade, the possibility of non-invasive cortical activity estimation has been highlighted by the application of the techniques known as high resolution EEG. These techniques include a subject's multi-compartment head model (scalp, skull, dura mater, cortex) constructed from individual magnetic resonance images, multi-dipole source model and regularized linear inverse source estimates of cortical current density. The appliance of such techniques has the potential to provide a better insight on the cortical activity than scalp EEG and can be used to on-line detection of mental states from EEG signals during motor imagery tasks. This study demonstrates that is possible to estimate cortical activity, resulting from non-invasive EEG during BCI sessions, on-line and the usefulness of such estimation to improve user performances.

INTRODUCTION

It has been shown that EEG-based BCI systems display a drop of classification accuracy when more than 2 mental states have to be classified, due to bad signal-to noise ratio (SNR) [1]. An alternative method is represented by direct implants into the brain as discussed by Nicolelis [2]. In this case, we have an excellent SNR but we are confronted with all the problems in association with a highly invasive system. On the other hand, linear inverse problem solutions (LI) has the potential to provide a better insight on the cortical activity. In the present study the usefulness of LI in the context of a BCI as compared with different scalp spatial filters generally used on-line [3] is demonstrated.

MATERIALS AND METHODS

The experimental setup: Six subjects (males, mean age 30.2 ± 2.9; subjects S1 to S6) voluntarily participated to the study. They underwent a series of recording while were trained to gain control on a mu-rhythm brain computer interface (BCI2000 recording software [4]). One of the subjects (S6) was confined to a wheelchair. In BCI2000 framework hand or foot movement imagination was executed to move a cursor upward or downward respectively, towards appearing targets which covered half screen (the cursor moved horizontally across the screen at a fixed rate, while the user controlled vertical movements). EEG was recorded by using a high resolution cap with 64 channels digitized at 200 Hz and stored for off-line analysis. A subset of the 64 channels was used to control cursor movement and was re-referenced to the common average reference (CAR). Training period lasted 10 weekly sessions. At the end of training each subject gained an accuracy higher than average 75 %.

The off-line paradigm: Four different scalp spatial filtering methods, e. g. ear referenced (RAW) potentials, common average reference (CAR), Small (SL), Large (LL) Laplacian, as considered in [3], and one cortical linear inverse source estimate (LI) were compared in term of topographical and spectral analysis of R-square (R2) values, both at the beginning and at the end of CAR training: "This measure proved very useful in choosing the best spatial filter method for extracting mu- or beta-rhythm signal features" [3].

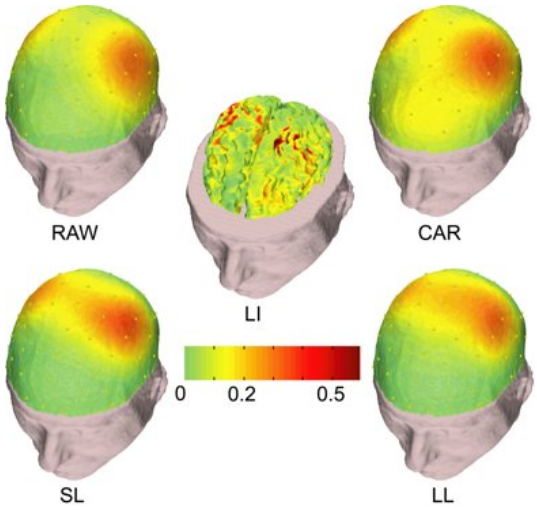

Figure 1: Topographical distributions of R-square for the spatial filters considered. All maps refer to the EEG frequency that shows the R-square peak.

The Linear inverse estimation: Sequential MR images were acquired and a three-shell realistic head models were generated with the help of the Curry 4.6 software (Compumedics Neuroscan Ltd., El Paso, Texas).With this approach, the cortical surface is tessellated into triangles and a dipolar source is modelled at each vertex (yielding about 5000 source locations). The strength of these sources was then estimated by using a linear inverse procedure according to a weighted-minimum norm approach as reported in details elsewhere [5]. Such estimation returns the pseudo-inverse transformation matrix (**G**) able to transform scalp EEG in dipoles current densities only by a matrix multiplication. **G** matrix, stored off-line can be used

on-line as an input filter of BCI2000 recording software [4].

The statistical analysis: The off-line R2 results were subjected to separate Analysis of Variance (ANOVA). The main factor of the ANOVAs was the FILTERING factor (with five levels: CAR, RAW, SL, LL, LI). Separate ANOVAs were performed on the off-line results obtained from the first and the last session of training. Moreover, post-hoc analysis with the Scheffes test was performed (significance level $p = 0.05$).

The on-line paradigm: To prove the easy utilization of LI without artefact rejection on-line, we realized an horizontal (left or right hand kinesthetic movement imagination) screening of all six subjects trained on the previous vertical task and selected the two more promising. In both cases the pseudo-inverse transformation **G** matrix stored off-line in the previous step was used as an input spatial filter for a standard recording software system as BCI2000 [4]. Since one of the more promising subject was the best vertical performer (S6), we test subject S1 and S6 with a horizontal and two-dimensional on-line tasks respectively.

RESULTS

The off-line results: All the spatial filters (CAR, RAW, SL, LL, LI) were compared by considering the maximum values of R2 taking into account the best usable feature (frequency/channel) of each subject both at the beginning and at the end of training. As showed in Figure 1 for a representative subject, all the features considered are associated with channels/dipoles above sensorimotor areas.

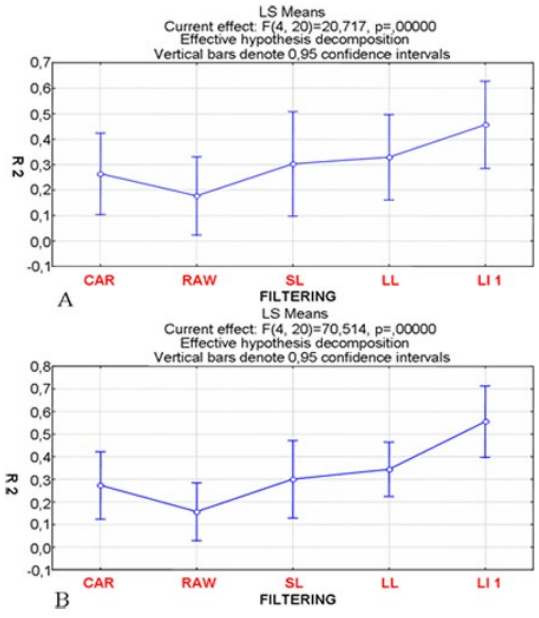

Figure 2: Spatial filters compared by average and standard deviation (on subjects) values of R2. Panel A and B take into account the first and last training session respectively.

The statistical analysis (ANOVA) revealed a strong influence of FILTERING factor on the R2 values ($p < 0.001$). This is illustrated in Figure 2 A and Figure 2 B for the first and the last training session respectively. It can be appreciated that, LI filtering procedure produces an average (on subjects) value of R2 higher than those obtained from all the other filtering methods as confirmed with a post hoc test with Scheffe's procedure.

The on-line results: Table 1 shows the on-line classification range obtained from the users in four sessions. In average, correct classifications exceed 80 % with a peak of 96 % considering the 1-dimensional task and 89 % considering the 2-dimensional task.

Table 1: On-line classification ranges obtained using linear inverse as spatial filter for BCI2000 recording software [1] for one and two dimensional horizontal task (4 sessions each)

1-D	**LI-1 on-line**	Corr. Class.	Uncorr. Class.
	MEAN	86.00 %	14.00 %
	ST.DEV	9.20 %	9.20 %
2-D	**LI-1 on-line**	Corr. Class.	Uncorr. Class.
	MEAN	80.09 %	19.91 %
	ST.DEV	7.02 %	9.01 %

DISCUSSION

The aim of this study was to to understand whether the use of cortical activity estimated from non-invasive EEG recording could be useful to improve performances in the context of a mu rhythm BCI. Furthermore, another objective was to demonstrate the on-line applicability of such method using a standard recording software (BCI2000 [4]). The data reported here suggest that LI procedure can be easily used on-line and improves performances. This can be explained with the natural ability of LI to improve signal to noise ratio as compared with scalp EEG data whatever spatial filter considered.

REFERENCES

[1] Wolpaw JR, et al. Brain-computer interfaces for communication and control. Clin Neurophysiol, 2002; 113(6): 767–791.

[2] Nicolelis MA. Actions from thoughts. Nature, 18-1-2001; 409(6818): 403–407.

[3] McFarland DJ, et al. Spatial filter selection for EEG-based communication. Electroencephalogr Clin Neurophysiol, 1997; 103(3): 386–394.

[4] Schalk G, et al. BCI2000: a general-purpose brain-computer interface (BCI) system. IEEE Trans Biomed Eng, 2004; 51(6): 1034–1043.

[5] Babiloni F, et al. High-resolution electroencephalogram: source estimates of Laplacian-transformed somatosensory-evoked potentials using a realistic subject head model constructed from magnetic resonance images. Med Biol Eng Comput, 2000; 38(5): 512–519.

AUTOREGRESSIVE SPECTRAL ANALYSIS IN BRAIN COMPUTER INTERFACE CONTEXT

S. Bufalari[1], D. Mattia[1], F. Babiloni[1,2], M. Mattiocco[1], M.G. Marciani[1,3], F. Cincotti[1]

[1]Clinical Neurophysiopathology Unit, Fondazione Santa Lucia IRCCS, Roma, Italy
[2]Dept. of Human Physiology and Pharmacology, Univ. of Rome "La Sapienza", Rome, Italy
[3]Dept. of Neuroscience, Univ. of Rome "Tor Vergata", Rome, Italy
E-mail: s.bufalari@hsantalucia.it

SUMMARY: In the context of mu-rhythm based Brain-Computer Interfaces, we present an analysis of the dependence of performance on the parameters of the feature extraction algorithm. In order to optimize user performances, we observed that a different model order value should be chosen corresponding to different EEG features used to control the system, according to the differences in the spectral power content of alpha and/or beta bands.

INTRODUCTION

In the context of Brain-Computer Interface signal processing, non-invasive data acquisition makes automated feature extraction challenging [1], since the signals of interest are 'hidden' in a highly noisy environment, so it is important to strive for robust signal processing methods that are as invariant as possible against such distortions (e. g. [2]). It was demonstrated that the spatial filtering operations improve the signal-to-noise ratio [3]. On the contrary, autoregressive modeling has been successfully used by many investigators for EEG signals analysis in BCI context (e. g. [2, 4]), but to our knowledge no clear guidelines exist on how to choose the parameters of the spectral estimation.

The aim of the present study is to perform a systematic analysis of the dependence of BCI performance on the parameters of the feature extraction algorithm, in order to improve both the accuracy and the generalization ability of the feature extraction.

MATERIALS AND METHODS

Recordings: Eight healthy subjects, 26–30 years old, participated to the study. Each subject's training consists in 6–10 recording sessions (BCI2000 software framework , D2box task with two vertical targets). Fifty-nine EEG channels, uniformly disposed on the scalp, were acquired. A subset of 1–3 channels (among C3, C4, Cz, CP3, CP4, and CPz), re-referenced to the common average reference (CAR), were used to control cursor movement. Subjects were instructed during the first session to perform hands/feet movement imagination to bring the cursor up/down. The cursor moves as a function of the amplitude of mu rhythm activity (8–12 Hz activity) or the amplitude of higher frequency (e. g. 18–30 Hz) beta rhythm activity, both focused over sensorimotor areas.

Data Analysis: A cross-comparison was performed between different autoregressive models by varying model order and the length of EEG segment data, according to the attitude of the estimated EEG segments to predict the target. Data are reported in term of topographical and spectral analysis of R^2 values, a measure proved very useful for extracting mu- or beta-rhythm signal features [2]. We evaluated performances for four epoch lengths: 200 ms, 250 ms, 500 ms and 1 s and then for the 1 s epoch length that maximize performances, according to the sampling frequency of 200 Hz, we ranged model order from a minimum of 10 to a maximum of 40, in order to approximate control signal's non parametric PSD (Welch PSD).

Simulations: Since results on real data show a dependence of optimal AR order on both scalp location and frequency of the responsive rhythms, with a strong interaction between these two variables, we reconstructed 5 different synthetic control signal's spectra that represent respectively 3 Hz alpha band desynchronization, 3 Hz or 6 Hz beta band desynchronization or the two simultaneous alpha and beta desynchronization, in order to find the differences in model order selection due to the "shape" of the control signals. For each of them we test the model order we had to select to optimize user's performances in the ideal case he had to control the system by means of the "built" synthetic signal.

RESULTS

The comparison of the distribution of R^2 values at the most responsive frequency/channel revealed that the ability of an AR spectral feature extracted from EEG data to predict the intended action, depends on the model order.

Three groups of responsive features were identified: A) Desynchronization in alpha band over bilateral sensorimotor cortex; B) Desynchronization in beta band over mesial cortex; C) Desynchronization in beta band over bilateral sensorimotor cortex. Not all subjects show the same dependence on model order.

Subjects in group A, who control the system by a desynchronization in alpha band over bilateral sensorimotor cortex (Figure 1), achieve the best performances with an higher order (between 22 and 30 depending on subject); while subjects in groups B or C, who control the system by a Desynchronization in beta band, respectively over mesial and bilateral cortex, maximize their performances by using a lower model order, from 10 to 20 among subjects.

Synthetic data confirmed real data results: in the case of desynchronization of mu-rhythm, R^2 value increase with model order from 0.32 (order 10) to 0.43 (order

32), while in the two different conditions of beta desynchronization (conditions B and C), the best order in terms of r-square maximization varied from 20 to 22 among different kind of beta desynchronization.
The use of EEG epochs of longer length produce more stable and reliable predictions. This not surprising result must be mediated with the consequent delay of the on-line feedback to the subject.

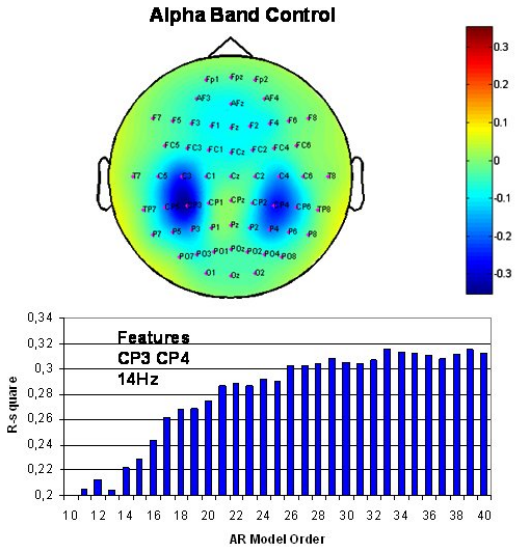

Figure 1: Topographical distributions of R^2 values for a representative subject in group A. The histogram represents R^2 peaks on control channels depending on the AR model order.

DISCUSSION

A statistical study, using about 200 training sessions, was performed to find a relationship between R^2 values, off-line computed on EEG data, and accuracy gained from users during on line sessions. According to this study the increase of R^2 value obtainable by optimizing model order selection corresponds in a different increase of performances related to the ability of the users: the increase of R^2 value we can obtain by varying model order is between 0.05 and 0.1, that means an increase of the on-line classification range from 5 % to 15 %.
These findings show that the performance of a BCI classifier can be enhanced by tuning to the individual subject the parameters for the feature extraction – a concept that is already well known for spatial selection of the features. Future work will extend this study to alternative (e. g. non-parametric) feature extraction algorithms.

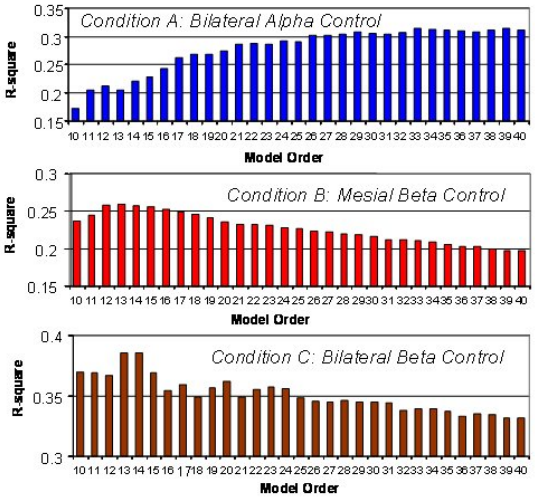

Figure 2: R^2 values varying the autoregressive model order for averaged real data in conditions A, B, and C.

REFERENCES

[1] Wolpaw JR, Birbaumer N, McFarland DJ, Pfurtscheller G, Vaughan TM. Braincomputer interfaces for communication and control. Invited Review, Clin Neurophysiol, 2002; 113(6): 767–791.

[2] Lemm S, Blankertz B, Curio G, Müller K-R. Spatio-Spectral Filters for Improving the Classification of Single Trial EEG. IEEE Trans Biomed Eng, 2005 Sep; 52(9): 1541–1548.

[3] McFarland DJ, Lynn M. McCane, Stephen V. David, Jonathan R. Wolpaw. Spatial filter selection for EEG-based communication. Electroencephalogr Clin Neurophysiol, 1997; 103(3): 386–394.

[4] Pfurtscheller G, Neuper C, Schlögl A, Lugger K. Separability of EEG signals recorded during right and left motor imagery using adaptive autoregressive parameters. IEEE Trans Rehabil Eng, 1998 Sep; 6(3): 316–325.

[5] Schalk G, McFarland DJ, Hinterberger T, Birbaumer N, Wolpaw JR. BCI2000: a general-purpose brain-computer interface (BCI) system. IEEE Trans Biomed Eng, 2004 Jun; 51(6): 1034–1043.

SELF-ADAPTING BCI BASED ON UNSUPERVISED LEARNING

J. Q. Gan

BCI Group, Department of Computer Science, University of Essex, Colchester CO4 3SQ, UK
E-mail: jqgan@essex.ac.uk

SUMMARY: This paper adopts a simple but effective unsupervised method for incrementally updating the means and variances that define LDA and Bayesian classifiers for real-time BCI. The method is evaluated using asynchronous BCI data from three subjects. Experimental results show that the proposed self-adaptation approach is stable and able to improve BCI performance consistently. This paper also aims to clarify the confusion between BCI that is capable of on-line training using true class labels and self-adapting BCI that is able to adapt without knowing true labels.

INTRODUCTION

It is well-known that EEG signals, particularly in EEG-based BCI systems, are non-stationary. The non-stationarities may be caused by the subject's brain conditions or dynamically changing environments. To some extent, a realistic BCI system has to be adaptive, even in application phases where the true labels of ongoing EEG trials are unknown.

Recent years have seen a few publications on adaptive BCI [3, 4, 5, 7, 8, 9, 10]. The adaptive BCI systems described in most of these publications are capable of on-line training or sequential learning using true class labels, but incapable of adapting without knowing true labels. Shenoy, et al. [7] have realized that "... in a realistic BCI scenario the labels of ongoing trials may not always be available; however, in some applications such as the use of a speller for communicating words, it is possible to estimate the labels a posteriori with high probability." In their paper, however, they only compared the results from on-line training using labeled data to the results from off-line training alone. Millan and Mourino [4] have also pointed out that "... online adaptation should be ongoing even when the subject's intention is not known instant by instant." They suggested that reinforcement learning techniques would be useful to address this issue, but no result on this has been reported so far. The reported adaptive BCI systems by Millan [3, 4, 5] are based on stochastic gradient descent updating of means and variances using labeled data. Adaptive BCI based on unlabeled data has been developed by Sykacek, et al. [8, 9], who used an adaptive variational Bayesian classifier. This is a kind of pseudo-supervised approach in which labels a posteriori estimated by the Bayesian classifier was used in the adaptation process. When the probability of correct estimation is not high enough, the incorrectly estimated labels would damage the parameter adaptation, similar to noise or outliers in supervised learning. Apart from adaptation of classifiers, adaptation of feature extractors is another important issue in adaptive BCI [10], but this paper will address classifier adaptation only.

This paper proposes to adopt a robust unsupervised method for updating means and variances, and subsequently adapting LDA and Bayesian classifiers for BCI applications. The method is evaluated on asynchronous BCI data, which has been used in BCI Competition III [5], in comparison with adaptation using true labels and labels estimated by classifiers.

SELF-ADAPTING BCI BASED ON UNSUPERVISED LEARNING

The basic issues in adaptive BCI systems include what to adapt, how to adapt, and when to adapt. For complicated nonlinear classifiers such as support vector machines (SVM) and other neural networks, there is no appropriate algorithm for on-line sequential learning, especially when class labels are not given. However, LDA and Bayesian classifiers have a big advantage, because they are completely determined by means and variances of the BCI data from individual classes and the number of samples from each class, which can be updated incrementally and robustly with new input data without knowing class labels. A two-pass method is necessary for accurate variance calculation, but it is not suitable for on-line or incremental updating. Some one-pass methods given in statistics textbooks for incrementally updating variances are often numerically unstable. This paper adopts the following numerically stable algorithm for updating the means and variances that define a LDA or Bayesian classifier:

Step 1: Given a new input $\boldsymbol{x}$, decide which class it belongs to by unsupervised clustering.

Step 2: If it belongs to class j, update the mean and variance of class j as follows [11]:

$$\mu_{new}^{(j)} = \mu_{old}^{(j)} + \frac{\boldsymbol{x} - \mu_{old}^{(j)}}{n_j + 1} \tag{1}$$

$$\Sigma_{new}^{(j)} = \frac{(n_j - 1)\Sigma_{old}^{(j)} + (\boldsymbol{x} - \mu_{new}^{(j)})(\boldsymbol{x} - \mu_{old}^{(j)})^T}{n_j} \tag{2}$$

where $\mu^{(j)}$ and $\Sigma^{(j)}$ are the mean and variance of the data from class j, n_j is the number of samples from class j, which will be increased by 1 after the above updating. The priors used in Bayesian classifier are estimated by $n_j / \sum_j n_j$. After the above updating, the associated LDA or Bayesian classifier can be easily updated. It can be seen that the above updating is completely incremental and instant by instant, and thus ideal for on-line BCI adaptation.

By now the issues on what to adapt and how to adapt have been addressed. As for when to adapt, a simple

solution is to adapt all the time. More delicate approaches could be based on checking the level of current classification confidence or whether there exist a trend of so-called error potentials in ongoing EEG [1, 6], or other novelty detection methods.
It should be noted that the proposed method can also be used for on-line training as in [4, 5, 7, 10] or pseudo-supervised adaptation as in [8, 9], if the class label of the new input is given from the training data or by the classifier's output. In the next section, the unsupervised learning based adaptation is evaluated in comparison with supervised and pseudo-supervised adaptation.

EXPERIMENTAL RESULTS

The data used here is for asynchronous BCI and from 3 subjects, each performing 3 mental tasks in a random order during 4 recording sessions respectively. EEG signals were recorded from 32 channels. Power spectral density (PSD) features were extracted and selected. Detailed description of data recording and preprocessing can be found in [5].

Table 1: Performance comparison of LDA (upper half) and Bayesian (lower half) classifiers using different adaptation methods

Adaption methods	Subj. 1 (%)	Subj. 2 (%)	Subj. 3 (%)	Ave (%)
None	81.80	67.19	48.17	65.45
Supervised	83.37	70.88	51.17	68.47
Pseudo-supervised	82.58	69.56	48.72	66.95
Unsupervised	83.65	69.95	50.11	67.90
None	83.50	65.45	45.70	64.88
Supervised	84.94	69.12	55.50	69.85
Pseudo-supervised	83.19	64.90	42.29	63.46
Unsupervised	84.53	66.45	49.75	66.91

The first 2 sessions from each subject were used to train off-line a LDA and a Bayesian classifier separately. The 3^{rd} and 4^{th} sessions from each subject were then used to evaluate the on-line adaptation (simulated on-line) of the trained classifiers by supervised, pseudo-supervised, and unsupervised methods respectively, in comparison with the situation of no adaptation. Using two sessions for evaluation is to test the stability of adaptation during a relatively long period. The classification rates of LDA classifiers and Bayesian classifiers on the evaluation data from the 3 subjects are given in Table 1. It can be seen that all the three adaptation methods improve the BCI performance of the LDA classifiers, but pseudo-supervised adaptation degrades the performance of the off-line trained Bayesian classifiers. Not surprisingly, supervised on-line training using true labels achieves the best result. It is interesting that unsupervised adaptation consistently outperforms pseudo-supervised adaptation, improving the performance of the Bayesian classifier for Subject 3 by over 4 %. It is also noticed that Bayesian classifiers perform better than LDA classifiers on Subject 1, but worse on Subjects 2 and 3.

CONCLUSION

Self-adaptation, without a need of class labels, is different from on-line training. The unsupervised learning approach for incrementally updating means and variances is simple but effective for self-adapting BCI, and it outperforms the pseudo-supervised approach. LDA and Bayesian classifiers are most suitable among other classification methods for adaptive BCI.

ACKNOWLEDGEMENT

The work was partly supported by the UK EPSRC under grant EP-D030552-1. The author would like to acknowledge with thanks the use of the asynchronous BCI data provided by J. del R. Millán, and thank Peter Sykacek, Steve Roberts, Carmen Vidaurre, and J. del R. Millán for useful discussions on adaptive BCI.

REFERENCES

[1] Ferrez PW, Millan JdR. You are wrong! – Automatic detection of interaction errors from brain waves. Proc IJCAI2005, 1413–1418.

[2] He X, Niyogi P. Locality preserving projections, Proc. NIPS 2003, Vancouver, Canada, 2003.

[3] Millán JdR. Adaptive brain interfaces. Communications of the ACM, 2003; 46(3): 74–80.

[4] Millán JdR, Mourino J. Asynchronous BCI and local neural classifiers: An overview of the adaptive brain interface project. IEEE Trans on Neural Syst and Rehab Eng, 2003; 11(2): 159–161.

[5] Millán JdR. On the need for on-line learning in brain-computer interfaces, in Proc. IJCNN 2004, Budapest, Hungary, 2004; 2877–2882.

[6] Schalk G, Wolpaw JR, McFarland DJ, Pfurtscheller G. EEG-based communication: presence of an error potential. Clin Neurophysiol, 2000; 111: 2138–2144.

[7] Shenoy P, Krauledat M, Blankertz B, Rao RPN, Müller K-R. Towards adaptive classification for BCI. J Neural Eng, 2006; 3: R13–R23.

[8] Sykacek P, Roberts S, Stokes M. Adaptive BCI based on variational Bayesian Kalman filtering: An empirical evaluation. IEEE Trans on Bio Med Eng, 2004; 51(5): 719–727.

[9] Sykacek P, Roberts S, Stokes M, Curran E, Gibbs M, Pickup L. Probabilistic methods in BCI research. IEEE Trans on Neural Syst and Rehab Eng, 2003; 11(2): 192–195.

[10] Vidaurre C, Schlögl A, Cabeza R, Scherer R, Pfurtscheller G. Adaptive on-line classification for EEG-based brain computer interfaces with AAR parameters and band power estimates. Biomed Tech (Berlin), 2005; 50(11): 350–354.

[11] West DHD. Updating mean and variance estimates: An improved method. Communications of the ACM, 1979; 22(9): 532–535.

SINGLE TRIAL ANALYSIS FOR ON-LINE ADAPTIVE CUE-BASED BRAIN-COMPUTER INTERFACES

C. Vidaurre[1], R. Cabeza[1], A. Schlögl[2]

[1]Dept. IEE, Public University of Navarre, Pamplona, Spain
[2]Institute of Human-Computer Interfaces, Graz University of Technology, Graz, Austria
E-mail: carmen.vidaurre@unavarra.es

SUMMARY: An alternative single-trial analysis for on-line adaptive cue-based brain-computer interfaces is presented. Usually the optimum value of the time course obtained by averaging trials was used as subjects' performance measurement. Instead we use an estimate of the most class-discriminative instants of each trial to calculate the performance of the subjects in each experimental session. The greatest separability between classes is calculated trial-based, using an estimate of the mutual information as performance measurement. This approximation is also employed to decide which samples of each trial should be used for on-line updating the classifier.

INTRODUCTION

On-line adaptive classifiers for brain-computer interfaces (BCIs) are currently a hot research topic in the field [1, 3, 4], although some kind of adaptation has always been performed in BCI systems due to the highly non-stationary nature of brain signals and more specifically, of electroencephalographic (EEG) signals.

Regarding the classification module we are interested in long-term changes that are for example caused by feedback training or tiredness. In order to deal with these variations, we have developed two adaptive classifiers, one of which is based on quadratic discriminant analysis (QDA) and the other on linear discriminant analysis (LDA). Our classifiers are parametric and are designed for cue-based synchronous systems, where the time is divided in trials, during which the subjects perform the task.

The single-trial analysis is used to analyse the subjects' performance and is specific to synchronous communication, in which the length of the trials is defined and the system knows when the trials start and end. Usually, single trial analysis is calculated as an average of the performance measurement, Mutual Information (MI, see [2]) and Error rate (ERR) at every point of time in a trial, using the most appropriate number of trials depending on the study. As a result of this analysis the time course of the selected performance measurement (ERR, MI or any other selected by the investigator) is obtained and its optimum value can be used to describe the subject's performance.

But in serveral works it has been shown that EEG is non-stationary and, therefore, the time point of most effective discrimination can change along the experiments [3, 1]. Moreover, selecting the optimum value from the single-trial analysis can be critised as the subjects' performance is described by only one specific instant. In order to solve these problems we could use the mean classification result at the window around the estimated time point of maximum class separability to calculate the performance of the subjects.

To accomplish this new single-trial analysis, we used two-class pre-recorded data from experiments performed with 3 unexperienced subjects who carried out three experimental sessions using on-line adaptive systems. The most discriminative instant of each trial was estimated and used to specify a window in which their performance was computed.

MATERIALS AND METHODS

The data used for the analysis was recorded in experiments carried out with 3 able-bodied naive subjects without previous BCI experience. They performed experiments using the "basket paradigm" with the timing shown in Figure 1. They received feedback with an on-line estimation of the best class-discrimination time in every trial.

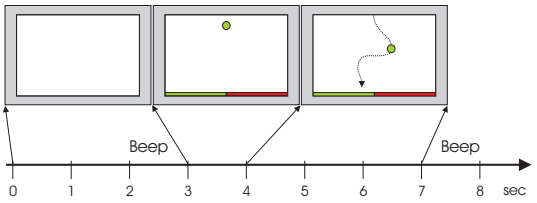

Figure 1: Timing of the experiments

The subjects conducted three different sessions, with 9 runs per session and 40 trials per run. 1080 trials were available for each of them (540 trials for each class). The system was a two-class cue-based and EEG-based BCI and the subjects had to perform motor imagery of the left or right hand depending on the cue. More specifically, they were not instructed to imagine any specific movement, but they were free to find their own strategy. They was asked to maintain their strategy for at least one run.

The estimation of the time point for the analysis was performed using an approximation of the MI. The original MI is computed using the principle of Shannon's communication theory and it is defined as the average amount of information that an observation (output) provides about a signal (input) and measured in bits. Comparing it to ERR, MI has some advantages: MI has no upper limit, indicating a large SNR, whereas ERR is limited to 0 %; ERR resolution is limited by the number of trials in consideration; and MI introduces the magnitude of the output and not only the sign.

A trial-based on-line estimation of MI ($\widehat{\mathbf{MI}}_t$) was used to determine the time when the adaptation of the classifier should start and to estimate the performance of the subject in each trial. $\widehat{\mathbf{MI}}_t$ was obtained using a moving average algorithm, see Equation 1.

$$\widehat{\mathbf{MI}}_t = \mathbf{mi} \cdot UC_{tini} + \widehat{\mathbf{MI}}_{t-1} \cdot (1 - UC_{tini}) \quad (1)$$

$$Tini = t|_{max(\widehat{\mathbf{MI}}_t)} \quad (2)$$

where $\boldsymbol{mi}$ is the output of the classifier multiplied by the class label of the current trial, and UC_{tini} is an update coefficient, the speed of adaptation of mutual information. The time when the maximum of $\widehat{\mathbf{MI}}_t$ appears is selected as $Tini$ for the next trial. The update coefficient is UC_{tini} and represents the "memory" of the process. Its value was selected by optimization over six subjects using exhaustive search due to the low number of iterations.
The subjects' performance was calculated by averaging the output of the classifier in the window selected for its adaptation in every trial with the use of $Tini$'s estimate. Therefore, one value was obtained in each trial and with the set of results of each session the ERR and an averaged MI ($\overline{MI}$) were computed.

RESULTS
Table 1 shows the subjects' performance each experimental session in terms of ERR and MI.

Table 1: Subjects' performance in each session

		Old method		New method	
Sub.	Sess.	ERR[%]	MI[bits]	ERR[%]	$\overline{MI}$[bits]
S1	Ses1	32.22	0.103	34.44	0.089
	Ses2	14.72	0.536	14.71	0.569
	Ses3	08.06	0.786	07.50	0.822
S2	Ses1	18.61	0.327	19.72	0.359
	Ses2	18.33	0.433	19.72	0.424
	Ses3	15.83	0.472	16.11	0.492
S3	Ses1	14.17	0.519	14.72	0.507
	Ses2	11.39	0.599	10.83	0.605
	Ses3	10.28	0.616	10.00	0.653

The old method refers to the optimum value of ERR and MI obtained with the traditional single-trial analysis. The new method is the single trial analysis accomplished with the estimate of $Tini$ for the calculation of both performance measurements. The results are shown for ERR and $\overline{MI}$.

DISCUSSION
Table 1 shows that the old and the new methods for single trial analysis yielded to similar results with the data recorded from three subjects. Nevertheless, it can be argued that the new method is preferable because is based on the parameter estimation used to perform the experiments; moreover, the description of the subjects' performance is not based on the selection of an optimum value which occurs in an specific instant of the trial, but on the group of samples around the estimate of the most class-discriminative moment of each trial.

REFERENCES

[1] Vidaurre C. On-line adaptive classification for brain-computer interfaces. Ph D Thesis Dp Electric and Electronic Engineering. Public University of Navarre, 2006.

[2] Schlögl A, Neuper C, Pfurtscheller G. Estimating the Mutual Information of an EEG-based Brain-Computer Interface. Biomedizinische Technik, 2002; 47: 3–8.

[3] Shenoy P, Krauledat M, Blankertz B, Rao RPN, Müller K-R. Towards adaptive classification for BCI. Journal of Neural Engineering, 2006; 3: R13–R23.

[4] Buttfield A, Ferrez PW, Millán JdR. Towards a robust BCI: Error recognition and online learning. IEEE Trans Neural Syst Rehabil Eng, 2006. To appear.

A BAYESIAN APPROACH FOR ADAPTIVE BCI CLASSIFICATION

M. Kawanabe[1], M. Krauledat[1,2], B. Blankertz[1]

[1]Fraunhofer FIRST (IDA), Berlin, Germany
[2]Technical University Berlin, Berlin, Germany
E-mail: nabe@first.fhg.de

SUMMARY: In this article, we present an adaptive classifier for BCI based on a mixture of Gaussian (moG) model of the features and a dynamical Bayesian model of the class means. We apply this approach to feedback data from the Berlin Brain-Computer Interface (BBCI). The proposed model can improve the classification performance by compensating for substantial changes of EEG signals between training and feedback sessions as well as for gradual nonstationarity in the feedback sessions.

INTRODUCTION

EEG-based BCI systems are often subject to nonstationarities that are caused by changes in the subject's mental state during an experiment (e. g. due to fatigue, change of task involvement and demands for visual processing etc.). Recently Shenoy et al. [2] showed that a simple bias recalculation for the classifier obtained from the training data can eliminate most detrimental effects of nonstationarities during feedback operation. In this paper, we propose a Bayesian version of such adaptive classifiers, where the class means are treated as random variables and their posterior distributions are approximated by a sequential manner as Kalman filters. The proposed method was applied to BBCI data collected from three subjects.

MATERIALS AND METHODS

We investigate data from a study of three subjects using the BBCI system similar to [1] but with very long feedback blocks without break. The experiments consisted of a calibration measurement and a feedback period. In the calibration measurement, visual stimuli L, R (for imagined left and right hand movement) and F (for imagined foot movement) were presented to the subjects. Based on the recorded signals, subject-specific features for the further analysis were calculated. The most discriminative frequency band for two of the three classes was selected manually by experts, and common spatial patterns (CSP) were calculated. For the data sets we analyzed, 6 (*al*), 2 (*aw*) and 4 (*VPt*) CSP channels were used, respectively. The bandpower of the CSP-projected channels was estimated using windows of 3 seconds length, and finally a linear classifier was trained by linear discriminant analysis (LDA).

In the feedback phase, bandpower estimations of CSP channels were calculated in a similar manner as in the calibration session for sliding windows of 1 second length. The real-valued output by the LDA classifier was used to move a cursor horizontally on the screen. The subjects were then using this cursor for the operation of a text input (speller) software.

We employ the following mixture of Gaussian (moG) model for each class distribution.

$$p(\boldsymbol{x}|y=1) := (1-p_p)\phi(\boldsymbol{x}|\boldsymbol{\mu}_p, \Sigma_p) + p_p\phi(\boldsymbol{x}|\boldsymbol{m}, V),$$

$$p(\boldsymbol{x}|y=-1) := (1-p_n)\phi(\boldsymbol{x}|\boldsymbol{\mu}_n, \Sigma_n) + p_n\phi(\boldsymbol{x}|\boldsymbol{m}, V),$$

where $\phi(\boldsymbol{x}|\boldsymbol{\mu}, \Sigma)$ is the Gaussian density function with mean $\boldsymbol{\mu}$ and covariance Σ. The first terms represent typical samples, while the common second term corresponds to outliers with large covariance V. Although we concentrated on the binary classification problem, the moG model also enables us to recognize outlying observations from typical samples. In the training session, we estimate the model parameters, i. e., the mean ($\boldsymbol{\mu}_p$, $\boldsymbol{\mu}_n$, $\boldsymbol{m}$) and the covariance (Σ_p, Σ_n, V) of each Gaussian prototype, their outlier ratios (p_p, p_n), and the class probability ($\pi := p(y=1)$) by EM algorithm with an extra restriction to keep the covariance V of the outlier large.

To cope with the difference of EEG signals between training and feedback and the gradual non-stationarity in the feedback session we assume that the centers of both classes are random variables and subject to the dynamical model ($t \geq 1$)

$$\boldsymbol{\mu}_p(t) = \boldsymbol{\mu}_p(t-1) + \epsilon_p(t)$$

$$\boldsymbol{\mu}_n(t) = \boldsymbol{\mu}_n(t-1) + \epsilon_n(t)$$

where $\epsilon_p(t) \sim N(\boldsymbol{0}, \Delta_p)$, $\epsilon_n(t) \sim N(\boldsymbol{0}, \Delta_n)$. The initial means are also assumed to be Gaussians centered at the estimators from the training session, i. e. $\boldsymbol{\mu}_p(0) \sim N(\widehat{\boldsymbol{\mu}}_p, \Gamma_p)$ and $\boldsymbol{\mu}_n(0) \sim N(\widehat{\boldsymbol{\mu}}_n, \Gamma_n)$, respectively. The covariances Δ_p, Δ_n, Γ_p and Γ_n control the speed of adaptation and should be chosen according to the magnitude of the initial covariances. The center $\boldsymbol{m}(t)$ of the outlier class is fixed at the average of the positive and negative classes. The required parameters are determined on the training data.

When the samples and the labels $\mathcal{D}_t = \{\boldsymbol{x}_\tau, y_\tau\}_{\tau=1}^t$ up to t-th trial are observed, we infer the posterior distribution $p(\boldsymbol{\mu}_p(t), \boldsymbol{\mu}_p(t)|\mathcal{D}_t)$ by a sequential scheme as Kalman filter. However in contrast to the case in Kalman filters, the posterior is not Gaussian in our moG model. Hence, we approximate it by a single Gaussian distribution with the same mean and covariance. We construct a classifier based on the posterior distribution in order to predict the label of the $(t+1)$th trial from the inputs. In this study we adopted the classifier based on the posterior probability of the typical positive minus that of the typical negative class, i. e. $f_t(\boldsymbol{x}) := P(y=1, z=0|\boldsymbol{x}, \mathcal{D}_t) - P(y=-1, z=$

$0|\boldsymbol{x}, \mathcal{D}_t)$, where the latent variable z equals 1 if the sample is an outlier and 0 otherwise.

RESULTS

In our Bayesian framework, the posterior distributions of the class means $\boldsymbol{\mu}_p(t)$ and $\boldsymbol{\mu}_n(t)$ are approximated by Gaussians. In order to visualize the nonstationarity of the data infered by the moG model, we plotted the time course of the posterior means in Figure 1, where the horizontal axis is the direction of the original classifier.

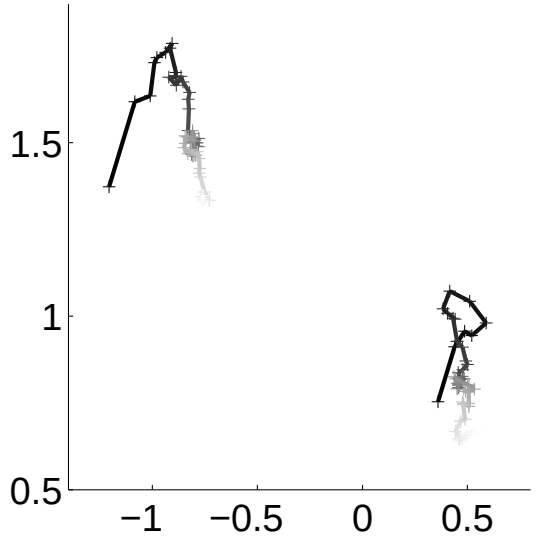

Figure 1: Time course of the class means. The posterior means of the random variables $\boldsymbol{\mu}_p(t)$ and $\boldsymbol{\mu}_n(t)$ for the subject *aw* were plotted so that the horizontal axis coincides with the direction of the original classifier.

Time is indicated by gray scale (black to white). At the beginning, because less information about the class means $\boldsymbol{\mu}_p(t)$ and $\boldsymbol{\mu}_n(t)$ is available, the posterior means can move by a large amount, while the changes get smaller as more trials are performed. For the subject *aw*, although the mean of the positive class again comes closer to the estimator from the training data after feedback learning, that of the negative class seems to stay away from the original estimator. This is the reason why classifier modification in the feedback session can improve the performance.

In Table 1, we compare the classification error in the feedback sessions of our approach (ADB) with the error of the original classifier (ORIG). ADB was much better for subject *aw*, equal for *VPt* and worse for *al*.

Table 1: Comparison of classification errors (window-wise, the feedback error in the BCI task was lower)

	ORIG	ADB
al	10.5	13.4
aw	22.5	9.0
VPt	18.5	18.3

DISCUSSION

The number of data sets limits the interpretation of our results so we can only speculate. In line with the results of [2], one possible reason for the difference in relative performance could be that the features which are extracted by the BBCI are often not strongly affected by nonstationarities (*al*, *VPt*). Accordingly adaptive methods can improve only for some datasets (*aw*). Another observation is that the in/decrease of performance correlates with the number of features. It could be that some parameters in the more complex method ADB are not accurately estimated. This issue and possible remedies are subject to further research.

REFERENCES

[1] Blankertz B, Dornhege G, Krauledat M, Müller K-R, Kunzmann V, Losch F, Curio G. The Berlin Brain-Computer Interface: EEG-based communication without subject training. IEEE Trans Neural Syst Rehabil Eng, 2006; 14(2) (in press).

[2] Shenoy P, Krauledat M, Blankertz B, Rao RPN, Müller KR. Towards adaptive classification for BCI. J Neural Eng, 2006; 3: R13–R23.

ONLINE CLASSIFIER ADAPTATION IN HIGH FREQUENCY EEG

A. Buttfield, P. W. Ferrez, J. del R. Millán

IDIAP Research Institute, Rue du Simplon 4, 1920 Martigny, Switzerland
E-mail: anna.buttfield@idiap.ch

SUMMARY: In recent years a number of non-invasive Brain-Computer Interfaces have been developed that determine the intent of a subject by analysing the Electroencephalograph (EEG) signals up to frequencies of 40 Hz. The use of high frequency EEG features have recently been proposed as alternative or additional features in EEG-based BCIs. In this paper we examine the performance of several feature bands, and evaluate the performance on online classifier adaptation on these features. Our analysis shows that the higher frequency band perform very well under online classifier adaptation for all the frequency bands, particularly for the higher bands.

INTRODUCTION

EEG-based BCIs have inherent instability due to the variation in EEG signals over time. Choosing more stable features is one way of reducing this variation. A different approach is to continually adapt the classifier as it is being used, in order to keep it tuned to the signals of the current session. Of course, ideally we would like the features that we are using to be as stable as possible so that the minimum possible adaptation is used. To this end we are investigating frequency bands higher than those traditionally used in BCIs. A comparison between different frequency bands has been performed by Ferrez et al. [1]. This paper investigates the performance of high frequency features in an adaptive classifier.

MATERIALS AND METHODS

This experimental setup is described more thoroughly in [1]. The data analysed in this paper were recorded from four healthy subjects performing three mental tasks (imagination of left and right hand movement and a language task), with EEG being recorded at 512 Hz from 64 scalp electrodes. The subjects were asked to perform each task for 5.5 seconds, of which the last 3 seconds was used in the analysis. The subjects received no feedback in order to prevent a bias towards one particular feature set. Each subject performed 15 sessions on two consecutive days, where each session comprised 18 trials with a delay of about 2.5 seconds between them.

Offline analysis was performed to determine the best feature bands as described in [1]. Fifteen feature bands of varying width were constructed by calculating the PSD over the given band, with narrower bands at low frequencies, covering the full range of frequencies from 2 Hz to 250 Hz. For each subject the 30 sessions were divided into six groups of five sessions. Feature selection was performed for each frequency band in each group to select the best electrodes. From the 64 electrodes the 10 with the highest discriminative power were chosen, creating a 10-element frequency-specific feature vector. For each group a Gaussian classifier was trained on the data from one group and tested on the five sessions of the next group.

From this analysis three frequency bands were chosen for further analysis with online classifier adaptation: 8–14 Hz, 72–90 Hz and 212–230 Hz. The online adaptation was performed on the Gaussian classifier by stochastic gradient descent (for details, see [2]). Each sample in turn was classified by the classifier, then used to update the classifier. In this analysis only the first second of every three was used to update the classifier in this way. This method of assessing the results gives us an idea of how the classifier would have performed online.

The Gaussian classifier outputs the posterior probabilities of the three classes. In general we set a minimum probability threshold level and reject samples that do not reach this confidence level. However, for the purpose of this study we are not rejecting any samples, so all samples are either classified correctly or incorrectly, making the chance level of good classifications 33.3 %.

RESULTS

Table 1 gives the classification results of the static classifier (trained on the sessions in the previous group) and the adapted classifier (initialised as the static classifier, then updated throughout the sessions) averaged over all 25 test sets of each subject, and the overall average. For all subjects and frequency bands, the adapted classifier significantly outperforms the static classifier. However, the statistical significance of comparisons between different frequency bands is less clear. When looking at the static classifier, the classification rates are similar for the three bands (the only statistically significant difference is between 8–14 Hz and 72–90 Hz), but the lower band has much smaller variation. When the adaptive classifier is used the lower band is more constantly outperformed by the higher bands (statistically significantly over the whole data set, and almost always significantly over the individual subjects), but the variation in the lower band is again much smaller than in the higher band.

Figure 1 shows the average correct decisions of the adaptive classifier over the five groups of five sessions that were used for testing. This shows the lower but more constant performance of the lower band, and the higher but more variable performance of the two higher bands.

Since the data was recorded over two days the first two groups are from the first day and the following three groups from the second day. As we are using the

data from the previous group to train the classifier, this means that the third group was trained on data from the previous day, a situation which generally results in poorer classification rates due to changes in the EEG signals. Interestingly, results obtained with online adaptation seem quite robust to this.

Table 1: Average % correct classifications of the static classifier (S) and the adapted classifier (A) for each subject (1-4), and averaged

		8–14 Hz	72–90 Hz	212–230 Hz
1	S	37.6 ± 6.1	45.9 ± 16.7	49.9 ± 20.5
	A	54.6 ± 5.8	70.1 ± 18.0	59.7 ± 22.9
2	S	51.2 ± 3.7	51.3 ± 13.0	49.3 ± 16.8
	A	58.9 ± 7.1	69.1 ± 23.5	77.7 ± 17.4
3	S	51.2 ± 3.7	47.6 ± 15.4	49.7 ± 18.0
	A	64.1 ± 8.0	78.5 ± 16.0	76.1 ± 17.7
4	S	46.0 ± 6.7	45.9 ± 14.8	49.3 ± 11.2
	A	59.0 ± 8.0	72.7 ± 17.8	83.7 ± 13.5
Av	S	45.4 ± 8.2	47.7 ± 15.0	49.5 ± 16.7
	A	59.2 ± 7.9	72.6 ± 19.1	74.3 ± 20.0

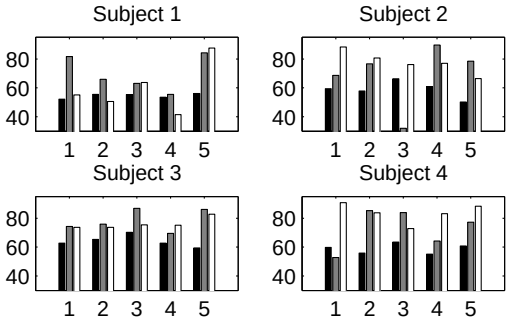

Figure 1: Performance of the adaptive classifier by group (average over 5 sessions), where the black bar is 8–12 Hz, the grey bar is 72–90 Hz and the white bar is 212–230 Hz.

Without online adaptation, classification rate of the low band on average decreased by 4.3 percentage points and the highest band dropped by 6.1 percentage points. With online adaptation the classification of the low band increased by 5.2 percentage points from the second to the third session, and the highest band dropped by only 0.2 percentage points on average (the figures for 72–90 Hz have not been quoted because of the distorting effect of the second subject on this band, where both the static and adaptive classifiers had the same very low classification rate on the third group). This indicates that the adaptive classifiers are able to incorporate quickly the signals in the new session and adjust themselves accordingly.
It is also interesting to note that the classification of the last group is often higher than the first group, especially in for the 72–90 Hz band, which might be an indication that the subject is becoming more used to the experiment and is generating more stable EEG.

DISCUSSION

The analysis in this paper demonstrated that online classifier adaptation was very effective when applied to high frequency features, as shown by the improvement in classification rates over the static classifier and the robustness to the difference in signals caused by the test and training data being from different days. The use of higher frequencies as features has potential and warrants further investigation. This analysis considered only the use of one frequency band at time and should be extended to using multiple bands together. However, while this analysis indicates that the average classification rates of the higher frequency bands are higher, particularly when used in conjunction with online classifier adaptation, the variation in the classification rates between sessions is much greater. Unless this variation is reduced it might make higher frequencies less desirable for a BCI than lower frequencies, despite their apparent promise.

ACKNOWLEDGEMENT

This work is supported by the European IST Programme FET Project FP6-003758 (MAIA) and the Swiss National Science Foundation NCCR "IM2".

REFERENCES

[1] Ferrez PW, Moles FG, Buttfield A, Gonzalez SL, de Peralta RG, and Millán JdR. High frequency bands and estimated local field potentials to improve single-trial classification of electroencephalographic signals. In Proc. of the 3rd Int. BCI Workshop & Training Course 2006 (Eds. Müller-Putz GR, Brunner C, Leeb R, Scherer R, Schlögl A, Wriessnegger S, Pfurtscheller G), Verlag TU Graz, Austria, 2006.

[2] Millán JdR, Buttfield A, Vidaurre C, Krauledat M, Schögl A, Shenoy P, et al. Adaptation in Brain-Computer Interfaces. In Towards Brain-Computer Interfacing (Eds. Dornhege G, Millán JdR, Hinterberger T, McFarland D and Müller K-R), MIT Press, Cambridge, Massachusetts, forthcoming, 2006.

AN ADAPTIVE, SPARSE-FEEDBACK EEG CLASSIFIER FOR SELF-PACED BCI

D. R. Lowne, C. J. Haw, S. J. Roberts

Pattern Analysis Research Group, Oxford University, Oxford, United Kingdom
E-mail: dlowne@robots.ox.ac.uk

SUMMARY: Generalized linear models (GLMs) are a very useful tool in data analysis. In this paper we project features from a dynamical system model of the EEG into a non-linear basis space. The responses from the basis functions are then mapped via a logistic classifier onto a class-posterior decision space. This mapping is parameterized via a set of weights which, importantly, we allow to be dynamically adaptive. This reflects our underlying belief that the EEG signals and subsequent decisions from BCI experiments are non-stationary. A sequential Bayesian learning paradigm gives a set of equations which may be implemented very efficiently via an extended Kalman filter (EKF). This paper shows that such adaptive classification gives good results and addresses the problem of running the method on data for which very few, or no, class labels are known – such as is the case for self-paced BCI experiments.

INTRODUCTION

An important problem in the field of online EEG analysis and many other online analysis problems is that of adaptive classification. The extended Kalman filter lends itself to this problem quite well due to the non-stationary nature of EEG signals. However, it is precisely this non-stationarity that renders simple linear systems ineffective in forming appropriate classifiers for BCI experiments.

The use of basis functions for nonlinear classification has been shown to be an effective method of increasing data separability [2]. Employing a Gaussian kernel to create a Hilbert expansion in this manner leads to a very effective classification system that is free of many of the pitfalls of a simple linear classifier. Using a Bayesian approach to evolve a time-dependent set of weights under a linear dynamical system yields a suitably adaptive system in the presence of a non-stationary data set [1].

In this paper, we present an extension of the dynamical linear model to accommodate adaptive and arbitrary non-linear two-class distinction when little or no feedback is available.

METHODS

Data acquisition: Using electrodes placed over C3 and C4 in the standard 10-20 placement system, one bipolar data channel was recorded at 384 Hz with a resolution of 16 bits using a g-Tec g.BSamp biosignal amplifier. Patients were prompted to perform imagined finger movements at regular intervals, though the classifier was left blind to the movement cues.

Feature extraction & basis formation: The second reflection coefficients of autoregressive (AR) models were calculated once every 54 ms using a sliding one-second long window forming a feature vector x. Using a set of Gaussian kernel functions, we created an expansion of the original feature set x

$$\Phi_t \equiv \left\{ \begin{array}{c} \vec{x}_t \\ \{\phi_j(\vec{x}_t)\} \\ 1 \end{array} \right\}$$

where $\phi_j(\vec{x}_t)$ are defined as:

$$\phi_j(\vec{x}_t) \equiv N\left(\vec{x}_t; \vec{\mu}_j, \sigma^2\right) \propto e^{-\frac{\left(\vec{x}_t - \vec{\mu}_j\right)^T (\vec{x}_t - \vec{\mu}_j)}{2\sigma^2}}$$

The location parameters $\vec{\mu}_j$ are selected once, without re-adjustments, from within the statistics of x.

EKF IMPLEMENTATION

The key variable of interest in our system is the posterior probability of movement, denoted by $\hat{y}_t$. This is obtained via a logistic regression of the form $\hat{y}_t = g(a_t)$ in which the intermediate variable a_t is given as $a_t = \vec{w}_t^T \vec{\Phi}_t$. By implementing sequential non-stationary Bayesian learning, we arrive at a set of update equations that can be implemented under the EKF framework. We begin by formulating the standard prediction and update steps of an EKF, with the latent space variable y_0 initialized to zero mean and unit variance.

Note that the weights $\vec{w}_t$ in this system, initialized to zero, are time-dependent and are evolved under a linear dynamical system as described further on.

Key to our EKF implementation is the use of quasi-targeting. This is incorporated as an extra step between the Kalman filter's prediction and update stages as described further on.

Prediction Step: The prediction step for the EKF implementation begins with calculating an adjustment value for the prior latent covariance by adding to the latter the weight diffusion vector q, initialized to 0 at time $t = 0$:

$$\Sigma_{t|t-1} = \Sigma_t + qI$$

where I is the identity matrix.

Next we calculate the latent variable $\hat{y}_t$ and its variance s_t^2:

$$\begin{aligned} s_t^2 &= \Phi_t^T \Sigma_{t|t-1} \Phi_t \\ \hat{y}_t &= \int g(a_t) p(a_t) da \approx g\left[\kappa\left(\sigma_\mu^2\right)\hat{a}\right] \end{aligned}$$

with $\kappa = 1/\sqrt{1 + \pi\sigma_\mu^2/8}$. We moderate $\hat{y}_t$ using the approximation in [3] to provide an estimate to the intractable integral.

Quasi-targeting and sparse feedback: In order to work with data in an environment where feedback is sparse, we must be able to deal with large amounts of unlabelled data. To do this, if Φ_t was generated from an unlabelled sample, we calculate from the latent variable an assumed target $z_t = \Theta\left(\hat{y}_t > 0.5\right)$, where Θ is the heaviside function

$$\Theta(x) = \begin{cases} 1 & \text{if } x \geq 0 \\ 0 & \text{otherwise} \end{cases}$$

Importantly, we consider a confidence metric $u_t = \hat{y}_t\left(1 - \hat{y}_t\right)$ on the distinction given by the latent variable. The implication of this is that when dealing with quasi-targeted data, the weight vector updates more strongly upon lower-certainty data.

Augmenting this approach, we optionally assign labels z_t to occasional samples known to have no motion planning. These labels are assigned to approximately one percent of all samples. Even in an online, asynchronous BCI system, obtaining baseline data from the user during use is a simple task, akin to displaying a "please wait" message box in a traditional graphical user interface.

Update step: Next, we assign the prior latent covariance matrix and weight vector for the next iteration of the filter:

$$\begin{aligned} \Sigma_{t+1} &= \Sigma_{t|t-1} - \left(\frac{u_t}{1 + u_t s_t^2}\right) \cdot \\ &\quad \cdot \left(\Sigma_{t|t-1}\Phi_t\right)\left(\Sigma_{t|t-1}\Phi_t\right)^T \\ \vec{w}_{t+1} &= \vec{w}_t \left(\frac{\Sigma_{t|t-1}}{1 + u_t s_t^2}\right) \Phi_t \left(z_t - \hat{y}_t\right) \end{aligned}$$

The inclusion of the value u in calculating the new covariance has the effect of contracting the area around a classification point when high-certainty data is presented to the system, and expanding the area when low-certainty data is seen. Prior to recalculating the weight diffusion vector, the latent space values must be updated according to the new weight and covariance:

$$\begin{aligned} y_t &= h\left(\underline{w}_{t+1}, \Sigma_{t+1}, 0\right) \\ \hat{u}_t &= y_t\left(1 - y_t\right) \end{aligned}$$

Finally we calculate the new weight diffusion vector:

$$q = \max\left(\hat{u}_t - u_t, 0\right).$$

If quasi-targeting was used for the most recent data point, then we add u to the new value of q, thus reflecting the calculated uncertainty of the assumed target and increasing the prior latent covariance in the next step accordingly. Obviously if a known target rather than a quasi-target was assigned to the data point, there is no need for this extra uncertainty measure in the weight diffusion vector and, by extension, the prior latent covariance for the next time step.

RESULTS

We show in Figure 1 a typical posterior class probability plot. Of principal importance are the distinct state changes from no movement ($y = 0$) to movement ($y = 1$) reflected in the posterior probability seen in relation to movement cues, denoted by brackets superimposed over the class probability plot.

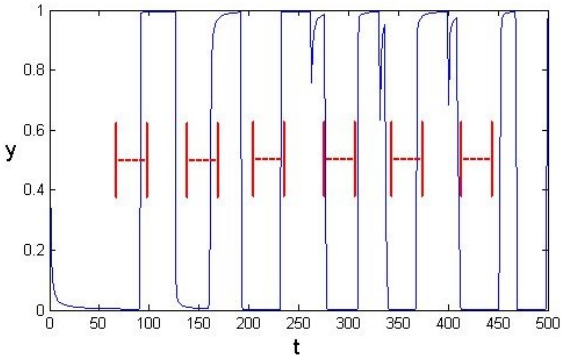

Figure 1: Posterior class probability plot in conjunction with movement cues (denoted by bracketed areas)

DISCUSSION

The $\Phi \Rightarrow y$ mapping characterized by the evolving system of weights attaches class labels to the mixture components, thus enabling localized data point classification that is relevant to the current system state. Periodic areas of no motion planning, easily solicited from the user in an on-line system and with high certainty of classification accuracy, act as a source of passive feedback to allow system parameter verification.

CONCLUSION

By evolving a series of weights tied to an EKF under a Bayesian framework, we generate a dynamic linear regressor that accurately responds to regime changes in a non-stationary data source. Moreover, by incorporating confidence-based quasi-targeting into our update equations, such a system presents an effective non-linear state classifier, well-suited to the problem of EEG classification in a self-paced BCI.

REFERENCES

[1] Bernardo JM, Smith AFM. Bayesian Theory. John Wiley, New York, 1994.

[2] Bishop C. Neural Networks for Pattern Recognition. Oxford University Press, Oxford, 1996.

[3] MacKay D. The evidence framework applied to classification. Neural Computation, 1992; 4(5): 720–736.

BRAIN STATE DIFFERENCES BETWEEN CALIBRATION AND APPLICATION SESSION INFLUENCE BCI CLASSIFICATION ACCURACY

M. Krauledat[1,2], F. Losch[3], G. Curio[3]

[1]Fraunhofer FIRST (IDA), Kekuléstr. 7, 12 489 Berlin, Germany
[2]Technical University Berlin, Str. des 17. Juni 135, 10 623 Berlin, Germany
[3]Dept. of Neurology, Campus Benjamin Franklin, Charité University Medicine Berlin, Hindenburgdamm 30, 12 203 Berlin, Germany

SUMMARY: The Berlin Brain-Computer Interface (BBCI) has been developed to transfer the main load of learning from the user to the machine. After a short calibration period of approx. 30 minutes, even untrained users with no previous BCI experience can achieve bit-rates of more than 35 bits/min. In some of these experiments, however, the classifier from the calibration period needs to be slightly adapted by adding a constant bias term to its output in order to maintain a stable performance throughout the feedback session. In this paper, we will provide evidence that a change in the brain states between calibration and feedback periods probably causes this need for adaptation.

INTRODUCTION

Operant conditioning, a classical approach to implementing BCI systems, relies on the ability of the brain to adapt to a fixed feedback application. It requires extensive training from the user to find a mental strategy which results in the desired effect in the feedback. The BBCI follows a different idea: driven by the motto "Let the machines learn", it minimizes the need for user adaptation by modifying the feedback application according to the individual brain signals, see [1]. This attempt is realized with an initial calibration ("training") period, where the users are switching between different mental states without receiving feedback from the computer. The brain signals are then used to generate a classifier which discriminates between the signals and which can then be used as the core of the feedback application.

The classification can only be successful if the brain signals produced in training and feedback session are similarly distributed, or if the change from training to feedback can be easily parameterized. It has been shown in [2] that if the distributions are sufficiently close, simple methods like adding a bias term to the classifier output can significantly increase the classification accuracy of the feedback session. In this paper, we demonstrate a change of brain states between the two sessions leading to a change in classification performance.

EXPERIMENTAL PARADIGM

For an intuitive use of the interface, imagined movements of hands and feet are used as mental states. The imagination of movements is known to entail a decreasing power in the alpha and beta frequency band of the electrodes over the corresponding motor cortex. This phenomenon is termed Event-Related Desynchronization (ERD). Since the exact location of the amplitude modulation varies strongly between subjects, a spatial filter is trained individually after each training session, projecting the data on few channels that maximize the variance for one class while minimizing it for the other class. The Common Spatial Patterns (CSP, see [3]) algorithm provides an analytical solution to this problem by simultaneous diagonalization of class-wise covariance matrices.

The study presented here comprised experiments with 9 healthy subjects. While sitting in a comfortable chair in front of a computer monitor, their EEG data was recorded using 64 electrodes. In each trial of the calibration period, one of the letters 'L', 'R' and 'F' was visually presented for 3.5–4 seconds to indicate the intended type of movement (left hand, right hand or foot). 140 trials of each target class were recorded. After training a classifier for the most discriminable pair of imagined movements, feedback was presented to the subjects. It consisted of a cursor whose horizontal position was controlled by the output of the classifier. The subjects then tried to navigate the cursor into a highlighted target. The classifier was applied to a window of the preceding 1000 ms. The data was projected on the CSP vectors, then a bandpass filter was applied and the bandpower was estimated by taking the logarithm of the variance.

Table 1: For this table, a window of 1000 ms length was extracted from each trial of calibration and feedback session. The first two rows show the classification error (in %) of the used classifier on training and feedback, respectively. The remaining rows show the neurophysiological change between these sessions. See text for details.

Subjects	TR error	FB error	Spec r^2	Alpha r
cm	16.5	19.0	1.36	0.18
cn	25.9	46.7	4.75	0.16
co	43.9	33.4	0.91	-0.08
cp	21.4	28.2	1.48	0.11
cr	29.3	35.3	3.45	0.04
ie	18.9	24.2	1.57	-0.00
cs	13.9	34.9	7.48	0.14
cu	32.9	23.0	0.66	-0.01
ct	14.3	25.0	2.79	0.00

RESULTS

Table 1 summarizes some changes that occured from calibration to test period. In 7 of 9 subjects, the classification rates in the feedback session were lower than

the performance on the trials from the calibration session. For the third row of Table 1, we calculated the squared r-value (the bi-serial correlation coefficient between the motor imagery conditions, a formula is given in [2]) of the most discriminative spectral frequency bin from the spectrum of laplace-filtered electrodes over the motor cortex. A large r^2-value indicates a high discriminability. Then we divided the resulting maximal value of the training session by the corresponding value from the feedback session. The results are greater than 1 in the same 7 subjects as before.

For the last row, the bandpower in the alpha band (8–14 Hz) has been calculated. By subtracting the values from the feedback session from the values from the training session, we calculated the r-value for each occipital electrode and averaged over all electrodes. It turns out that for 5 of the 7 subjects the average r-value is greater than zero, which proves that the bandpower during the training session is higher.

A typical subject is shown in Figure 1. The figure reveals a strong shift of alpha bandpower over the occipital electrodes and decreasing significance levels for the class discriminability.

DISCUSSION

In this series of experiments, the classification performance in the feedback session was often different from the expected accuracy. Table 1 shows that in most of the subjects the performance dropped considerably. This can be accounted to the generally lower discriminability of spectral features in the feedback session, as it has been demonstrated by comparing the most informative spectral frequency bins of calibration and application session. Therefore, the performance of every other classifier relying on spectral features would have deteriorated in the feedback session.

In the calibration session the demand for visual processing is low as compared to the feedback session, where visual attention is high. Furthermore imagining movements in the calibration session leads to high and less distributed activity in the pericentral regions. By contrast in the feedback session subjects have to follow correct effectiveness of their imagined movements by high visual attention and more distributed cortical activity. On this account as one can see in Figure 1 pericentral activity in most of our subjects in feedback condition decreases whereas occipital visual activity increases and vice versa for the calibration session.

As the brain states between training and test apparently differ strongly, it is likely that a classifier will perform better when it is adapted to the data of the feedback session.

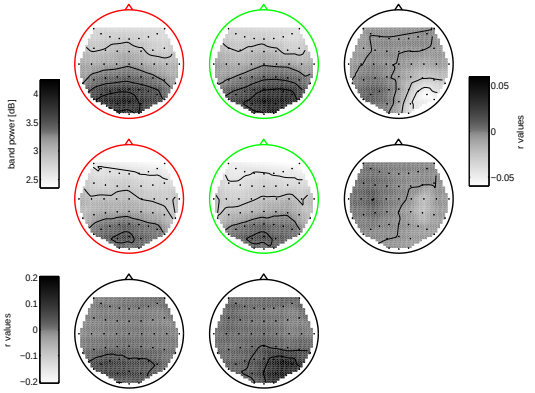

Figure 1: The differences of brain states in training and feedback condition for subject *cm*. The first row shows the bandpower during the training session for left hand (first column) and right hand (second column) movement, and the difference between these conditions in terms of r-values. In the second row, the same evaluation is made for the feedback session. The third row shows the difference between the sessions.

ACKNOWLEDGEMENT

This work was supported in part by grants of the Bundesministerium für Bildung und Forschung (BMBF), FKZ 01 IBE 01A/B and by the IST Programme of the European Community, under the PASCAL Network of Excellence, IST-2002-506778.

REFERENCES

[1] Blankertz B, Dornhege G, Krauledat M, Müller K-R, Curio G. The Berlin Brain-Computer Interface: Report from the feedback sessions. Tech Rep 1, Fraunhofer FIRST, 2005.

[2] Shenoy P, Krauledat M, Blankertz B, Rao RPN, Müller K-R. Towards adaptive classification for BCI. J of Neural Eng, 2006; 3: R13-R23.

[3] Guger C, Ramoser H, Pfurtscheller G. Real-time EEG analysis with subject-specific spatial patterns for a Brain Computer Interface (BCI). IEEE Trans Neural Syst Rehab Eng, 2000; 8(4): 447-456.

VIEWING MOTION ANIMATIONS DURING MOTOR IMAGERY: EFFECTS ON EEG RHYTHMS

P. S. Hammon[1], J. A. Pineda[2], V. R. de Sa[2]

[1]Department of Electrical and Computer Engineering,
University of California at San Diego, La Jolla, CA, United States
[2]Department of Cognitive Science,
University of California at San Diego, La Jolla, CA, United States
E-mail: phammon@ucsd.edu

SUMMARY: The mu rhythm is an 8–13 Hz oscillation which can be detected over human sensorimotor cortex in brain signals such as the electroencephalogram (EEG). This rhythm is desynchronized by movement, observing the movement of others, and imagined self movement [3]. In this study we combine motor imagery and movement observation. We show that the majority of subjects tested produce an enhanced mu desynchronization over sensorimotor cortex when motor imagery and movement observation are combined, compared to motor imagery alone.

INTRODUCTION

Both motor imagery and movement observation have been shown to decrease mu power over sensorimotor cortex (known as an event-related desynchronization or ERD) [3], and there is some speculation that these two different findings may involve the same brain system [4]. In this study, we analyze the effects on mu rhythms of combining motor imagery and movement observation. Our technique for enhancing mu ERD during motor imagery tasks may be useful for improving brain-computer interfaces based on this signal.

METHODS

Experimental paradigm: Ten healthy, right-handed volunteers participated in this study (6 male and 4 female aged 22–32 years, mean 25). Subjects were seated in a comfortable chair approximately 85 cm from a 19 inch monitor in an electrically shielded, soundproof room.

The experiment consisted of 10-second trials during which the subject performed a motor imagery task. There were two experimental conditions which differ in the stimulus presented to the subject: fixation cross (FIX) or realistic animated video of a clenching and unclenching right-hand fist (VID). Each trial consisted of a 2.5 second presentation of a fixation cross, which brightened from second 2.5 to second 3 to indicate that the active portion of the trial was about to begin. At second 3, one of the two stimuli {FIX, VID} was displayed for 4 seconds, during which the subject was instructed to imagine clenching and unclenching his or her right hand in a manner similar to the animation. The final 3 seconds of the trial consisted of a rest period with a blank screen. The two conditions were presented in random order in 7 blocks of 20 trials, with 1–3 min rest periods between blocks, for a total of 70 trials for each condition.

EEG Recording: Continuous EEG signals were recorded from 13 scalp sites located according to the 10-20 system using an electrode cap (Electro-Cap, USA). Signals were recorded using tin electrodes with a ground at AFz and a linked mastoid reference. Voltages were amplified and digitized at 500 Hz using a NeuroScan Synamps amplifier and were bandpassed from 0.3 to 50 Hz. Data were re-referenced to a common reference and the 3-second rest period was discarded. The data were visually inspected for blink or movement artifacts, and affected trials were discarded.

Analysis: Our analysis focused on electrode position C3 because of its location near the sensorimotor hand area contralateral to the imagined movement, which makes it a good choice for detecting mu ERD from motor imagery tasks [3].

Analysis was carried out in the frequency domain using Welch's averaged modified periodogram [1] for spectral estimates. Spectra for the two trial conditions were computed for the 4 second active period of each trial, while baseline spectra were computed for the first 2.5 seconds of each trial. In order to compute the mu ERD, we first determine the peak mu frequency for each subject by locating the frequency of the average peak power of the baseline period, restricted to the expected mu frequency range of 8–13 Hz. A 2 Hz wide frequency window centered about the peak mu frequency is used to compute the mu power for each trial.

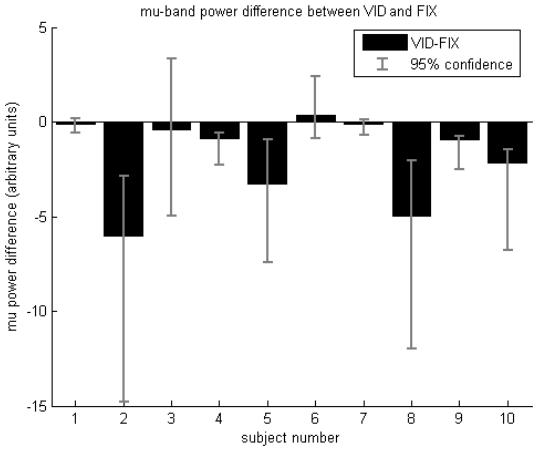

Figure 1: Mean mu power difference between conditions VID and FIX with 95 % confidence intervals. Negative values indicate enhanced mu ERD in the VID condition relative to FIX.

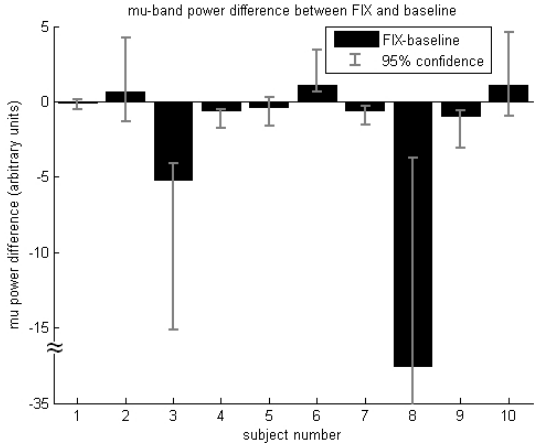

Figure 2: Mean mu power difference between FIX condition and baseline with 95 % confidence intervals. Negative values indicate enhanced mu ERD in the FIX condition relative to baseline.

RESULTS

We analyzed the effect on the mu ERD of movement observation during imagined movement by comparing mu power of FIX, VID, and baseline conditions. Our analysis used a percentile-t bootstrap [5] to compute 95 % confidence intervals on power differences. A mean difference is considered significant if the 95 % confidence interval does not include 0.

The mu power difference VID-FIX is shown for all subjects in Figure 1. 9 out of 10 subjects showed an enhanced mu ERD in condition VID relative to FIX, with statistical significance in 6 subjects. Figure 2 shows the mu power difference FIX-baseline, which indicates each subject's mu ERD for motor imagery without feedback. Comparing these figures reveals that some subjects (e. g. subjects 2 and 10) with poor ERD performance in the FIX condition show marked improvement with the addition of movement observation in the VID condition.

DISCUSSION

This study indicates that presenting realistic human motion animations during motor imagery enhances the mu ERD in most subjects. Although some subjects failed to show a significant ERD enhancement in the VID condition, no subjects displayed a significant ERD decrease, indicating that there is little negative interference from observing the video.

It may be possible to increase this effect by employing imagery and animations which are more goal-directed [2] and by exploring movement observation in virtual reality settings. It is also possible that the effect would be further increased in an online setting where the user's imagined movements affect the animated hand in real time. We intend to further explore these options and eventually use the results to improve upon current mu-rhythm-based brain-computer interfaces.

ACKNOWLEDGEMENT

This work was supported by NSF Grant DGE-0333451 to GW Cottrell, NSF CAREER Award 0133996, and the Cure Autism Now fund.

REFERENCES

[1] Hayes MH. Statistical Digital Signal Processing and Modeling. John Wiley & Sons, 1996.

[2] Muthukumaraswamy SD, Johnson BW, McNair NA. Mu rhythm modulation during observation of an object-directed grasp. Cognitive Brain Research, 2004; 19: 195–201.

[3] Neuper C, Scherer R, Reiner M, Pfurtscheller G. Imagery of motor actions: differential effects of kinesthetic and visual-motor mode of imagery in single-trial EEG. Cognitive Brain Research, 2005; 25: 668–677.

[4] Pineda JA. The functional significance of mu rhythms: Translating "seeing" and "hearing" into "doing". Brain Research Reviews, 2005; 50(1): 57–68.

[5] Wilcox RR. Fundamentals of Modern Statistical Methods: Substantially Improving Power and Accuracy. Springer, New York, 2001.

"BRAIN SWITCH" BCI SYSTEM BASED ON EEG DURING FOOT MOVEMENT IMAGERY

S. Kanoh[1], R. Scherer[2], T. Yoshinobu[1], N. Hoshimiya[3], G. Pfurtscheller[2]

[1]Graduate School of Engineering, Tohoku University, Sendai, Japan
[2]Institute for Knowledge Discovery, Graz University of Technology, Graz, Austria
[3]Tohoku Gakuin University, Sendai, Japan
E-mail: kanoh@ecei.tohoku.ac.jp

SUMMARY: EEG-based asynchronous brain-computer interface (BCI) system to realize binary switch by using simple thresholding of EEG beta band power was tested on six healthy subjects. EEG signal was measured from a bipolar channel on the vertex of the head, and was band-pass filtered, squared and smoothed on-line to extract the band power of beta oscillation. Subjects were requested to imagine foot movement, and if the band power exceeded a pre-defined threshold value, a command was generated. It was shown that two subjects out of six were able to induce bursts of beta oscillations by foot movement imagery, and binary commands could be detected in higher correct rates by these subjects.

INTRODUCTION

To provide better communication abilities to severely paralyzed patients, the EEG-based asynchronous (user-driven) brain-computer interface (BCI) that enabled binary switch by detecting the patients' foot motor imagery was studied.

We have developed a BCI to realize binary switch by detecting bursts of beta oscillation. Such a system, so called "Brain Switch", has been applied successfully to one paralyzed patient for controlling external FES (functional electrical stimulation) system [1].

In previous BCI studies, it was common to extract and classify features from preprocessed multi-channel EEG data by complex mathematical data analyses for increasing both information transfer rate and accuracy of the obtained commands. But for robust and easy–to–apply BCI for paralyzed patients, the binary switch with only a single channel would be reasonable.

In this study, the "Brain Switch" was tested on six healthy subjects to show the applicability of this system.

MATERIALS AND METHODS

Six healthy subjects took part in the experiments. From each subject, bipolar EEG (Cz-FCz) was measured by two Ag-AgCl electrodes with a forehead ground. Measured signal was amplified (sensitivity 50 μV) between 0.5 and 100 Hz with a biosignal amplifier and sampled with 250 Hz.

In the present method, the power increase of beta oscillation elicited by foot movement imagery was detected as a command. To estimate the band power of beta oscillation, signal was processed on-line by bandpass filtering (20–30 Hz), squaring and smoothing (moving average: 1 s). A white bar (power bar), whose length was propotional to the calculated power value, was displayed onto a LCD display as a feedback.

The experiments consisted of two parts. One was a free training session, in which subjects were requested to control the length of the power bar by foot movement imagery on his/her own pace. It was intended to help subjects to develop their own mental strategy for motor imagery. The other was a cue-based training session. Subjects were instructed to imagine foot movement during the presence of cue (from 0 to 6 s) onto the display, and to try and keep the length of the power bar longer during imagination.

To subjects with significant increase of beta band power during imagery, the free/cue-based training with command detection were applied. In these paradigms, the total numbers of desired/undesired detections were displayed together with the power bar. Beep signals were also presented when the events were detected as commands.

The criteria to detect events of motor imagery was as follows [1, 3]: An event was detected if the band power of beta oscillation exceeded a pre-defined threshold value for a certain time period (dwell time). To avoid undesired successive detections, refractory period was taken into account. These three parameters for command detection were initially set by ROC analysis [3], and were adjusted according to subjects' performances.

In this study, the change of beta band power due to foot movement imagery was evaluated for detecting commands. Generally, mu oscillation whose frequency range is similar to that of occipital alpha oscillation is also responsible to motor imagery. But this component was not used for detection, because it was very hard to separate it from alpha oscillation by using a single channel bipolar signal.

RESULTS AND DISCUSSION

From two subjects, significant bursts of ERS and ERD (event-related (de)synchronization [2]: increase and decrease of magnitude on specific frequency range) were observed. A weak ERD on wider frequency range (mu and lower beta bands) was observed from the rest four subjects.

An example of time-frequency map of EEG activity on cue-based training is shown in Figure 1. As shown in this figure, the following ERS and ERD components could be observed from those two subjects: (a) ERD after onset of motor imagery on lower beta band (20–25 Hz), which was related to motor planning, (b) sus-

tained ERS on upper beta band (25–30 Hz), (c) sustained ERD on mu band, (d) ERS after offset of motor imagery (rebound) on lower beta band.

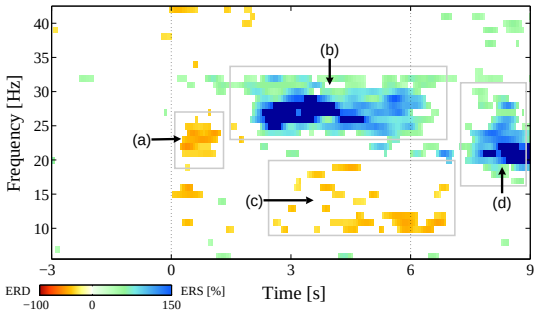

Figure 1: An example of time-frequency map of EEG activity related to foot movement imagery task during cue-based training for one subject. ERD (a and c), ERS (b and d).

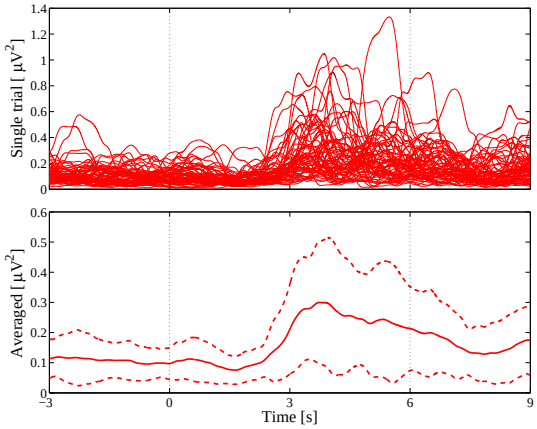

Figure 2: Single trial (upper) and averaged (lower, with standard deviation) band power of beta oscillation (25–30 Hz) induced by foot movement imagery for one subject.

Especially, the band power of upper beta range activities during foot motor imagery (b) was slightly stronger on these two subjects. The single-trial and averaged band power activities on this frequency range are shown in Figure 2 (results in Figure 1 and Figure 2 were given from the same data). As shown in this figure, an increase of upper beta (25–30 Hz) band power was observed from both single-trial and averaged activities.

The two subjects above participated in the experiments with command detection. Events were treated as true positives if it were detected during imagery period, otherwise they were treated as false positives. By these experiments, it was shown that the true events of foot motor imagery were detected with a probability of 60–90 %.

CONCLUSION

Applicability of the EEG-based asynchronous BCI system to realize a binary switch was tested on six subjects. It was shown that the bursts of EEG beta oscillations in the vertex of the head were induced by foot movement imagery on two subjects, and binary commands based on motor imagery could be detected in higher correct rates from these subjects. The present system detects foot motor imagery by simple thresholding, and it requires only one bipolar channel (three electrodes) for measurement. The “Brain Switch” would be a robust and easy–to–apply BCI system for paralyzed patients. Investigation of training effect and development of training strategies to improve the performance are left to future study.

REFERENCES

[1] Pfurtscheller G, Müller-Putz GR, Pfurtscheller J, Rupp R. EEG-based asynchronous BCI controls functional electrical stimulation in a tetraplegic patient. EURASIP Journal on Applied Signal Processing, 2005; 19: 3152–3155.

[2] Pfurtscheller G, Lopes da Silva FH. Event-related EEG/MEG synchronization and desynchronization: basic principles. Clin Neurophysiol, 1999; 110: 1842–1857.

[3] Townsend G, Graimann B, Pfurtscheller G. Continuous EEG classification during motor imagery – Simulation of an asynchronous BCI. IEEE Trans Neural Syst Rehab Eng, 2004; 12(2): 258–265.

HAPTIC FEEDBACK COMPARED WITH VISUAL FEEDBACK FOR BCI

L. Kauhanen[1], T. Palomäki[1], P. Jylänki[1], F. Aloise[2], M. Nuttin[3], J. del R. Millán[4]

[1]Laboratory of Computational Engineering, Helsinki Univerisity of Technology, Espoo, Finland
[2]Neurophysiopathology Unit, Fondazione Santa Lucia IRCCS, Rome, Italy
[3]Dept. of Mechanical Engineering, K.U.Leuven, Belgium
[4]IDIAP Research Institute, Martigny, Switzerland
E-mail: laura.kauhanen@tkk.fi

SUMMARY: Feedback plays an important role when learning to use a BCI. Here we compare visual and haptic feedback in a short experiment. By imagining left and right hand movements, six novice subjects tried to control a BCI with the help of either visual or haptic feedback every 1 s. Alpha band EEG signals from C3 and C4 were classified. The classifier was updated after each prediction using correct class information. Thus feedback could be given throughout the experiment. Subjects got better at controlling the BCI during the experiment independent of the feedback modality. Haptic feedback did not present any artifacts to the classified brain signals. More research is required on haptic feedback for BCI applications because it frees visual attention to other tasks.

INTRODUCTION

EEG signals associated to mental tasks can be classified accurately enough to be transferred into computer commands in a Brain-Computer Interface (BCI) [1, 2]. Feedback plays an important role when subjects learn to control their brain signals. Nevertheless, just a few studies have addressed the role of feedback in BCIs (see e. g. [3, 4, 5]), where only the effect of removing visual feedback from well-trained subjects [3], comparison of discrete and continuous visual feedback [4], and the use of auditory feedback has been examined [5]. To our knowledge the use of other feedback modalities, such as haptic feedback, has not been studied. The aim of this study was to compare haptic and visual feedback in a short experiment.

MATERIALS AND METHODS

Subjects: Six right-handed subjects (20–30 years).

Recordings: EEG was measured at 12 locations (international 10-20 system, sampling frequency was 500 Hz). The reference was situated between Cz and Fz.

Experimental setup: Subjects were shown a visual target either on the right, left, or upper side of a small screen. The subjects were to imagine either left or right hand movements, or do nothing (target up). The targets were changed randomly every 10–15 s. S1–S3 received haptic feedback in the first three sessions and visual feedback in the following three sessions. The order was reversed for S4–S6. Each session lasted ∼7 min.

Features: Movement-related activity (7–13 Hz) from C3 and C4 was used. FFT components were calculated from a 1 s time window, resulting in 2 channels × 7 frequencies = 14 features. The window was moved and features were re-calculated once the classifier function had finished with the previous sample (∼ every 100 ms).

Classification and Feedback: A linear model with logistic output function was used to classify the features. The model was re-trained after each new feature (∼ every 100 ms) using a maximum of 300 previous labelled samples from both classes (less in the beginning of the experiment). The iterative least squares algorithm was used to update the model parameters. Classification and training was done only when the subject was performing either the left or right task. Haptic feedback was delivered through a vibrotactile transducer driven by a custom board connected to the PC. It consisted of 100 ms of 200 Hz vibration either to the left or the right lower neck. The amplitude was set to a value that the subjects reported being clearly perceivable. Visual feedback showed for ∼100 ms an arrow on the screen either to the left or right. Feedback was given every 1 s if the averaged posterior probabilities of 10 previous predictions exceeded 70 % (S1 & S4) or 60 % (others) for either of the two classes, i. e. feedback was not given in uncertain cases. Feedback was given from the beginning of the experiment.

RESULTS

Table 1 shows the mean classification accuracy averaged over three sessions with different feedback modalities. Even during a short 42 minute experiment high classification accuracies (means 56–80 %) were possible.

Table 1: Mean classification accuracies for 3 sessions (%) (HF, VF: Haptic and Visual Feedback, respectively)

	S1	S2	S3	S4	S5	S6	**Mean ± SD**
HF	77	71	56	71	64	67	**68 ± 7**
VF	80	67	64	70	67	58	**68 ± 7**

Table 2: Average feedback time interval (s) for subjects

	S1	S2	S3	S4	S5	S6	**Mean ± SD**
HF	3	2	3	6	3	2	**3.3 ± 1.5**
VF	2	2	3	5	3	2	**3.8 ± 0.9**

Table 2 shows how often the subjects received feedback. The best subjects got on average feedback every 2 s and the worst subject every 6 s. The posterior probability threshold was higher for S1 and S4, thus

they had to perform better to get the same amount of feedback.
Figure 1 displays the classification accuracies for the individual sessions for the different subjects. No clear differences can be seen between haptic and visual feedback. Subjects S2–S6 got tired towards the end of the experiment which explains the worse results in the last session. Three out of six subjects show a decrease in classification accuracy when the feedback modality was changed. Subjects got better during the experiment irrespective of feedback modality.

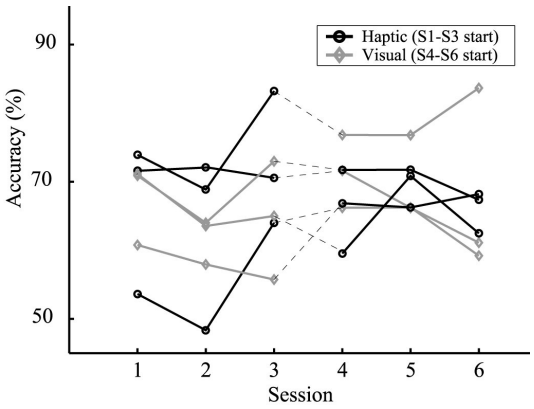

Figure 1: Classification accuracies in the different sessions

The left side of Figure 2 displays the event-related potentials for the visual (grey) and haptic feedback (black) from channel C3 and corresponding standard error. The slow somatosensory evoked potential (SEP) can be detected in all subjects at ∼200 ms. The visual feedback does not evoke any response. The right side of Figure 2 displays the corresponding spectrum (calculated using FFT for 0.5 s time window after stimulus onset). The haptic feedback does not show significant difference in the alpha band frequencies that could interfere with the classification of motor imaginary.

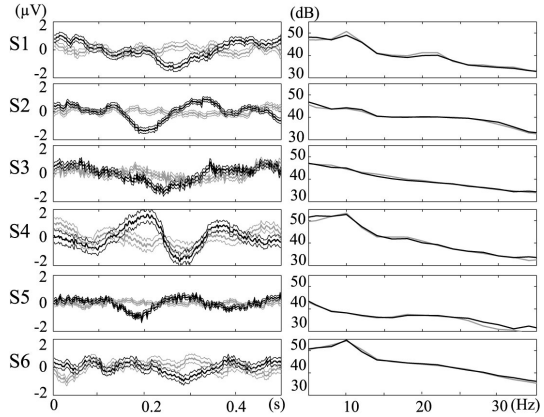

Figure 2: Left: Evoked-responses of feedback related activity (N = 200–400). Right: Corresponding spectra.

DISCUSSION

No differences were found between training using haptic or visual feedback during the 42 min experiment. Even though SEPs can be detected in the averaged signals, the haptic feedback did not interfere with the classified brain signals in the 7–13 Hz range. When asked, most subjects thought haptic feedback felt more natural. However, one subject said that it sometimes, especially during misclassifications, interfered with the imagination of movements. Visual feedback was given discretely only once a second because continuous haptic feedback was not possible due to technical difficulties. Otherwise the different feedback modalities would not be comparable.
The preliminary results of this study show that haptic feedback could be used as an alternative to visual feedback if e. g. visual attention is needed for other tasks. Haptic feedback could also be used as additional information to visual feedback. For example, when controlling an intelligent application, haptic feedback could present the user with the output of the classifier and visual feedback the control of the application. For example, in a wheelchair simulator with intelligent assistance to avoid obstacles, the movement of the wheelchair does not directly describe the classification performance. These results should be verified with more subjects. Especially the long term effects when learning to use a BCI with the help of haptic feedback should be investigated as well as the effect of discrete and continuous feedback.

ACKNOWLEDGEMENT

This work was supported by the Academy of Finland (projects 200849 and 49881), the European IST Programme FET Project MAIA FP6-003758, and the Swiss National Science Foundation NCCR “IM2”.

REFERENCES

[1] Wolpaw JR, Birbaumer N, McFarland DJ, Pfurtscheller G, Vaughan TM. Brain-computer interfaces for communication and control. Clinical Neurophysiology, 2002; 113: 767-791.

[2] Millán JdR. Brain-computer interfaces, MA Arbib (ed.) Handbook of Brain Theory and Neural Networks, 2nd ed, Cambridge, MA: MIT Press, 2002.

[3] McFarland DJ, McCane LM, Wolpaw JR. EEG-based communication and control: short-term role of feedback. IEEE Trans Rehab Eng, 1998; 6: 7-11.

[4] Neuper C, Schlögl A, Pfurtscheller G. Enhancement of left-right sensorimotor EEG differences during feedback-regulated motor imagery. J Clin Neurophysiol, 1999; 4: 373-382.

[5] Hinterberger T, Neumann N, Pham M, Kübler A, Grether A, Hofmayer N, Wilhelm B, Flor H, Birbaumer N. A multimodal brain-based feedback and communication system. Experimental Brain Research, 2004; 154: 521–526.

BRAIN-COMPUTER INTERFACE BASED ON NON-MOTOR IMAGERY

A. F. Cabrera, M. E. Lund, D. M. Christensen, T. N. Nielsen,
G. Skov-Madsen, K. D. Nielsen

Centre for Sensory-Motor Interaction, Department of Health Science and Technology
Aalborg University, Denmark
E-mail: vhooraz@hst.aau.dk

SUMMARY: We describe a brain-computer interface system based on two non-motor imagery tasks, namely auditory imagery of a familiar tune (AI) and imagination of spatial navigation (SN) through a familiar environment. 10 healthy subjects were used in this experiment and EEG activity was recorded from 18 electrodes over the temporal and parietal lobes. Features were extracted using autoregressive modeling (AR), and classification was performed with a Bayesian classifier. The two classes were differentiated with an average classification accuracy of 73 % based on the entire feature space, 69 % based on the best pair from all combinations of two electrodes and 65 % based on two optimal electrodes selected with a feature selection method.

INTRODUCTION

Motor imagery is the most commonly task used in brain-computer interface systems (BCI). It consists of imagining a movement without actually performing it, which produces changes in the EEG activity that are fairly easy to recognize. Use of motor imagery task if effectively used in BCI systems, however may be difficult for a person who has been paralyzed for several years. Also has been shown that patients with spinal cord injuries do not perform motor imagery tasks as well as able-bodied persons [1]. These facts indicate the need for BCI systems based on non-motor imagery, which feasibility has been shown by [2].

METHODS

Equipment: The EEG data acquisition was performed using the Quick-Cap EEG positioning system, the NuAmp digital amplifier and the Scan 4.3 Data Acquisition Software (Neuroscan). Data was sampled at 500 Hz using a band pass filter set to 0.1–100 Hz and a standard resolution of 32 bit.

Subjects: Ten naive healthy subjects (5 males) aged 21–28 participated in the experiment.

Imaginary tasks: Two non-motor imaginary tasks were used and subjects were instructed to perform them as follow.

1. *Spatial Navigation (SN):* The subject was instructed to imagine being in a familiar environment, scanning the surroundings noticing details while going from room to room and around rooms. The importance that the imagination involved examining the rooms rather than walking around them was stressed, as the latter could cause motor activity [2].
2. *Auditory Imagery (AI):* The subject was asked to think of a familiar tune. They were instructed to listen to it in their head, without mouthing the words or melody [2]. Well known melodies were presented to the subjects and they had to choose the most familiar one.

Electrode placement: Both hemispheres of temporal and parietal lobes were partially covered by 18 electrodes according to the extended 10-20 positioning system at FT7, T7, TP7, C5, FT8, T8, TP8, C6, P5, CP3, PO5,3, P1, P6, CP4, PO6, P4 and P2, referenced to the average between both ear lobes.

Performance of the imaginary tasks: Subjects were asked to stay still during the EEG recordings. Oral and written instructions were given to them regarding imaginary tasks. Each task was performed for 10 s and repeated 10 times with an inter-trial interval of 15 s. Tasks were performed alternatively. An external trigger marked the beginning of both tasks and warned the subject before the start of each trial with a 5 s countdown.

Signal Processing: The entire analysis was performed on segments of 1 s with an overlap equal to 0.5 s.

Pre-processing: The EEG signal was assumed to be wide sense stationary (WSS), nevertheless the 1 s segment might still nor be WSS, thus, the segments were detrended by taking the first order difference of the signal. All segments were re-referenced using common average reference (CAR), as described in [3].

Feature extraction: Autoregressive (AR) analysis was used to extract features. In this method the signal is modeled as a linear combination of the input (white Gaussian noise) and the P last outputs. The AR coefficients were found using the Burg-lattice method, which predicts the forward and backward error. The AR model order was settled to 6.

Channels selection: Two methods were used:

1. *SEPCOR:* The name stands for SEParability and CORrelation. The algorithm is based on a separability measure, $S(i)$, and a normalized correlation coefficient C, defined as follows:

$$S(i) = \frac{1}{2}\frac{(\mu_{1i} - \mu_{2i})^2}{\sigma_{1i}^2 + \sigma_{2i}^2};\ C = \left|\frac{\sigma_{ij}}{\sqrt{\sigma_{ii}\sigma_{jj}}}\right| \quad (1)$$

where μ_{ji} denotes the mean of class j on the ith component and σ_{ji}^2 denotes the variance of class j on the ith component, in the second equation σ_{ij} corresponds to the covariance between feature i and j, and σ_{ii} is the variance of feature i.

Assume the features are listed in decreasing order according to the separability value $S(i)$ (1). Then the algorithm is described as follows (as done by [5]):

(a) Select from the list the feature with highest $S(i)$ value and remove it from the list.

(b) Obtain the overall correlation C between (all) the selected feature(s) and each of those remaining in the list, and remove from the list all features which have a higher correlation value than a certain threshold (MAXCOR) with any of the selected features.

(c) If the list is not empty and more features are required, then repeat from (a).

In this study MAXCOR was settled to 0.4 and the two channels with highest separability value were chosen as feature space.

2. *Exhaustive search:* To find the two electrodes that gave the best classification all combinations of two electrodes were classified. The pair that gave the best classification was chosen.

Fisher's Linear Discriminant (FLD): Projects high dimensional data onto a line. The projection maximizes the distances between the means of the classes while minimizing the variance within each class. The orientation that separates best the two classes is chosen.
Classification: This process was performed separately for each subject. Three feature spaces (previously projected onto a line with FLD) were classified; all channels, all combinations of two electrodes (only the best pair is presented in the final results) and the 2 channels that gave best separability using SEPCOR.
Based on these reduced feature spaces, classification was performed using a Bayesian classifier. For description of this classifier see [4], chapter 2. Features were randomly separated into two equally sized test and training sets. To avoid unfortunate permutations of the features, the random-splitting procedure was repeated 40 times to generate 40 classifiers. The final results are an average of these 40 classification procedures.

RESULTS AND DISCUSSION

The classification result for each subject is reported in Table 1. The average results show a classification accuracy of 73 % ($\sigma = 6$ %) based on the entire feature based on the best two electrodes using SEPCOR. By using channels T8 and P4 for all the subjects, as done by [2], the average classification accuracy was 60 % ($\sigma = 4$ %). For electrodes pairs it was found that it was significantly better ($p = 0.02$) selecting the optimal pair of electrodes using exhaustive search for each subject compared to using the same two electrodes for all subjects.
Exhaustive search showed a slightly better classification accuracy than SEPCOR ($p = 0.01$) but a much higher computational time. The difference between using exhaustive search and all 18 electrodes was not significant ($p = 0.06$). No pattern could be observed in the chosen electrode pairs among subjects neither using exhaustive search nor SEPCOR, as seen in Table 1.

Table 1: Classification accuracy for all 10 subjects. The electrodes chosen for classification are marked with E for exhaustive search and S for SEPCOR.

	FT7	T7	TP7	C5	P5	CP3	P3	PO5	P1	P2	CP4	P4	PO6	P6	FT8	T8	TP8	C6	EXH.	SEP.	COR.	ALL
sub.1												E	S		ES				70%	67%	71%	
sub.2	E			S						E			S						62%	62%	63%	
sub.3							S	E									ES		76%	68%	77%	
sub.4	E			ES						S									64%	62%	70%	
sub.5						E				ES					S				68%	67%	71%	
sub.6		E									S		S	E					63%	60%	67%	
sub.7						S		ES	E										70%	64%	76%	
sub.8				S	S				E								E		72%	70%	83%	
sub.9		E			S				E				S						66%	61%	68%	
sub.10	S	E		S	E														77%	69%	80%	
																AVERAGE			***69%***	***65%***	***73%***	

Classification Accuracy

CONCLUSION

The two tasks investigated in this study, FT and SN, showed to have good classification accuracy, which makes them suitable for online systems. The lack of a pattern in the selection of the best two channels suggests that training sessions must be carried with a large electrodes setup to find the optimal feature space to feed the classifier, and then reduce it to the desired number of channels. For this, SEPCOR seems to be the most appropriate method since the computational time required is substantially less than for exhaustive search, giving similar results.

REFERENCES

[1] Birch G, Bozorgzadeh Z, Mason S. Initial online evaluations of the LF-ASD brain-computer interface with able-bodied and spinal-cord subjects using imagined voluntary motor potentials. IEEE Trans Neural Sys Rehab Eng, 2002; 10(4): 219–224.

[2] Curran E, Sykaceck P, Stokes M, Roberts S. Cognitive tasks for driving a brain-computer interfacing system: A pilot study. IEEE Trans Neural Sys Rehab Eng, 2003; 12(1): 48–54.

[3] McFarland D, McCane L, David S, Wolpaw J. Spatial filter selection for EEG-based communication. Electroencephalogr Clin Neurophysiol, 1997; 103(3): 386–394.

[4] Duda R, Hart P, Stork D. Pattern Classification, John Wiley & Sons, Inc., New York, 2001.

[5] Granum E. Application of statistical and syntactical methods of analysis and classification to chromosome data. In: Kittler J, Fu K, Pau L (Ed.). Pattern Recognition. Theory and Applications. D. Reidel Publishing Company, Dordrecht, Holland–Boston–London, 1982; 373–398.

CLASSIFICATION OF MOVEMENT-RELATED CORTICAL POTENTIALS ACCORDING TO VARIATIONS OF RATE OF TORQUE DEVELOPMENT DURING IMAGINARY ISOMETRIC PLANTAR-FLEXION

O. F. do Nascimento, D. Farina

Centre for Sensory-Motor Interaction, Department of Health Science and Technology
Aalborg University, Denmark
E-mail: omar@hst.aau.dk

SUMMARY: The aim of this study was to discriminate cortical activity related to different rates of torque development of imaginary isometric plantar-flexion on a single-trial basis. Electroencephalographic (EEG), electrooculographic (EOG) and electromyographic (EMG) signals were recorded while six subjects imagined two right-sided isometric ankle plantar-flexions tasks comprising moderate and ballistic rate of torque developments (RTDs). Feature extraction was based on the marginal distribution of a discrete wavelet transform with optimization of the mother wavelet. Classification was performed with a support vector machine (SVM) approach. Minimum misclassification rate from the best channel was 12 % with wavelet optimization and 17 % with Daubechies 4 wavelet.

INTRODUCTION

It has recently been shown that movement-related cortical potentials (MRCPs) are function of force-related parameters in both real and imaginary movements [1,2]. This is the basis for the use of these signals in brain-computer interface (BCI) applications.

Therefore, this study aims to identify and classify two rates of torque development (RTD) of imaginary isometric plantar-flexions on a single-trial basis using electroencephalographic (EEG) recordings. The method used for classification is based on signal-based wavelet optimization, which has shown satisfactory results with EMG signals when compared to spectral-based or catalogue wavelet-based approaches [3].

MATERIALS AND METHODS

Experimental Setup: Six right-handed healthy volunteers participated in the experiment (3 males and 3 females, mean age 24.3 years, SD 1.5 years). The experimental procedures were approved by the local ethical committee and informed consent was obtained.

The subjects were asked to perform voluntary real and imaginary right-sided isometric plantar flexion under two RTD (moderate and ballistic) ending at 60 % of the maximum voluntary contraction (MVC).

The ballistic task was defined as the attainment of 60 % MVC as fast as possible, whereas the moderate task was defined as a 4 s linear torque increase followed by a plateau of 1 s.

Each task comprised 74 and 26 trials of imaginary and real movements, respectively, randomly distributed. Trials of real movements were included to keep the subject focused on the specific motor task. Auditory warnings were sent to the subjects in order to indicate when to get ready to perform a task; with either one or two beeps indicating imaginary or real movement, respectively.

For real movements, the subjects had torque feedback on an oscilloscope which displayed an output voltage proportional to the torque exerted on a pedal instrumented with strain gauges.

For imaginary movements, the subjects were asked to imagine the movement as they recalled the experience, having compute-generated traces on the oscilloscope for visual guidance.

EEG recordings were performed with standard 10-20 system. The channels FC1, FC2, C1, CZ, C4, CP3, CP1, CPZ, P3, PZ and P4 were recorded with reference to electrodes on the earlobes (A1, A2). Vertical and horizontal EOGs were recorded as well. Surface EMG was recorded from soleus and tibialis anterior muscles.

Data Preprocessing: Only data of imaginary motor tasks were analyzed. Trials were excluded if the EMG activity exceeded by 25 % the EMG noise root mean square, estimated as average over all trials during rest periods. Trials were also excluded if the peak-to-peak EOG amplitude exceeded 75 μV in one of the four EOG channels. EEG and EOG signals were high-pass filtered at 0.25 Hz and notch filtered at 50 Hz to eliminate baseline drift and power line noise, respectively. Signal epochs of 1024 samples were used for further analysis.

Wavelet transformation: A discrete wavelet transform (DWT) was used for extracting features from EEG signals. By restriction to orthogonal wavelets and using the multiresolution analysis framework, it was possible to define mother wavelets by varying design parameters of Finite Impulse Response (FIR) filters, which are associated to the scaling and wavelet functions [4]. For feature extraction an analysis filter of length 4 was used, resulting in one free design parameter. All ten levels of wavelet coefficients were include. The optimal wavelet was selected by varying this parameter in steps of 0.1 from $-\pi$ to $+\pi$, and by estimating the classification error from a training set (supervised classification). For comparison, Daubechies wavelet with filter length 4 (DB4) was also used for classification. Further details on the actual wavelet optimization, feature extraction and classification are presented in [5].

Feature extraction: Features were obtained by computing the marginal distribution (integrating over

time) of the discrete wavelet transform [3].
Classification: A Support Vector Machine (SVM) classifier was used with cross validation procedure (3 subsets of trials) for reporting misclassification errors [6].
Statistical Analysis: The resultant misclassification rates were statistically tested with a two-way repeated measures analysis of variance (ANOVA), with channels and wavelet type (optimal vs. DB4) as within levels. Significant differences were localized by Student-Newman-Keuls (SNK) test for multiple comparisons.

RESULTS

Minimum misclassification rate was obtained in channel C4 with an average of 21.6 % ($\pm$ 8.3) with the optimal wavelet, whereas the misclassification rate with DB4 wavelet in the same channel was 26.9 % ($\pm$ 11.7). The topographical distributions of average misclassification rates over all subjects are reported in Figure 1.

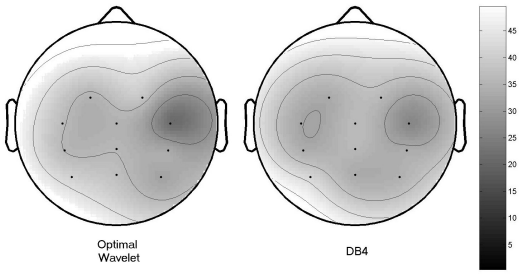

Figure 1: Topographical distributions of average misclassification rates over all subjects in case of wavelet optimization (left) and Daubechies 4 wavelet (right).

Within subjects, C4 was also the electrode that presented the lowest misclassification rate, i. e. 12 % and 17 % for optimal and DB4 wavelets, respectively.
Statistical analysis showed the results obtained with optimal and DB4 could not be differentiated, but C4 electrode showed a "close to significant" difference ($p = 0.069$). Moreover C4 electrode was significantly different from all other electrodes when using the optimal wavelet ($p < 0.05$), while for DB4 wavelet, the only significant difference was found between electrodes C4 and P3 ($p = 0.022$).

DISCUSSION

This study shows for the first time that MRCPs have a potential as control signals in BCIs, considering that variation of RTD of a same imaginary motor task can be detected in a single trial basis. The classification results obtained with optimal wavelet showed better performance than with DB4 wavelets, with an average decrease in the misclassification rate with optimization of $\sim$4.5 %. A tendency for significant difference ($p < 0.07$) was found in C4 and this electrode was significantly different from all other electrodes when using the optimal wavelet, while such a trend was not observed when using DB4 wavelet.
The lowest misclassification rates found in electrode C4 corroborates our previous findings were differentiation of average MRCPs between force-related tasks were mainly seen ipsilateral to the side of the imaginary movement [2]. Most likely, this outcome indicates a dipolar projection of the contralateral cortical site responsible for ankle/foot movements. Nevertheless, it cannot be excluded that ipsilaterality may be an effect of handedness [7], considering that all subjects were right-handed and imaginary motor tasks probably generate a diffuse cortical activity that may be strongly influenced by handedness dominance.

CONCLUSION

The results show that imaginary movements with different RTDs can be classified from EEG with a misclassification rate of $\sim$20 % in subjects without any specific training. These results are considered promising for the use of MRCPs in BCIs since training of subjects and multi-channel classification approaches are expected to further decrease the misclassification rates.

REFERENCES

[1] Do Nascimento OF, Nielsen KD, Voigt M. Relationship between plantar-flexor torque generation and the magnitude of the movement-related potential. Exp Brain Res, 2005; 160: 154–165.

[2] Do Nascimento OF, Nielsen KD, Voigt M. Movement-related parameters modulate cortical activity during imaginary isometric plantar-flexions. Exp Brain Res, 2006; 171: 78–90.

[3] Maitrot A, Lucas MF, Doncarli C, Farina D. Signal-dependent wavelets for electromyogram classification. Med Biol Eng Comput, 2005; 43(4): 487–92.

[4] Mallat SG. A theory of multiresolution signal decomposition: the wavelet representation. IEEE Trans Pattern Anal Machine Intell, 1989; 11(7): 674–693.

[5] Farina D, do Nascimento OF, Lucas MF, Doncarli C. Parameterization of wavelets for optimized signal representation in the classification of movement-related cortical potentials. 3^{rd} International BCI Workshop, Graz, Austria, Sept 22–23 2006.

[6] Saunders C, Stitson MO, Weston J, Bottou L, Schlkopf B, Smola A. Support Vector Machine Reference Manual, Technical Report, CSD-TR-98-03, Royal Holloway Univ. of London Egham UK, March 1998; http://svm.cs.rhbnc.ac.uk/.

[7] Beisteiner R, Hollinger P, Lindinger G, Lang W, Berthoz A. Mental representations of movements, Brain potentials associated with imagination of hand movements. Electroencephalogr Clin Neurophysiol, 1995; 96(2): 183–93.

EFFECTS OF MULTIMODAL USER INTERFACE IN BCI PERFORMANCE

R. Ron-Angevin, A. Díaz-Estrella.

Dpto. Tecnología Electrónica. University of Málaga, Málaga, Spain
E-mail: rra@dte.uma.es

SUMMARY: A multimodal interface such as virtual reality can combine 3D display and sound, improving BCI feedback presentation to help subjects to get better control of EEG signals. This paper describes a BCI system based on virtual reality techniques to provide feedback with more immersive and motivating effect. Preliminary results suggest that EEG behaviour can be modified via feedback presentation.

INTRODUCTION

A brain-computer interface (BCI) is based on the analysis of the electroencephalographic signals (EEG), recorded during certain mental activities, to control an external device. One of its main uses could be in the field of medicine and especially in rehabilitation. It helps to establish a communication and control channel for people with serious motor function problems but without brain function disorder.

Performance of BCI will depend, especially, on the ability of subjects to control their EEG patterns. Appropriate training is very important, which can sometimes take up to several months [1]. It is also very important to provide some type of feedback allowing subjects to see their progress [2].

Nowadays, conventional systems of feedback are based on cursor control and horizontal bar extension. Due to the lengthy training in BCI systems, this type of feedback may result tiring or somewhat boring, leading to a lack of motivation [2]. In order to improve the effectiveness of the training process and reduce training time, feedback needs to be attractive, thus motivating subjects to control their EEG signals. For this, as proposed in [3], a good option is the use of techniques based on virtual reality (VR), combining 3D display with sophisticated graphics and sound. Using these techniques, a more natural interaction can be achieved, providing a more immersed and motivating environment.

The purpose of this paper is to continue the work developed in previous research [4] in which subjects were trained using a BCI system based on virtual reality techniques and had to act within a familiar environment, such as controlling a car to avoid puddles. The obtained results showed how subjects were motivated throughout the feedback period to control the car's movement to avoid the puddle, achieving a good control of EEG signals. However, a worsening of this control was noticed during the last second of feedback, probably due to the fact that subjects did not make an effort when they realised the puddle was almost behind them. In the study presented in this paper, the same BCI system has been used but different obstacles (walls, logs and ramps) are incorporated at the end of the puddle with the purpose of improving the control of the BCI.

MATERIALS AND METHODS

Signal recording and signal processing: The EEG was recorded from two bipolar channels with electrodes placed over the right and left hand sensorimotor area. The signal processing includes EEG feature extraction and classification. The feature extraction consists of estimating the average band power of each channel in predefined, subject specific reactive frequency, and the classification is based on linear discriminant analysis.

Training protocol: The training protocol consisted of different training sessions, combining sessions with no feedback and sessions with continuous feedback. During each session, subjects were instructed to carry out 160 trials. The duration of each trial was 8 seconds. The training was carried out discriminating between two mental tasks: a relaxed state and imagined right hand movements.

Trial time: Subjects were to carry out some trials, the timing of which is shown in Figure 1. In a scene of continuous movement, initially the car would be moving in the middle of three lanes. At 2 s, a puddle, in the left or right lane, would appear at the end of the road. If this appeared in the left lane, subjects should imagine right hand movements. If it appeared on the right, they should remain in a relaxed state. At 4.25 s, the puddle was situated beside the car, starting the feedback period when subjects were able to control the car to avoid the puddle and the obstacle located at the end of the puddle (a wall in Figure 1). In the case of sessions without feedback, the car would stay in the central lane.

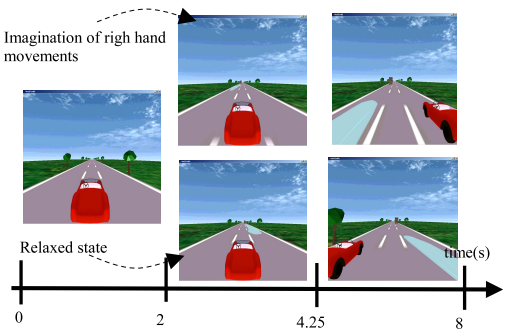

Figure 1: Trial time

In this system, to make interface even more entertaining, different scenes were developed (Figure 2): controlling the car to avoid crashing into a wall, to avoid logs in the road, or to reach a ramp that would make

the car jump (in this scene, the ramp is not an obstacle but a target, and it is also located at the end of the puddle but on the opposite lane with the aim being to drive over the ramp). With the aim of achieving a more realistic environment, sounds simulating a car engine, puddle splashes and effects of the obstacles were introduced.

Figure 2: Different obstacles

RESULTS

Only one of the subjects who took part in the previous research [4], participated in this study. To obtain comparative results, error percentage of all sessions with feedback have been considered, as shown in Figure 3. Discontinuous lines represent the error curves obtained in previous experiments [4] in which the subject was to control the car's movement to avoid only the puddle (5 sessions). Continuous lines represent the error curves obtained in this experiment in which the subject was to control the car to avoid the puddle and the obstacle located at the end of the puddle (3 sessions). In this study, the obstacles presented in each trial were randomised between the wall and the ramp. Thick lines represent error percentage average from all sessions with feedback for each experiment.

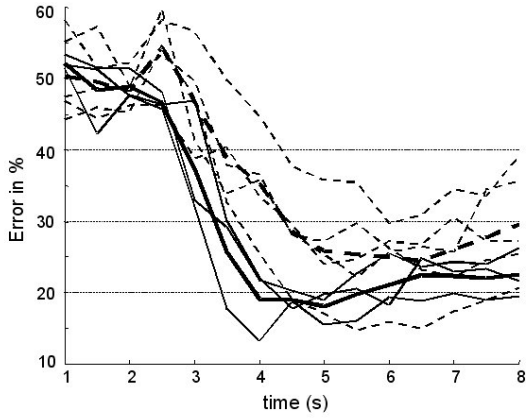

Figure 3: On-line classification results

Curves show how, effectively, in almost all sessions the error rates worsen during the last second of feedback (specially from 6.5 s to 8 s) when the subject has to avoid only the puddle (results obtained in [4]), while the presence of an obstacle located at the end of it seems to help the subject to maintain the control of the EEG signals until the end of the feedback period.

DISCUSSION

The obtained results suggest that changing the feedback presentation make it possible to modify the behaviour of the subject and in turn their capacity to control the EEG signals. The incorporation of an obstacle at the end of the puddle, at the end of the feedback period, allows the subject to feel immersed and to be taking part in the task of avoiding the puddle during the whole feedback period. The subject manages to maintain concentration until the end of the trial avoiding a loss of control of the BCI. Furthermore, mixing different scenes, or obstacles, seems very important to make interface even more entertaining, and to avoid that feedback effects become frustrating or could prove somewhat boring.

CONCLUSION

In BCI systems, training must be as easy and attractive as possible, being sometimes necessary to adapt training protocol to be effective. The preliminary results obtained in the study carried out suggest how it is possible to improve the EEG control presenting feedback whose effects are more immersive and motivating. The graphical possibilities of a multimodal interface combining 3D display and sound seems a good option to develop training techniques helping subjects to achieve a better control of the BCI.

ACKNOWLEDGEMENT

This research has been partially supported by the Spanish Ministry of Science and Technology, and ERDF funds (Project TIC2002-04348-C02-01).

REFERENCES

[1] Wolpaw JR, Ramoser H, McFarland DJ, Pfurtscheller G. EEG-Based Communication: Improved Accuracy by Response Verification. IEEE Trans Rehab Eng, 1998; 6(3): 326–333.

[2] Wolpaw JR, Birbaumer N, Heetderks WJ, McFarland DJ, Peckham PH, Schalk G, et al. Brain-computer interface technology: A review of the first international meeting. IEEE Trans Rehab Eng, 2000, 8(2): 164–173.

[3] Pineda JA, Silverman DS, Vankov A, Hestenes J. Learning to Control Brain Rhythm: Making a Brain-Computer Interface Possible. IEEE Trans Neural Syst Rehab Eng, 2003; 11(2): 181–184.

[4] Ron-Angevin R, Reyes-Lecuona A, Díaz-Estrella A. The use of virtual reality to improve BCI training techniques. Proceedings of the 2nd International Brain-Computer Interface Workshop and Training Course, Graz, Austria, 2004; 65–66.

CLASSIFICATION OF CORTICAL POTENTIALS EVOKED BY MODULATION OF FORCE IN PERCEIVED AND REAL WRIST FLEXION IN AN AMPUTEE

Y. Gu, O. F. do Nascimento, N. Mazzaro, T. Sinkjaer, D. Farina

Center for Sensory-Motor Interaction (SMI), Department of Health Science and Technology, Aalborg University, Aalborg, Denmark

E-mail: yinggu@hst.aau.dk

SUMMARY: This study investigated if changes in rate of force development, during perceived and real wrist flexion performed by an amputee, could be classified from multichannel electroencephalographic (EEG) data. An approach based on optimization of wavelets for feature extraction and K-nearest neighbor for classification has been applied. As a main result, classification of perceived wrist flexion at the amputated side presented errors as low as 5 %.

INTRODUCTION

Differentiation of movement-related parameters in movement-related cortical potentials (MRCP) during motor imagination can considerably improve EEG-based brain-computer interfaces (BCI). Previous studies have demonstrated the correlation between MRCPs and motor tasks involving different rates of torque development and levels of torque both during actual execution and imagination of motor tasks [1, 2]. The present study was designed to identify similar movement parameters in tasks performed by an amputee.

MATERIALS AND METHODS

Experiment setup: A 28 years old male with an amputation of the left hand/wrist participated in the experiment. The amputation, about 5 cm above the left wrist, occurred approximately 2 years prior to the experiment. The experimental procedures were approved by the local ethical committee and informed consent was obtained before the experiment.

The experimental tasks consisted of voluntary real (right side) and perceived/imaginary (left and right sides, respectively) isometric wrist flexions at two rates of force development (moderate and ballistic tasks). The ballistic task was defined as the attainment of 60 % of maximum voluntary contraction (MVC) as fast as possible, whereas the moderate task as a 4-s linear force increase followed by a plateau of 1 s. A total of 6 tasks were performed in random order and evaluated: Ballistic Real Right (BRR), Moderate Real Right (MRR), Ballistic Imaginary Left (BIL), Moderate Imaginary Left (MIL), Ballistic Imaginary Right (BIR) and Moderate Imaginary Right (MIR) wrist flexions. Each task consisted of 50 trials.

The isometric wrist flexion was measured as the downwards force exertion on a multi-axis force transducer set as a handlebar (FS-6, AMTI) with force signal acquired and sampled at 500 Hz.

The EEG recordings were performed with standard 10-20 system. The channels FP1, FP2, F7, F3, FZ, F4, F8, FC1, FC2, T7, T8, C3, C1, CZ, C2, C4, CP3, CP1, CPZ, CP2, CP4, P7, P3, PZ, P4, P8, PO7, PO8, O1 and O2 were recorded with reference to electrodes (tin) on the earlobes (A1, A2). The EOG were recorded by four standard tin electrodes. The EEG/EOG signals were digitized at 500 Hz.

Surface electromyography (EMG) was recorded from digital flexors and extensor muscles of both forearms using standard self-adhesive disposable Ag/AgCl electrodes and digitized at 2000 Hz. The raw EMG data were high-pass filtered at 10 Hz, rectified and low-pass filtered at 6 Hz.

Data pre-processing: Pre-processing included:

1. Setting exact movement onset by means of threshold and extracting time intervals for EEG: 1 s before and after movement onset.
2. Discarding trials contaminated by EOG activity that exceeded 75 μV.
3. High-pass filtering EEG signals at 0.05 Hz to remove baseline drift and notch filtering at 50 Hz to remove power line noise.

Discrete Wavelet Transform (DWT): The DWT is based on the Multi Resolution Analysis (MRA). Mother wavelet can be parameterized through Finite Impulse Response (FIR) filters h and g associated respectively to the scaling function ϕ and wavelet function ψ by the two-scale relations:

$$\phi(t/2) = \sqrt{2}\sum_n h[n]\phi(t-n) \quad (1)$$

$$\psi(t/2) = \sqrt{2}\sum_n g[n]\psi(t-n) \quad (2)$$

In order to generate an orthogonal MRA wavelet, h must satisfy some conditions. g can be deduced from h according to the relationship $g[n] = (-1)^n h[1-n]$. When the length of h is L, the number of free parameters to design h is $L/2-1$ to allow perfect reconstruction. Each free parameter θ varies independently from 0 to π. In our application, with $L = 4$, we need one design parameter θ and h is given by Sherlock and Monro [3].

$$\begin{aligned} h(1) &= (1/\sqrt{2})\cos(\theta)\cos(\pi/4-\theta) \\ h(2) &= (1/\sqrt{2})\sin(\theta)\cos(\pi/4-\theta) \\ h(3) &= -(1/\sqrt{2})\sin(\theta)\sin(\pi/4-\theta) \\ h(4) &= (1/\sqrt{2})\cos(\theta)\sin(\pi/4-\theta) \end{aligned}$$

In this study, 20 parameters θ between 0 and π with equal step were used to design h, therefore 20 mother wavelets were obtained for optimization.
Feature Extraction: The features for classification were extracted from the DWT coefficients by Root-Mean Square (RMS) for each subband:

$$y(j) = \sqrt{\frac{\sum_{i=1}^{j} \sum_{n_i} D_i[n]^2}{\sum_{i=1}^{j} n_i}} \qquad (3)$$

where D_i and n_i are the detail coefficients and the number of detail coefficients at i^{th} level. The feature vector was obtained by $y(j), (j = 1 \dots N)$. N was the deepest level of decomposition.
Classification: The K-Nearest Neighbor classifier was used. In our application, K, the number of nearest neighbors, was chosen as 5. Leave-one-out approach was applied for estimation of the probability of error: the tested signal is not used for training [4].
Optimization: The probability of classification error is represented by $P_e^{\theta}(\omega_i)$ for a given free parameter θ and given class ω_i. The overall probability of classification error is the average of N (number of classes) probabilities $P_e^{\theta}(\omega_i)$:

$$P_e^{\theta} = \frac{1}{N} \sum_{i=1}^{N} P_e^{\theta}(\omega_i) \qquad (4)$$

Then θ is optimized by minimizing the criterion (4) [5].

RESULTS

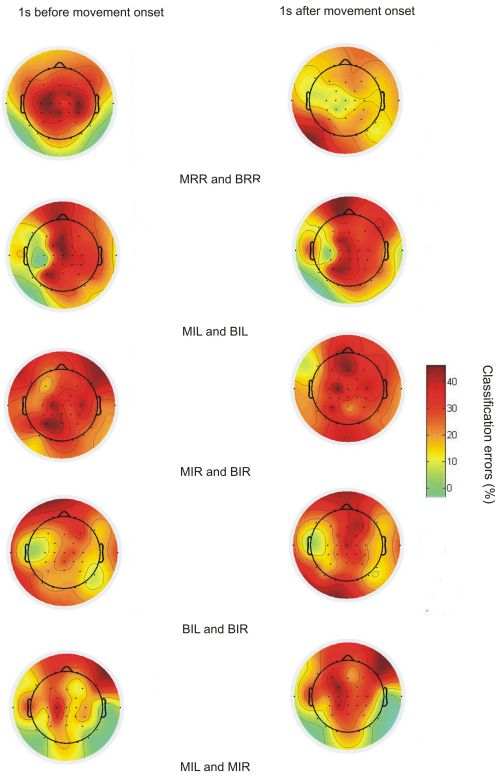

Figure 1: Interpolated scalp maps of classification errors (%) between two classes, 1 s before (left) and 1 s after (right) movement onset.

Classification has been done between two tasks on multiple channels. Each channel has its own optimized DWT and accordingly a lowest classification error. Results are shown in Figure 1. For classification of MRR and BRR, after movement onset, MRCP in primary motor cortex result in best performance. MIL and BIL can be classified with classification error lower than 5 % in channels C3, located in the shoulder to wrist area of primary motor cortex [6] and CP3. For MIR and BIR, F3 gives lowest (11 %) classification error among channels before movement onset, while F7 and T7 give lowest (11 %) classification error after movement onset. For BIL and BIR, T7 gives lowest (5 %) classification error among channels. For MIL and MIR, they can be classified with lowest classification error (0 %) on T8.

DISCUSSION

The low classification error in the differentiation between moderate and ballistic imaginary/perceived wrist flexion in the amputated side is particularly interesting and inspiring. According to the purpose of this experiment, the main outcome is the possibility of discriminating between two different rates of force development in the amputated side, which open the possibility for the development of BCIs for control of force-related parameters in prosthetic devices.
Since performance of classification between two classes are dependant on channels that show the locations of brain activities, the future work on classification will combine the spatial information.

ACKNOWLEDGEMENT

The authors would like to thank the support provided by Danish Technical Research Council.

REFERENCES

[1] Do Nascimento OF, Nielsen KD, Voigt M. Relationship between plantar-flexor torque generation and the magnitude of the movement-related potential. Exp Brain Res, 2005; 160: 154–165.

[2] Do Nascimento OF, Nielsen KD, Voigt M. Movement-related parameters modulate cortical activity during imaginary isometric plantar-flexions. Exp Brain Res, 2006; 171: 78–90.

[3] Sherlock BG, Monro DM. On the space of orthonormal wavelets. IEEE Trans on Signal Processing, 1998; 46: 1716–1720.

[4] Duda RO, Hart PE, Stork DG. Pattern classification, John Wiley & Sons, Inc, New York, USA, 2001.

[5] Maitrot A, Lucas MF, Doncarli C, Farina D. Signal-dependent wavelets for electromyogram classification. Med Biol Eng Comput, 2005; 43(4): 487–492.

[6] Homan RW, Herman J, Purdy P. Cerebral location of international 10–20 system electrode placement. Electroenceph Clin Neurophysiol, 1987; 66: 376–382.

IS THE LOCUS OF CONTROL OF REINFORCEMENT A PREDICTOR OF BRAIN-COMPUTER INTERFACE PERFORMANCE?

W. Burde[1,2], B. Blankertz[2]

[1]Institut of Psychology, Humboldt University of Berlin, Berlin, Germany
[2]Fraunhofer FIRST (IDA), Berlin, Germany
E-mail: wenke.burde@first.fhg.de

SUMMARY: Brain-Computer Interfaces (BCIs) provide a direct communication channel from the brain to an output device. This paper focuses on the pyschological concept of the "locus of control of reinforcement" (LOC) developed by Julian Rotter. Here we report from a study with twelve subjects who had no prior experience with BCI feedback. In the beginning of the experiment the subjects filled out two questionnaires for assessing different aspects of LOC. After a calibration measurement the subjects performed a feedback run in which they could BCI-control a cursor horizontally. The analysis pointed out a positive correlation between a LOC score related to dealing with technology and the accuracy of BCI control. These preliminary results suggest that a LOC score can be used as predictor of BCI performance.

INTRODUCTION

One major goal of Brain-Computer Interface (BCI) research [6] is to improve performance. While great efforts are being made to develop better algorithms, it is conjectured that also many different psychological variables influence the performance. Nevertheless only few studies on this topic exist (e. g. [3]). Here we focus on the "locus of control of reinforcement" (LOC) introduced in [5] which has so far not been considered in BCI context. This concept was developed in Rotter's theory of social learning. The fundamental idea is that a specific behavior in a specific situation can be explained by subjective reinforcement of performance results, and by subjective expectations, that a specific result will appear as an action result.

The subject of investigations was to see whether a LOC related score of a subject measured before an experiment is a predictor of her/his BCI performance. If this is the case, a further strategy to enhance BCI usage could be to influence the LOC of BCI users to be more internal.

THEORY

Locus of control of reinforcement (LOC): The concept "locus of control of reinforcement" [5] roughly divides people into two groups according to their tendency to ascribe their chances either to external or internal causes. Persons with an *external LOC* perceive the results of their actions not as a result of their own performance but as a result of good or bad luck, coincidence, destiny, not predictable or dependent by other people. Persons with an *internal LOC* perceive reinforcement and events, that follow their own actions, as dependent to their own performance or personality.

For a detailed assessment of the LOC characteristics of a person there exist several different questionnaires that allow to quantify the LOC with respect to various aspects. For this study we used the german questionnaires IPC [4] to determine external (condensed PC-Scale) and internal (I-Scale) LOC, and the KUT [1], which has a focus on the LOC with regard to dealing with technology. It is a one dimensional construction of LOC, that was developed to analyse technology.

The Berlin Brain-Computer Interface: This study was carried out using the Berlin Brain-Computer Interface (BBCI) which is an EEG-based system operating on the spatio-spectral changes during different kinds of motor imagery. The BBCI uses machine learning techniques to adapt to the specific brain signatures of each user. This concept allows to achieve high quality feedback already in the very first session without subject training [2]. This unique feature makes the BBCI particularly attractive for studies like this.

MATERIALS AND METHODS

Seventeen subjects (12 male, 5 female, with a mean age of 26) took part in the experiment. All subjects had been novices for BCI experiments. The brain-activity was recorded with multi-channel EEG amplifiers using 64 channels. Surface EMG at both forearms and the right leg was additionally recorded. They were not used for generating feedback but only to ensure (on- and off-line) that no real movements were performed. In a calibration measurement subjects performed motor imagery regarding the left hand, the right hand and the right foot according to visual stimuli (L/R/F). Then the two classes given the best discrimination were identified. For twelve subjects (9 male, 3 female) this discrimination was satisfactory and a binary classifier was trained. These subjects then performed a feedback run of 50 trials in which they could control a cursor horizontally by using motor imagery. The cursor started in the center of the screen and was to be moved to either the left or the right edge of the screen as indicated by a highlighted target (25 left and 25 right targets in random order). A trial ended when the cursor touched one of the edges of the screen or after a time limit of 5 seconds. When the cursor was on the target side, the trial was counted as a HIT.

For the current study we analysed the correlation between LOC and coping with the BBCI feedback as explained above. The used *independent variables* were IV1: internal locus of control of reinforcement (IPC-I-Scale), IV2: external locus of control of reinforcement (IPC condensed PC-Scale) and IV3: locus of control

by dealing with technology (KUT). The only *dependent variable* to operationalise the performance was: DV1: Number of hits (HITS).

RESULTS

The one tailed correlation (Pearson) for the independent variables with the dependent variables showed a significant correlation of 0.59 ($\alpha = 0.05$) for KUT and HITS. No significant correlation was found for the I-, and the condensed PC-Scale of the IPC.

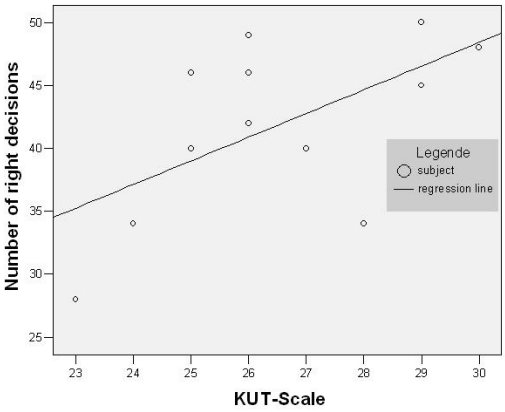

Figure 1: The scatter plot of HITS and KUT.

DISCUSSION

The results implicate that a person who has a strong internal LOC can perform better with the BBCI than somebody who has ordinary or below average LOC. This was specially found in the analysis of the correlation between the KUT and the HITS. The higher the KUT results were the better was the performance. The IPC is a more general questionnaire to look at LOC. In view of the fact that we analyse interaction with technology it is understandable that only the questionnaire that focuses specially on this aspect shows a significant correlation.

The results of the study suggest that a specific aspect of the LOC may be a predictor of BCI performance. People who feel very comfortable with technology and believe in their own abilities seem to be good in this kind of experiments. Furthermore a novel method for improving BCI performance is conceiveable. When users can successfully be confirmed in their internal LOC, it can be expected that their BCI-performance will increase. However, this was to be verified in further studies.

This study can only give preliminary indications due to the limited number of subjects. Furthermore it remains open, whether similar implications are true for other BCI systems, e. g. ones involving subject training.

ACKNOWLEDGEMENT

This work was supported in part by a grant of the Bundesministerium für Bildung und Forschung (BMBF), FKZ 01 IBE 01A.

REFERENCES

[1] Beier G. Kontrollüberzeugungen im Umgang mit Technik: ein Persönlichkeitsmerkmal mit Relevanz für die Gestaltung technischer Systeme. dissertation, de, 2004.

[2] Blankertz B, Dornhege G, Krauledat M, Müller K-R, Kunzmann V, Losch F, Curio G. The Berlin Brain-Computer Interface: EEG-based communication without subject training. IEEE Transactions on Neural Systems and Rehabil Eng, 2006; 14(2): 147-152.

[3] Kotchoubey B, Haist S, Daum I, Schugens M, Birbaumer N. Learning and self-regulation of slow cortical potentials in older adults. Experimental Aging Research, 2000; 26(1): 15-36.

[4] Krampen CJ, IPC-Fragebogen zu Kontrollüberzeugungen, 1981.

[5] Rotter JB, Generalized expectancies for internal versus external control of reinforcement. Psychological Monographs, 1966; 609.

[6] Wolpaw JR, Birbaumer N, McFarland DJ, Pfurtscheller G, Vaughan TM. Brain-computer interfaces for communication and control. Clin Neurophysiol, 2002; 113: 767-791.

THE RELEVANCE OF FEEDBACK TYPE ON BCI CLASSIFICATION RESULTS

S. Wriessnegger[2] , R. Scherer[1], C. Maier[2], K. Mörth[2], G. Pfurtscheller [1], C. Neuper[2]

[1]BCI-Lab, Institute for Knowledge Discovery, Graz University of Technology
[2]Department of Psychology, University of Graz

SUMMARY: In the present paper we describe the results of two different types of feedback, abstract versus concrete, on classification results obtained with the Graz Brain-Computer-Interface. The EEG of thirty-four healthy subjects, performing a left or right motor imagery task, was recorded in a primary screening session. Afterwards the subjects were divided into two comparable groups based on their mean classification values, resulting in 10 subjects per group. In the experimental session, one group obtained abstract feedback (moving bar), whereas the other group obtained concrete feedback (moving hand). The classification results show no difference between the two feedback groups.

INTRODUCTION

Brain-Computer Interfaces (BCI) provide users with an alternative output channel other than the normal output path of the brain, i. e. the efferent nervous system and muscles. The purpose of a BCI is to detect physiological signals from the brain, typically electrical signals resulting from neural firing and to translate this signal in order to control an output device.

To control such a BCI, several technical, physiological and psychological factors play an important role. The Graz-BCI, presented in this paper, is based on the classification and detection of changes in the sensorimotor electroencephalogram (EEG, usually two bipolar channels), induced by the imagination of motor activity (e. g. hand movement) [1]. Important factors for the identification of the changing oscillatory brain activity are 1) electrode location and 2) reactive frequency components.

Second, but also important are some psychological factors like motivation, attention or excitement. Such factors, which are closely related to the learning process, could be influenced by the choice of feedback presentation, which might determine the success in following BCI applications [2, 3]. In the present paper two types of feedback (abstract vs. concrete) were investigated regarding their impact on classification results.

METHODS

The EEG from thirty-four healthy, naive subjects (19 females, age 24.1 ± 2.0, 15 males, age 28.2 ± 8.7) was recorded from 6 sintered Ag/AgCl electrodes placed over the cortical hand areas (at positions C3 and C4 as well as positions 2.5 cm anterior and posterior to these (Figure 1). The subjects were without any medical or psychological diseases, had normal or corrected to normal vision and got paid for attending to the experiments. The acquired signal was analog filtered between 0.5 and 100 Hz (2^{nd} order, attenuation 40 dB) and sampled with 250 Hz.

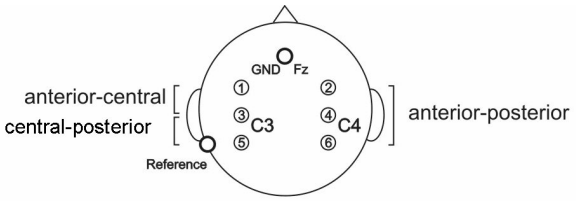

Figure 1: Electrode setup and analyzed bipolar derivations

Sitting in a comfortable armchair, subjects had to imagine left and right hand movements, following a fixed repetitive time scheme. In the screening session each trial started with the presentation of an acoustical warning tone and a fixation cross. One second later, an arrow (cue) pointing to the left (left hand) or to the right (right hand) specified the motor imagery task to perform. Each subject had to perform the motor imagery for 4 seconds, until the screen content was erased. After a short pause (random duration) the next trial started. Each training run consisted of 40 trials with 20 trials per class (left/right) presented in randomized order.

Five training runs were recorded for each subject and according to their accuracy they have been divided in two comparable groups (median based), receiving different types of feedback (Figure 2).

Band power features were computed by bandpass filtering the EEG signal, squaring and averaging the samples in the analyzed 1-second time window. From this averaged value the logarithm was calculated. For classification Fisher's linear discriminant analysis (LDA) was applied to the band power estimates. In subsequent sessions, the system uses the classifier to translate the user's motor imagery into a continuous output, which is presented to the subjects as online feedback on a computer screen.

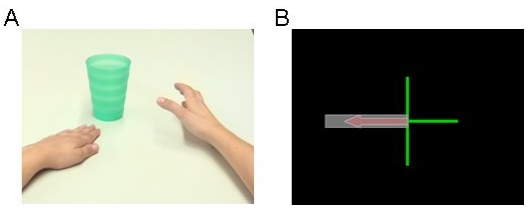

Figure 2. A: Concrete Feedback; B: Abstract Feedback

One group received concrete feedback, where according to their brain states caused by the required motor

imagery a real hand starts moving to reach a glass. The second group received abstract feedback by manipulating a bar in the predefined direction (Figure 2). For example, if the subject has to imagine a right hand movement in the concrete feedback, the right hand starts moving to reach the green glass. In the abstract feedback condition the subjects had to expand a grey bar in the required direction previously indicated by a red arrow (Figure 2). Subjects performed 3 feedback sessions with 40 trials each.

RESULTS

A one-way ANOVA was computed comparing the classification results of three feedback sessions from subjects who received concrete versus abstract feedback. No significant difference was found between the types of feedback obtained in session one (FB1: $F(1, 18) = 0.275$; $p = 0.606$), session two (FB2: $F(1, 18) = 1.151$; $p = 0.297$) and session three (FB3: $F(1, 18) = 0.512$; $p = 0.484$). Furthermore no significant differences were found within the three feedback sessions. The individual classification results for each feedback group (abstract vs. concrete) are illustrated in Figure 3. The mean classification results over all feedback sessions and subjects were 62.95 (SD = 6.80) for concrete FB and 60.06 (SD = 8.94) for abstract FB.

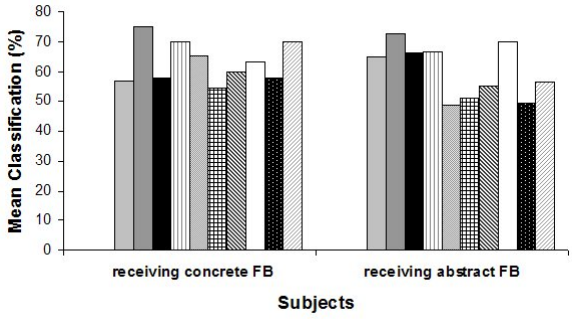

Figure 3: Mean classification results for concrete and abstract FB of all subjects overall sessions (FB1, FB2, FB3).

DISCUSSION

The results of this study indicate that feedback is a necessary and useful method improving learning, attention and motivation in BCI applications, but the type of feedback (concrete vs. abstract) does not influence the performance, at least in initial feedback sessions. These results are contrary to the assumptions of Pineda et al. (2003), who suggested that feedback conditions in a stimulus-rich, more realistic environment (e. g. shooter games) led to better performance and shorter training times. This could be attributed to the low number of training sessions (3 sessions) in our study and the third person movement imagery arising by observation of the moving hand, which is known to be less effective compared to first person imagery [4].

CONCLUSION

The type of feedback (concrete/abstract) does not influence classification results. Particularly, to move a virtual bar (abstract FB) seems to be enough information for individuals to perform accurately. However the number of feedback sessions should be extended in further experiments.

ACKNOWLEDGMENTS

This work was supported by the 'Fonds zur Förderung der Wissenschaftlichen Forschung' in Austria, project P16326-B02.

REFERENCES

[1] Pfurtscheller G,Neuper C. Motor Imagery and Direct Brain-Computer Communication. Proceedings of the IEEE, 2001; 89(7): 1123–1134.

[2] Pineda JA,Silverman DS, Vankov A, Hestenes J. Learning to control brain rhythms: Making a Brain-Computer Interface possible. IEEE Trans Neural Syst Rehab Eng, 2003; 11: 181–184.

[3] Pfurtscheller G. Importance of motor imagery and of feedback by observation of a moving object in BCI research. Proc. of the 2nd Int. BCI Workshop & Training Course 2004, Suppl. Vol. Biomed. Tech.(Berlin), 2004; 49(1): 23–28.

[4] Neuper C, Scherer R, Reiner M, Pfurtscheller G. Imagery of motor actions: differential effects of kinesthetic and visual-motor mode of imagery in single-trial EEG. Cogn Brain Res, 2005; 25: 668–677.

SINGLE-TRIAL EEG CLASSIFICATION OF EXECUTED AND IMAGINED HAND MOVEMENTS IN HEMIPARETIC STROKE PATIENTS

A. Mohapp[1,2], R. Scherer[1,3], C. Keinrath[1], P. Grieshofer[3], G. Pfurtscheller[1], C. Neuper[2]

[1]Laboratory of Brain-Computer Interfaces, Institute for Knowledge Discovery,
Graz University of Technology, Austria
[2]Department of Psychology, University of Graz, Austria
[3]Klinik Judendorf-Straßengel, Judendorf-Straßengel, Austria

SUMMARY: The goal of the study was to identify relevant features from the ongoing electroen-cephalogram (EEG, i. e. electrode location and reactive frequency components) that represent the specific mental processes during execution and imagination of hand movements in stroke patients with hemiparesis. The results of this first study show that single-trial analysis represents an appropriate method to detect task-related EEG patterns in stroke patients.

INTRODUCTION

Rehabilitation of hemiparesis after stroke is well established for lower limbs, whereas therapy of upper limb motor skills is less developed. One way of intervention is to treat the paretic upper limb actively or passively [1]. Another therapeutic approach may be the concept of motor imagery, i. e. to imagine or simulate the movement of the affected limb [2]. Based on this idea the main goal of this study was to develop an additional rehabilitation method to improve the motor function of the affected upper limb on the basis of the electroencephalogram (EEG)-based Graz Brain-Computer Interface (BCI) operated by motor imagery [3]. For this purpose, in a first step, we investigated, whether there are EEG patterns in stroke patients which are detectable and stable enough to be used for BCI feedback training. Single-trial classification of executed and imagined hand movements was performed. At the same time, we tried to identify the relevant frequency components, which can be used for BCI training to enhance the cortical activity on the lesional hemisphere.

MATERIALS AND METHODS

Subjects and data acquisition: Ten right-handed patients (5 females, 5 males, mean age 45.7 years, SD = 11.6) gave their informed consent to participate in this study after the experimental procedure had been explained to them. They had sustained their first-time stroke between 2 and 36 months prior to the study (mean time since onset: 12 months, SD = 12.9). All subjects suffered from unilateral lesion (cortical and/or subcortical) as a consequence of the cerebrovascular damage. The lesions were located either in the left ($n = 3$) or right ($n = 7$) hemisphere and had led to hemiparesis of the contalateral upper extremity directly after stroke onset. Three bipolar EEG-channels were recorded from 6 Ag/AgCl scalp electrodes placed over hand and foot representation areas (2.5 cm anterior and posterior to electrode positions C3, Cz and C4, 10-20 system). The EEG signal was acquired and band pass filtered between 0.5 and 30 Hz with notch on. The recordings, including trigger signals indicating movement/imagination onset, were sampled at 125 Hz.
Experimental Procedure: Each participant performed each of the two experimental conditions twice with each hand, starting with the unaffected hand:

1. Motor execution (ME). Participants were asked to clench or even move their fingers considering the severity code of the hemiparesis (approximately 2 s).

2. Motor imagery (MI). Participants were asked to imagine the movement they were asked to perform within the first experimental task.

Throughout the experiment subjects sat relaxed on their chair with their eyes open. Within one experimental condition the participant had to repeat (cue-based, trial duration randomly selected between 8–10 s) the movement/imagination 30 times (resulting in 60 repetitions per hand and condition). Before the beginning of each run, the researcher explained the task by using simple instructions and showing the sequence of movements that should be performed with his own hands. MI consisted of imagining the performance of motor sequences and the kinesthesic sensations associated with it while holding the finger still.

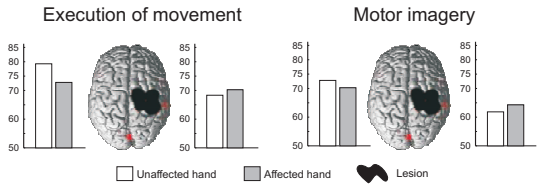

Figure 1: Mean DSLVQ classification accuracy

Signal processing: From the continuous EEG time segments with a length of 8 s each (2 s before and 6 s after cue onset) were analysed. All trials were visually controlled for artefacts and affected trials were excluded from further analyses. For single-trial classification and identification of reactive frequency components the Distinction Sensitive Learning Vector Quantization (DSLVQ) algorithm was used [4]. Two time segments of 1 s length were extracted, one was taken from 0.5–1.5 s (reference period, class 1) the other from 3.5–4.5 s (task period, class 2) and classified against each

other. For each segment, 21 overlapping (1 Hz) frequency components between 8 and 30 Hz with a bandwidth of 2 Hz were calculated. Separately for each task and for each electrode position, a DSLVQ classification was performed. The analysis was repeated for the task period defined from 4.5–5.5 s (class 2).

RESULTS

The mean DSLVQ single-trial classification results are summarized in Figure 1. Table 1 gives a more detailed overview of all patients. The classification accuracies were subjected to a repeated measures ANOVA with the factors TASK (2 levels: ME, MI), HEMISPHERE (2 levels: unaffected, affected) and LIMB (2 levels: unaffected, affected) as within subject variables. Aside from the prominent TASK effect ($F(1,9) = 8.55$; $p < 0.05$) for the "real" motor versus imagined task conditions, indicating higher recognition rate for ME than for MI, we found also a significant 2-way interaction between LIMB × HEMISPHERE ($F(1,9) = 7.58$; $p < 0.05$). Post-hoc comparisons of the respective means support that the recognition rate was higher at the contralesional than at the affected hemisphere, irrespectively whether the motor task involved the affected or intact hand. The accuracy rate at the contralesional hemisphere was higher for the healthy hand area than for the affected one.

The relevance values of different frequency components between 8 and 30 Hz pointed out that basically the frequency components of the lower beta (16–22) and alpha or mu (9–14) play an important role for ME as well as MI.

DISCUSSION

The results demonstrate more pronounced cortical activity changes as reflected in higher classification rates, at the contralesional than at the affected hemisphere, independent of whether the hand movement was executed or imagined at the unaffected or affected side. This finding is in line with previous studies suggesting increased task-related activation of the ipsilateral cerebral motor cortex in stroke patients with hemiparesis [5, 6]. It was shown that for unrecovered stroke patients, most task-related information flow between the sensorimotor cortices in the low beta band of the EEG came from the ipsilateral (undamaged) hemisphere during a movement with the affected hand.

Of interest is that a similar pattern of results, i. e. contralesional preponderance, was also found for the imagery task in our study. The lower classification rate obtained for MI than for ME is in agreement with a previous study in healthy subjects [4]. Moreover, considering the task relevant frequency ranges, the present data confirm that during ME as well as MI, mainly the frequency components between 16–22 Hz and 9–14 Hz play a very important role for the intact as well as the paretic hand.

Table 1: Classification accuracy rates (%, highest accuracy of the two analyzed time periods) for the different tasks (ME, MI), hand movement (unaffected limb: UL; affected limb: AL) and hemisphere (unaffected hemisphere: UH; affected hemisphere: AH). Side of lesion: L

		ME				MI			
		UL		AL		UL		AL	
Subj.	L	UH	AH	UH	AH	UH	AH	UH	AH
V02	R	87.0	53.1	66.9	70.4	73.3	57.3	66.6	61.9
V05	R	77.4	58.0	68.0	59.8	64.8	47.0	70.7	55.1
V10	R	77.7	66.9	77.1	56.4	79.7	61.7	69.8	59.8
V12	R	78.2	57.7	70.6	54.1	80.8	53.7	70.8	47.6
V14	R	94.4	82.3	85.4	83.9	81.2	69.3	78.9	72.2
V15	R	68.2	59.5	66.2	62.3	91.2	59.7	75.5	61.3
V22	R	69.9	68.4	61.4	76.1	62.6	60.3	59.6	66.0
V01	L	70.0	66.4	73.2	76.3	59.0	65.9	56.3	68.1
V18	L	73.1	73.7	73.6	72.9	60.4	68.7	68.0	67.1
V19	L	94.0	93.9	82.7	86.6	71.6	71.6	82.7	86.6
Mean		79.0	68.0	72.5	69.9	72.5	61.5	69.9	64.6
SD		9.7	12.5	7.5	11.3	10.7	7.7	8.0	10.4

The main objective of this study was to find out, which classification rates can be achieved in single trial analysis of motor imagery related EEG in stroke patients, and which task-related frequencies are the most important for this classification. In this regard, the present study revealed moderate classification accuracy rates for MI in stroke patients.

ACKNOWLEDGMENT

This work was supported by the "Steiermärkische Landesregierung" project GZ: A3-16 B 74-05/1.

REFERENCES

[1] Schaechter JD. Motor rehabilitation and brain plasticity after hemiparetic stroke. Progr Neurobiol, 2004; 73: 61–72.

[2] Stevens JA, Stoykov ME. Using motor imagery in the rehabilitation of hemiparesis. Arch Phys Med Rehabil, 2003; 84: 1090–1092.

[3] Pfurtscheller G, Müller-Putz G, Schlögl A, et al. 15 years of BCI research at Graz University of Technology: current projects. IEEE Trans Neural Syst Rehabil Eng, 2006; 14(2): 205–210.

[4] Neuper C, Scherer R, Reiner M, Pfurtscheller G. Imagery of motor actions: differential effects of kinesthetic and visual-motor mode of imagery in single-trial EEG. Cogn Brain Res, 2005; 25: 668–677.

[5] Serrien D, Strens LHA, Cassidy MJ, et al. Functional significance of the ipsilateral hemisphere during movement of the affected hand after stroke. Experimental Neurol, 2004; 190: 425–432.

[6] Verleger R, Adam S, Rose M, et al. Control of hand movements after striatocapsular stroke: high-resolution temporal analysis of the function of ipsilateral activation. Clin Neurophysiol, 2003; 114: 1468–1476.

VISUALIZATION OF THE DELTA-PHASE FEATURE AND ITS CORRELATION TO EVENT-RELATED DESYNCHRONIZATION

Y. Feng

Department of Computer Science, Algoma University, Sault Ste. Marie, Ontario
E-mail: feng@algomau.ca

SUMMARY: The new phase-related feature called "delta-phase" first introduced in [1] is investigated here as a physiological phenomenon. We present and discuss here for the first time a visualization tool called the delta-phase map used to visualize the occurrence of this feature over the time courses of motor imagery trials. In this study, the delta-phase feature is shown to be proportional to instantaneous frequency and is presented here in that context. It was found that the most reactive delta phase features are highly correlated with the most reactive band power feature during an event-related desynchronization.

INTRODUCTION

With an increase in the number of groups focusing on Brain-Computer Interfaces (BCIs) [2], more researchers are beginning to look at ways to improve the restricted data throughput. One way to accomplish this is to discover new features such as the Complex Band Power (CBP) features discussed in [1]. This feature set contains two components, delta-phase and amplitude (a band power-like component), which were used together to achieve improved results. Unlike band power however, which has been extensively studied and analyzed in many ways, delta-phase has only been exploited to improve classification results, but never studied as a physiological phenomenon. Phase information contained in EEG has been studied indirectly, appearing implicitly in some other kind of feature, however it has not been visualized explicitly before in the same way as band power. For example, the ERD/ERS map gives a consolidated view of the available data, and is ideally suited as a visualization tool for this purpose. It is only natural to extend the concept of an ERD/ERS map to the new delta-phase map considered here. This new visualization tool is used here to show a correlation between ERD and delta-phase. The data from [1] is used along with the CBP features originally used in that study. Since these features were already shown to produce good classification results with the data set in question, the goal of the present study was to determine why this was so, or in other words, to determine what physiological phenomenon was being captured by the features used. The data recordings used were available on the Graz site during the 2005 BCI competition.

MATERIALS AND METHODS

The CBP features produced from EEG recordings during a four-class BCI motor imagery experiment were used for this study. Details of the experiment can be found in [1]. Only left and right hand imagery are considered here. Each trial was 10 s in length. Motor imagery began at $t = 3$ s. Features derived from electrodes C3 and C4 were considered in this experiment since they reveal the most important signals [4] for this motor imagery. The instantaneous phase angle is derived from an FFT of the raw EEG as described in [1], and differentiated to form the delta-phase feature. This step is described in (1). Δt corresponds to one sample.

$$\hat{\phi}_f = \frac{\Delta\phi_f}{\Delta t} = \phi_f - \phi_{f-1} \tag{1}$$

In the original study [1], the delta-phase feature was the difference in phase angle of two adjacent samples. Clearly the units of delta-phase are radians/second, however this is simply frequency. With 2π radians in a cycle, and a 250 Hz sampling rate, the original delta-phase feature can be converted directly to Hertz by multiplying by $2\pi/250$. This is the perspective taken in this study. The CBP amplitude component, was used to produce ERD/ERS maps. The delta-phase component was shown in a similar way to provide the "delta-phase" maps shown here, however the feature was scaled as discussed above to produce a frequency in Hertz, and then normalized by subtracting out the mean of the frequency in the pre-trigger period so that the result captures the change in frequency during motor imagery. Since 4 Hz bands are used in the FFT, this scaled delta-phase feature will range from ± 4 Hz. In the description above, the original delta-phase feature is not only scaled to a frequency expressed in Hertz, but also offset to 0 Hz based on the mean frequency prior to the trigger. Similarly, based on the definition of ERD/ERS, the amplitude information is also normalized in the same way so that the mean of the band power prior to the trigger is considered to be 100 %. To review for clarity, in the pre-trigger trial period, the delta-phase component is normalized to 0 Hz, and the amplitude component is normalized to 100 %.

RESULTS

In all cases, the 12–16 Hz band showed the most predominant ERD activity, consistent with [3]. In all but one subject, the most predominant ERD activity was at C3 for right trials and C4 for left. For one subject, immediately adjacent electrodes were predominant. All subjects and trials showed the following phenomenon. In the 12–16 Hz band, the delta-phase activity wanders around at 0 Hz. The most predominant delta-phase activity occurs in the next higher and next lower bands. In the higher band, the frequency of the delta-phase feature rises in lock-step with the

ERD activity, while in the lower band, it falls. For subjects s1 and s4, who produced very good classification results [1], the frequency change is on the order of ±2 Hz. The other subjects showed similar behavior, but with changes under ±1 Hz. Figure 1 shows the time-courses of the ERD and delta-phase activities for the averaged left trials of subject s1.

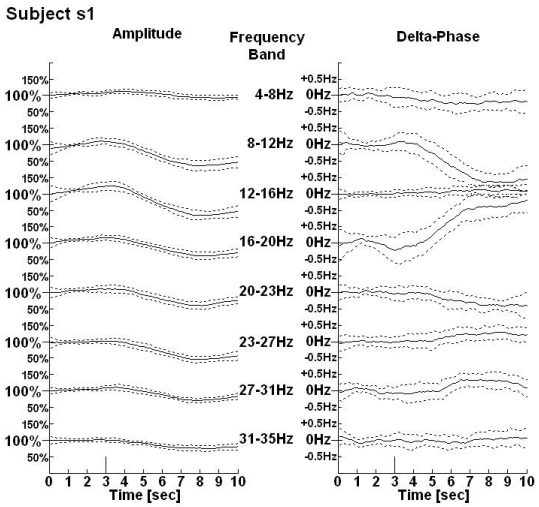

Figure 1: Time courses for ERD/ERS (left) and delta-phase (right) for averaged left hand motor imagery from subject s1, electrode C4. Onset of motor imagery begins at $t = 3$ s. The most predominate ERD occurs in 12–16 Hz band, while most predominate delta-phase activity occurs in adjacent bands above and below. Dotted lines give standard deviation above/below mean.

Figure 2 shows ERD/ERS and delta-phase activity in visual maps. Activity at values near the baseline has been suppressed for clarity. White indicates that no activity being shown. Where other shades of grey appear, the lighter shades indicate ERS activity or increased frequency in the case of the ERD/ERS maps and delta-phase maps respectively, while the darker shades indicate ERD activity or decreased frequency correspondingly.

DISCUSSION

The results show that ERD is accompanied by frequency increases and decreases in the bands above and below the band in which the ERD occurs. Alternatively, this can also be viewed as a positive phase shift in the upper adjacent band, and a negative phase shift in the lower one. Since the band power in the adjacent bands decreases, the frequency changes must be due to oscillations already present in other nearby networks "pulling" the observed frequency further away from what was the predominant signal in each band prior to the ERD. In any case, the results show a clear correlation between ERD and delta-phase.

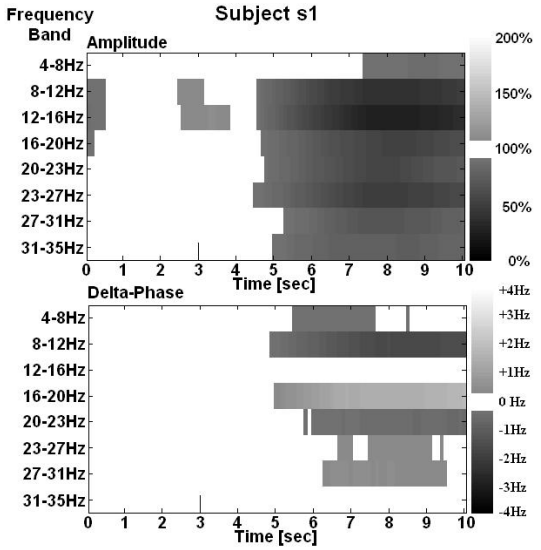

Figure 2: ERD/ERS (upper) and delta-phase maps (lower) for averaged left hand motor imagery from subject s1, electrode C4. Onset of imagery begins at $t = 3$ s. Most predominate ERD is in 12–16 Hz band, while the most predominate delta-phase activity occurs in adjacent bands.

REFERENCES

[1] Townsend G, Graimann B, Pfurtscheller G. A comparison of common spatial patterns with complex band power features in a four-class BCI experiment. IEEE Trans Biomed Eng, 2006; 53: 642–651.

[2] Vaughan TM. Guest editorial brain-computer interface technology: a review of the second international meeting. IEEE Trans Neural Syst Rehab Eng, 2003; 11(2): 94–109.

[3] Pfurtscheller G, Neuper C, Krausz G. Functional dissociation of lower and upper frequency mu rhythms in relation to voluntary limb movement. Clin Neurophysiol, 2000; 111: 1873–1879.

[4] Pfurtscheller G. Event-related desnchronization, handbook of electroencephalography and clinical neurophysiology. Amsterdam, Elsevier, 1999.

CORRELATION IN PAIRED ONE-DIMENSIONAL, CLOSED LOOP, OVERT, MOTOR CONTROLLED BCI

K. J. Miller[1,2,3], G. Schalk[4], E. C. Leuthardt[2], P. Shenoy[3], R. P. N. Rao[3], J. G. Ojemann[2]

Depts of Physics[1], Neurosurgery[2], and Computer Science[3];
University of Washington, Seattle, WA
[4]Wadsworth Institute, Albany, NY, United States
E-mail: kjmiller@u.washington.edu

SUMMARY: Electrocorticographically-based (ECoG-based), closed loop cursor control paradigms for three patients are examined. Each patient obtained control in two separate control paradigms: a left-right cursor to target task mediated by overt hand movement and an up-down task mediated by overt tongue movement. The relationship between the signals used for the two independent movement related-features are evaluated using the cross-correlation values from each feature during relevant states in each task.

INTRODUCTION

One-dimensional BCI has been demonstrated using the BCI2000 program [1] for cursor control with narrow spectral bands from single electrodes [2, 3]. This paper examines separate one dimensional control paradigms to quantify cross talk between control features. Such quantification is important because the independence of control features will dictate whether simultaneous control of separate degrees of freedom is feasible.

MATERIALS AND METHODS

Electrode Arrays: Epileptic patients were implanted with subdural electrode arrays for monitoring prior to seizure focus resection. During their monitoring duration, the patients participated in BCI screening and online control experiments.

Screening: Thirty 3-second interval stimuli for hand movement, and thirty 3-second intervals for tongue movement (shown in random order) were interleaved with three-second rest periods. Comparisons of intervals for each movement type with rest intervals were used to identify appropriate channel-frequency band features for closed loop control.

$$p_{ab}^2 = \frac{\left(\overline{a} - \overline{b}\right)}{\sigma_c} \frac{N_a N_b}{N_c} \qquad (1)$$

$$c = a \cup b$$

BCI: Features identified during screening tasks were coupled with cursor movement for control of a cursor in either the horizontal or vertical dimension. In a left-right target experiment, patients controlled a cursor using the hand movement feature. In a separate, up-down target experiment, patients used the tongue movement feature. Cursor feedback was based upon the ratio between the instantaneous power in the given feature vs. a dynamically calculated mean [1, 2, 3].

Feature significance: The significance of each feature during screening and feedback was quantified using the square of the cross-correlation coefficient (1).

Table 1

Patient	Mode	Freq (Hz)	Electrode Location	Accuracy (L. T.)
1	Hand	79–85	-60, -3, 30	100 % (2)
	Tongue	79–87	-44, -14, 56	97 % (8)
2	Hand	77–83	54, -29, 49	85 % (0)
	Tongue	29–35	63, -1, 17	76 % (20)
3	Hand	97–103	-42, -14, 55	98 % (0)
	Tongue	77–83	-25, 21, -28	98 % (22)

RESULTS AND DISCUSSION

Task Perfomance: Table 1 shows the features used and the results of one-dimensional control tasks. The frequency ranges used for control varied from 29–103 Hz, although the majority of feature ranges were centered around 80 Hz. Five of the six electrode locations used were in somatosensory cortex, while one was subtemporal (pt 3, tongue feature). Patients 1 and 3 obtained complete control in both tasks (97–100 % target accuracy), while Patient 2 had more difficulty. The learning times (L.T.) required before the listed results ranged from 0 to 22 minutes.

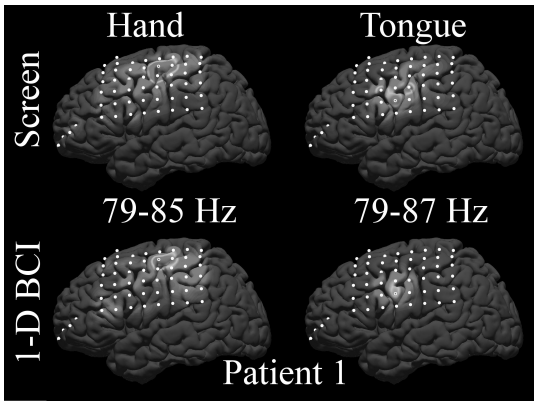

Figure 1

Figures 1-3 [5]*:* These figures illustrate the spatial distribution of the cross-correlation coefficients of select frequency bands during each screening task and the associated one-dimensional feedback BCI task, for patients 1 and 2. Light shading indicates higher activation. Electrode locations are shown with white dots. Patients 1 and 2 exhibited contrasting strategies: Patient 1's cortical changes became more focused and less

extreme with feedback, whereas Patient 2's became less focused and more extreme. This suggests either that the features hand picked in Patient 1's case were better as a control schema, or that the two simply adopted two different strategies in response to feedback. The case of Patient 2 may reflect the idea that low frequency changes with motor movement are more broadly distributed spatially [4].

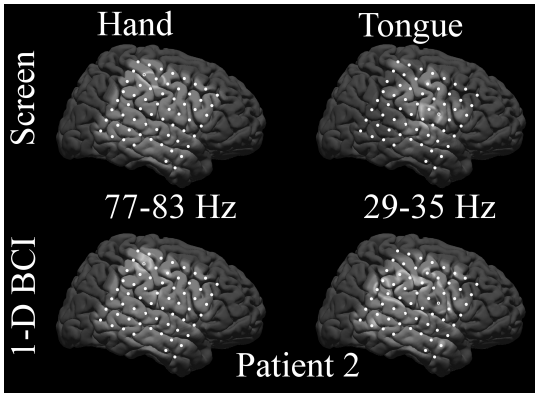

Figure 2

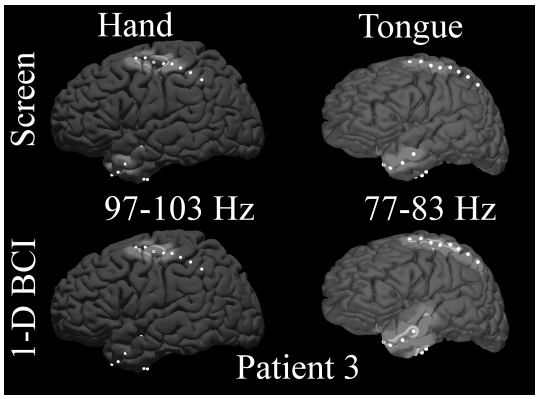

Figure 3

Table 2: The squared cross-correlation across many tasks quantifies the involvement of each feature. Patient 1's features were significant only for the appropriate screening movement intervals, and both could discriminate between the two motor screen intervals. Patient 1 also had significant correlation for each feature during the proper one dimensional task, but not during the other task, suggesting a smooth transition to simultaneous two-dimensional control. Patient 2 had mediocre hand feature resolution in the screening task and even worse during the closed loop one dimensional task. The tongue feature was more highly correlated with the target task than the hand feature during the closed loop hand control task. This implies that this patient would need a significant amount of cortical feature separation during feedback tasks to obtain viable two dimensional cursor control. Patient 3's screening for hand produced a strongly discernable feature. Tongue movement, however, did not, and so a subtemporal site was chosen which did not show strong change during the hand intervals, but showed a reasonable (0.3) change during the tongue intervals. The patient, who appeared to have little control over this feature, learned (over the course of 22 minutes) to elicit a broad hemispheric change (Figure 3) which ranged over the entire range of surveyed cortex, including the feature chosen for the closed-loop hand movement paradigm. This might present difficulty when combining the two features for simultaneous control.

CONCLUSION

The significant cross correlation between features chosen in individual one dimensional cursor control tasks suggest that, in some cases, significant changes during two dimensional feedback will be required for control of independent degrees of freedom.

REFERENCES

[1] Schalk G, McFarland DJ, Hinterberger T, Birbaumer N, Wolpaw JR. BCI2000: development of a general purpose brain-computer interface (BCI) system. IEEE Trans Biomed Eng, 2001; 51: 1034–1043.

[2] Leuthardt EC, Schalk G, Wolpaw JW, Ojemann JG, Moran DW. A brain computer interface using electrocorticographic signals in humans. J Neural Eng, 2004; 1(2): 63–62.

[3] Leuthardt EC, Miller KJ, Schalk G, Rao RPN, Ojemann JG. Electrocorticography-Based Brain Computer Interface - The Seattle Experience. IEEE Trans Neural Syst Rehabil Eng, June 2006.

[4] Miller KJ, et al. Electrocorticographic spectral changes with motor movement. In submission.

[5] Miller KJ, et al. Cortical surface localization from X-Ray and simple mapping for electrocorticographic research: The Location-On-Cortex Package. In submission.

Table 2

Squared Cross-correlation values	Patient 1: hand	Patient 1: tongue	Patient 2: hand	Patient 2: tongue	Patient 3: hand	Patient 3: tongue
screening: rest cue vs. tongue cue	0.06	0.58	0.19	0.03	0.73	0.06
screening: hand cue vs. rest cue	0.76	0.004	0.03	0.45	0.002	0.30
screening: hand cue vs. tongue cue	0.85	0.57	0.22	0.61	0.82	0.06
hand feedback task: target vs. target	0.74	0.0001	0.17	0.28	0.79	0.39
tongue feedback task: target vs. target	0.02	0.66	0.40	0.54	0.41	0.60

ROBUST CLASSIFICATION OF ELECTROCORTICOGRAPHIC SIGNALS FOR BCI

P. Shenoy[1], K. J. Miller[1,2,3], N. Evans[1], J. Ojemann[3], R. P. N. Rao[1]

Depts of [1]Comp. Science, [2]Physics, [3]Neurosurgery, U. Washington, Seattle, WA, USA
E-mail: pshenoy@cs.washington.edu

SUMMARY: We examine the problem of classifying electrocorticographic changes during overt movement of two different body parts (tongue and hand) for designing closed-loop BCI control. We overcome the problem of extremely small training data sets via judicious feature selection and the use of powerful sparse classification methods (LPM). Our results show very high accuracy on quarter-second windows of data, and in addition succeed in identifying neurophysiologically relevant spatial features.

INTRODUCTION

Electrocorticography (ECoG) [1,2,3] has gained attention as a potential *minimally invasive* recording technique for use in brain-computer interfaces. ECoG has a much higher signal-to-noise ratio than EEG, as well as higher spectral and spatial resolution. However, using ECoG for BCI necessitates a reengineering of the signal processing and classification techniques used in traditional EEG-based BCIs, to accomodate these characteristics.

We present a choice of features and classification methods that reliably captures the difference between the chosen motor tasks. A single set of simple spatial and spectral features is used across a large number of patients to obtain reproducible classification results. Our methods naively identify the neurophysiologically relevant cortical areas involved in these tasks. While our results are for overt motor actions, we have shown that overt and covert motor actions elicit similar spectral changes in motor cortex [4]. This has also been shown for EEG signals [5].

MATERIALS AND METHODS

Data Collection: Each subject performed an interval-based motor repetition task consisting of randomly interspersed hand clenching and tongue protrusion with alternating rest periods. A total of 30 trials of each class were recorded, each trial being 3 s of repetitive movement, cued visually. 26–104 ECoG channels were recorded at 1000 Hz, and stored along with stimulus times.

Feature Selection: Each specified window of data from a channel is processed into two bandpower features, the *lowband* (11–40 Hz) and *highband* features (71–100 Hz) (see Figure 1). Our choice of feature selection was motivated by two compelling reasons. Firstly, we have consistently seen quantitative differences in these bands between average spectra for motor and rest across patients and motor actions [6], showing that this is a general physiological phenomenon. Secondly, the extreme paucity of data (only 30 trials per class, for upto 100 channels) forces us to use a single, simple set of features across all patients in order to prevent overfitting.

Classification: We use the linear programming machine (LPM, see [7] for details), a sparse variant of the support vector machine, for classification. The LPM uses a weight vector w that linearly combines the features of a data point to compute the distance of the data point from a classification boundary. The advantage of the LPM is that it computes highly sparse vectors w (i. e., most of the entries are zero or close to zero), automatically performing feature selection in addition to classification. The components of the vector w can be visualized as a spatial distribution over the cortical electrode positions in order to interpret the significance w attaches to each channel.

Evaluation: We use double-crossvalidation to measure the performance of our classifier. Specifically, we randomly divide the trials into 6 blocks, using 5 for training and 1 for testing. For each train step, we minimize 5-fold cross-validation error over the data in order to pick a cost parameter C for the LPM. This process is repeated 5 times, and the resulting error averaged. The features for the training data are computed on a 2 second window (1–3 s) from each trial. The trained classifier is tested on non-overlapping 0.25 s windows of the test trials from 1 s to 3 s, yielding 8 independent data points per trial.

BRIEF RESULTS

We evaluated our algorithms on data collected from 9 patients.

Classifier Performance: The LPM classification error averaged across all subjects was 13.7 %, for individual quarter-second windows of data (see evaluation above). These errors do not take into account the benefit obtainable from temporal integration of classifier output.

Figure 3 displays the classification time course, and classifier output for a single subject, averaged across all test trials, with standard deviation (hatching). This demonstrates that the two classes are quickly disambiguated, and that the performance of the LPM is excellent on even 0.25 s slices of data. Each trial begins with a visual stimulus, and the low initial classification rate reflects the behavioral response time of the subjects. Smoothing over time brings down the error rate further (not shown).

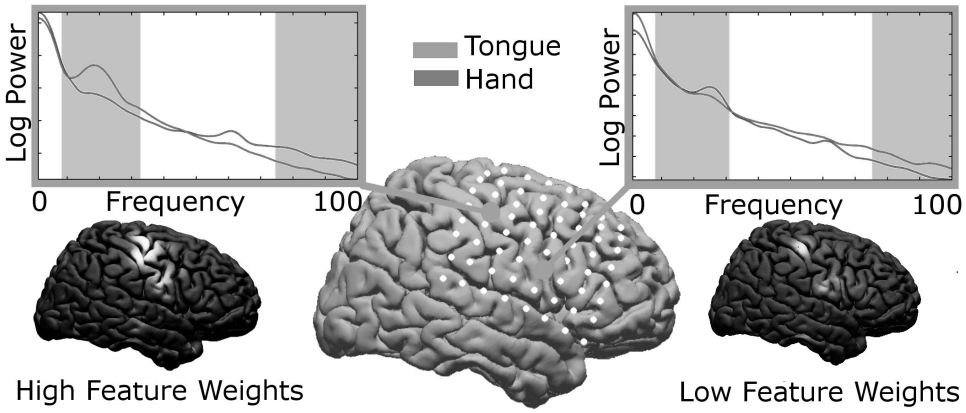

Figure 1: Spatial and Spectral Feature Selection: We choose two simple features, bandpower in low and high bands, that have consistently shown modulation during motor actions. Shown are average spectra for two electrodes in the classical tongue and hand areas, respectively. The bottom left and right figures show features selected by the sparse classifier (LPM).

Spatial Feature Selection: We use the electrode positions [8] for each subject to project the electrode weights onto a standard brain, to visualize the low-band and highband features selected by the classifier. The data is interpolated by linearly superimposing gaussian kernels of fixed width about each electrode (Figure 1, lower left and right). The figure clearly shows general agreement across subjects on the actual electrode positions picked by the LPM classifier. This sparse selection also corresponds to classically described neuroanatomy.

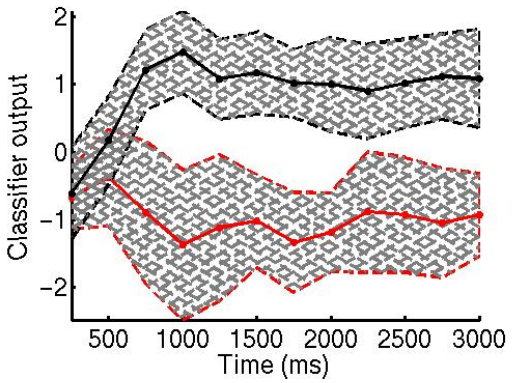

Figure 3: LPM classifier output on independent 0.25 s windows of data across the trial. Hatching shows standard deviation.

DISCUSSION AND CONCLUSION

We have presented a method for binary classification of ECoG signals recorded during motor actions. Our method can classify 0.25 s slices of data as "tongue" or "hand" movement with an average error of 13.7 % across 9 patients, and is currently being evaluated online in closed-loop scenarios. We have shown that a simple set of spatial and spectral features produces robust classifiability across many subjects, and naively converges upon the underlying neuroanatomical features.

REFERENCES

[1] Leuthardt EC, Schalk G, Wolpaw JR, Ojemann JG, Moran DW. A brain-computer interface using electrocorticographic signals in humans. J Neural Eng 1, 2004; 2.

[2] Lal TN, Hinterberger T, Widman G, Schröder M, Hill J, Rosenstiel W, Elger CE, Schölkopf B, Birbaumer N. Methods Towards Invasive Human Brain Computer Interfaces. NIPS 17, 2005.

[3] Graimann B, Huggins JE, Levine SP, Pfurtscheller G. Towards a direct brain interface based on human subdural recordings and wavelet packet analysis. IEEE Trans BME, 2004; 51(6).

[4] Miller KJ, Schalk G, Ojemann JG, Rao RPN. Real and imagined sources in electrocorticography. International BCI workshop, Graz, Austria, 2004.

[5] Pfurtscheller G, Lopes da Silva FH. Handbook of Electroencephalography and Clinical Neurophysiology – Event-related desynchronization, Elsevier, Amsterdam, Netherlands, 1999.

[6] KJ Miller et al. Electrocorticographic spectral changes with motor movement. Technical Report, Computer Science Dept, University of Washington, 2006.

[7] Müller K-R, Krauledat M, Dornhege G, Curio G, Blankertz B. Machine learning techniques for brain-computer interfaces. Biomed Tech; 49(1).

[8] KJ Miller et al. Cortical surface localization from X-Ray and simple mapping for electrocorticographic research: The Location-On-Cortex Package. Technical Report, Computer Science Dept, University of Washington, 2006.

MOVEMENT ONSET RELATED CHANGES IN ECOG RECORDINGS

J. Blumberg[1,2,3], A. Schulze-Bonhage[1,2], C. Mehring[1,4], A. Aertsen[1,3], T. Ball[1,2]

[1]Bernstein Center for Computational Neuroscience, Freiburg, Germany
[2]Epilepsy Center, University Hospital, Albert-Ludwigs-University, Freiburg, Germany
[3]Neurobiology & Biophysics, Institute of Biology III, Albert-Ludwigs-University, Freiburg
[4]Neurobiology & Animal Physiology, Institute of Biology II, Albert-Ludwigs-University, Freiburg
E-mail: julie.blumberg@uniklinik-freiburg.de

SUMMARY: In former studies on movement direction inference during self-paced movement, our group found the highest decoding power in electrodes in primary and premotor cortex, but less information in inferior parietal regions [1]. In the present study we have detected groups of electrodes with a reproducibly similar dynamic behavior around movement onset irrespective of movement direction. In contrast to directional decoding, movement onset related changes showed an additional peak in the inferior parietal lobule (IPL). The IPL therefore is a promising region for movement detection in brain-machine-interfacing applications.

INTRODUCTION

For brain-machine interfacing aiming at the restoration of movement capabilities in paralysed patients it is not only crucial to extract movement parameters such as movement direction from brain signals, but it is also important to distinguish movement per se from rest, i. e. to achieve movement detection. In an ongoing project we have shown that movement direction specific electrocorticographic signals (ECoG) are generated in the human frontal lobe, allowing for single trial decoding of arm movement direction [1]. In this work, we have investigated arm movement direction *un*specific potentials which might still be useful for detection of movement in ongoing recordings.

MATERIALS AND METHODS

An epilepsy patient with electrodes implanted for preneurosurgical diagnostics (Figure 1) performed center-out arm reaching movements to four targets.

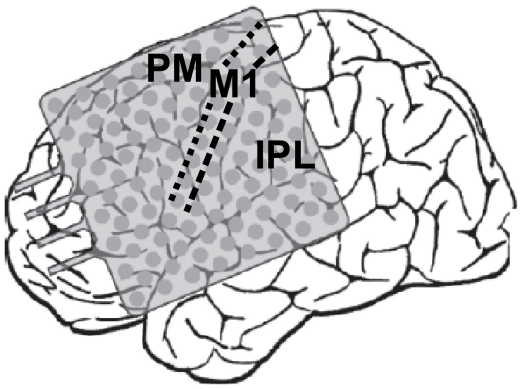

Figure 1: Subdural Electrocorticogram grid on the premotor (PM), primary motor cortex (M1) and the inferior parietal lobule (IPL). Modified from [2].

To record ECoG we used a densely spaced electrode grid of 112 electrodes with 4 mm diameter covering an area of approximately $7 \times 7\,\mathrm{cm}^2$ of the fronto-temporo-parietal cortex. The function of the cortex underlying the individual electrode contacts was determined by direct electrical cortical stimulation. We investigated ECoG time series of ± 2 seconds around movement onset.

In order to identify optimal electrodes for movement detection, we developed the following three step procedure:

1. *Detection of electrodes with a reproducible movement onset behavior across trials:* For each electrode the pair wise correlation between all 88 trials in different directions was calculated and the significantly reliable electrodes were determined. The significance level was assessed by comparison with the distribution of equally preprocessed white noise.

2. *Classification of groups of electrodes with similar response:* To classify different groups of electrodes exhibiting a similar averaged temporal behavior around movement onset, we used a correlation based hierarchical clustering with distance metric
$$d = 1 - |< x_i(t), x_j(t) >|\,,$$
with $x_i(t)$ being the ECoG signal of electrode i at time point t.

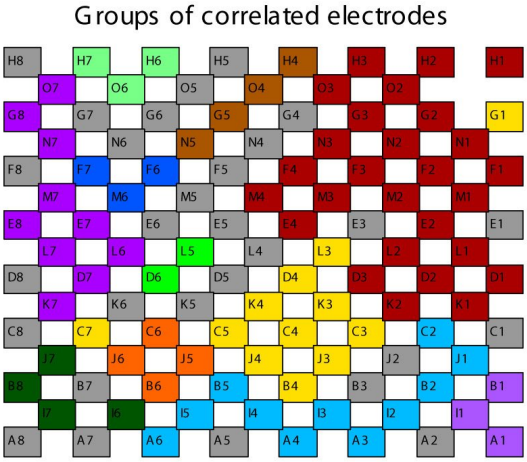

Figure 2: For a threshold correlation of 0.65, the clustered electrodes formed twelve distinct groups

3. *Determination of electrodes with specific movement onset behavior:* In the third part of our analysis we determined the electrodes with the highest significance of ECoG differences between pre- and post-movement onset periods. Therefore we tested whether a channel's mean potential over all trials irrespective of movement direction at a pre-movement time point was significantly different from the mean potential of the distribution of any of the following time points using a Student's t-test. The significance of the signal change is visualized in Figure 3. The dark areas in the center of lighter ones indicate highly significant differences between pre-movement potentials and later movement related potentials.

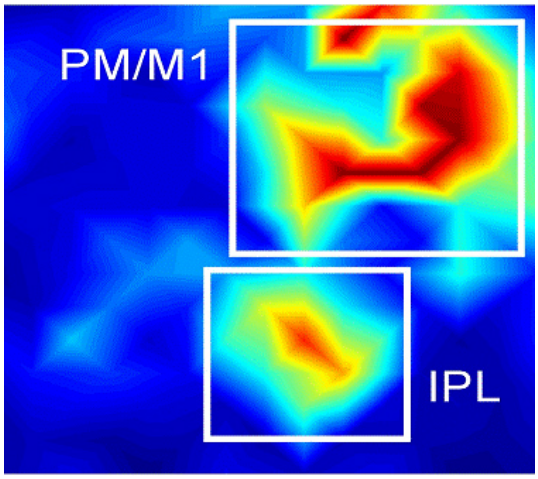

Figure 3: Areas of electrodes with significant potential differences before and after movement onset

RESULTS

Groups of electrodes with a reproducible, similar potential behavior around movement onset were detected. Electrodes above motor cortex gave the most reproducible movement onset related ECoG response. With a threshold correlation of 0.65, twelve groups of recording channels could be determined (Figure 2). The remaining thirty electrodes were not correlated. The two largest groups of similarly behaving electrodes were located around the superior part of the central sulcus (darkest gray) as well as in the inferior part of the postcentral gyrus and the inferior parietal lobule (IPL) (lightest gray). Regarding the differences between pre- and post-movement onset time series, in the resulting cortical map (Figure 3) local peaks were not only found in the primary motor cortex (M1) and premotor cortex (PM), marked by the upper white box, but also in a second area in the inferior parietal lobule.

DISCUSSION

As a preparation for future online movement detection for BMI applications, we investigated the temporal behavior of cortical potentials around movement onset. Based on a cluster analysis, the two largest groups of correlated electrodes were found in the region of PM/M1 and of IPL. Generally, the IPL is often found to be activated during voluntary movement tasks [3, 4] and shows activity already early during movement preparation [3]. The same two regions also showed significant differences between pre- and post-movement onset ECoG amplitude. As these two areas were separated by the cluster analysis, it will be interesting to further investigate whether the two regions actually contain non-redundant information about movement onset. Further, by combining the most efficient electrodes, movement detection could be facilitated for future online analysis where movement onset is unknown.

CONCLUSION

Among the discovered robust electrodes, several groups with similar movement onset specific behavior could be identified. The two largest groups were located above PM/M1 and IPL, respectively. Such groups of electrodes may be helpful for an online application where averaged signals can not be obtained from several trials, but across a group of electrodes.
Highly significant differences between pre-movement potentials and potentials occurring later during movement preparation and execution were located not only in the region of the primary motor arm and hand representations, where ECoG signals were also movement direction specific, but an additional maximum in the topographical distribution was found in the inferior parietal cortex. Therefore, in addition to M1 and PM, this region might be a useful source of information for movement detection in BMI applications.

ACKNOWLEDGMENT

Supported by the WIN-Kolleg of the Heidelberg Academy of Science. BMBF-DIP D3.2 and BMBF 01GQ0420 to BCCN-Freiburg.

REFERENCES

[1] Ball T, Schulze-Bonhage A, Aertsen A, Mehring C. Inference of Arm Movement Direction from Epicortical Field Potentials of the Human Frontal Lobe. Submitted.

[2] Ball T, Nawrot MP, Schulze-Bonhage A, Aertsen A, Mehring C. Towards a brain-machine interface based on epicortical field potentials. Biomed Eng (Berlin), 2004; 49(Suppl. 2): 756–759.

[3] Ball T, Schreiber A, Feige B, Wagner M, Lcking CH, Kristeva-Feige R. The role of higher-order motor areas in voluntary movement as revealed by high-resolution EEG and fMRI. Neuroimage, 1999 Dec; 10(6): 682–694.

[4] Mehring C, Nawrot MP, Cardoso de Oliveira S, Vaadia E, Schulze-Bonhage A, Aertsen A, Ball T. Comparing information about arm movement direction in single channels of local and epicortical field potentials from monkey and human motor cortex. J Physiol (Paris), 2005; 98: 498–506.

SSVEP DETECTION USING SUBSPACE METHODS

T. Solis-Escalante, O. Yañez-Suárez

Neuroimaging Laboratory, Universidad Autónoma Metropolitana-Iztapalapa,
Mexico City, Mexico
E-mail: teosoet@gmail.com

SUMMARY: In this work we validate the results of using the Multiple Signal Classification algorithm to determine the presence of stimulation frequency in EEG recordings of steady-state visual evoked potentials. Support vector machines were used to detect one out of two stimulation frequencies in a number of averaged epochs using pseudospectral features. The results show advantages over the Fourier transform-based approaches.

INTRODUCTION

The detection of a stimulation frequency in recordings of steady-state visual evoked potentials (SSVEP) is usually solved by means of spectral computations using the fast Fourier transform (FFT) algorithm followed by power averaging at specific frecuencies. Although this method is useful and simple to implement, other alternatives are still available. The main problem is to detect a nearly sinusoidal signal, the SSVEP, immerse in noise, background EEG. The Multiple Signal Classification (MUSIC) algorithm is a statistical subspace method specifically aimed at this kind of detection task [1]. The evaluation of MUSIC-based SSVEP detection is described in this paper.

MATERIALS AND METHODS

SSVEP recordings and stimuli: The SSVEP recordings used in this work were kindly facilitated by Dr. Brendan Allison from the Scripps Research Institute, La Jolla, CA and Dr. Jonathan Wolpaw from the Wadsworth Center, Albany, NY. The data collection was made with a 64-channel electrode cap, EEG channels were referenced to an electrode attached to the right earlobe, a ground electrode was placed behind the right mastoid. All data were sampled at 160 Hz and band-pass filtered between 0.1–50 Hz. Data were collected in a work area with occasional uncontrolled distractions. SSVEP were induced with two checkerboxes oscillating at 6 Hz and 15 Hz.

Feature extraction: The MUSIC algorithm is a subspace projection method that uses the fact that for an observed signal $x[n]$ composed of a sinusoidal signal $s[n] = Ae^{j\omega_s n}$ of frequency ω_s, embedded in white noise $\eta[n]$

$$x[n] = s[n] + \eta[n] \tag{1}$$

the sinusoid $e^{j\omega_s n}$ is an eigenvector of the observed sequence's correlation matrix $R_x = E\{\mathbf{x}\mathbf{x}'\}$

$$R_x\mathbf{s} = \lambda\mathbf{s} \tag{2}$$

where $\mathbf{s} = \left[1, e^{j\omega_s}, e^{j2\omega_s}, \ldots, e^{j(N-1)\omega_s}\right]'$ [1, 2]. Since the rest of the eigensubspace (the *noise* subspace) will be orthogonal to the observed sinusoid, and so will be any sinusoid of a different frequency ω_k, the projection of $x[n]$ onto the noise subspace is expected to be very close to zero. Any signal not containing the sinusoid at the reference frequency will have a non-zero projection over the noise subspace.

Based on the previous fact, a principal component decomposition $R_x\nu = \Lambda\nu$, is made to find the eigenvectors, $\nu = [\mathbf{e}_0 \ldots \mathbf{e}_{N-1}]$, of the estimated correlation matrix and its corresponding eigenvalues, $\Lambda = diag(\lambda_i)$.

Those eigenvectors associated with the eigenvalues smaller than or equal to some chosen threshold, σ_0, are selected to form the basis of the noise subspace, E_{noise}:

$$E_{noise} = \left[\mathbf{e}_{N-(M+1)} \ldots \mathbf{e}_{N-1}\right] \tag{3}$$

where

$$\lambda_k \leq \sigma_0,\ k \in \{N-(M+1) : N-1\}. \tag{4}$$

A probe vector W is then formed by sampling a sinusoid of the frequency being investigated, ω:

$$W = \left[1\ e^{j\omega} \ldots e^{j(N-1)\omega}\right]' \tag{5}$$

The next step in the MUSIC algorithm is to calculate the pseudospectrum of $x[n]$, this is accomplished by the function:

$$\hat{P}(e^{j\omega}) = \frac{1}{W^{*'}E_{noise}E_{noise}^{*'}W} \tag{6}$$

which is the inverse of the norm of the projection of W onto the noise subspace. When $\omega = \omega_s$, since W is orthogonal to the noise subspace, its projection onto E_{noise} is close or equal to zero, therefore the function $\hat{P}(e^{j\omega})$ will show a peak at frequency ω_s. It is important to remark that $\hat{P}(e^{j\omega})$ is not a spectral estimator because it does not provide information about the signal power, however it is useful to spot the frequencies contained in a signal. Pseudospectral values at specific frequencies can be used as features to describe the signal content of an observation.

Analysis: The MUSIC algorithm was implemented in Octave [3] and the threshold was experimentally choosen as $\sigma_0 = 0.1\sum_{i=0}^{N-1}\lambda_i$. The pseudospectrum was calculated for 240 one-second SSVEP epochs over electrodes O1 and O2 of the international 10-20 standard; the features chosen were the pseudospectrum values at the first subharmonic, the stimulation frequencies and their first two harmonics. Different numbers of epochs were averaged and measurements of ac-

curacy were made to establish the performance of the classifiers, Support Vector Machines with radial basis function (rbf-SVM) and linear kernels (lin-SVM) [4], as function of the number of averaged epochs. The measurements were made in a leave-one-out scheme using the libSVM library [5].

RESULTS

The measurements of accuracy for one to five averaged epochs are shown in Table 1.

Table 1: Accuracy for k averaged epochs

k	1	2	3	4	5
linear_{O1}	88.75	95.00	97.91	98.75	100.00
linear_{O2}	85.83	95.00	97.91	98.33	99.16
rbf_{O1}	91.66	95.00	97.91	99.58	99.58
rbf_{O2}	86.66	96.25	98.33	98.33	100.00

The results show an excellent performance for all the SVM, reaching accuracies close to the ninety percent in single epoch classification. All the SVM used in this work reach one hundred percent accuracy for ten and fifteen averaged epochs.

DISCUSSION

Application of MUSIC algorithm to the SSVEP detection task showed a better performance, in terms of both accuracy and time, than the results reported in [6, 7, 8] which are FFT-based. Moreover, there is no need to calculate a full pseudospectrum, to extract features it is sufficient to calculate the values of the pseudospectrum in a reduced collection of frequencies as there is theoretically infinite resolution to the algorithm. The current epoch length to detect a SSVEP is one second, but smaller lengths (450 to 600 ms) could be used.

CONCLUSIONS

We have introduced the use of the MUSIC algorithm to solve the SSVEP detection task. It showed to behave better than the typical FFT-based approaches and might constitute an alternative way to improve the bit rate in the SSVEP based BCI.

REFERENCES

[1] Schmidt R. Multiple emitter location and signal parameter estimation. IEEE Trans on Antennas and Propagation March 1986, 34(3): 276–280.

[2] Therrien CW. Discrete Random Signals and Statistical Processing. Prentice-Hall Signal Processing Series, 1992.

[3] Eaton JW, Octave GNU. Software available at www.gnu.org/software/octave/.

[4] Müller KR, Mika S, Rätsch G, Tsuda K, Schölkopf B. An introduction to kernel-based learning algorithms. IEEE Trans Neural Networks, February 2001; 12: 181–201.

[5] Chang C, Lin C. LIBSVM: A Library for Support Vector Machines, 2001. Software available at www.csie.ntu.edu.tw/cjlin/libsvm, last update November 2005.

[6] Gao X, Xu D, Cheng M, Gao S. A BCI-Based Enviromental Controller for the Motion-Disabled. IEEE Trans Neural Systems and Rehabilitation Engineering, June 2003; 11(2).

[7] Wang Y, Zhang Z, Gao X, Gao S. Lead selection for SSVEP-based brain-computer interface. Proc 26$^{\text{th}}$ IEEE EMBC, San Francisco, CA, USA, September 1–5, 2004.

[8] Müller-Putz G, Scherer R, Brauneis C, Pfurtscheller G. Steady-state visual evoked potential (SSVEP)-based communication: Impact of harmonic frecuency components. J Neural Eng, December 2005; 2(4): 123–130 .

ANALOGUE P300-BASED BCI POINTING DEVICE

L. Citi[1,2], R. Poli[1], C. Cinel[3]

[1]Department of Computer Science, University of Essex, UK
[2]IMT Institute for Advanced Studies Lucca, Italy
[3]Department of Psychology, University of Essex, UK
E-mail: {lciti,rpoli,ccinel}@essex.ac.uk

SUMMARY: We propose a P300-based BCI mouse. The system is analogue: the pointer is controlled by directly combining the amplitudes of the outputs produced by a filter in the presence of different stimuli. The system is optimised by a genetic algorithm.

INTRODUCTION

We present a P300-based system for the two-dimensional control of a pointer on a computer screen, inspired by Donchin's Speller [1]. In our BCI mouse, four unobtrusive rectangles are superimposed on the screen, near its edges, and are used to represent the directions up, right, down and left (Figure 1). The rectangles are flashed in random order at 180 ms intervals. To limit the risk of perceptual errors [2], the same rectangle is not allowed to flash twice in a row.

By focusing their attention to one particular rectangle, users produce P300s when the rectangle flashes. The system processes responses and moves the mouse pointer in the appropriate direction. The approach is similar to that used in [3] but with a substantial difference: logically *our BCI mouse is an analogue device*, since the responses for the four directions directly affect the movement of the pointer without requiring any binary classification.

Unlike previous approaches, we use a genetic algorithm (GA) to optimise the parameters of the system for each user and each session – a technology which provided promising results in our earlier work in medical signal processing [4, 5] and BCI [6].

The system makes it possible for a person with no previous training and within 15 minutes of wearing the electrode cap, to move a pointer to any location of a computer screen.

SYSTEM

We used the 19 channels corresponding to the 10-20 international system to acquire EEG. The analysis of the P300 components is preceeded by a preprocessing phase in which: a) each channel is low-pass filtered using a FIR filter (order 30, $f_{pass} = 34\,\text{Hz}$, $f_{stop} = 47\,\text{Hz}$), b) the signal is decimated to a sampling rate of 128 Hz, c) the Continuous Wavelet Transform (CWT) of each EEG channel is performed. CWT was done at 30 different scales between 2 and 40 and for a temporal window from 235 ms and 540 ms after the presentation of stimuli. So, the ERP response to each stimulus gives us a 3–D array $\mathbf{V}(c, s, t)$ of features, where c indexes the channel, s the scale and t the time corresponding to a feature. In total we have $19 \cdot 30 \cdot 40 = 22,800$ components.

Because of the large numbers of features we performed feature selection using a wrapper approach where the selection of features and the training of a classifier are performed jointly.

Computer mice are fundamentally analogue devices. So, it seemed inappropriate to turn analogue brain activity recorded in the EEG into binary form, as it is done traditionally in P300-based BCI by thresholding the output of classifiers, to later turn the signal in analogue form again. So, we felt that an analogic BCI approach would offer the potential to better use the information present in P300s.

To obtain this, the motion of the pointer is directly determined by the output of a filter. More precisely, the vertical motion of the pointer is proportional to the difference between the output produced by the filter when processing an epoch where the "up" rectangle was flashed and the output produced by the filter when processing an epoch where the "down" rectangle was flashed. Horizontal motion is determined similarly.

Therefore, the task of the GA is not just selecting features and designing detectors to best discriminate between P300 and non-P300 responses, but also to do so in such a way that the responses to pairs of stimuli provide the fastest and most precise way of moving the pointer in the desired direction.

To control the motion we used the output of the following filter which combines a subset of elements of the feature matrix $\mathbf{V}$:

$$O(\mathbf{V}) = \arctan\left(a_0 + \sum_{j=1}^{N} a_j \cdot \mathbf{V}(c_j, s_j, t_j)\right) \qquad (1)$$

where N is the number of terms in the filter, the coefficients c_j, s_j, t_j identify which component of $\mathbf{V}$ is used as the j^{th} feature, and finally the values a_j are coefficients weighing the relative effect of each term. We take a *single trial* approach. This allows our mice to move approximately once per second.

Each individual in the GA represents a tentative solution to the problem, i. e. it is a collection of the parameters a_j, c_j, s_j and t_j that need optimising. In the GA runs we used tournament selection, blend crossover, headless-chicken mutation, populations of size 50,000, and 40 generations.

The problem of evolving a mouse is multi-objective: we want to obtain both maximum motion in the desired direction *and* minimal motion in the orthogonal direction. To achieve this we used the following fitness

function:

$$f = \alpha \left(\sum_{t=1}^{N} \sum_{i=1}^{30} \left(v_d^{i,t} - 0.2 \left| v_o^{i,t} \right| \right) - 0.2 \left| \sum_{t=1}^{N} \sum_{i=1}^{30} v_o^{i,t} \right| \right)$$

where $\alpha = 1/(30N)$, N is the number of groups of 30 repetitions of a command (up, down, left or right), $v_d^{i,t}$ represents the motion in the target direction produced at repetition i in the t^{th} group of 30, while $v_o^{i,t}$ represents the motion produced in the direction orthogonal to the desired direction.

RESULTS

We report results with 3 participants: A (male, age 25), B (male, age 28) and C (female, age 35). During the phases of acquisition of training and validation sets, the experimenter selected one of the rectangles on the screen as a target, and participants were asked to count the number of flashes of the target. During testing, participants are asked to perform the same task, except the trajectory of the mouse pointer produced by their efforts was also shown. Each run of our experiment involved presenting a full series of 4 flashing rectangles for 30 times. The process was repeated multiple times for each direction. For participant A, 12 runs were recorded while B and C performed 16 runs.

3- and 4-fold cross-validation was used to train the filters and test their performance and generalisation ability. For each participant a total of 12 different classifiers have been evolved.

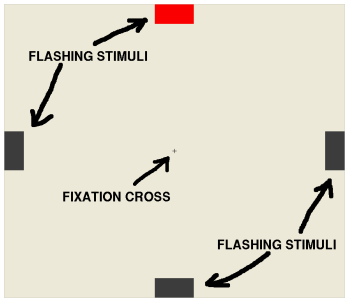

Figure 1: The stimuli used for BCI mouse control.

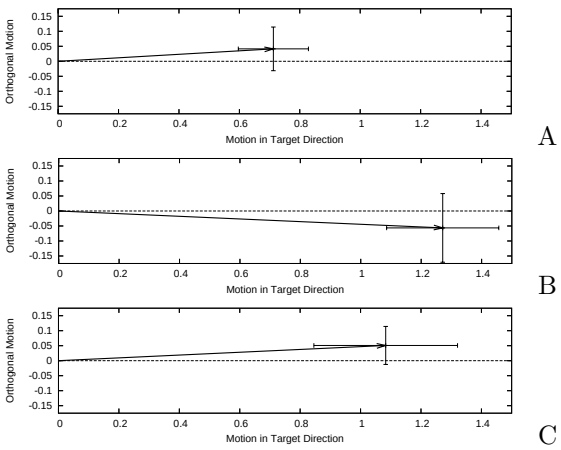

Figure 2: Performance on validation set.

The accuracy results for the validation set are depicted in Figure 2. The arrows represent the average distance travelled in the direction of the target and in a direction orthogonal to the target. The crosses represent standard deviations over the performance of different classifiers. Clearly users were able to move the mouse pointer in the desired direction with only minor inaccuracies.

CONCLUSIONS

In this paper we have proposed a BCI mouse based on the manipulation of P300s. The system is analogue, in that at no point a binary decision is made as to whether or not a P300 was actually produced in response to a particular stimulus. Instead, the motion of the pointer on the screen is controlled by directly combining the amplitudes of the output produced by a filter in the presence of different stimuli.

The performance of our BCI mouse is very encouraging. Control in testing was accurate and all participants were able to use the system within 15 minutes of wearing the electrode cap.

The hardest part of the design in this system (i. e. the feature selection and the selection of the order and parameters of the controller) was entirely left to a genetic algorithm. We only provided carefully designed stimuli, a rich set of features (wavelet coefficients) and a simple combination mechanism (a squashed linear filter) through which we thought a solution to the problem of controlling a pointer via EEG could be found.

The GA has been very effective and efficient at finding good designs for the system. Indeed, it succeed in every run, suggesting that we had chosen a good infrastructure and feature set for the system.

REFERENCES

[1] Farwell LA, Donchin E. Talking off the top of your head: A mental prosthesis utilizing event-related brain potentials. Electroencephalography and Clinical Neurophysiology, 1988; 70: 510–523.

[2] Cinel C, Poli R, Citi L. Possible sources of perceptual errors in P300-based speller paradigm. Proc. of the 2nd Int. BCI Workshop & Training Course 2004, Suppl. Vol. Biomed. Tech.(Berlin), 2004; 49(1): 39–40.

[3] Beverina F, Palmas G, Silvoni S, Piccione F, Giove S. User adaptive BCIs: SSVEP and P300 based interfaces. Psychology Journal, 2003; 1(4): 331–354.

[4] Poli R, Cagnoni S, Valli G. Genetic design of optimum linear and non-linear QRS detectors. IEEE Trans Biomed Eng, Nov 1995; 42: 1137–1141.

[5] Cagnoni S, Dobrzeniecki AB, Poli R, Yanch JC. Genetic algorithm-based interactive segmentation of 3D medical images. Image and Vision Computing, 1999; 17: 881–895.

[6] Citi L, Poli R, Sepulveda F. An evolutionary approach to feature selection and classification in P300-based BCI. Proc. of the 2nd Int. BCI Workshop & Training Course 2004, Suppl. Vol. Biomed. Tech.(Berlin), 2004; 49(1): 41–42.

P300-BASED BRAIN COMPUTER INTERFACE: MULTIPLE LETTER KEYS VS. FOUR ARROWS DISPLAYS

F. Piccione[1], G. Palmas[2], F. Beverina[2], F. Giorgi[1], K. Priftis[3], L. Piron[1], M. Cavinato[1], S. Silvoni[1]

[1]Department of Neuro-rehabilitation, S. Camillo Hospital, Alberoni, Venice, Italy
[2]STMicroelectronics - AST Group, Agrate Brianza, Italy
[3]Department of General Psychology, University of Padova, Padova, Italy
E-mail: piccioneparrinello@aliceposta.it

SUMMARY: Two of actual BCIs system requirements are the improvement of the communication speed and the classification accuracy. The higher speed and accuracy, the greater use of BCI system to solve difficult tasks. To tackle this problem in a P300-based BCI system, the elicitation paradigm and the stimuli presentation should be deeply considered [2]. Also the data processing and the classification system should not be neglected. Our study evaluates three visual elicitation paradigms which use a different number of stimuli with dissimilar meaning. The four arrows paradigm [5] is compared with variants of Farwell and Donchin [3] spelling paradigm (multiple letter keys paradigm). A comparison between the two methods suggests that increasing the paradigm complexity, the correct single-sweep ERPs recognition task becomes more difficult.

INTRODUCTION

In the P300-based BCI research, recent studies investigate accuracy of ERPs recognition using traces average method [7] and different classification algorithms. These studies have shown that this type of system can be potentially used to help locked-in subjects to communicate with the environment. Differently, few studies have focused the attention to the structure of elicitation paradigm, the modality of stimulus presentation, the complexity of stimulus meaning, in order to permit a single-sweep P300 wave detection [1, 6]. As reported in literature, the P300 wave parameters (latency, amplitude) and its morphology strongly depend on these variants [4]. Our study evaluates the recorded ERPs behaviour related to different paradigms in order to check the single-sweep P300 wave recognition capability.

MATERIALS AND METHODS

Subjects: 5 healthy subjects voluntarily participated to the study (2 females and 3 males, mean age of 36 years, range 26–43 years). Participants did not present cognitive deficits and had P300 wave parameters within the normative guidelines.

Tasks and stimulation paradigms: The first paradigm is described in a previous report [5] (P1: four arrows): the task is to move a cursor until it reaches a target, using the directional meaning of each stimulus. The second and third alphabetical paradigms are variants of Farwell and Donchin spelling paradigm [3] (respectively, P2: colored keys; P3: grey-scale keys): the task is to compose a word of 5 letters length (such as "bread", etc.), then to select the *"ok"* button, using a multiple letter keypad. The stimulus (single trial) consists in a single flash of a key border at a time (flash time equal to 200 ms); the inter-stimulus interval (ISI) is 2 s, and a stimulus is called *target* if the flashed key contains the target character (Figure 1), otherwise it is called *non-target*. The main hypothesis is that every *target* stimulus elicits a P300. All ten keys are highlighted with an occurrence probability of 0.1 in a randomize sequence of trials. We call "session" the whole trials sequence until the *"ok"* button is selected (after the five characters selection). In this context we carry out only *learning* sessions, where the feedback for the subject is the appearance of the target letter when it is selected. Each subject is tested by 5 *learning* sessions per paradigm (one paradigm a day).

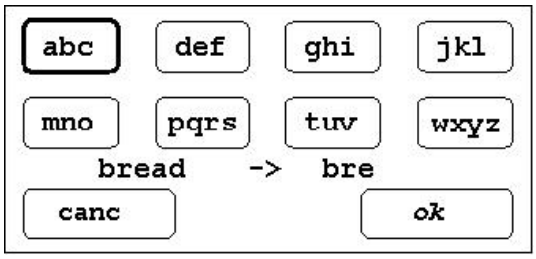

Figure 1: Multiple letters keypad interface.

Data acquisition: Registration electrodes were placed according to the international 10-20 system at Fz, Cz, Pz and Oz; the EOG was placed at SO2; all electrodes are referenced to bilateral earlobes. The five channels were amplified, band-pass filtered between 0.15 Hz and 30 Hz, and digitized (with a 16-bit resolution) at 200 Hz sampling rate. Every ERP epoch, synchronized with the stimulus, began 100 ms before the stimulus onset, up to 900 ms after stimulus trigger signal (tot. 1000 ms). Thus, after every stimulus the system recorded a matrix of 200 samples per 5 channels, available for the *off-line* data processing.

Data analysis: During *off-line* operations we primarily extracted a direct index (called *"ra"*) of the difference between the two types of ERPs response for each subject and each paradigm session sequence; thus, considering a subject and a paradigm, we evaluated the 5 sessions raw traces average of the channel PZ, then the *"ra"* index as follow: the sum of absolute differences between *target* and *non-target* average traces (respectively $avg_2^{PZ}(k)$ and $avg_1^{PZ}(k)$, $k \in [1, 200]$) in the

interval 200–700 ms (1):

$$ra = \sum_{k} \left| avg_2^{PZ}(k) - avg_1^{PZ}(k) \right|, k \in [60, 160] \quad (1)$$

Secondarily, we applied the procedure described in [5] to assess the single-sweep P300 wave recognition; for each subject and each paradigm, we trained a specific classifier extracting the target traces recognition error ratio (2):

$$ep3 = \frac{n2 - p3ok}{n2} \quad (2)$$

where $n2$ is the number of *target* stimuli and $p3ok$ is the number of *target* traces correctly recognised.

Table 1: P1, P2 and P3 paradigms comparison (ra, $ep3$)

	P1		P2		P3	
subject	ra (uV)	ep3	ra (uV)	ep3	ra (uV)	ep3
1	714	0.42	167	0.83	419	0.83
2	521	0.44	307	0.83	102	0.83
3	312	0.72	145	0.83	105	0.83
4	331	0.59	162	0.83	256	0.83
5	201	0.52	201	0.83	107	0.83

RESULTS

We reported the results (Table 1) of our analysis in terms of *"ra"* index and error ratio in the target traces recognition ($ep3$). Friedman's Analysis of Variance (ANOVA) for repeated measures revealed a significant difference in the distribution of the PZ *"ra"* index for the three paradigms, $\chi^2(2) = 7.6$, $p < 0.05$. Pairwise comparisons for repeated measures using the Wilcoxon test showed significant differences between P1 and P2 ($p < 0.05$) and between P1 and P3 ($p < 0.05$). In contrast, the difference between P2 and P3 was not significant. Figure 2 underlines the differences between *target* and *non-target* average traces for each paradigm.

DISCUSSION

The results indicate that relevant distinctions between the paradigm P1 and the paradigms P2 and P3 exist. As we can see (Table 1, $ep3$ parameter), all subjects elicit a single sweep detectable P300 wave during paradigm P1; conversely, a slight detectable single sweep P300 was elicited by means of P2 and P3. In this case a correct ERPs recognition is possible as well, using traces average method. Moreover, we observe significant differences also comparing the *"ra"* index (see Table 1, Figure 2). The dissimilarities between the first two paradigms are related to the number of stimuli, 4 vs. 10 stimuli, and the meaning of each stimulus target, directional vs. alphabetical ones; the third paradigm differs from the second one only for the black/white vision. Others differentiation regard the position of the flashed stimuli, screen border arrows vs. equally positioned keys, and the stimuli shape, arrows vs. smoothed rectangles. The number of stimuli difference implies that in the multiple letter keys paradigms the occurrence of a target stimulus decreases from 0.25 to 0.1; besides, by a cognitive point of view, all other differences yield to an increment of the subjects recognition task complexity. Altogether, the increment of the task difficulty can be quantitatively observed evaluating the recorded ERPs behaviour.

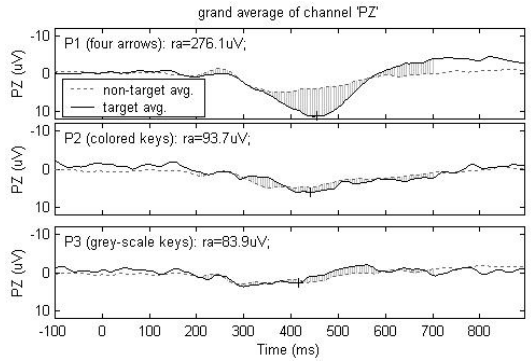

Figure 2: Comparison of the *target* and *non-target* grand average traces (for each paradigm the average of all subjects traces was considered, channel PZ).

CONCLUSION

In this paper, we have analysed the ERPs response of three paradigms that can be used in a P300-based BCI environment. Many factors influence the cognitive potential elicitation, modifying the differences between the *target* and *non-target* response. Comparing the three methods, the ERPs behaviour changes reflecting the increment of the task difficulty.

REFERENCES

[1] Bayliss JD, Inverso SA, Tentler A. Changing the P300 brain computer interface. Cyberpsychol Behav, 2004; 7(6): 694–704.

[2] Birbaumer N. Brain-computer-interface research: Coming of age. Clin Neurophysiol, 2006; 117(3): 479–483.

[3] Farwell LA, Donchin E. Talking off the top of your head: toward a mental prosthesis utilizing event-related potentials. Electroenceph Clin Neurophysiol, 1988; 70: 510–523.

[4] Nobre AC. Orienting attention to instants in time. Neuropsychologia, 2001; 39: 1317–1328.

[5] Piccione F, Giorgi F, Tonin P, Priftis K, Giove S, Silvoni S, Palmas G, Beverina F. P300-based brain computer interface: Reliability and performance in healthy and paralised participants. Clin Neurophysiol, 2006; 117(3): 531–537.

[6] Sellers EW, Donchin E. A P300-based brain computer-interface: Initial tests by ALS patients. Clin Neurophysiol, 2006; 117(3): 538–548.

[7] Thulasidas M, Guan C, Wu J. Robust Classification of EEG Signal for Brain-Computer Interface. IEEE Trans Neural Syst Rehab Eng, 2006; 14(1): 24–29.

IMPROVING BIT-RATE IN P300-BASED BCI USING GRAMMATICAL RULES AND LANGUAGE PROBABILITY

A. Jiménez-Ramos, O. Yañez-Suárez

Neuroimaging Laboratory, Universidad Autónoma Metropolitana-Iztapalapa, México.
E-mail: biomedicoajr@gmail.com

SUMMARY: An ensemble of EEG recordings of event related potentials from the P300 speller BCI is typically used to detect the character being communicated. As more trials in the ensemble are used, the detection accuracy increases. However, the price to be paid is a reduced bit rate. In this paper, an algorithm using grammatical rules and language probability is coupled with support vector machine classifiers in order to reduce both the number of misclassified characters and the number of trials required for accurate detection, so that the highest possible bit-rate is achieved with a minimum loss of accuracy. The prediction model proposed is independent from the chosen language and can be utilized in any method of P300 based spelling.

INTRODUCTION

The P300 is a characteristic waveform in the human EEG that occurs as a response to rare event-stimuli. Farwell and Donchin were the first to introduce the use of the P300 potential into BCI [1]. In the P300 speller, the key task is to detect P300 events in the EEG recording, both accurately and immediately, to ensure the highest possible bit-rate transfer between human and computer.

In a P300-based BCI system, P300 events are usually detected using signal enhancement and pattern recognition techniques on the basis of ensemble averaging of several trials. In general, the more averaged trials, the higher the detection accuracy. But, at the same time, the more averaged trials, the lower the bit-rate. Therefore, the performance in terms of BCI communication rate is determined by both the number of trials and the detection accuracy.

The introduction of grammatical rules and language probability in a P300 speller system could minimize the number of trials used to infer a symbol, especially when the data doesn't have good quality due to common online BCI artifacts such as EOG or EMG.

METHODS

EEG Recording and Experimental Paradigm: One hundred and seventy 64-channel EEG recordings, corresponding to the training data set II provided for the BCI Competition III [2] were utilized in this study. Such recordings were obtained from two different subjects (85 records each) performing a visual speller task, following the paradigm described by Donchin et. al. [1], which evokes P300 event related potentials (ERP) under directed spelling. Each record corresponds to 15 trials of speller matrix intensifications.

Data pre-processing: Every character epoch was bandpass filtered with a zero-phase, 120^{th} order FIR filter with low cutoff at 0.5 Hz and high cutoff at 10 Hz, and undersampled accordingly. Temporal windows from 0 to 850 ms were extracted and divided into row- and column-wise stimuli. All epochs were biased and scaled to attain zero mean and unit standard deviation normalization. EEG recordings were not restored nor manually intervened to select or reject components.

Classification: Non-linear (RBF) support vector machine (SVM) classifiers were trained per trial and repetition, to differentiate patterns with and without P300 events. Subsampling of the non-P300 class pattern pool in the training set was performed to equalize prior probabilities. Outputs of the SVM's were transformed into estimates of posterior probability through logistic regression. Independent SVM's were designed for row- or column-wise stimuli and a subset of the 10 channels providing the best classification efficiency was selected per subject. Cumulative values of the row and column posterior probabilities along several trials were used for decision-making, selecting the character with the largest value of cumulative posterior probability [3]. Classification efficiency was estimated by six-fold cross validation.

Word Formation: Assuming that in the P300 speller, the ERPs are independent events from character to character, the pool of 170 character responses was used to assemble a collection of 50 words in Spanish (although the approach is independent of the chosen language). Whenever more that one response associated to the same character was available, it was chosen randomly among the options. The words built were chosen randomly as well, but trying to incorporate all the characters.

Word Prediction: An algorithm using grammatical rules and language probability, based on the Prediction by Partial Matching algorithm (PPM) [4] is introduced once the cumulative values of the row and column posterior probabilities are available. The next character is predicted using the k previous characters, with the prediction order of the model increasing dynamically with the number of characters in the word. The prediction model uses a suite of fixed-order context with different values of k, from 1 up to some pre-determined maximum given by the length of the word itself. The first character in a word is always determined using cumulatives of the row and column posterior probabilities after N trials, to ensure that the first character will be maximally correct. Given the first character, obtained solely from ERP classification, the prediction procedure can be summarized as follows:

1. Using grammatical rules, only cumulative posterior probabilities for characters with probability not equal to zero are considered. For example, having detected letter 'p', letter 'x' has probability zero to occur.

2. For characters with probability not equal to zero, a relevance score is computed as the product of cumulative values of the row and column posterior probabilities and the language probability. Language probability is the conditional probability of the i^{th} character given the previous $i-1$ detected characters. These probabilities are precomputed based on a language dictionary of more than 3000 words [5], in terms of relative frequencies of occurrence of the letter sequence.

3. A dynamic score threshold for prediction is then established, as the value of the maximum score minus n-times the standard deviation of all possible character products ($n = 0.8, 1.0, 1.5$).

4. If there is just one product score above the threshold, the corresponding character is selected. If more than one character exceeds the threshold, the next EEG trial is used (from the 15 available) and the process is repeated until only one character is selected.

5. The next character is predicted repeating steps 1–4, but with language prediction order k increased by one.

RESULTS

Table 1: Electrode subsets used for classification

Channels used for analysis in the classification	
Subject A	{Fcz,C1,Cz,Cpz,Fp1,Fp2,F3,Pz,Po3,Po8}
Subject B	{Fc4,C2,Cp2,F2,Pz,Po7,Po4,Po8,O1,O2}

Table 2: Number of trials and prediction accuracy, where * is the value of decision threshold, while ** means the use of the same threshold as in (a) but without considering language probability. Using the largest value of cumulative posterior probability after 10 trials for all characters 100 % accuracy was achieved.

Method of Word Prediction	Number of trials/character (mean)	Bit-rate (bits/min)	Accuracy (%)
SVM + language model			
(a) $n = 1.5^*$	6.83	19.52	95.42
(b) $n = 1.0^*$	5.39	23.32	92.57
(c) $n = 0.8^*$	4.70	25.76	90.28
*SVM alone***	8.43	10.47	75.42

Table 1 lists the electrodes used in classification for each subject. Table 2 shows the number of trials, bitrate and detection accuracy obtained for different values of decision threshold, on the set of 50 different words for both subjects. The first character within a word was determined using 10 EEG trials in all cases.

DISCUSSION

The prediction model has a direct impact on the number of trials used to ensure a high accuracy in character detection. Its use accelerates BCI communication by improving character classification with a minimum loss of accuracy, due to the introduction of language probability.

There are some considerations to include in the algorithm described above. If we have just one possibility given by the language probability we infer the upcoming character in just one trial. When we have a difficult decision, (the statistical threshold is unable to select a maximum), we choose that character that has been selected 3 consecutive times in the last trials.

The model proposed in this work can be used as an auxiliary tool for any other method of P300 detection in the speller task. Furthermore, the algorithm of language prediction implemented is independent of the language, which makes it flexible and reliable.

ACKNOWLEDGEMENT

The authors are grateful to M. Sc. Gerardo Gabriel Gentiletti (Universidad Nacional de Entre Ríos, Argentina and Neuroimaging Laboratory, UAM) for his support in providing the classification software and data processing.

REFERENCES

[1] Farwell LA, Donchin E. Talking off the top of your head: Toward a mental prothesis utilizing event-related brain potentials. Electroenceph Clin Neurophysiol, 1988; 70: 510–523.

[2] Blankertz B. The BCI competition III, 2004.

[3] Gentiletti G, Thesis PD. Universidad Autónoma Metropolitana Iztapalapa, México, 2006.

[4] Cleary JG, Teahan WJ, Witten IH. Unbounded length contexts for PPM. The Computer Journal, 1997 comjnl.oxfordjournals.org

[5] Online Spanish dictionary, available at http://www.proyectosalonhogar.com; accessed 08/05/2006.

BRAIN-COMPUTER INTERFACING USING SELECTIVE ATTENTION AND FREQUENCY-TAGGED STIMULI

P. Desain[1], A. M. G. Hupse[1], M. G. J. Kallenberg[1], B. J. de Kruif[1,2], R. S. Schaefer[1]

[1]Music, Mind, Machine Group, NICI, Radboud University Nijmegen, The Netherlands
[2]Department of Biophysics, Radboud University Nijmegen, The Netherlands
E-mail: desain@nici.ru.nl

SUMMARY: Selective attention can offer new possibilities for Brain Computer Interfacing (BCI) by separating compound streams of presented stimuli. An added watermark in the stimuli that can easily be extracted from the EEG signals yields possibilities for increased reliability in classification. The effect strength of the watermarks on cerebral activity is influenced by purposefully directed attention.

INTRODUCTION

Imagining temporal patterns (auditory, tactile, motor) as a cognitive task is a viable means of driving a BCI. As such, no stimulus is needed. However, asynchronous BCI analyses, not needing information on when a pattern of brain activity is generated, are complicated because of the weak and noisy signals, and thus some synchronization, or time-lock, is used. However, the time-lock in such tasks often becomes rather loosely coupled to brain activity, as the lock is only based on a prompting cue. Due to the high frequency and the short duration of the waveforms, the jitter in the time-lock should however be kept minimal.

For patterns which can be represented on a regular temporal grid (such as a musical rhythm) the grid can be presented (e. g. as a metronome), inducing a framework against which to imagine the pattern, thus minimising the jitter. Instead of imagining events that strictly fall on this grid, the cognitive task can be shifted to focusing attention on only part of the stimulus presented by the metronome. The task of BCI analysis is to distinguish between attended and non-attended events. In the auditory domain sequential selective attention occurs spontaneously in the so called clock-illusion, in which an identical train of isochronous beats is heard as a 'tick-tock' percept [1]. This has been shown to elicit attention-modulated differences in EEG P300 traces [2].

Adding to sequentially varying attention, one can also selectively attend to one of several simultaneously presented stimuli, consisting e. g. of a mixture of tones, tactile stimuli, or spatially divided auditory sources. Natural cognitive mechanisms that mute non-attended streams of information from the environment can be used towards driving a BCI. Imprinting the different streams with unique and easily identifiable watermarks, the BCI only needs to detect the strongest watermark and as an added advantage, the time-lock will be tight.

The auditory stimulus used here is a combination of two frequencies. The subject is instructed to focus on one of them, each is watermarked by an AM modulation of a different frequency. Although the fundamental pitch of a presented tones may not be easily recovered from measurement of brain activity, the AM frequency can be detected, making this a suitable method for hearing tests [3]. For BCI, the AM frequency tag is used as a watermark whose salience is modulated by selective attention [4]. Likewise, the trill-frequency of vibration can be used for the tactile sense [5, 6]. The signal processing needed for detection of such tags is relatively easy (filtering at a known frequency, power and phase estimation) and the BCI performance depends on the amount and robustness of the modulation of these signals by attention, and the classification of these features (albeit possibly in many channels and with a specific spatio-temporal evolution).

MATERIALS AND METHODS

Apparatus: Frequency tagged stimuli are presented in two modalities; auditory (presented through passive loudspeakers) and tactile. For the tactile stimuli, a device was designed and made using 8 separately moveable pins that produce braille-like patterns that can be presented to one or more fingers in parallel, using different frequencies of stimulation (see Figure 1).

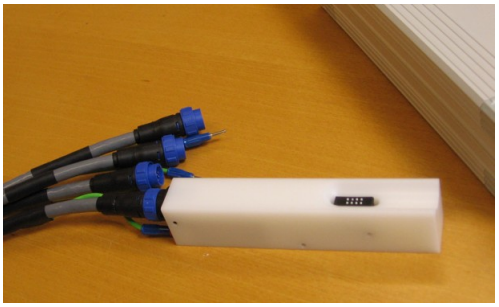

Figure 1: Tactile stimulator

Data-analysis: When attending to a frequency-tagged stimulus, the EEG signal is processed in two steps (see Figure 2): First, two filters are applied in parallel to the data, each with a pass-band of one of the frequencies that have been added to the stimulus. Second, a Hilbert transform is applied, which – by taking the absolute value and the angle respectively – yieds the amplitude and phase of the frequency of interest. These features are then fed to a classifier.

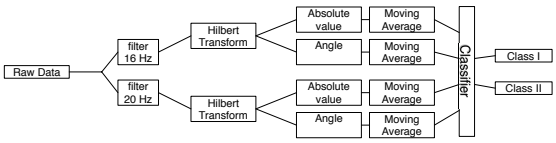

Figure 2: Data analysis schema

RESULTS

In order to examine the proper configuration of the data-analysis, a simulation was performed. Here, the two attention effects reported in the literature (an increased power and a phase-shift of the oscillation of the AM frequency in a frequency tagged sine tone) are implemented.

The output of the analysis of these simulated data is shown in Figure 3. The top plot of the figure shows the simulated EEG measurement. It consists of a 16 Hz and a 20 Hz sine wave, corrupted by noise. In the first half, the 16 Hz was larger in amplitude and leading in phase, while for the second half the 20 Hz component was larger in amplitude and leading in phase. This is predicted when shifting the focus from the 16 Hz modulated sine to the 20 Hz modulated sine [3].

The second plot from the top shows the output of the bandpass filters, while the third plot shows the estimate of the phase and magnitude of both filter outputs. The bottom plot shows the amplitude and phase for 100 repeated trials.

DISCUSSION

The analysis on the simulated data shows that the data-analysis is able to reveal the effects that have been described in the literature. Although these simulated results do not yield any conclusive evidence, they support the feasibility of using selective attention towards driving a BCI device given the reported findings of the processing of frequency-tagged stimuli. Eventually, the combination of two modalities could produce binding effects that can improve classification even further. That possibility is, however, still to be investigated.

CONCLUSION

By using stimuli to respond (or attend) to when driving a BCI device, the problem of synchronization or time-locking of EEG activity is tackled in an efficient and natural way. As the time dimension is extremely precise in EEG measurements, not exploiting this in developing methods for BCI appears to be a missed opportunity for increased reliability and speed.

REFERENCES

[1] London J. Hearing in time. Psychological aspects of musical meter. Oxford University Press, 2004.

[2] Brochard R, Abecasis D, Potter D, Ragot R, Drake C. The "ticktock" of our internal clock: Direct brain evidence of subjective accents in isochronous sequences. Psychol Sci, 2003; 14(4): 362–366.

[3] Picton TW, Skinner CR, Champagne SC, Kellett AJC, Maiste AC. Potentials evoked by the sinusoidal modulation of the amplitude or frequency of a tone. J Acoustical Society of America, 1987; 82(1): 165–178.

[4] Ross B, Picton TW, Herdman AT, Hillyard SA, Pantev C. The effect of attention on the auditory steady-state response. Neurol Clin Neurophysiol, 2004; 22: 1–4.

[5] Bauer M, Oostenveld R, Peeters M, Fries P. Tactile spatial attention enhances gamma-band activity in somatosensory cortex and reduces low-frequency activity in parieto-occipital areas. J Neurosci, 2006; 26(2): 490–501.

[6] Müller-Putz G, Scherer R, Neuper C, Pfurtscheller G. Steady-state somatosensory evoked potentials: suitable brain signals for Brain-Computer Interfaces. IEEE Trans Neural Syst Rehabil Eng, 2006; 14(1), 30-37

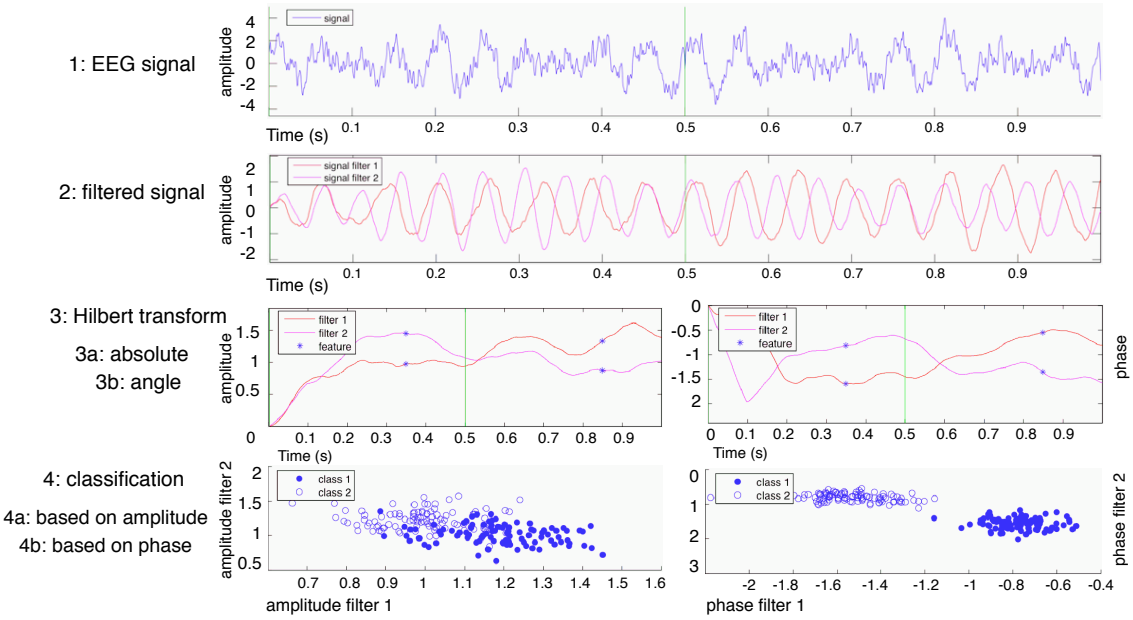

Figure 3: Data-analysis on simulated data

HEART RATE-CONTROLLED EEG-BASED BCI: THE GRAZ HYBRID BCI

G. Pfurtscheller, R. Scherer, G. R. Müller-Putz

Laboratory of Brain-Computer Interfaces (BCI-Lab), Institute for Knowledge Discovery, Graz University of Technology, Austria
E-mail: pfurtscheller@tugraz.at

SUMMARY: A novel steady state visual evoked potential-based (SSVEP) BCI is introduced where the battery of flicking lights is switched on and off by the respiratory heart rate (HR) response. This "Graz hybrid BCI" has two modes, the slow intentional control based on the detection of the respiratory HR response and the fast intentional control based on SSVEP detection. Preliminary data of 3 healthy subjects are reported. One important aspect is that the Graz hybrid BCI needs only one EEG and one ECG signal and operates satisfactorily also during verbal interaction with the user.

INTRODUCTION

A Brain-Computer Interface (BCI) can be operated by different mental strategies such as operant conditioning, motor imagery, P300 paradigm or focused visual-spatial attention to a flickering light [1, 2]. Of special interest in terms of speed, accuracy and simple EEG recording is the induced oscillatory response due to periodic light stimulation known as steady-state visual evoked potential (SSVEP) [3]. In the case of an e. g. prosthetic control, longer breaks can occur between 2 control states and therefore it is recommended to switch "on" the lights only when needed for control. One possibility to realize such a switch-function is to use the ECG for detecting transient heart rate (HR) changes associated with a brisk inspiration. The HR is influenced by a number of physiological mechanisms. Beside others, reflex mechanisms and high level brain stimuli (central commands) modulate sympathetic and vagal outflow from the brain stem. For example, a single, brisk inspiration results in a HR response in form of an initial acceleration, followed by a deceleration and return to the baseline.
The goal of this paper is to introduce a novel SSVEP-based 4-class asynchronous BCI which is controlled by the HR response.

MATERIALS AND METHODS

Three subjects aged between 18 and 30 participated in the study. All had normal vision and were seated 1 m in front of the stimulation unit (SU) during the training session. The SU was composed of 4 light-emitting diods (LEDs) flickering with 6, 7, 8 and 13 Hz. For the prosthetic device control (hand prosthesis, Otto Bock, Vienna, Austria) 4 LEDs were fixed on different parts of the prosthesis with the goal to control different types of movement (with different flicker frequencies): lateral 5^{th} finger → turn left (6 Hz), lateral index finger → turn right (7 Hz), wrist → hand open (8 Hz) and wrist → hand close (13 Hz) (Figure 1).

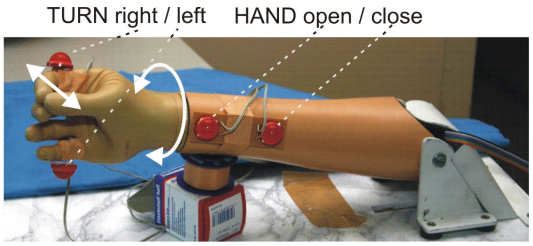

Figure 1: Hand prosthesis with LEDs mounted

Continuous EEG signals were recorded bipolarly over the occipital cortex, filtered between 0.5 and 30 Hz and digitalized at a rate of 256 Hz. Simultaneously the ECG was recorded bipolarly from the thorax and also sampled with 256 Hz.
The EEG was analyzed by calculating 1-s power spectra in steps of 250 ms. For classification the sums of the harmonic components were computed at each stimulation frequency. The maximum of the harmonic sums (HS) was used to define the detection threshold which had to be exceeded for at least 1 s (dwell time). After this 1-s period a prosthetic movement was triggered, followed by a refractory period of 8 s (details see [3]).
The instantaneous heart rate (IHR) was computed by the detection of beat-to-beat intervals in the ECG. From the IHR the first derivative was calculated and a subject-specific threshold (TH_{ECG}) was determined by help of ROC curves. When this differentiated IHR time series (dIHR) exceeded TH_{ECG} a switch operation (switching on or off the flickering lights) was triggered.
The following experimental protocol was used for optimizing the subject-specific threshold of the HR-switch:

1. Cue-based brisk inspiration in randomized intervals over a period of 380 s (20 trials, mean duration 19 s).

2. Alternating periods of resting and activity, like loud reading of a newspaper, SSVEP-control and an interview, over a period of 900 s.

Experiment 1 was primarily used to define the true positive and false negative (TP and FN) and experiment 2 was necessary especially to define the true negative (TN) and the false positive (FP) responses. The analysis was done sample-by-sample (beat-to-beat), with the same threshold for both experiments and a cue-based time window of 4 s to define the TP. In the case of a duration of 1240 s (340 + 900) for both experiments and a mean beat-to-beat interval of 1 s (corresponding to 60 bpm) the total number of samples (TN + TP + FP + FN) was 1240.

The optimized HR-detector was used to switch on/off the flickering lights of the 4-class (2-axis hand prosthetic control) SSVEP-based BCI. The subjects were instructed to autonomously start and finish the SSVEP-based BCI operation within a 10 min period and perform the following movement sequence: turn right (TR), hand open (HO), hand close (HC), turn left (TL), HO, TR, TL and HC.

RESULTS

An example of different time courses of one representative subject for the experiments 1 and 2 are displayed in Figure 2. IHR and dIHR curves are displayed below the respiratory signal. The vertical lines indicate the cue-stimulus presentation in experiment 1 and the changes of different conditions in experiment 2. The horizontal line marks the threshold defined by ROC analyses. The results of the ROC analyses and the corresponding performance of the "HR-Switch" is summarized in Table 1. The averaged IHR and the average derivative IHR (dIHR) of the cue-based training experiment 1 are shown in Figure 3.

Altogether 1 to 3 repetitions of the predefined prosthetic hand movement sequence were realized. The SSVEP performance is summarized in Table 2. During the experiment for 2 subjects only 1 FP HR-change was detected.

Table 1: Performance measures of the HR-switch (ROC-Analysis). The detection threshold (TH_{ECG}) and TP/FP rates are listed for each subject. Additionally to the FP rate also the number of FP (FP#) and total number of TN are reported.

Subject	TH_{ECG}	TP%	FP%	FP# (TN#)
s1	-0.046	90.0	11.0	151 (1369)
s2	-0.024	90.0	3.3	50 (1515)
s3	-0.070	90.0	10.0	125 (1252)

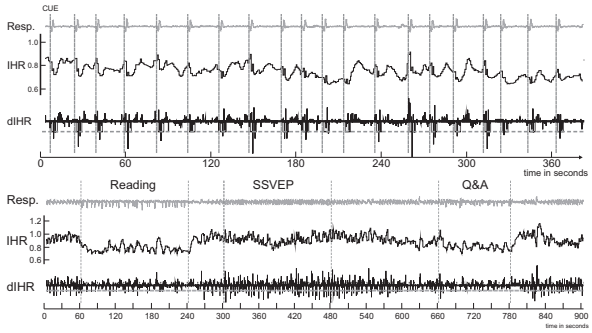

Figure 2: Example of respiratory signal, IHR and differentiated IHR (dIHR) for experiment 1 (upper panel) and experiment 2 (lower panel)

Table 2: True positives (TP) and false negatives (FN) for best peformance of a predefined sequence of 8 prosthetic movements for 3 subjects. "moves" indicate the number of correct movements.

Subject	TP	FN	moves
s1	9	1	8
s2	9	1	8
s3	12	18	7

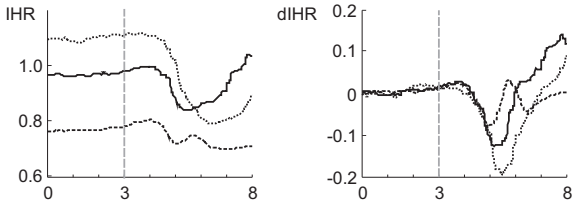

Figure 3: Averaged IHR (RR-interval) (left) and average dIHR (right) for 3 subjects

DISCUSSION

It was demonstrated for the first time that both, EEG and ECG recording can be used to create a hybrid BCI with two modes. One mode is the slow intentional control (SIC) based on the detection of the respiratory heart rate response, the other is the fast intentional control (FIC) based on the induced EEG oscillations while focusing on one of 4 flickering light sources. After a short training time of some minutes subjects were able to obtain SIC control and to deliberately switch on and off a battery of 4 flickering lights. The robustness of the method can further be improved by using a multistream approach with e. g. both dIHR and template matching. Details about FIC with SSVEP were reported elsewhere [3]. Of interest is that during relative long periods (minutes) when no control was intended, only a relative small number of false positive control signals (non-intentional control) were obtained. The aspect of relative immunity to verbal interactions and the simple recording of the ECG signal with 2 chest electrodes are advantages of the Graz hybrid BCI with slow and fast intentional control.

ACKNOWLEDGMENT

This work was supported by the EU Project PRESENCCIA (IST-2006-27731), the Steiermärkische Landesregierung project GZ: A3-16 B 74-05/1 and the Lorenz-Böhler Foundation. We are indebted to C. Keinrath for assistance in data recording.

REFERENCES

[1] Wolpaw JR, Birbaumer N, McFarland DJ, et al. Brain-computer interfaces for communication and control. Clin Neurophysiol, 2002; 113: 767–791.

[2] Pfurtscheller G, Müller-Putz GR, Schlögl A, et al. 15 years of BCI research at Graz University of Technology: Current projects. IEEE Trans Neural Sys Rehab Eng, 2006; 14(2): 205–10.

[3] Müller-Putz GR, Scherer R, Brauneis C, Pfurtscheller G. Steady-state visual evoked potential (SSVEP)-based communication: impact of harmonic frequency components. J Neural Eng, 2005 Dec; 2(4): 123–30.

FIRST STEPS TOWARDS THE NIRS-BASED GRAZ-BCI

R. Leeb[1], G. Bauernfeind[1], S. Wriessnegger[2], H. Scharfetter[3], G. Pfurtscheller[1]

[1]Institute of Knowledge Discovery, BCI-Lab, Graz University of Technology, Austria
[2]Department of Psychology, University of Graz, Austria
[3]Institute of Medical Engineering, Graz University of Technology, Austria
E-mail: robert.leeb@tugraz.at

SUMMARY: In a Brain-Computer Interface (BCI), the electrical activity of the cortex (EEG) is mostly used as input signal. Beside that also the functional activity of the cerebral cortex, the alteration in the cerebral blood circulation in terms of concentration changes of the hemoglobin can be detected with near-infrared spectroscopy (NIRS). In this work, a custom-built NIRS-based BCI is used and the results of the first measurements and the emerging problems, especially the influence of artifacts, are discussed.

INTRODUCTION

A Brain-Computer Interface (BCI) allows users who suffer from neuromuscular impairments the possibility to communicate or interact through thought processes alone. Neural activity (EEG) within the motor cortex is a typical physiological signal used in this context [1]. On the other hand non-invasive near-infrared techniques (NIRS) can also be used to detect functional activity of the cerebral cortex. Thus, the optical response denoting functional brain activation can be used as an alternative to electrical signals. The intention of such a NIRS-based BCI is to develop a more practical, user-friendly BCI and to overcome the limitations and restrictions of EEG acquisition, such as the influence of electrooculogram (EOG), electromyogram (EMG), electrode failures and conductivity problems. An area where it may be disadvantaged, when compared to EEG, is its slower temporal response after brain stimulation. A full description of a BCI we have developed using the above principles [2] is given elsewhere [3].

MATERIALS AND METHODS

NIRS measurement: NIRS measures concentration changes in hemoglobin in the human brain non-invasively. It relies on the principle that light absorption depends on the oxygenation level of the blood, in particular the absorption coefficients of oxy-hemoglobin (HbO_2) and deoxy-hemoglobin (Hb). Oxy-hemoglobin and deoxy-hemoglobin, which are the main absorbers, have different attenuation spectra (see Figure 1). Near-infrared light in the range of the tissue window (630–1300 nm) can penetrate the human adult head to sufficient depths so as to allow functional mapping of the cerebral cortex [4]. The photons are mostly scattered and absorbed, but some are reflected and exit the head at positions up to a few centimeters away from their original source location, thereby the photons travel in an arc-shaped path from source to detector [5]. By measuring the optical attenuation changes at various wavelengths, qualitative measures of brain activity can be obtained [6]. The concentrations of all other absorbers in the blood such as water, lipids and surface tissue are assumed to remain constant over the measurement time.

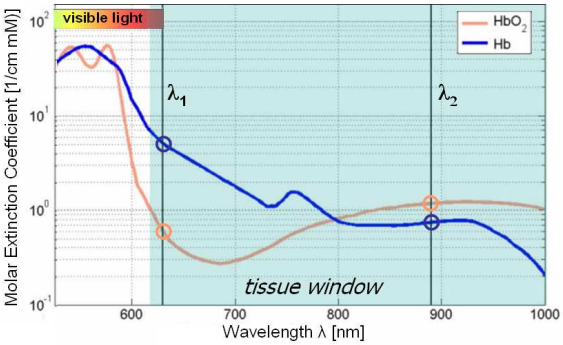

Figure 1: Absorption spectra of Hb and HbO_2

The absorption of light can be described by the Beer-Lambert Law $A = \log(I_0/I) = a \cdot c \cdot x \cdot d$, where A is the attenuation, I_0 is the light intensity entering the tissue, I is the light intensity exiting the tissue, a is the specific extinction coefficient, c is the concentration of the absorption, x is the differential path length factor and d is the geometrical distance between emitter and detector. The NIRS response in the brain is comprised of two signals: 1) there is a slow response (around 5–8 s) as a result of attenuation changes due to cerebral hemodynamics (yielding localized blood circulation and oxygenation changes) [6] and 2) a fast response (in the order of milliseconds) that is thought to be due to changes in the scattering properties of the neuronal membranes during firing [7]. Our current BCI system focuses on the slow vascular response, which can be continuously monitored in real-time.
As sources, LEDs at 670 nm and 890 nm are modulated with a sine at 3 kHz and 7 kHz and placed in direct contact with the scalp. The detector is an avalanche photodiode (APD), which is placed around 3 cm from the light source. With a dual lock-in amplifier the intensities of the two wavelengths are obtained and the oxy- and deoxy-hemoglobin can be determined. It is important to note that the chosen modulation frequencies have no influence on the absorptions and therefore on the detected signals, because the absorptions are only determined by the wavelengths of the LED lights (see Figure 1). With the implemented continuous wave method only relative absorption changes can be detected. Modulation of the light sources and lock-in amplification allows the hemoglobin-detection

to be almost insensitive to ambient light. Nevertheless the room has to be darkened during the experiment to prevent the APD going into saturation.
Experiment: The subject was seated in a comfortable arm-chair. The sources and the detector was placed 1.5 cm to the left and right of position FP1 according to the international 10/20 system. After a visual cue the subject had to subtract two presented numbers from each other within 10 seconds, afterwards a pause of 30 seconds was given. One recording lasted over 4.5 minutes with 6 cues. For each subject two recordings have been performed in minimum.
Artifact reduction: As seen in Figure 2 the pulse strongly influences the recorded signals. The frequency of the pulse waves is in the range between 1 Hz (60 bpm) and 2 Hz (120 bpm), and the responses of the oxy- and deoxy-hemoglobin are much slower. Therefore a digital lowpass butterworth filter of order 5 with a ripple of 60 dB in the stop band was designed to remove the pulse (see enlarged picture in Figure 2). In one subject the effects of respiration could still be found in the results because this subject aligned his respiration with the given task, that is, he always stopped breathing during the calculation. The result of this subject has been discarded. It can be observed that the effects of the pulse and the respiration are much stronger on the oxy- than on the deoxy-hemoglobin (see Figure 2).

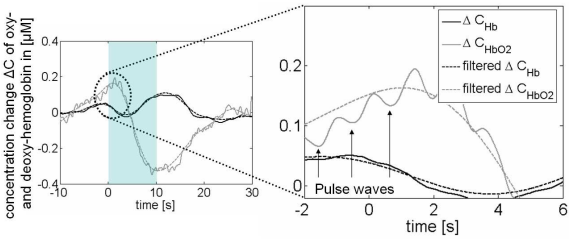

Figure 2: Pulse influences on hemodynamic response

RESULTS
The results on three subjects can be reported. The mean concentration change of oxy- and deoxy-hemoglobin during the averaged arithmetic tasks are displayed in Figure 3.

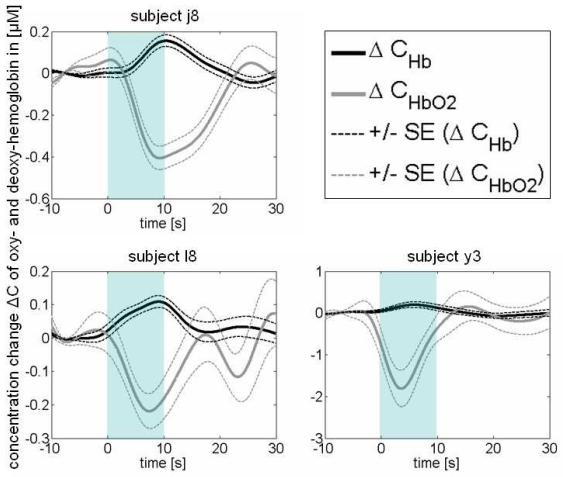

Figure 3: Hemodynamic response

The mental task was always performed between second 0 and 10 (marked with a rectangle). The results demonstrate that independently of the recording, the day of the experiment and the subject, the same results could be obtained. During the mental task the concentration change of the oxy-hemoglobin $\Delta C_{\mathrm{HbO}_2}$ and deoxy-hemoglobin ΔC_{Hb} (both in μ molar) shows an opposite characteristic. The maximum change occurs when the task is fulfilled and after that both curves returns to their baseline. It must be noted that the absolute values are different between the subjects, but the trends are the same.

DISCUSSION
Near-infrared spectroscopy is a cost-effective, very easy to use and non-invasive technology for physiological monitoring and future BCI-applications. With the presented results it could be demonstrated that the system is working very reliably and that hemodynamic changes in the oxy- and deoxy-hemoglobin during mental tasks can be detected. At the moment only a single channel setup was used, but in a further step we want to duplicate the hardware and build a multi-channel system. Especially the replacement of the hardware lock-in amplifier with a software solution, e. g. in Simulink, would remove the most expensive component which is currently one of the existing limiting factors in the current setup.

ACKNOWLEDGEMENT
This work was funded by the European PRESENCCIA project (IST-2006-27731).

REFERENCES

[1] Wolpaw JR, Birbaumer N, et al. Brain-computer interfaces for communication and control. Clin Neurophysiol, 2002; 11(6): 767–791.

[2] Coyle S, Ward T, et al. On the Suitability of Near-Infrared Systems for Next Generation Brain Computer Interfaces. Physiol Meas, 2004; 25: 815–822.

[3] Bauernfeind G, Leeb R, et al. Setup of the NIRS based Graz-BCI, in Proc BMT'06, Zuerich, 2006.

[4] Jobsis F. Non-invasive infrared monitoring of cerebral and myocardial oxygen sufficiency and circulatory parameters. Science, 1997; 198: 1264–1267.

[5] Chance B, Villringer A. Non-invasive optical spectroscopy and imaging of human brain function. Trends in Neurosci, 1997; 20(10): 435–442.

[6] Villringer A, Planck J, et al. Near infrared spectroscopy (NIRS): a new tool to study hemodynamic changes during activation of brain function in human adults. Neurosci Lett, 1993; 154: 101–104.

[7] Gratton G, Fabiani M. Shedding light on brain function: the event-related optical signal. Trends Cogn Sci, 2001; 5: 357–363.

NEAR INFRARED SPECTROSCOPY FOR BRAIN-COMPUTER INTERFACE DEVELOPMENT

R. Sitaram[1,2], Z. Haihong[2], K. Uludag[3], G. Cuntai[2], Y. Hoshi[4], N. Birbaumer[1,5]

[1]Institute of Medical Psychology and Behavioral Neurobiology, University of Tübingen, Tübingen, Germany
[2]Institute for Infocomm Research, Singapore
[3]Max Planck Institute of Biological Cybernetics, Tübingen, Germany
[4]Tokyo Institute of Psychiatry, Tokyo
[5]National Institute of Health (NIH), Human Cortical Physiology, Bethesda, USA
E-mail: sitaram.ranganatha@uni-tuebingen.de

SUMMARY: A Brain-computer Interface (BCI) can be developed using the optical response of Near Infrared Spectroscopy (NIRS) which measures metabolic brain activation. NIRS can localize brain regions with a spatial resolution in mm and temporal resolution in hundreds of ms. NIRS has the advantages of non-invasiveness, portability and affordability. We have developed a multi-channel NIRS-BCI that distinguishes the brain activation during imagination of left hand and right hand movement. This mechanism is being incorporated in a word speller, in an on-going research project, to help severely disabled persons to communicate.

INTRODUCTION

Infrared light at a wavelength in the range from 670 nm to about 850 nm penetrates tissue, goes through the skull, and reaches about 2 cm below the skull's surface all the way to the cortex area where most of the grey matter is located. Regional brain activation is accompanied by increase in oxygenated hemoglobin (oxy-hb) and decrease in deoxygenated hemoglobin (deoxy-hb) [1]. This signal occurs in the range of 5–8 seconds after the onset of stimulation and reflects mainly changes in light absorption. NIRS signal is recently reported to be well correlated with the fMRI BOLD signal, providing a sound basis for NIRS-BCI research [2]. Previous electrophysiological studies have reported that brain activation during motor imagery is similar to the activation during actual execution of movement [3]. Sitaram et al. [4, 5] and Coyle et al. [6] reported optical response during overt and covert hand movements for implementing BCIs.

MATERIALS AND METHODS

Figure 1 gives a schematic overview of our NIRS-BCI system. It has the following subsystems: signal acquisition, signal processing and classification, signal feedback, application e. g. word speller, and the participant. The signal acquisition subsystem acquires the hemodynamic response from both hemispheres over the motor cortex in real-time using a multi-channel NIRS instrument. We have explored the use of two commercially available instruments for our NIRS-BCI development: 1) OMM1000 from Shimadzu Corporation, Japan, and 2) Imagent Functional Brain Imaging System from ISS Inc., USA.

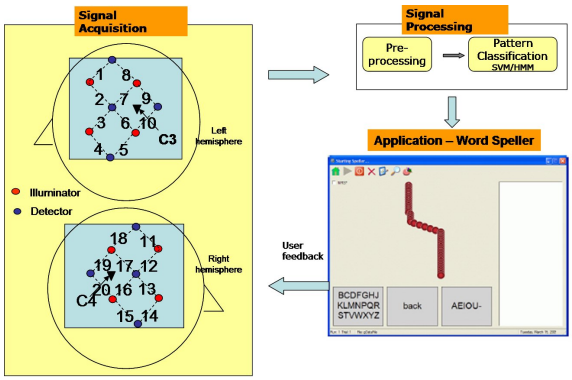

Figure 1: Overview of the NIRS-BCI system

The experiment was conducted on a right handed male subject aged 33 years. A set of 4 illuminator and 4 detector optodes were arranged to form 10 channels on each hemisphere as shown in Figure 1, around C3 (left hemisphere) and C4 (right hemisphere) areas (International 10-20 System). Infrared rays leave each illuminator, pass through the skull and the brain tissue of the cortex, and are received by the detector optodes. The NIRS photomultiplier cycles through all the illuminator-detector pairings (channels) to acquire data at every sampling period. The data are acquired at a sampling rate of 14 Hz and digitized by the analog to digital converter. The change in concentration of oxy-hb and deoxy-hb are calculated by the system in real-time based on the modified Beer-Lambert equation [1]. The signals are preprocessed by applying the Chebyshev type II filter (cutoff frequency ∼0.7 Hz) for removing artifacts from heart beat and high frequency noise such as from muscle activity. Motor imagery produces an increase in oxy-hb and a decrease in deoxy-hb in the NIRS optodes in the contralateral hemisphere. Amplitudes of oxy-hb and deoxy-hb after stimulation for each trial is extracted from the preprocessed data and fed to a pattern classification system. In total, we used NIRS data from 4 sessions, each session having 4 runs, each run comprising 20 trials each of left hand and right hand imagery. We have explored the application of two different types of classifiers: Support Vector Machine (SVM) and Hidden Markov Model (HMM). For the SVM, the acquired sig-

nals were combined in a joint feature vector per trial to train a linear SVM kernel. We conducted 8 runs of 5-fold cross-validation to evaluate the classification accuracy. Single trials data during real and imagined hand movements usually exhibit rather dynamic and complex patterns. Hence, it is beneficial to capture the patterns using dynamic Bayes networks like HMM. We designed different HMM models for left and right hand movements. The HMMs was implemented using the Hidden Markov Model Toolkit (HTK) from the Department of Engineering of Cambridge University, United Kingdom. Each model is trained using the data described above. When an un-labeled NIRS trial is presented, the machine will estimate the hidden states using the Viterbi algorithm. In this method, likelihood is calculated for each model, and the classification is then made using the maximum likelihood criterion.

The word speller application provides a means to use NIRS responses created by left and right hand motor imagery to spell words, create sentences and eventually write messages. The letters of the alphabet are divided between left and right boxes at the bottom of the word speller application window (Figure 1). The program works in the synchronous mode of BCI execution. During its operation, a cursor moves at a constant speed from the top-center of the speller window towards the bottom. The user has to use left or right hand imagery to move the cursor in the left or right direction, respectively, to select a box that contains the letter of choice. The pattern classifier classifies the real-time NIRS response as left or right imagery. Aided by the cursor feedback in this manner, the user learns to adjust the execution of motor imagery to select a letter of his choice.

RESULTS AND DISCUSSION

Figure 2 shows sample oxy-hb and deoxy-hb data from 3 channels on the left hemisphere during right hand imagery. Our experiments with the volunteer have shown that the HMM classifier performers better (average accuracy of 91.29 %) than the SVM classifier (average accuracy of 75.62 %). This might be due to considerable variations in the temporal domain in the performance of the tasks, and such variations may be better dealt with by dynamic machines like HMM.

NIRS avoids the noise prominent in the EEG, and is less cumbersome to use, as there is no need for applying conducting gel. The most important advantage of the NIRS is its ability to localize brain activity non-invasively. This provides us with an excellent opportunity to use a variety of motor and cognitive tasks, and to detect signals from specific regions of the cortex for the development of powerful and user-friendly BCIs.

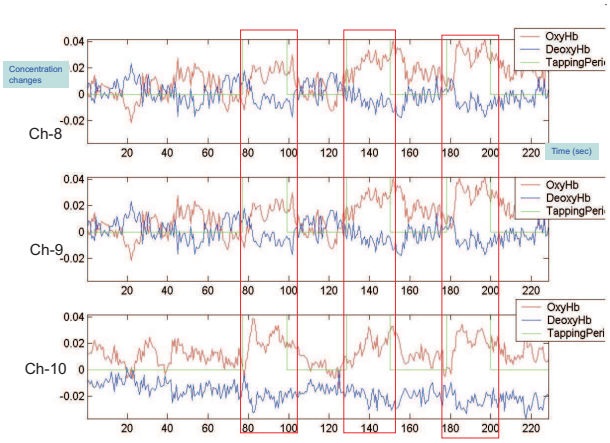

Figure 2: oxy-hb and deoxy-hb sample data from left hemisphere during right hand imagery

ACKNOWLEDGEMENT

Author R. S. is supported by the Deutsche Forschungsgemeinschaft (DFG), and author N. B. by DFG and the National Institute of Health (NIH).

REFERENCES

[1] Villringer A, Obrig H. Near Infrared Spectroscopy and Imaging. Brain Mapping: The Methods. 2nd Edition ed 2002: Elsevier Science, USA.

[2] Huppert TJ, et al. A temporal comparison of BOLD, ASL, and NIRS hemodynamic responses to motor stimuli in adult humans. Neuroimage, 2006; 29(2): 368–82.

[3] Pfurtscheller G, et al. EEG-based discrimination between imagination of right and left hand movement. Electroencephalogr Clin Neurophysiol, 1997; 103(6): 642–51.

[4] Sitaram R, et al. A Novel Brain-Computer Interface Using Multi-channel Near Infrared Spectroscopy. Submitted to Neuroimage, 2006.

[5] Sitaram R, Hoshi Y, Cuntai G. (Eds.) Near Infrared Spectroscopy based Brain-Computer Interface. Fundamental Problems of Optoelectronics and Microelectronics II. ed Kulchin YN, Vitrik OB, Proc of the SPIE, Stroganov VI, 2005; 5852: 434–442.

[6] Coyle S, et al. On the Suitability of Near-Infrared Systems for Next Generation Brain-Computer Interfaces. Physiological Measurement, 2004; 25: 815–822.

FUNCTIONAL MAGNETIC RESONANCE IMAGING BASED BCI FOR NEUROREHABILITATION

R. Sitaram[1], A. Caria[1], R. Veit[1,3], K.Uludag[3], T. Gaber[1,3], A. Kübler[1], N. Birbaumer[1,2]

[1]Institute of Medical Psychology and Behavioral Neurobiology, University of Tübingen, Germany
[2]National Institute of Health (NIH), Human Cortical Physiology, Bethesda, USA
[3]Max Planck Institute for Biological Cybernetics, Tübingen, Germany
E-mail: sitaram.ranganatha@uni-tuebingen.de

SUMMARY: We have developed a Brain-Computer Interface (BCI) based on functional magnetic resonance imaging (fMRI) that provides real-time feedback of blood oxygen level-dependent (BOLD) response from specific, localized regions of the brain. The approach presents new opportunities for behaviour therapy by training patients to control abnormal activity in selected brain regions. Study of neuroplasticity and functional reorganisation for recovery after neurological diseases, such as stroke, is of clinical importance. Here, we report results of self-regulation training of supplementary motor area (SMA) on 4 healthy volunteers.

INTRODUCTION

Functional brain imaging is a non-invasive measurement of task induced blood oxygen level-dependent (BOLD) response. With innovations in high performance magnetic resonance scanners, computers, and developments in techniques for faster acquisition, processing and analysis of MR images, fMRI-BCI has recently become a topic of research and development [1, 2]. Hemiparesis (paralysis or weakness affecting one side of the body) is a common neurological deficit after stroke [3]. Recent studies have suggested that the recovery after stroke is facilitated by the reorganization of cortical motor areas in both damaged and non-damaged hemispheres. A treatment modality consists of training patients first to learn to modulate brain areas involved in the process of functional reorganization, such as the motor cortex, basal ganglia and cerebellum. This re-organizational process of the brain could be assisted by fMRI-BCI. The aim of our study was to investigate the effect of training subjects to self-regulate the supplementary motor area (SMA) on their cortical activity and re-organization.

MATERIALS AND METHODS

The study was performed using our fMRI-BCI system, a closed loop system having the following major components: 1) Signal Acquisition, 2) Signal Analysis, 3) Signal Feedback, and 4) the Participant. The first 3 components are usually executed on separate computers for optimizing the system performance, and are connected together by a local area network (LAN). Commonly, fMRI signals are acquired by echo planar imaging (EPI). After on-line reconstruction of images by the scanner, the Signal Analysis component, based on the software Turbo-Brain Voyager (TBV) (Brain Innovations, Maastricht, the Netherlands) retrieves the reconstructed images and performs data preprocessing, including 3D motion correction, and statistical analysis to display brain activation maps in real-time. We have developed a custom software called *BCI-GUI* that provides a graphical user interface to configure the fMRI-BCI experiment, enter user input, choose one among a variety of feedback modalities, present feedback to the subject in real-time, and report experimental results as graphs and charts at the end of the training session.

Four healthy right handed volunteers (2 male and 2 female, mean age 25) participated in this study. Each participant gave written informed consent. The study was approved by the medical faculty of the University of Tuebingen, Germany. The experiment was conducted in a Siemens 1.5 T Vision scanner using Echo Planar Imaging (EPI) with the following parameters: repetition time TR = 1.5 s, echo time TE = 45 ms, flip angle = 70°, 16 slices, $\mathrm{FOV_{PE}} = 210$, $\mathrm{FOV_{RO}} = 210$, image matrix = 64×64, voxel size $3 \times 3 \times 5\,\mathrm{mm}^3$. Each participant had to undergo a functional localizer session followed by 5 feedback sessions. During the functional localizer session, participants were asked to perform finger tapping in alternating blocks of 30 s activation and 20 s rest. Rectangular region of interest (ROI) of SMA containing an average of 36 voxels was then selected by visual examination of the activation maps (see Figure 1c). During the feedback session, participants were asked to self-regulate the ROI in 2 alternating blocks: up-regulation block (45 s), and baseline block (30 s). There were in total 5 up-regulation blocks and 6 baseline blocks in each feedback session. Participants were given feedback, updated approximately every 1.8 s, of the average BOLD activity in the selected ROI subtracted by the average BOLD activity in the baseline blocks, using one of the two methods: 1) Thermometer display, or 2) Virtual reality (VR) game, called 'Seaworld'. Two participants were given the thermometer feedback and two others were given the VR feedback. The first feedback method shows snapshots of BOLD activity in the ROI (as computed above) as graduations in a thermometer (see Figure 1a). Using this feedback participants have an intuitive grasp of increasing or decreasing the thermometer variations during self-regulation. In the second method (see Figure 1b), participants have to control a 3D animated fish, to move the fish towards a food item (a smaller fish) to eat it. During up-regulation, participants have to increase their BOLD activity in the SMA

by motor imagery in order to increase the red graduations in the thermometer, or move the fish towards the food item, depending on the type of feedback. During the baseline block, participants had to count numbers. Offline analysis of the images was carried out using SPM2 (Wellcome Department of Cognitive Neurology, Queens Square, London, UK).

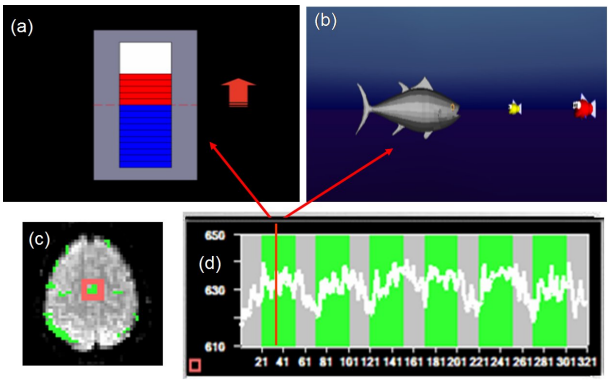

Figure 1: Figure (a) shows the thermometer feedback that gives a regularly updated snap shot of brain activity as graduations in the thermometer. Positive BOLD activity with respect to baseline activity can be shown in one color (red) to differentiate negative BOLD activity (blue). Figure (b) shows the virtual reality environment for feedback. Volunteers have to control a 3D animated character, a fish in water, by self-regulating their BOLD response to carry out a task of moving the 3D fish towards a food item (a smaller fish) for eating it. Figure (c) shows the localization of supplementary motor area (SMA) as the region of interest (ROI). Figure (d) shows a participant's time series of self-regulation of BOLD response from SMA after 3 training sessions. Green and gray bars indicate activation and baseline blocks, respectively.

RESULTS AND DISCUSSION

All the participants learned to self-regulate BOLD activity in the SMA successfully by the end of 5 feedback sessions. Figure 1 (d) shows exemplary BOLD time-series after 3 feedback sessions for subject 2. There was no significant difference in performance between participants who used the thermometer feedback and the VR feedback. However, participants who used the VR feedback reported that the game was fun and encouraged them to continue training. Importantly, significant activation ($P < 0.05$, FEW corrected) was observed for each participant in the SMA during the up-regulation blocks as compared to baseline blocks. Furthermore, we observed focussed SMA activation and less widespread activation in other regions with increasing training. Figure 2 shows this aspect of our observation for subject 2 during the first session, mid-session and the last session. Our results indicate that fMRI-BCI can be potentially applied in neuroscientific research and clinical treatment of patients with motor deficits due to brain lesions and stroke.

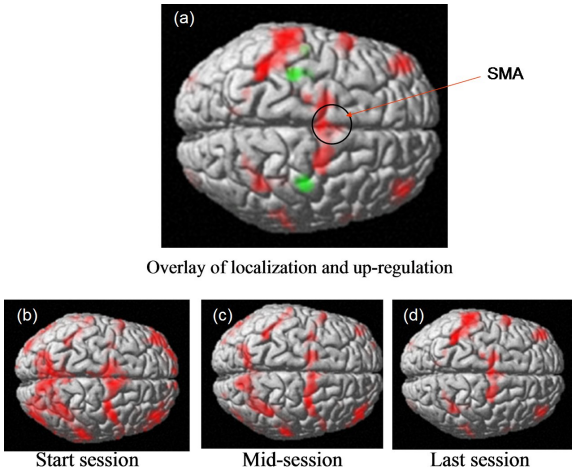

Figure 2: Figure (a) shows significant activity around the SMA (marked by a circle) during the functional localization session when the volunteer carried out self-paced finger tapping task. Figures (b)–(d) show brain activity during the first, middle and last session of self-regulation training.

ACKNOWLEDGEMENT

This work was supported by grants from the Deutsche Forschungsgemeinschaft (SFB 437/F1), the Marie Curie Host Fellowship for Early Stage Researchers Training, and the National Institute of Health. We are indebted to M. Erb and W. Grodd for technical assistance in data acquisition and helpful discussions.

REFERENCES

[1] Weiskopf N, et al. Self-regulation of local brain activity using real-time functional magnetic resonance imaging (fMRI). J Physiol Paris, 2004; 98(4–6): 357–373. Epub 2005 Nov 10.

[2] Sitaram R, et al. fMRI Brain-Computer Interface: A New Tool for Neuroscientific Research and Psycho-physiological Treatment. J of Int Society for Psychophysiological Research. In Press.

[3] Kato H, et al. Near Infrared Spectroscopy Topography as a Tool to Monitor Motor Reorganisation after Hemiparetic Stroke. A Comparison with Functional MRI. Stroke, 2002; 33: 2032–2036.

THE BERLIN BRAIN-COMPUTER INTERFACE PRESENTS THE NOVEL MENTAL TYPEWRITER HEX-O-SPELL

B. Blankertz[1], G. Dornhege[1], M. Krauledat[1,2], M. Schröder[1], J. Williamson[3], R. Murray-Smith[3,4], K.-R. Müller[1,2]

[1]Fraunhofer FIRST (IDA), Berlin, Germany
[2]Technical University Berlin, Berlin, Germany
[3]University of Glasgow, Glasgow, Scotland
[4]Hamilton Institute, NUI Maynooth, Ireland

E-mail: benjamin.blankertz@first.fhg.de

SUMMARY: We present a novel typewriter application 'Hex-o-Spell' that is specifically tailored to the characteristics of direct brain-to-computer interaction. The high bandwidth at which a user may perceive information from the display is used in an appealing visualization based on hexagons. On the other hand the control of the application is possible at low bandwidth using only two control commands (mental states) and is relatively stable against delays and the like. The effectiveness and robustness of the interface was demonstrated at the CeBIT 2006 (world's largest IT fair) where two subjects operated the mental typewriter at a speed of up to 7.6 char/min. It was developed within the Berlin Brain-Computer Interface project in cooperation with specialists for Human Computer Interaction.

INTRODUCTION

Brain-Computer Interfaces (BCIs) translate the intent of a subject measured from brain signals directly into control commands, e. g. for a computer application or a neuroprosthesis [3]. Although the proof-of-concept of BCI systems was given decades ago, several major challenges are still to be faced. One of those challenges is to develop BCI applications which take the specific characteristics of BCI communication into account. Apart from being prone to error and having a rather uncontrolled variability in timing, its bandwidth is heavily unbalanced: BCI users can perceive a high rate of information transfer from the display, but have a low-bandwidth communication in their control actions.

The Berlin Brain-Computer Interface (BBCI) is an EEG-based BCI system which operates on the spatio-spectral changes during different kinds of motor imagery. It uses machine learning techniques to adapt to the specific brain signatures of each user, thereby achieving high quality feedback already in the first session [1]. The mental typewriter presented here incorporates state-of-the-art knowledge from Human Computer Interaction (HCI) and report results of a public performance with two subjects.

METHODOLOGY

The challenge in designing a mental typewriter is to map a small number of BCI control states (typically two) to the high number of symbols (26 letters plus punctuation marks) while accounting for the low signal to noise ratio in the control signal. The more fluid interaction in the BBCI system was made possible by introducing an approach which combined probabilistic data and dynamic systems theory based on our earlier work [2] on mobile interfaces.

Here we take the example that the typewriter is controlled by the two mental states *imagined right hand movement* and *imagined right foot movement*. The initial configuration is shown in the leftmost plot of Figure 1. Six hexagonal fields are surrounding a circle. In each of them five letters or other symbols (including '<' for backspace) are arranged. For the selection of a symbol there is an arrow in the center of the circle. By imagining a right hand movement the arrow turns clockwise. An imagined foot movement stops the rotation and the arrow starts extending. If this imagination is performed in a longer period the arrow touches the hexagon and thereby selects it. Then all other hexagons are cleared and the five symbols of the selected hexagon are moved to individual hexagons as shown in Figure 1. The arrow is reset to its minimal length. Now the same procedure (rotation if desired and extension of the arrow) is repeated to select one symbol.

A language model determines the order of the symbols in one hexagon depending on the context, but this and many more important details go beyond the scope of this note.

RESULTS

On two days in the course of the CeBIT fair 2006 in Hannover, Germany, live demonstrations were given with two subjects simultaneously using the BBCI system. These demonstrations turned out to be BBCI robustness tests *par excellence*. All over the fair pavilion, noise sources of different kinds (electric, acoustic, ...) were potentially jeopardizing the performance. A low air humidity made the EEG electrode gel dry out and last but not least the subjects were under psychological pressure to perform well for instance in front of several running TV cameras or in the presence of the German minister of research. The preparation of the experiments started at 9:15 a.m. and the live performance at 11 a.m. The two subjects were either playing 'Brain-Pong' against each other or writing sentences with the typewriter Hex-o-Spell. Except for short breaks

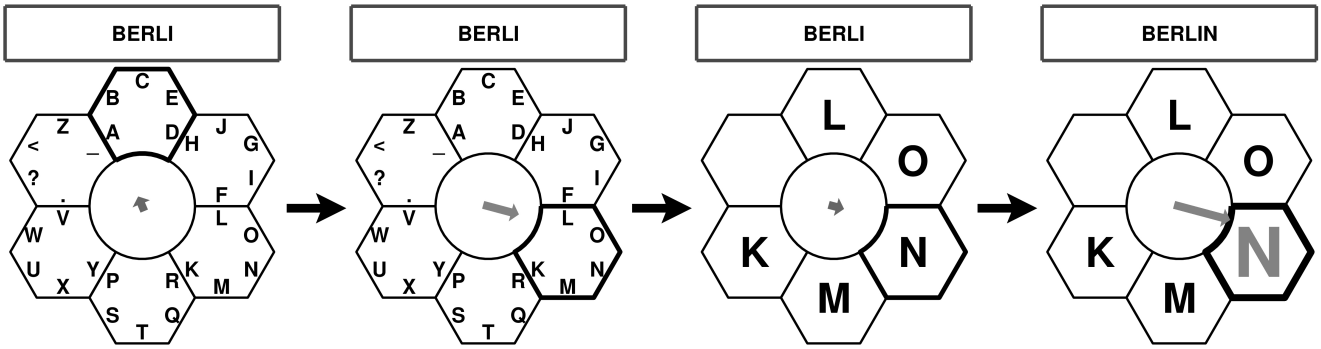

Figure 1: The mental typewriter 'Hex-o-Spell'. The two states classified by the BBCI system control the turning and growing of the gray arrow respectively (see also text). Letters can thus be chosen in a two step procedure.

and a longer lunch break, the subjects continued until 5 p.m. without degradation of performance over time which is a demonstration of great stability. The typing speed was between 2.3 and 5 char/min for one subject and between 4.6 and 7.6 char/min for the other subject. This speed was measured for error-free, completed phrases, i. e. all typing errors that have been committed had to be corrected by using the backspace of the mental typewriter. The total number of characters spelled in error-free phrases was up to 560 per subject per day.

For a BCI driven typewriter not operating on evoked potentials this is a world class spelling speed, especially taking into account the environment and the fact that the subjects did not train the usage of the BBCI typewriter interface: the subjects used the typewriter application only twice before.

DISCUSSION

The prospective value of BCI research for rehabilitation is well known. In light of the work presented here we would advocate a further point. BCI provides stimulation to HCI researchers as an extreme example of the sort of interaction which is becoming more common: interaction with 'unconventional' computers in mobile phones, or with devices embedded in the environment. These have a number of shared attributes: high-dimensional, noisy inputs, which describe intrinsically low-dimensional content; data with content at multiple time-scales; and a significant uncontrolled variability. The mismatch in the bandwidth between the display and control channels (as explained in the introduction) and the slow, frustrating error correction motivate a more 'negotiated' style of interaction, where commitments are withheld until appropriate levels of evidence have been accumulated (i. e. the entropy of the beliefs inferred from the behavior of the joint human-computer system should change smoothly, limited by the maximum input bandwidth). The dynamics of a cursor, given such noisy inputs, should be stabilized by controllers which infer potential actions, as well as the structure of the variability in the sensed data. Hex-o-Spell demonstrates the potential of such intelligent stabilising dynamics in a noisy, but richly-sensed medium. The results suggest that the approach is a fruitful one, and one which leaving open the potential for incorporating sophisticated models without *ad hoc* modifications.

ACKNOWLEDGEMENTS

This work was supported in part by a grant of the BMBF (FKZ 01IBE01A), by the SFI (00/PI.1/C067), and by the IST Programme of the EU under the PASCAL NoE (IST-2002-506778).

REFERENCES

[1] Blankertz B, Dornhege G, Krauledat M, Müller K-R, Kunzmann V, Losch F, Curio G. The Berlin Brain-Computer Interface: EEG-based communication without subject training. IEEE Trans Neural Syst Rehab Eng, 2006; 14(2): 147–152.

[2] Williamson J, Murray-Smith R. Dynamics and probabilistic text entry. Proc of the Hamilton Summer School on Switching and Learning in Feedback systems (Murray-Smith R and Shorten R, eds.). LNCS, 2005; 3355: 333–342.

[3] Wolpaw JR, Birbaumer N, McFarland DJ, Pfurtscheller G, Vaughan TM. Brain-computer interfaces for communication and control. Clin Neurophysiol, 2002; 113: 767–791.

ASYNCHRONOUS (SELF-PACED) BRAIN-COMPUTER COMMUNICATION: EXPLORING THE "FREESPACE" VIRTUAL ENVIRONMENT

R. Scherer[1], F. Lee[2], H. Bischof[2], G. Pfurtscheller[1]

[1]Laboratory of Brain-Computer Interfaces, Institute for Knowledge Discovery, Graz University of Technology, Austria
[2]Institute for Computer Graphics and Vision, Graz University of Technology, Austria
E-mail: Reinhold.Scherer@TUGraz.at

SUMMARY: In this paper, we present how subjects learned to operate an asynchronously (self-based) controlled Brain-Computer Interface and with it to navigate through a Virtual Environment (VE). Similar to computer games, the task was to pick-up items within a limited time period. In doing so, motor imagery related mental activity was mapped to the following three navigation commands: rotate left, rotate right and move forward. No cues, routing directives or instructions were given to the subjects who had to make self-paced decisions on type and duration of mental activity. Three able-bodied subjects participated in the experiments and each was able to navigate through the VE and collect the hidden items. Two succeeded in collecting all items within the time limit.

INTRODUCTION

The majority of Brain-Computer Interfaces (BCIs) are designed for the cue-based or synchronous operation mode. Following a fixed repetitive procedure subjects have to wait for a cue-signal from the system before switching to the next mental state. Since the changes in the brain patterns are time-locked to the cue, only data in a defined time window is analyzed and used for classification. A more natural interaction would require that the user is in command of timing and speed of communication. Only a minority of BCIs are designed to operate in the self-paced or asynchronous mode. Each time the user needs BCI-based interaction he can autonomously switch into corresponding mental states. The task of the BCI is to detect voluntarily induced mental patterns (intentional control, IC) in the ongoing brain activity (non-intentional control, NC). In this paper, we present an enhanced version of the asynchronously controlled 3-class Graz-BCI [1], based on the detection of changes in the sensorimotor electroencephalogram (EEG) induced by motor imagery (MI). With the proposed system three healthy subjects had the task of exploring a Virtual Environment (VE) with the goal to find scattered items.

MATERIALS AND METHODS

Subjects and data acquisition: Three healthy subjects (s1, s2 and s3) participated in the experiments. Three bipolar EEG-channels were recorded from 6 sintered Ag/AgCl electrodes placed over hand and foot representation areas. The EEG was analog band pass filtered between 0.5 and 100 Hz and sampled with 250 Hz.

Signal processing: Logarithmic band power (BP) features were extracted from the ongoing EEG (band pass filtering, squaring and moving average over one second) and classified using Fisher's linear discriminant analysis (LDA). To ensure that EEG was used to control the BCI on-line detection and reduction of electrooculographic (EOG) and electromyographic (EMG) artifacts was performed [2]. Since Fisher's LDA is designed for 2-class problems, 3 independently trained LDAs in combination with majority voting was used to solve the 3-class problem.

Gaining asynchronous control: Subjects participated in cue-based 3-class feedback training after identifying highly subject-specific parameters like electrode positions, reactive frequency components and MI task by means of Distinction Sensitive Learning Vector Quantization (DSLVQ, [3]). For each subject maximal 6 band power features in the range between 8–30 Hz were selected from maximal 3 bipolar channels arranged symmetrically over both hemispheres. 5 to 7 sessions with 4 runs (10 trials per class) were recorded. During this training subjects and classifier CFR#1 (3 LDAs) were mutually adapting to each other. From the collected cue-based data, as well as from additionally EEG recordings without MI, a second classifier (CFR#2) was computed. CFR#2 (single LDA) was trained to identify the collected MI patterns (left, right and foot or tongue MI mixed) in the ongoing EEG. To increase the robustness of CFR#2 a threshold had to be exceeded for a certain time (transition time) in order to cause a switch between NC and IC and vice versa. Receiver Operator Characteristic (ROC) analysis was performed with the criteria to maximize true positive detections within the MI-period and minimizes false positives (FP) anywhere else. Again DSLVQ was used to identify the 6 most reactive frequency bands. By combining both, CFR#1 (3-classes) and CFR#2 (MI vs. NC), we created a system able to discriminate between 4 classes: 1) left hand, 2) right hand, 3) foot or tongue MI and 4) non-control. The output of CFR#1 was triggered by CFR#2: Each time IC was detected the classification result of CFR#1 was feed trough. Otherwise the output was "zero".

Virtual environment and experimental setup: The 3-D modeling software Maya (Alias Wavefront, Toronto, Canada) was used to create and the Qt application framework (Trolltech, Oslo, Norway) to visualize and to animate the "freeSpace" Virtual Environment (VE). The virtual park, dimension 30×30 units,

consisted of a flat meadow, several hedges and a tree. Three items (coins) were positioned on fixed locations inside the park. Subjects had the task of picking up the three coins within a three minute time limit. From a randomly selected starting point (same positions for all subject), subjects could explore (first-person view) the park in the following way: Left/right hand MI resulted in a rotation to the left/right (45°/s) whereas foot or tongue MI resulted in a forward motion (1 unit/s). Whenever NC was detected, no action was performed. With this control, each part of the park could be reached. Like in computer games, the coins were automatically collected by contact; hedges or the three had to be bypassed (collision detection). For orientation a bird view map of the VE, showing the actual position was presented. Figure 1 A shows a screen snapshot.

No instructions on how to reach the coins were given to the subjects. Two sessions with 3 feedback training runs were recorded. Each session started with free-training lasting about 20 minutes.

RESULTS

Each subject was able to navigate through the VE and collect items. Subjects s2 and s3 succeeded in collecting all three items within the 3 minutes time limit. Subject s1 was able to collect only 2 of the 3 coins. While s1 and s2 could improve their performance (reflected in the covered distance and number of collected items), the results of session two for s3 were poor compared to the first. The best performance for each subject is shown in Figure 1 B. Interesting is that best results were achieved from each subject independently when starting from the same initial position. The routes, however, show that subjects had different strategies (depending also on the ability to control the BCI) and consequently choose different ways to collect the coins.

The distribution of the BCI classification output, summarized in Table 1, show that all four classes occurred during the experiment. Interviews with the subjects confirmed that all 3 motor imagery mental states as well as NC were deliberately used for navigation. It was necessary that no navigation command was send to the VE during non-MI related mental activity, like e. g. orientation or routing, or whenever subjects needed a break.

CONCLUSION

The "freeSpace" paradigm was introduced because no instructions, except the overall aim to collect coins, had to be given to the subjects. The paradigm is motivating, entertaining and most important there is an endless number of ways to reach the goal.

The results of the experiments show that subjects learned to successfully navigate through the "freeSpace" VE and were able to collect coins by autonomously switching between different mental states. These properties make BCIs become a real alternative to standard communication channels.

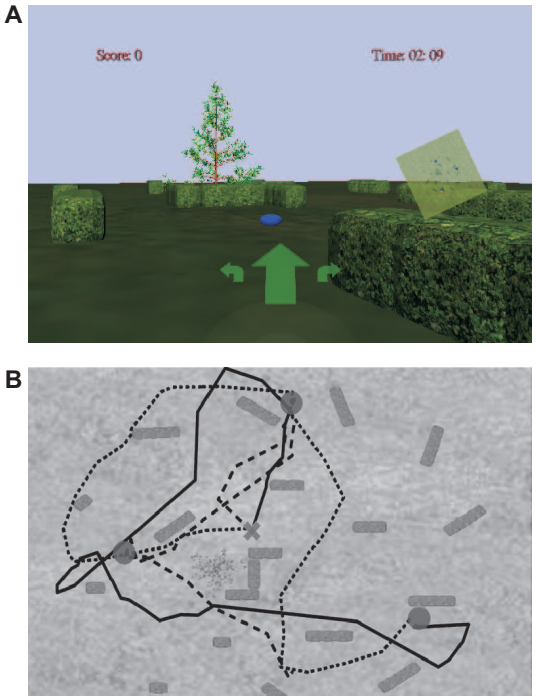

Figure 1: A: Screenshot of the "freeSpace" VE. The big arrow indicates the selected navigation command (here forward movement). During NC the three arrows had the same (small) size. B: Map of the freeSpace virtual environment showing the best performance (route) for each subject (s1, dashed; s2, continuous; s3, dotted line).

Table 1: Motor imagery task distribution (percentage)

Subject	Left	Right	Foot/Tongue	NC
s1	13.8	16.7	12.3	57.2
s2	18.7	19.0	30.8	31.5
s3	15.0	14.5	25.5	45.0

ACKNOWLEDGEMENT

This work is supported by the "Fonds zur Förderung der Wissenschaftlichen Forschung" in Austria, project P16326-BO2 and funded in part by the EU research project PRESENCCIA IST 2006-27731.

REFERENCES

[1] Scherer R, Müller GR, Neuper C, Graimann B, Pfurtscheller G. An asynchronously controlled EEG-based virtual keyboard: improvement of the spelling rate. IEEE Trans Biomed Eng, 2004; 51(6): 979–84.

[2] Scherer R, Schlögl A, Pfurtscheller G. Online detection and reduction of electrooculographic (EOG) and electromyographic (EMG) artifacts, BMT 3-Ländertreffen, 6.–9. September 2006, ETH Zürich, Schweiz, accepted.

[3] Pregenzer M, Pfurtscheller G. Frequency component selection for an EEG-based brain to computer interface. IEEE Trans Rehabil Eng, 1999; 7(4): 413–419.

NON-INVASIVE BRAIN-COMPUTER INTERFACE FOR MENTAL CONTROL OF A SIMULATED WHEELCHAIR

E. Lew[1], M. Nuttin[2], P. W. Ferrez[1], A. Degeest[2], A. Buttfield[1], G. Vanacker[2], J. del R. Millán[1]

[1]IDIAP Research Institute, Martigny, Switzerland
[2]Department of Mechanical Engineering, Katholieke Universiteit Leuven, Leuven, Belgium
E-mail: {elylee, jose.millan}@idiap.ch

SUMMARY: This poster presents results obtained from experiments of driving a brain-actuated simulated wheelchair that incorporates the shared-control intelligence method. The simulated wheelchair is controlled offline using band power features. The task is to drive the wheelchair along a corridor avoiding two obstacles. We have analyzed data from 4 nave subjects during 25 sessions carried out in two days. To measure the performance of the brain-actuated wheelchair we have compared the final position of the wheelchair with the end point of the desired trajectory. The experiments show that the incorporation of a higher intelligence level in the control device significantly helps the subject to drive the robot device.

INTRODUCTION

Recent experiments have shown the possibility of using the brain electrical activity to directly control the movement of robots or prosthetic devices in real time [1]. In order to provide a more practical environment for the subject to use the BCI for control, there is a need to have an adaptive shared autonomy between two intelligent agents – the human user and the robot – so that the user only conveys intents that the robot performs autonomously [2]. Although the initial brain-actuated robot had already some form of cooperative control, shared autonomy is a more principled and flexible framework.

METHODS

In this paper, the experiment protocol is similar to that described in [3]. In order to control the simulated wheelchair, the classifier embedded in the BCI is fed with the power of the frequency band 8–14 Hz from 10 scalp EEG electrodes and it sent its output every 0.5 s to the robot. The simulated wheelchair has two levels of intelligence, namely A0 (it allows the wheelchair to detect obstacles and stop before colliding) and A1 (it detects obstacles and avoids them). The task is to drive the wheelchair along a corridor avoiding two obstacles (Figure 1). We have analyzed data from 4 naive subjects during 25 sessions carried out in two days. The classifier embedded in the BCI was trained with data from 5 consecutive sessions and tested over the next 5 consecutive sessions. To measure the performance of the brain-actuated wheelchair we have compared the final position of the wheelchair with the end point of the desired trajectory.

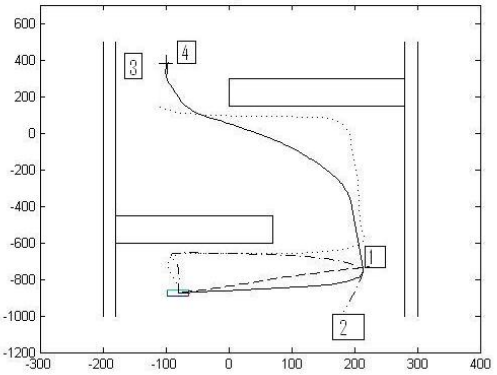

Figure 1: Example of trajectories in the simulated environment. The starting point for the wheelchair is at the bottom left in front of the obstacle. The axes give the coordinates of the simulated environment in centimeters.

RESULTS

Figure 1 shows a few trajectories obtained from the experiments. Using intelligence level A0, most of the time, the wheelchair stops moving whenever it comes across any obstacles, causing it to stay near the starting point as in the dashed line path (labeled 1) in Figure 1. The solid line (labeled 4) is the desired trajectory and the end point of this trajectory is used as a reference for comparison with other end points reached by the brain-actuated wheelchair for each session and subject. The dotted line (labeled 3) is an example of a trajectory reaching the target. Distance from starting point to the target is 1262 cm. The dotted-dash line (labeled 2) shows the wheelchair turning to the opposite direction further away from the starting point. If the simulated wheelchair ends within 50 cm from the target, it is considered the task has been achieved. Results for the 4 subjects are tested with the simulator using intelligence level A1 as shown in the graphs of Figures 2 to 5 with the comparison between trajectories generated with online learning [4] and without online learning. In these figures, distances of more than 1262 cm correspond to trajectories where the subject sent a series of wrong mental commands at the beginning and the wheelchair turned away from the target as in the case of trajectory labeled 2 in Figure 1.

DISCUSSION

Despite the fact that the subjects' performance are quite far from optimal – because among other reason, they are novel – the results show that the incorpo-

ration of shared autonomy with A1 intelligence level allows subjects to achieve the task a considerable number of times. This is not the case when the simulated wheelchair has only A0 intelligence level, when the target is never reached.

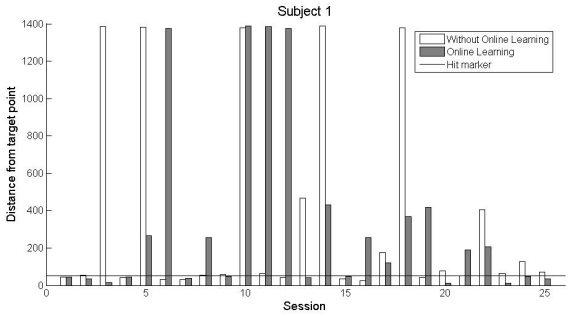

Figure 2: Subject 1 hits the target in 8 (without online learning) vs. 12 (with online learning) out of 25 sessions

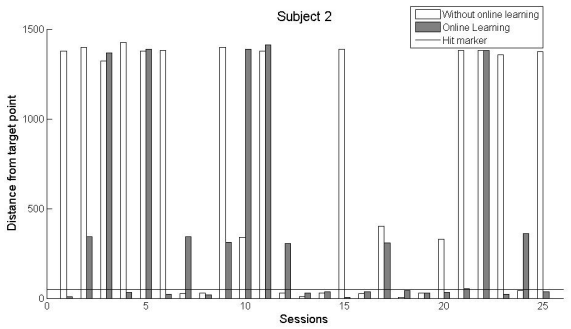

Figure 3: Subject 2 hits the target in 9 (without online learning) vs. 13 (with online learning) out of 25 sessions

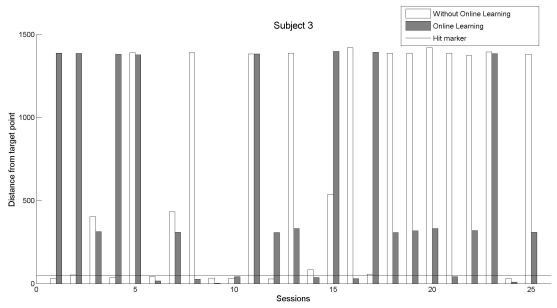

Figure 4: Subject 3 hits the target in 7 (without online learning) vs. 8 (with online learning) out of 25 sessions

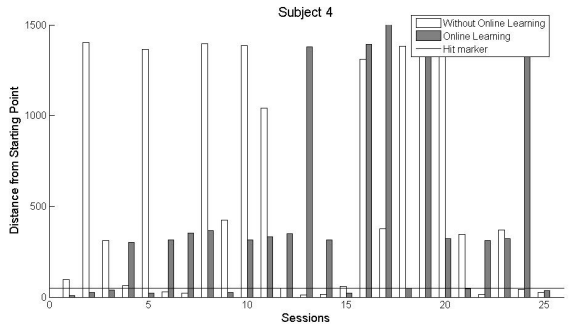

Figure 5: Subject 4 hits the target in 8 (without online learning) vs. 9 (with online learning) out of 25 sessions

It is also worth noting that the performance of subject 1 and subject 4 increased at the last few sessions while subject 3 performs best in the beginning of the sessions and subject 2 is able to reach the target more frequent in the middle of the sessions. Finally, as expected, the incorporation of online learning [4], improves the performance for all the subjects especially subjects 1 and 2 with more drastic increase in number of times hitting the target with online learning.

CONCLUSION

This paper shows the importance of having a higher intelligence level in the wheelchair (or control device) to help the subject achieve the task with a high probability from the very first trial, although performance between subjects varies across sessions. For future work, we plan to estimate the subject's intention using a probabilistic framework, as in [2], and to incorporate learning capabilities in the robot controller to improve the entire brain-actuated device.

ACKNOWLEDGEMENT

This work is supported by the European IST Programme FET Project FP6-003758 and by the Swiss National Science Foundation NCCR IM2.

REFERENCES

[1] Millán JdR, Renkens F, Mourino J, Gerstner W. Non-invasive brain-actuated control of a mobile robot by human EEG. IEEE Trans Biomed Eng, 2004; 51: 1026-1033.

[2] Demeester E, Nuttin M, Vanhooydonck D, Van Brussel H. A model-based, probabilistic framework for plan recognition in shared wheelchair control: Experiments and evaluation. IEEE/RSJ Int Conf Intelligent Robots and Systems, 2003.

[3] Ferrez PW, Galan F, Buttfield A, Gonzalez SL, Grave de Peralta R, Millán JdR. High frequency bands and estimated local field potentials to improve single-trial classification of electroencephalographic signals. In Proc. of the 3rd Int. BCI Workshop & Training Course 2006 (Eds. Müller-Putz GR, Brunner C, Leeb R, Scherer R, Schlögl A, Wriessnegger S, Pfurtscheller G), Verlag TU Graz, Austria, 2006.

[4] Buttfield A, Ferrez PW, and Millán JdR. Online Classifier Adaptation in High Frequency EEG. In Proc. of the 3rd Int. BCI Workshop & Training Course 2006 (Eds. Müller-Putz GR, Brunner C, Leeb R, Scherer R, Schlögl A, Wriessnegger S, Pfurtscheller G), Verlag TU Graz, Austria, 2006.

NEURAL INTERNET FOR ALS PATIENTS

A. A. Karim [1,2], M. Bensch[3], J. Mellinger[1], T. Hinterberger[1], M. Schröder[3], M. Bogdan[3], N. Neumann[1], A. Kübler[1], W. Rosenstiel[3], N. Birbaumer[1,4]

[1]Institute of Medical Psychology, University of Tübingen, Tübingen, Germany
[2]International Max Planck Research School of Neural & Behavioral Sciences, Tübingen, Germany
[3]Department of Computer Engineering, University of Tübingen, Germany
[4]Human Cortical Physiology Section, NINDS, National Institutes of Health, Bethesda, USA
E-mail: ahmed.karim@uni-tuebingen.de

SUMMARY: Neural Internet is a system which uses neuronal signals from the brain and transforms them to binary or multidimensional computer commands enabling severely paralysed patients to surf the internet, read and send e-mails independently of any voluntary muscle control. Here we introduce two types of EEG controlled web browsers based on self-regulation of slow cortical potentials (SCP): *Descartes* and *Nessi*. The functioning of Neural Internet and its clinical implications for motor impaired patients are highlighted.

INTRODUCTION

Amyotrophic lateral sclerosis (ALS), also known as "Lou Gehrig's disease", is a progressive neurodegenerative disease that causes widespread loss of both upper and lower motor neurons [1]. With voluntary muscle action progressively affected, patients in the later stages of the disease may become totally paralysed. Yet, for the vast majority of ALS patients, their sensory and cognitive functions remain largely unaffected [2]. One of the most terrifying aspects of this "locked-in syndrome" is that the loss of muscle control prevents the expression of even the most basic needs. Therefore, we developed a brain-computer interface (BCI) controlled by SCP self-regulation enabling ALS patients to write messages independently of voluntary muscle control [3]. The goal of this study was to investigate the feasibility of a web browser based on self-regulation of brain potentials for locked-in patients. This technology, which we call Neural Internet, could enable severely paralysed patients to regain autonomy by using the unique communication and interaction possibilities of the world wide web independently of any voluntary muscle control. Here, we introduce two types of EEG controlled web browsers, which can be operated by SCP self-regulation: *Descartes* and *Nessi*.

PATIENTS

Descartes has been developed and tested since 1999 with a locked-in patient (HPS) diagnosed with ALS, rendering him the first paralysed patient to surf the internet only with his brain waves [4]. Usability tests with *Nessi* are currently ongoing with five ALS patients.

WEB SURFING WITH DESCARTES

In *Descartes* the commands are arranged in a dichotomous decision tree based on a modified Huffman's algorithm. EEG data acquisition, online signal processing and classification was performed using the Thought Translation Device software [3]. SCP were extracted by appropriate filtering, corrected for EOG activity and fed back to the patient as a cursor movement on a laptop screen. For *selecting* a command the patient produces positive SCP shifts (above a predefined threshold of 7 μV), which move the cursor downwards. For *rejecting* a command the patient produces negative SCP shifts, which move a cursor on a computer screen upwards. At the first level of the decision tree the patient can choose whether to write an e-mail or to surf the internet. If the patient decides to write an e-mail, the e-mail address and the text body has to be spelled out using the BCI spelling device [3]. If the patient decides to surf the internet, he/she first receives a number of predefined links arranged in the dichotomous decision tree. Each web page is offered successively for selection at the bottom of the monitor (cf. Figure 1).

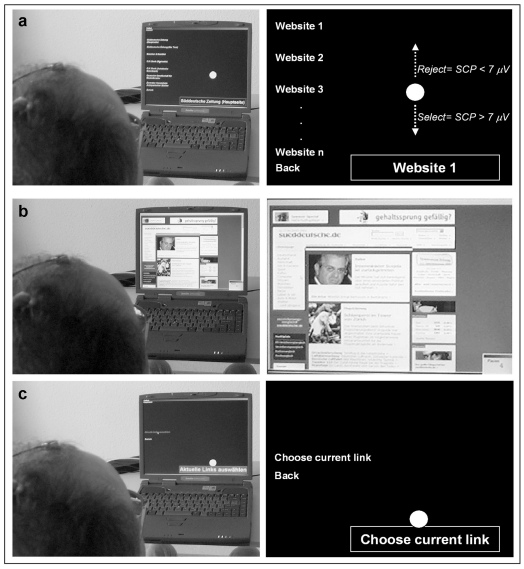

Figure 1: Web surfing with *Descartes*

Once the patient has selected a web page it will be automatically loaded and shown for a predefined time until the SCP feedback mode will start again offering the patient to choose a link from the selected web page, to go one page back or to start from the initial list again. In order to test the patient's ability to reliably operate *Descartes*, two or three test runs

were conducted at the beginning of each web surfing session. Patient HPS has achieved a mean accuracy of 80 % (± SD 6.2 %), which varies on different days from 68 % to 95 %. HPS is now using *Descartes* regularly 1–2 times a week, for example to read his favourite German newspaper online, to search and order recently published law books especially those of his former colleagues, or to read and write e-mails to friends and relatives (for more BCI data from this patient using *Descartes* see [4]).
However, due to modern web coding practices, it is quite often impossible to obtain a textual label associated with a link on a web page. Very often, links are associated with graphics instead of a descriptive text, but even for a textual link its semantic content may depend on its position on the web page. To overcome this problem we developed a second Neural Internet system, called *Nessi*, which uses graphical "in-place" markers instead of textual labelling, whereas different brain responses correspond to two different frame colours placed around selectable items on a web page.

WEB SURFING WITH NESSI

In *Nessi* (Neural Signal Surfing Interface) the open-source browser Mozilla was extended by graphical "in-place" markers. Coloured frames are placed around selectable items on a web page, circumventing any need to maintain a separate presentation of choices (cf. Figure 2). By default, red frames are selected by producing cortical negativity and green frames are selected by the production of cortical positivity. As an aid, feedback is displayed at the left rim of the screen by depicting the vertical movement of a cursor that can be moved upwards into a red area or downwards into a green area. By presenting a series of brain responses as indicated by changing colour of the frame around that link, it can be chosen with binary decision neglecting any knowledge about its position in a selection tree [5].

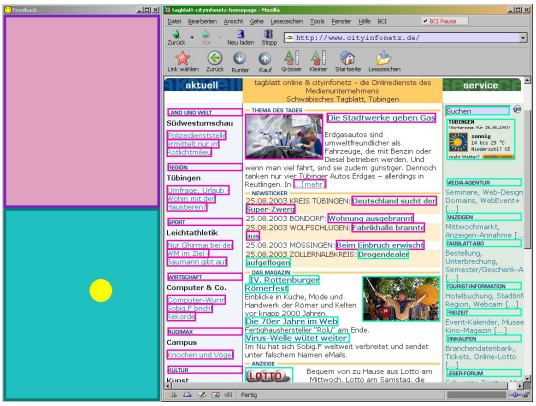

Figure 2: Web surfing with *Nessi*

Besides links, other interactive elements on web pages are accessible to the user, particularly text fields for which a virtual keyboard is provided, opening up a wide range of hypertext based applications. However, to avoid overexertion the number of navigation elements can be reduced while the patient is learning to operate the web browser. First usability tests with five ALS patients showed difficulties only when a web page contained too many links.

CONCLUSION

We have shown here that an EEG controlled web browser based on self-regulation of SCP can be reliably operated by a nearly completely paralysed ALS patient. To avoid constraints in web surfing caused by problems in identifying the textual labelling of a web link, we are currently testing the usability of graphical "in-place" markers instead of textual labelling, whereas different brain responses correspond to two different frame colours placed around selectable items. Neural Internet seems to be a very promising approach for connecting motor-impaired users to the world wide web and offering them unique communication and interaction possibilities with the outside world, which they would not otherwise be able to use due to their motor disability, such as shopping, receiving information or even running a business. Moreover, using options like e-mail with a BCI web browser may offer for completely paralysed patients the only possibility to read, write and send confidential letters to relatives or friends without an intermediator (a caregiver or a nurse). Thus, Neural Internet can help motor impaired patients to regain a certain level of *autonomy* in the interaction with the outside world and thereby enhance their quality of life.

ACKNOWLEDGEMENT

This project was supported by the DFG and by the United States National Institutes of Health (NIH).

REFERENCES

[1] Rowland LP, Shneider NA. Amyotrophic lateral sclerosis. N Engl J Med, 2001; 344: 1688–700.

[2] Strong MJ, Grace GM, Orange JB, Leeper HA, Menon RS, Aere C. A prospective study of cognitive impairment in ALS. Neurology, 1999; 53: 1665–1670.

[3] Birbaumer N, Flor H, Ghanayim N, Hinterberger T, Iverson I, Taub E, et al. A Spelling Device for the Paralyzed. Nature, 1999; 398: 297–298.

[4] Karim AA, Hinterberger T, Richter J, Mellinger J, Neumann N, Flor H, et al. (in press). Neural Internet: Web surfing with brain potentials for the completely paralysed. Neurorehabilitation and Neural Repair.

[5] Mellinger J, Hinterberger T, Bensch M, Schröder M, Birbaumer N. Surfing the Web with Electrical Brain Signals. Proceedings of the 2nd World Congress of the Intern. Soc. of Physical and Rehabilitation Medicine ISPRM, Prague, 2003.

ROBOT OPERATION BASED ON PATTERN RECOGNITION OF EEG SIGNALS

K. Inoue[1], K. Kumamaru[1], G. Pfurtscheller[2]

[1]Department of Systems Innovation and Informatics, Kyushu Institute of Technology, Iiduka, Fukuoka, Japan
[2]Laboratory of Brain-Computer Interface, Graz University of Technology, Graz, Austria
E-mail: inoue@ces.kyutech.ac.jp

SUMMARY: Electroencephalograph (EEG) recordings during right and left motor imagery can be used to move a cursor to a target on a computer screen. Such an EEG-based brain-computer interface (BCI) can provide a new communication channel to replace an impaired motor function. It can be used by e. g., handicap users with amyotrophic lateral sclerosis (ALS). In this study, statistical pattern recognition method based on AR model was introduced to discriminate the EEG signals recorded during right and left motor imagery, and is applied to operate a robot. The effectiveness of our method was confirmed through the experimental studies.

INTRODUCTION

Classification of EEG signals during motor imagery can be used to control an electronic device. Such a system which transforms signals from the brain into control signals is known as a brain-computer interface (BCI) [1, 2, 3]. We also have proposed such a system based on AR model [4], and investigated the learning effects of subjects on our system [5]. In these studies, it was confirmed that the detection of the operation imagination of the hand was possible with high accuracy for the subject who trained enough. This fact suggests that robot operation will be possible by using our method. In this study, robot (AIBO: SONY entertainment robot) operation was tried by using the statistical pattern recognition method based on AR model. And the effectiveness of our method was confirmed through the experimental studies.

MATERIALS AND METHODS

Three subjects (22–24 years old) participated in this study. All were right-handed, and were free of medication and central nervous system abnormality. Electrode positions are shown in Figure 1. The EEG signals were amplified by a Nihon Khoden amplifier and then were sampled at 128 Hz. In this study, the small Laplacian filtered signals (SL signals) are used.

Pattern Recognition Method Based on AR Model: Following Bayes decision rule is adopted.

$$k^* = \arg\max_k \Pr\frac{\omega_k}{Z_{DN}} \qquad (1)$$

$$\begin{aligned} Z_{DN} &= \{Y_{1N}, Y_{2N}\} \\ Y_{1N} &= \{y_{11}, y_{12} \ldots y_{1N}\} : \text{Signals (C3)} \\ Y_{2N} &= \{y_{21}, y_{22} \ldots y_{2N}\} : \text{Signals (C4)} \\ \omega_k : &\quad \text{Class (Right or Left)} \end{aligned}$$

A posteriori probability function $\Pr(\omega_k/Z_{DN})$ can be expressed as explicit form by assuming that the EEG signals are generated from an autoregressive (AR) model [4].

Training of the subject: Each of the subjects participated in 10 sessions, all on different days. Timing chart of feedback session are shown in Figure 2. Each session consisted of 3 experimental runs of 60 trials (30 'left' and 30 'right' trials) and lasted for about 1 hour. The sequence of 'left' and 'right' trials, as well as the duration of the breaks between consecutive trials (ranging between 500 and 2500 ms), were randomized throughout each experimental run.

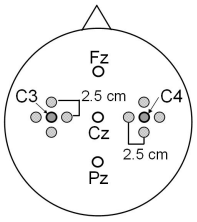

Figure 1: Position of the electrodes

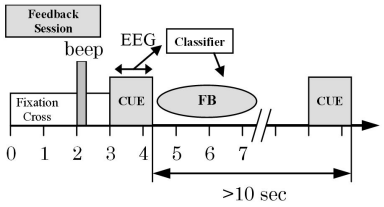

Figure 2: Timing chart of feedback session

Robot operation: The robot is programmed to execute the following two kinds of instructions. One is one-step-walking to the right-front direction. Another is one-step-walking to the left-front direction. The time required to execute each instruction is 1.5 seconds. The control system is shown in Figure 3. The control system sends the instruction to AIBO every 1.5 seconds according to the pattern recognition result of the previous 2.0 seconds data. The timing chart of control is shown in Figure 4.

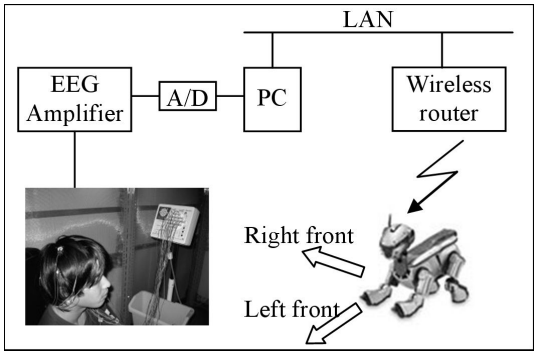

Figure 3: Control system of robot (AIBO)

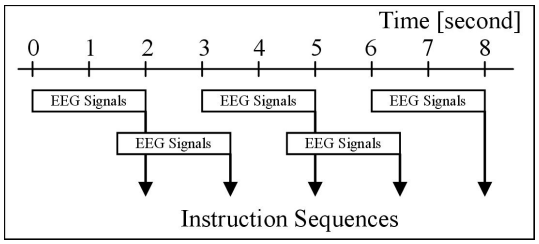

Figure 4: Timing chart of AIBO control

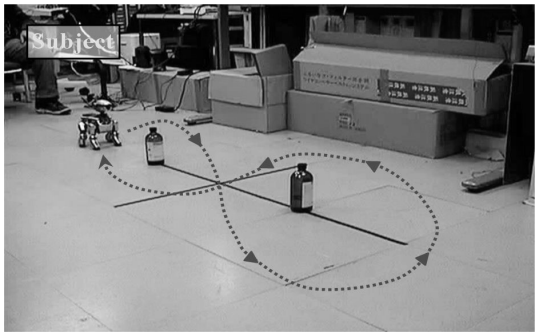

Figure 5: Environment of Experiment 2

In this study, two kinds of experiment were tried.

Experiment 1: Single direction walking Subjects try to let AIBO walking to only one direction (right or left) during experiments (about 50 s).

Experiment 2: Walking like the character eight. Subjects try to let AIBO walking like the character eight to avoid two obstacles (see Figure 5). The AR parameters which are estimated from the data (data length: 2.0 s, data period: 6.0–8.0 s) of final session (10^{th} session) are used in the the control system.

RESULTS AND DISCUSSION

Pattern recognition results are shown in Figure 6. This results suggest that number of the sessions which is needed for the training depends on each subject. The results of Experiment 1 (Single direction walking) are shown in Figure 7, which is the histograms concerning the moved distance in direction of right and left (Left: 30 trials, Right: 30 trials). These results suggest that only subject m2 can completely control AIBO by only thinking. Therefore, only subject m2 participated in next experiment (Experiment 2). Figure 8 shows the trace of AIBO movement. This result shows that he could control the AIBO as he wills.

CONCLUSION

In this paper, robot operation system by the control method built in EEG recognition method was developed.

And it was confirmed that the subject trained enough was able to control the AIBO only by thinking about the operation. This system is prototype system of BCI. It is necessary to increase the kind of available operation in order to make the system to a more practicable system. These studies are under consideration.

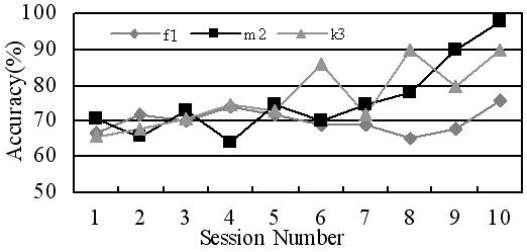

Figure 6: Pattern recognition results (Subject: f1, m2, k3)

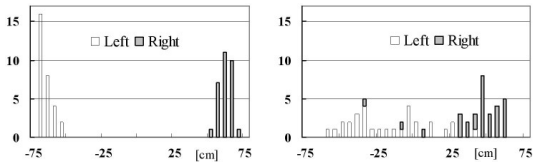

Figure 7: Walking distance (Left: Subject m2, Right: Subject k3)

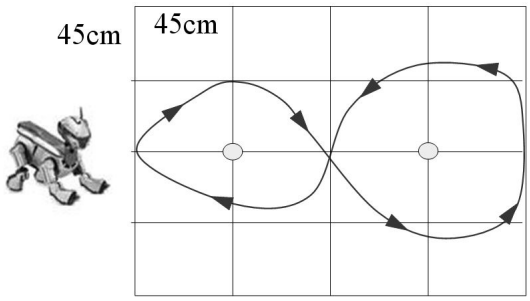

Figure 8: Trace of the AIBO movement (subject m2)

REFERENCES

[1] Pfurtscheller G, Neuper C, Schlögl A, Lugger K. Separability of EEG Signals Recorded During Right and Left Motor Imagery Using Adaptive Autoregressive Parameters. IEEE Trans Rehabil Eng, 1998; 6–3: 316–325.

[2] Vidal J. Toward direct brain-computer communication, Annual Rev Biophysics Bioengineering, 1973; 157–180.

[3] Wolpaw J, McFarland D. Control of a two-dimensional movement signal by a noninvasive brain-computer interface in humans, PNAS December 21, 2004; 101–51: 17849–17854.

[4] Inoue K, Pfurtscheller G, Neuper C, Kumamaru K. Pattern Recognition of EEG Signals During Right and Left Motor Imagery. Proc of the 13^{th} IFAC Symposium on System Identification, 2003; 138–143.

[5] Inoue K, Mori D, Pfurtscheller G, Kumamaru K. Pattern Recognition of EEG Signals During Right and Left Motor Imagery -Learning Effects of the Subjects-. Proc of the First International Conference on Complex Medical Engineering, CME2005, 2005; 665–670.

BCI IN A CLINICAL CONTEXT: THE ASPICE PROJECT

F. Aloise[1], D. Mattia[1], D. Morelli[1],F. Babiloni[1,2], M. G. Marciani[1,3], F. Cincotti[1]

[1]Clinical Neurophysiopathology Unit, Fondazione Santa Lucia IRCCS, Roma, Italy
[2]Dept. of Human Physiology and Pharmacology, Univ. of Rome "La Sapienza", Rome, Italy
[3]Dept. of Neuroscience, Univ. of Rome "Tor Vergata", Rome, Italy
E-mail: fabio.aloise@aspice.it

SUMMARY: The ASPICE project aims to develop an Assistive System for Patient's Increase of Communication, ambient control and mobility in absence of muscular Effort. Different disability level means different system users: from people confined to a wheelchair to neuromotor disabled persons. ASPICE tries to improve or recover their mobility (directly or by emulation) and communication within the surrounding environment. The system pivots around a software controller running on a portable computer to offer a proper interface for the user through different interfaces, selected by the individual's residual abilities. This system links to the concept of user-centered interface promoted by human-computer interaction researchers. Each person has an own "individual ability", thus the system must provide the possibility to use an adaptive interface customized to their own ability and requirements, which stems from contingent factors or simple preferences, depending on the user and on his or her life stage, task, and environment.

INTRODUCTION

The main goal in rehabilitation are the reduction of the disability caused by any pathological condition using orthesis, and the management of the social disadvantage related to disability, using different aids.
The project described in this paper offers the opportunity to integrate a technological core (Brain Computer Interface, Domotics, Robotics) into a prototype, taking into account different disabilty levels, in order to prove that a real application is always possible, though the residual muscular strength (e. g. considering diseases as Spinal Muscular Atrophy, Duchenne Dystrophy, Amyotrophic Lateral Sclerosis) cannot be adequate for the utilization of conventional aids.

MATERIALS AND METHODS

The ASPICE project (Assistive System for Patient's Increase of Communication, ambient control and mobility in absence of muscular Effort) fosters its aims through the integration of disciplines brought from the partners of the development consortium. The constitutive elements of the system are:

1. *Input devices*
2. *System core*
3. *Feedback*
4. *Actuator*

The ASPICE architecture, with its input and output devices, is outlined in Figure 1.

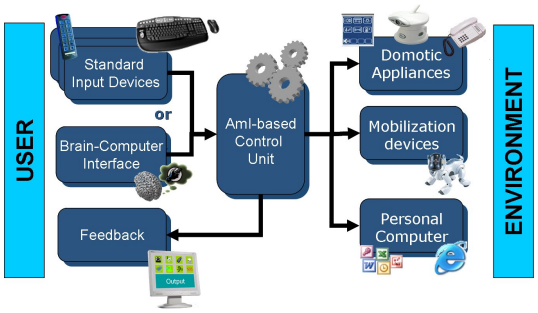

Figure 1: Outline of the architecture of the ASPICE project. The figure shows that the system interfaces the user to the surrounding environment. The modularity is assured by the use of a core unit that takes inputs by one of the possible input devices and sends commands to one or more of the possible actuators. A feedback is provided to keep the user informed about the status of the system.

The system input devices are customized on the users' residual motor abilities: users can access the system through the aids they are already familiar with, and that have been interfaced to provide a low level input to a more sophisticated assistive device. On the other hand, the variety of input devices provides robustness against worsening of patients' abilities, which is a typical consequence of degenerative diseases. The software implementation of this modular attitude benefited from the use of the ICon package [1].
An extreme instance of input devices that can be interfaced to the system are Braincomputer interfaces [2]. The ability to control the system via a brain computer interface relies on the BCI2000 software system. The users learn to control their own mu rhythm by being fed back during a training period. This acquired skill is used to move a cursor on a screen and the interface allows him to navigate an icon based menu [3–6].
The System core receives the logical signals from the input devices and converts them into commands that can be used to drive the output devices. Whenever the user selects an action that, rather than changing the internal context of the core (i. e. selects a non-leaf item of the cascaded menu), it instructs the system to undertake a physical action, the Control Unit fulfils the user's demands by sending the appropriate control signals to the output appliances. Drivers are used to offer a homogeneous interface from the Control Unit's point of view.
Feedback: The user can select the commands and monitor the system's behaviour through a Graphic Interface. Like all other modules, inter-module communica-

tion is transported via TCP/IP socket; among others, this allows each module to run on a different computers. The Feedback can significantly benefit from this, since a lighter an low power computer such as a palmtop PC or even a smart phone can be used to give the subject the feedback he/she needs, while being of minimum burden for the user. Figure 2 shows a possible appearance of the feedback screen.

Figure 2: Appearance of the feedback screen. The Feedback application has been instructed to divide the window into three panels. In the top panel, the available selections (commands) appear as icons. In the bottom right panel, a feedback stimulus by the BCI. In the bottom left panel, the Feedback module displays the video stream.

Actuators: The Aspice system allows the user to operate remotely with electric devices (e. g. TV, fan, lights) as well as monitoring the environment with remotely controlled video-cameras. Moreover, a robot navigation system has been developed, based on a small set of commands, which has been interfaced with the Aspice system [7].

RESULTS

Clinical validation of the prototype has been carried out with the voluntary collaboration of 15 adult subjects affected by motor disability of variable degree due to neuromuscular diseases. These subjects were asked to interact with the prototype and to provide information about how it was perceived in terms of augmented independence in daily life activity. The results indicated that the individual's needs and interest must be analyzed and reinforced. Environmental control is a strong positive reinforcement even if the subject partially regains some independency in operating domotic devices. It remains to be tested how these positive reinforces could be integrated into a general training framework.

CONCLUSION

The quality of the life of an individual, suffering from severe motor impairments, is mainly affected by its complete dependence upon the caregivers. An assistive device, even the most advanced, cannot substitute, at the state of the art, the assistance provided by a human skill. Nevertheless, it can contribute to relief the caregiver from a continuous presence in the room of the patient. Most importantly, the perception of the patient is that he has no more to rely on the caregiver for any action. The ASPICE system can increase the sense of independence of a patient, granting a sense of privacy, that is almost absent if another person has to take his care. For these reasons, the quality of life of the patient can be sensibly improved.

ACKNOWLEDGEMENT

This work is partially supported by the Italian Telethon Foundation, Grant GUP03562. The robot navigation system has been developed by prof. G. Oriolo and collaborators at the Dept. of Systems and Computer Science, La Sapienza University, Rome.

REFERENCES

[1] Dragicevic P, Fekete JD. Input Device Selection and Interaction Configuration with ICON. Proc IHM-HCI, 2001.

[2] Wolpaw JR, Birbaumer N, McFarland DJ, Pfurtscheller G, Vaughan TM. Braincomputer interfaces for communication and control. Clin Neurophysiol, March 2002; 113: 767–791.

[3] Pfurtscheller G, Neuper C. Motor imagery and direct brain-computer communication. Proc IEEE, 2001; 89: 1123–1134.

[4] Birbaumer N, Elbert T, Caravan AGM, Roch B. Slow potentials of the cerebral cortex and behavior. Physiol Rev, 1990; 70: 1–41.

[5] Schalk G, McFarland DJ, Hinterberger T, Birbaumer N, Wolpaw JR. BCI2000: A general-purpose brain-computer interface (BCI) system. IEEE Trans Biomed Eng, 2004; 51: 1034–1043.

[6] Millán JdR, Renkens F, Mouriño J, Gerstner W. Non-invasive brain-actuated control of a mobile robot by human EEG. IEEE Trans on Biomed Eng, 2004; 51: 1026–1033.

[7] Oriolo G, Ulivi G, Vendittelli M. Real-time map building and navigation for autonomous robots in unknown environments. IEEE Trans on Systems, Man, and Cybernetics, 1998; 28(3): 316–333.

A PLATFORM INDEPENDENT FRAMEWORK FOR THE DEVELOPMENT OF REAL-TIME ALGORITHMS: APPLICATION TO THE SSVEP BCI PROTOCOL

L. Mazzucco[1], S. Parini[1], L. Maggi[1], L. Piccini[1], G. Andreoni[1], L. Arnone[2]

[1]Bio-engineering Department, Polytechnic of Milan, Italy
[2]STMicroelectronics, AST Group: Research & Innovation, Agrate Br., Italy
E-mail: lucamazzu@tim.it

SUMMARY: In our work we addressed the problem of porting BCI algorithms to different platforms especially the those not supporting Matlab® based development, and focused our attention mainly to embedded devices. A careful management of the programming code was realized after a deep analysis of the hardware characteristics of the computers: all the necessary optimizations were adopted in order to obtain fast execution of functions. Special attention was also dedicated to the management of the memory. The here presented C4M library is a powerful tool for the efficient porting of generic algorithms on single chip embedded system, which have limited performances in terms of speed and memory resources, when compared with those available in a standard PC.

INTRODUCTION

For a real usability Brain Computer Interface is a new man machine interface which can lead many disabled people to an higher quality of life. In order to avoid undesired or unsafe behavior of the controlled system, algorithms have to operate in real-time. Many state of the art BCI algorithms have been designed using specific mathematical languages strictly dependant from the use of a PC or similar devices [1]. Notwithstanding the importance of studying and developing more reliable algorithms, the possible future diffusion of daily life application, will also face the problems related to the possibility to transport the BCI from the traditional PC to the devices and systems used by the disabled people.

Furthermore we point out that the most of the high level digital signal processing languages are typically oriented to the reduction of the developing time rather than optimizing the resources and the real-time execution. Considering those assumptions, in our work we addressed the problem of providing a framework able to facilitate the porting of BCI algorithms to any platform, devoting a special attention to the embedded solutions and without affecting the realization time.

Table 1: The c4mMatrix struct

c4mMatrix	
*pdata	void
rows	uint32
cols	uint32
esize	uint8

This work was based on the development of a library of mathematical functions written in C language (the C4M library) allowing numerical computation and signal processing either on PC, using standard instruments and on specific devices with less resources.

MATERIALS AND METHODS

Since the most diffused tool for the prototyping of BCI algorithms is Matlab® (Mathworks Inc., Massachusetts, USA) [1, 2], the structure of the proposed library was organized in order to simplify the porting from Matlab to C language. The features that make Matlab suitable to design signal processing solutions are the matrix-based architecture and the availability of several basic and recurrent functions able to address both time and frequency domain operations. In order to obtain the maximum performances, portability and usability the C4M proposed and used some specific rules, structures and functions:

- the C4M functions are atomic operators: the function can not dynamically allocate memory (the program that operates in the higher level must provide the necessary memory);
- in order to adapt the algorithm to the architecture of the CPU and to the requirements in terms of precision, both single and double floating-point precision version of each function should be provided;
- in order to avoid waste of memory, each function should use the input variables space to store the output variables: the calling level function will make a copy of the input variables if necessary.

Input and output arguments are in the form of matrices and are represented using a c4mMatrix struct:
The *pdata* member points to the memory area where the data are stored; the *rows* and the *cols* elements provide information about the matrix dimension; the *esize* variable is the size of the single element of the matrix and it allows the users to retrieve the amount of memory used by the matrix. The *C4M functions* implement recurrent mathematical methods: they provide the most common operations supplied by Matlab libraries. The library is under continuous improvement: the basic functions related to matrix operations (e. g. matrix sum, product and inversion), frequency and time domain functions (e. g. fast Fourier transform and convolution) were developed. For every C4M function a mex-file was created in order to execute it directly from Matlab, taking advantage of the graphical and the data management tools provided by the

IDE (Integrated Development Environment) and to test the speed and the reliability of each function. The C4M library has been used in a SSVEP (Steady State Visual Evoked Potential) protocol based BCI previously working fine with Matlab. The host system was the complete BCI system previously developed by our group[3] based on a wearable EEG acquisition device and a Windows® based software which managed the graphical user interface, the protocol execution and the visual stimulation. The SSVEP protocol was applied to a five state selection. Four high efficiency LEDs provided the visual stimulation; the idle state was considered as the fifth class.

RESULTS AND CONCLUSION

The C4M-based algorithm was integrated in the BCI software using a C++ objects oriented programming. In this way it has been possible to remove the calls to Matlab and replace them with the calls to the newly created algorithm. Figure 1 shows the structure of the algorithm.

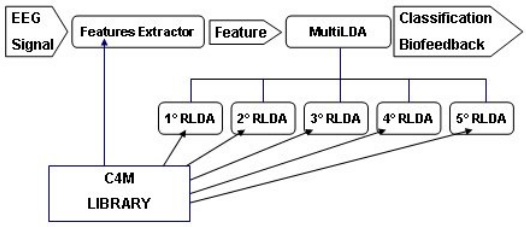

Figure 1: Structure of the algorithm

The Feature Extractor is the object that computed the features vector from EEG signal, by means of some spectral parameters. The BCI algorithm was based on a supervised multiclass classifier obtained by combining different sub-classifiers. Each RLDA object operated a one versus all-type binary Regularized Linear Discriminant Analysis [4]. The derived MultiLDA object made a multiple classification taking the results of 5 RLDA (4 associated to the luminous stimuli and last one to the idle state), moreover it generated the biofeedback by combining the resultant time signed distance with quality index related to the number of coherent identification.

Table 2: Time comparison obtained by using the real-time counter of the CPU

	Matlab version	C version
Mean elaboration time	137.5 ms	0.89 ms

Some tests were conducted in order to compare the performances obtained by the original Matlab-version algorithm with the one based on the C4M library. Table 2 shows the mean computation time during the real-time operation of a trained system, on the same platform. The software run on a laptop PC (Pentium IV, 2.8 GHz). The C version software had a considerably higher execution speed if compared to the Matlab version software. As a matter of fact some platforms do not offer the possibility to allocate the memory dynamically; the C4M library provides a useful module that enables the emulation of the dynamic allocation. These special functions also allow the monitoring of the memory during the execution of the program so avoiding lack of resources due to omitted deallocations, and for memory requirements characterization. Figure 2 shows the amount of allocated memory during the training phase of the algorithm, both working with single precision and double precision floating-point variables.

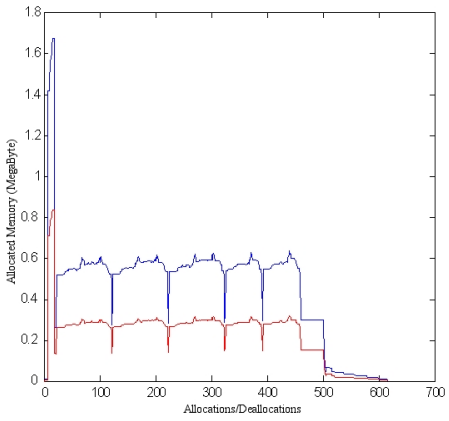

Figure 2: Memory allocation

The porting to C language made the operation of features extraction and classification much faster than the same operations executed using through the Matlab environment. The Matlab algorithm was real time capable, it was possible to perform two classifications per second: thanks to this improvement it was possible to obtain a hard real-time behaviour. Next steps will be taken to move part of the elaboration load into the EEG acquisition system CPU: by extracting the useful information of the signal rather than sending the whole acquired signal, it will be possible to reduce the amount of data to be sent to the PC minimizing the power consumption due to wireless transmission. At the moment the library is available only for developers: a proper license agreement will be proposed soon.

ACKNOWLEDGEMENT

This work was partially supported by a grant from ST Microelectronics and a grant from Istituto Italiano di Tecnologia (IIT).

REFERENCES

[1] Scherer R, et al. Inside the Graz-BCI: rtsBCI. Biomedizinische Technik, 2004; 49: 81–82.

[2] Shalk G, et al. BCI2000: A General-Purpose Brain-Computer Interface (BCI) System. IEEE Trans Biomed Eng, 2004; 51(11): 1034–1043.

[3] Piccini L, et al. A Wearable Home BCI system: preliminary results with SSVEP protocol. Proc IEEE EMBC, Sept. 1-4, 2005; Shanghai (China).

[4] Poggio T, Girosi F. Regularization algorithms for learning that are equivalent to multilayer networks. Science, 1990; 247: 978–982.

BCI-INFO.ORG – AN INTERNATIONAL INTERNET-PLATFORM FOR THE BCI COMMUNITY

B. Graimann, G. Pfurtscheller

Institute of Knowledge Discovery, Graz University of Technology, Graz, Austria
E-mail: graimann@tugraz.at

SUMMARY: BCI-info.org is an international internet-platform for the BCI community that facilitates the exchange and discussion of BCI related information. It is intended to be a repository for everything related to BCI research, containing information for researchers and patients alike. Membership to BCI-info.org is free and everyone is invited to contribute to the site.

INTRODUCTION

The past few years have seen an increased interest in BCI research resulting in a large number of new research groups. BCI research is an interdisciplinary field integrating knowledge from neuroscience, psychology, engineering, computer science, and rehabilitation.

Seldom does any single group have the expertise in all these fields required to develop and improve a workable BCI. Therefore, it is important to have forums in which results and problems common to BCI researchers from these diverse disciplines can be discussed. Unfortunately, these are usually limited to conferences and special workshops, the rarity of which often stifles the required discussion and exchange of information.

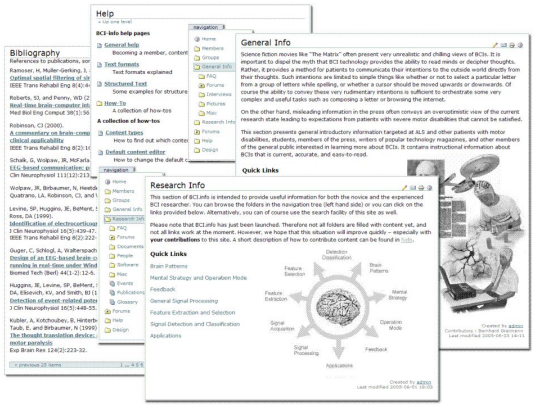

Figure 1: Screenshots of BCI-info.org

Further, useful information about BCI research is scattered over scientific publications and websites maintained by individual research groups. In order to mitigate this situation, we suggest an internet platform for BCI research. This platform is intended to be a repository of everything related to BCI research, containing information for researchers and patients alike (e. g. ALS patients). The site will also contain instructional materials written for a lay audience, so that students, media, and others from the general public can find current, accurate, and easy-to-read information about BCIs. A second prototype of the suggested platform is already available at http://www.bci-info.org (Figure 1).

In this article we explain the technology upon which BCI-info.org is based, the structure used to organize content, and how anyone can become a member of BCI-info.org and contribute content to the site.

MATERIALS AND METHODS

Content management system: BCI-info.org is based on Plone [1]. Plone is a powerful and flexible open-source content-management system (CMS) that is easy to use and maintain. Most of the functionality of BCI-info.org is already provided by Plone. This, however, is only one reason why Plone is a suitable basis for a community site like BCI-info.org. Other reasons are [1]: It is open source and is licensed under the GNU General Public License [2]. Unlike many other open source CMS available, Plone is an already mature product and is supported by a strong and large development team. It complies with standards for usability and accessibility. And further, extensions such as new content types can be created rather easily by a programming framework called Archetypes [3]. Since Plone is open source, a large number of useful extensions are freely available.

In order to facilitate the organization of the content and information available, BCI-info.org is structured in different sections as depicted in Figure 1. Detailed information about the content available in the individual sections can be found in the help section of BCI-info.org. The sections are either moderated (grey boxes) or unmoderated (white boxes). Only reviewers and site managers can directly contribute to moderated sections.

Figure 2: Structure of BCI-info.org

Standard users are supposed to store their contributions in their member folders and can then submit

them for publication. The submissions are reviewed by the BCI-info.org review board[1] and are either accepted for publication on the site or rejected. Figure 2 shows the complete workflow for content on BCI-info.org as it is currently implemented.
Published content will be listed in the appropriate moderated sections or listed by the search facility of the site. Rejected content and content retracted by the user can remain in the user's folder as public draft where other site members or visitors can access it. Content can also be made private. In this case, it is invisible for other members except the content owner. This workflow is maintained to ensure a certain quality of the information provided in the moderated sections and to avoid duplication and reduce redundancy.

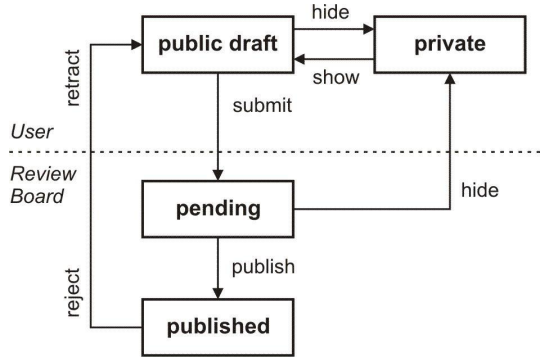

Figure 3: Default workflow for content on BCI-info.org

Available content types: The content type that most closely represents a typical web page is a page item. Therefore it can be used for static, general information. Other standard content types are: news items (can be used e. g. to announce new papers or press releases), event items (e. g. upcoming conferences), and files (e. g. data or multimedia files). Besides these standard types provided by Plone, BCI-info.org also provides customized content types particularly suitable for BCI research: bibliography items (references to articles, books, etc), journal items (descriptions of journals that publish BCI research), group items (short descriptions of BCI groups), contact items (personal contact information), job items (open vacancies), software items (descriptions and links to useful software), and web resource items (interesting resources on the web).
Joining BCI-info.org and adding content: Only registered members of BCI-info.org can add content. Becoming a member is easy, and anyone can do it. For the registration process, one has to provide their name and a valid email address, which is used for sending a provisional password. BCI-info.org guarantees that the email address is not used for anything else except the communication between the user and the platform. After registration, the user will have an account on the server, which can be used to add content to the site.
Adding content is also a simple process that always follows the same basic procedure: The content type appropriate for the information that is to be provided has to be selected from a drop-down list and the corresponding form has to be filled in. After completing the form, it can be submitted for publication. Usually, a submitted content item is then published within a view days and can be found in search results or is listed in the appropriate moderated sections. Detailed information about adding content can be found in the help section of BCI-info.org.

DISCUSSION

There are currently more than 220 registered users on BCI-info.org. Considering that BCI research is a rather small field, this is a surprisingly large number of members. Obviously, there is an interest for a platform dedicated to BCI research. However, only a small percentage of the members (about 2 percent) have contributed content to the site. Compared with other community sites, this is a small number of active users. Since a community site depends on the contributions of its members, we improved the documentation of BCI-info.org in the hope that short and simple guidelines for contributing content will encourage and improve the number of contributions. Further, a mailing-list/newsgroup and a discussion forum have been established to facilitate unmoderated, immediate communication between members. Every member is invited to participate in the forums and contribute at least simple content like contact information, bibliography items, news, or events. Members that want to support BCI-info.org more actively (e. g. as reviewer) are also welcome. BCI-info.org is not intended to be the product of one single BCI group. In fact, it is meant to serve the BCI community as a useful platform, and as such it needs the help and participation of the community.

REFERENCES

[1] The Plone Foundation, Plone, http://www.plone.org.

[2] Free Software Foundation, GNU General Public License, http://www.gnu.org/copyleft/gpl.html

[3] McKay A. The definitive guide to Plone. New York, Apress, 2004.

[1] A list of members of the review board can be found at http://www.bci-info.org/about

OFFLINE DATA ANALYSIS FOR THE BCI2000 FRAMEWORK: THE MARIO PROJECT

F. Cincotti[1], M. Mattiocco[1], A. E. Fiorilla[1], F. Babiloni[1,2], D. Mattia[1], S. Salinari[3], M. G. Marciani[1,4], G. Schalk[5]

[1]Clinical Neurophysiopathology Unit, Fondazione Santa Lucia IRCCS, Roma, Italy
[2]Department of Human Physiology and Pharmacology, La Sapienza University, Rome, Italy
[3]Department of Systems and Computer Science, La Sapienza University, Rome, Italy
[4]Department of Neuroscience, Tor Vergata University, Rome, Italy
[5]Brain-Computer Interface R&D Program, Wadsworth Center, New York State Dept. of Health, Albany, New York, USA

E-mail: f.cincotti@hsantalucia.it

SUMMARY: Signals from the brain could provide a non-muscular communication system, a brain-computer interface (BCI), for people who are paralyzed. The BCI2000 software framework facilitates real-time implementations of BCI systems. The MARIO Project aims at complementing BCI2000 by building a software tool for offline analyses of brain signals. These analyses can be performed within a graphic environment or using modules written in the Matlab language. At present, Mario supports mu rhythm and P300 analyses. The combination of graphical and script-based use provides a rapid learning curve and also facilitates more comprehensive analyses by advanced users.

INTRODUCTION

Brain-Computer Interfaces (BCIs) are systems that depend on two adaptive controllers – the user and the system. In order to optimize decoding of the user's intent and also to facilitate user learning, appropriate machine adaptation should be ideally matched to a specific user in the particular stage of his/her training. While current algorithms have some adaptive capacities, human intervention and expert supervision is still required. Progress requires the evaluation of different approaches and the use of the resulting algorithms for real-time communication and control.

BCI is a highly interdisciplinary research field. Thus, not all research groups have the expertise to develop and implement all aspects of effective BCI systems. The BCI2000 project [1] marked an important milestone, because BCI2000 already supports a number of important BCI methods and facilitates implementation of modules to support new data acquisition systems, signal processing algorithms, or user tasks, to be used for online experiments. At the same time, offline analyses and their appropriate interpretation and integration in subsequent online experiments are currently not adequately addressed by BCI2000 and are also not documented in the literature.

The MARIO project aims at addressing this problem by providing support for standard and more comprehensive analyses and by also providing adequate documentation.

MATERIALS AND METHODS

MARIO is an off-line analysis software, developed using the Matlab environment (The Mathworks, Inc., Natick, MA, USA). It is modular and object-oriented, and can be easily integrated with other software packages for data analysis and visualization. MARIO can be used for the analysis of data acquired with a BCI2000 environment in mu-rhythm and P300 setups.

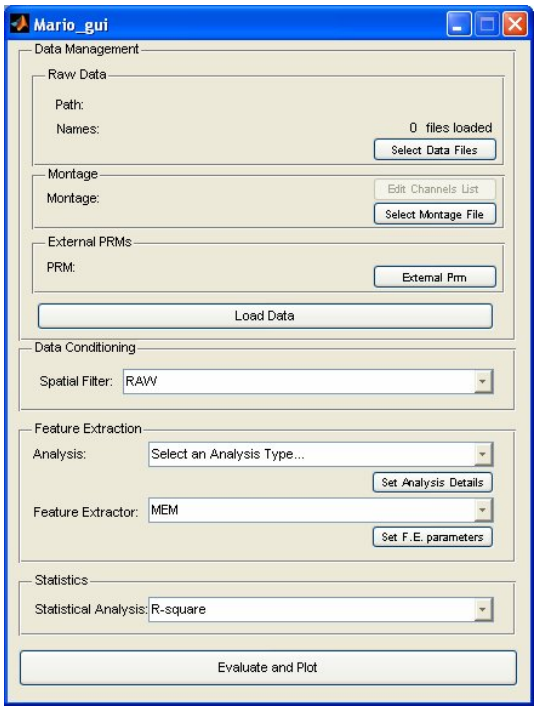

Figure 1: Main graphical interface of the Matlab implementation of the MARIO Toolbox

It is targeted towards two classes of uses routine analysis by non-experts and more comprehensive analysis by experts in signal analysis. The first use benefits from a Graphical User Interface (GUI) that guides users through standard analysis processes. The second use benefits from software modules that are available for batch processing. This capacity will facilitate 1) repeating the same analysis on a large number of recordings; 2) performing exhaustive analyses (using different parameters) on a specific dataset; 3) experi-

menting with custom algorithms with no need to reimplement the entire processing pipeline.

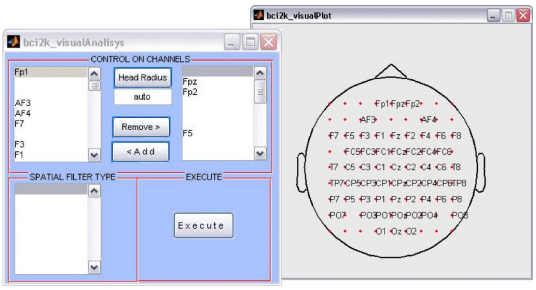

Figure 2: Screenshot of one of the parameter dialogs (montage set-up)

Internally, MARIO is decomposed into functional and cascaded modules as described below:

- Data import (BCI2000 .dat or Matlab .mat files)
- Signal conditioning (spatial filtering, ...)
- Feature extraction (spectral estimation, averaging)
- Feature combination (manual selection, exhaustive monovariate testing, LDA, ...)
- Statistical analysis (r^2, ANOVA)
- Visualization (feature matrix, topographic maps, spectra, ...)

All these modules are hidden in the graphical user interface, but can be directly accessed in the batch scripts. Each of these modules can be easily replaced with an improved version, a custom version, or a different analysis.

RESULTS

An executable implementation of MARIO, and the Matlab source code for mu-rhythm and P300 analysis are included in the BCI2000 distribution [2]. Documentation can be also found on the Internet [3].
MARIO offers a wide set of visualization graphs that can be combined to have a complete visualization of the produced data.

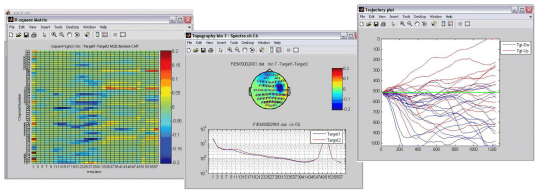

Figure 3: Screenshot of some results of the mu rhythm analysis: r^2 matrix (channels by frequency); r^2 topographical distribution and spectrum; cursor trajectories for a training session.

For a mu rhythm analysis, a user can request to visualize:

- a trajectory plot that shows the actual (i. e. online) cursor position for any sample in a BCI2000 trial;
- a matrix (channel × bin) that shows in color the r^2 value of any feature. A colorbar shows the displayed range of r^2 values;
- Another panel shows a detail of the previous matrix. The upper topographic plot shows the r^2 value for any channel in the selected bin of frequencies; the lower one is the spectrum of the selected channel for all the frequencies.

For a P300 analysis user can choose between:

- An r^2 matrix
- An amplitude waveform graph;
- A topographic plot;
- An ERP response graph;
- A string prediction form.

All these results visualizations are shown by the GUI, but can be also generated by the Matlab scripts.

DISCUSSION

We introduced the MARIO project, which complements BCI2000 with offline analysis capabilities. Using signal acquisition equipment, an installation of BCI2000 for on-line operation, and of MARIO for offline analysis, is sufficient for a research group with basic knowledge on brain signals and PC management to start BCI research efforts. We anticipate that this will represent a strong "democratization" of the BCI procedure that should allow for even greater diffusion of BCI research. As the wide dissemination of BCI2000 demonstrates, the use of common systems can facilitate collaborations between research groups and possibly the creation of consortia whose aim is large-scale experimentation.
A second advantage of this scenario is that individual groups with specific expertise or consortia of groups with complementary expertise can carry on research in one of the disciplines that compose BCI research, without being forced to acquire detailed competence in all of the others. As an example, a group involved in machine learning could study, either offline or online, a new classification strategy by simply plugging their new analysis technique into the analysis pipeline of MARIO or BCI2000, respectively, or a group involved in assistive technology could test the effectiveness of their brain-controlled keyboard in a clinical environment.

REFERENCES

[1] Schalk G, McFarland DJ, Hinterberger T, Birbaumer N, Wolpaw JR. BCI2000:A general-purpose brain-computer interface(BCI) system. IEEE Trans Biomed Eng, 2004; 51(6): 1034–43.

[2] The BCI2000 project web site, www.bci2000.org/

[3] The MARIO Project online documentation, mario.neilab-fsl.it/wiki/

USAGE OF SIMULINK FOR BRAIN-COMPUTER INTERFACE EXPERIMENTS

C. Guger, F. Laundl, G. Krausz, I. Niedermayer, G. Edlinger

g.tec medical engineering GmbH, Schiedlberg, Austria
Guger Technologies OEG, Graz, Austria
E-mail: guger@gtec.at

SUMMARY: A brain-computer interface requires the real-time analysis of brain signals. A new high-speed online processing environment allows the easy usage of Simulink for this task. Properties of this new technology are discussed.

INTRODUCTION

A brain-computer interface (BCI) analyzes brain waves in order to control external devices [1, 2]. BCI input signals can be the Electroencephalogram (EEG), the Electrocorticogram (ECoG) or even action potentials. The subjects' task is to imagine specific thoughts in order to control the system. Therefore the biosignal acquisition, the analysis and the experimental control must be done in real-time.

A big advantage for the development and specific adaptations is that a BCI system facilitates the real-time implementation of EEG-analysis algorithms under a Rapid Prototyping environment [3]. The developed system is based on MATLAB and Simulink. Simulink is a signal-flow oriented programming language that allows setting up the biosignal analysis with graphical blocks. The Real-Time Workshop generates then the code for real-time applications. This C code is directly generated, compiled and linked from the Simulink model and downloaded to a real-time Kernel under Windows. This allows to run the whole Simulink model in real-time.

This approach has several disadvantages:

1. *Requirement of C code for analysis functions:* The Simulink blocks for the analysis must be written in C code

2. *Slow communication channel:* The analysis model loaded into the real-time Kernel of Windows communicates over a communication channel with the graphical representation of the Simulink model. Through this channel biosignal data is sent to the Scope blocks or to MATLAB S-functions (Simulink blocks) which are used to program experimental paradigms. However, this communication channel is very slow and therefore the achieved sampling frequencies, number of channels and update times are limited.

3. *Limitation of standard Simulink blocks and C functions:* The Real-time Workshop is used to compile the Simulink model and to download the generated code into the Real-time Kernel. The compilation is not possible for functions containing a graphical output. Therefore standard functions such as the *FFT Scope* of Simulink can not be compiled and therefore not be used. It is furthermore not possible to compile graphical output commands into C functions.

The current work discusses the recently developed high-speed online processing environment which overcomes all of these limitations.

MATERIALS AND METHODS

For the biosignal acquisition a 16 channel biosignal amplifier with 24 bit and an internal DSP was developed (g.USBamp). The amplifier can be directly connected to a PC or notebook with an USB connector. No additional data acquisition devices are therefore needed. 16 analog to digital converters perform the simultaneous sampling. Each analog to digital converter is operating at 2.5476 MHz and performs a 64 times oversampling. This results in a sampling rate of 38.500 Hz for each channel. A powerful floating point DSP performs an additional oversampling and the real-time filtering of the biosignal data. The sampling frequency can be adjusted between 16 Hz and 38.400 Hz. Therefore, a sampling frequency of 128 Hz yields to an over-sampling rate of 19.200 with a very high signal to noise ratio.

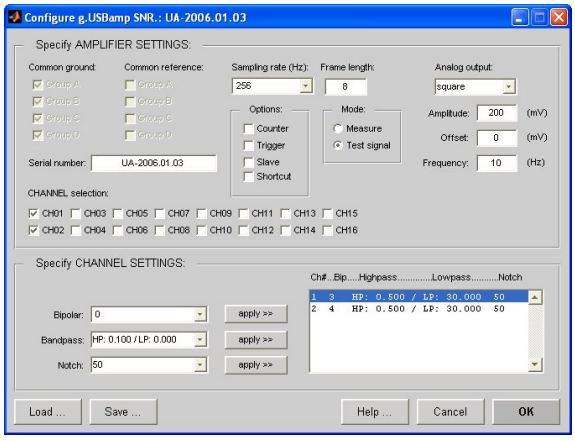

Figure 1: Graphical controls of the amplifier unit

The g.USBamp high-speed block provides a graphical interface to the g.USBamp hardware which can be used under Simulink to specify the amplifier properties and to acquire the data. The g.USBamp block output contains the biosignal data. The block transmits the data with a specific frame size depending on the sampling frequency. The data format is float32 with 4 Byte. The graphical interface (see Figure 1)

allows to select the channels that shall be acquired, to select a band pass filter (Butterworth characteristics) and to select a notch filter for suppressing the power line interferences. Additionally, a bipolar derivation can be performed between specific channels. The bipolar derivation is calculated on the DSP directly after the over-sampling is done. Therefore, the band pass and notch filtering is already performed for the bipolar derivation.
An *Unbuffer* block follows the g.USBamp block separating the bytes transmitted in one frame. Therefore the Simulink model can work with the data sample by sample. Important to note is, that the Simulink model is driven by a special hardware interrupt control of the g.USBamp and works therefore in real-time. Then the data channels are split with a *Demux* block and converted into double precision for the following signal analysis. In Figure 2 the Simulink model calculates the bandpower in the alpha (8–12 Hz) and beta (16–24 Hz) ranges of each channel resulting in 4 parameters for each sample.

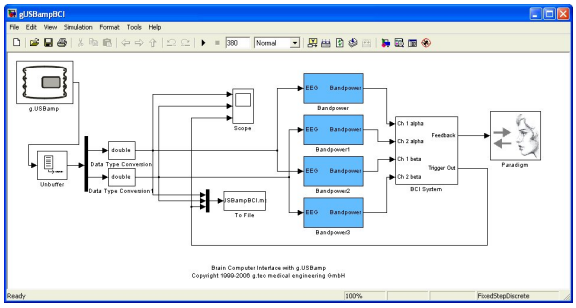

Figure 2: Simulink model operating in real-time with the hardware interrupt driven g.USBamp block

Then an on-line linear discriminant analysis is calculated to obtain the control signal for the experimental paradigm. The paradigm is programmed as MATLAB S-function to transform the BCI control signal into cursor movement. The biosignal raw data is visualized with the *Scope* block and stored in MATLAB file format. Therefore the off-line analysis can easily be done in MATLAB.

RESULTS

The presented new approach with the hardware interrupt driven g.USBamp block allows to operate the whole model in real-time. The exact timing is provided by the external biosignal amplifier. Data is transmitted to the Simulink model every ms. As soon as new samples are sent into the Simulink model the analysis is performed as fast as possible on the PC.
The computational demand of the algorithms must be low enough to allow the PC to process the data without a buffer overflow.
With this approach a sampling frequency of 38.400 Hz per channel for all 16 channels can be obtained. If more channels are required the g.USBamp block has to be copied multiple times into the model. The synchronization is done directly on the amplifiers themselves. Therefore the data is exactly synchronized.

DISCUSSION

A very important advantage of this approach is that all standard Simulink blocks can be used in the individual models. This can be done because the real-time code generation with the Real-time Workshop was eliminated with the hardware interrupt driven g.USBamp block. Therefore, also blocks having graphical outputs can be used.
The achievable sampling frequencies and therefore update rates of the Simulink model are much higher than those obtained with the Real-time Kernel, because the timing is done by the external amplifier hardware. Additionally, the slow communication channel between the Real-time Kernel and the graphical Simulink model was eliminated. This results in very fast updates of the *Scope* and *Paradigm* blocks and eliminates the additional step of compiling the model.

CONCLUSION

The new approach allows an easier handling of biosignal analysis under Simulink and enables higher sampling frequencies and update rates. Additionally all Simulink blocks can be used for the signal analysis and this increases the Rapid Prototyping speed.

ACKNOWLEDGEMENT

This work was supported by EU IST project Presencia and by the FFG in Austria.

REFERENCES

[1] Wolpaw JR, McFarland DJ, Neat GW, Forneris CA. An EEG-based brain-computer interface for cursor control. Electroenceph Clin Neurophy, 1991; 78: 252–259.

[2] Pfurtscheller G, Neuper C, Schlögl A, Lugger K. Separability of EEG signals recorded during right and left motor imagery using adaptive autoregressive parameters. IEEE Trans Rehab Eng, 1998; 6: 316–325.

[3] Guger C, Schlögl A, Neuper C, Walterspacher D, Strein T, Pfurtscheller G. Rapid prototyping of an EEG-based brain-computer interface (BCI). IEEE Trans Rehab Eng, 2001; 9(1): 49–58.

INDEX